ELSEVIER

Physics Reports 354 (2001) 243–409

PHYSICS REPORTS

www.elsevier.com/locate/physrep

The nuclear physics of muon capture

D.F. Measday *

University of British Columbia, 6224 Agricultural Rd., Vancouver, BC, Canada V6T 1Z1

Received December 2000; editor: G.E. Brown

Contents

* Tel.: +1-604-822-5098; fax: +1-604-822-5098.
E-mail address: measday@triumf.ca (D.F. Measday).

0370-1573/01/$ - see front matter
PII: S0370-1573(01)00012-6

Abstract

We review the topic of muon capture in nuclei and show that significant nuclear physics is being learnt from recent experiments. The focus of many earlier experiments had been the particle physics and weak interactions aspects of the subject. Although these were useful confirmation of basic ideas, defining experiments mostly came from other areas. Thus, we focus on what can be learnt about nuclei especially 1^+, 1^- and 2^- magnetic transitions. Valuable comparisons can be made to other charge exchange reactions such as (π^-, γ), (π^-, π^0), (n, p), $(d, {}^2\mathrm{He})$ and $(t, {}^3\mathrm{He})$. However, all those experiments have resolutions of 300 keV to 1 MeV, or even worse, so γ-ray studies of muon capture provide resolutions 100–1000 times better, and thus define the levels unambiguously. For even–even nuclei one can also compare to (e, e') at 180°, or (p, p') at forward angles, for which the resolution is reasonable, typically 50–100 keV, but isospin mixing complicates the comparison. With the recent substantial progress in Shell Model calculations, we anticipate significant developments in our understanding of nuclear structure in the next few years.

PACS: 23.40.Hc

1. Introduction

1.1. Prologue

Muon capture in nuclei has been a secluded garden slightly off the main tourist routes of particle and nuclear physics. Few major discoveries have been made there, but it has often been a refuge where one could admire the beauty of nature and verify the ideas which were created elsewhere. The weak interaction has been a fertile zone of sub-atomic physics. Many major discoveries have been made therein and these are the foundation of many of our paradigms of particle physics such as "The Standard Model". Muon physics has been a major part of that development, and muon capture in nuclei a useful adjunct. The field grew upon the research at the old synchrocyclotrons in the 1950s and 1960s and most of the basic concepts date from that era.

There was a second coming at the meson factories in the 1980s and 1990s; improved equipment resolved many old problems although many remain. We postulate that these unresolved problems are due to the complexity of the nuclear environment and not due to an imperfect understanding of the weak interactions. Thus, we can now turn this around to use muon capture as an excellent test of our understanding of complex nuclei. With the recent improvement in calculational technology for the shell model in quite heavy nuclei, there is a very real hope that significant improvement in our knowledge will emerge.

There are many existing reviews on muon capture but almost all written from the point of view of a theorist. This perspective is very valuable, but much information which is relevant to an experiment is omitted from such an approach. An obvious example is the subject of muonic X-rays which for a theorist is legitimately considered another topic. In an experiment however, muonic X-rays are both a curse and a blessing, but certainly cannot be ignored. Thus this review is written for those who may pursue such muon capture experiments in the future. We shall show that we now know what were the problems with previous experiments. To overcome these difficulties will take resources which may become available in new facilities such as the Joint Project for High Intensity Proton Accelerators at Tokai, Japan.

1.2. General introduction

Ever since its discovery in 1937, the muon has been an enigma which has fascinated and frustrated physicists of several generations (not only the second). We shall take the point of view that the general properties of the muon have been established in particle experiments and that any new discoveries, as important as they will be, will not substantially affect the problems addressed in muon capture. We shall also assume that lepton universality holds better than we need, so that the many lessons learned from β decay can be transferred over to muon capture which thus can be considered as an extension of electron capture, though with many more states available.

Muon capture centres on the simple semi-leptonic reaction

$$\mu^- + p \rightarrow n + \nu_\mu \,, \tag{1.1}$$

which occurs via the charged current of the weak interactions. A feature which turns out to be critical is the extreme spin sensitivity of this reaction for μp atoms in the $1s$ state. The singlet capture rate is about $660\,s^{-1}$ whereas the triplet rate is only $12\,s^{-1}$ or so. Many experiments performed at the old synchrocyclotrons showed that these capture rates for hydrogen are roughly correct, but the experiments are hard, and complicated by the fact that absorption actually takes place from a $p\mu p$ molecule. Recently, however, a remarkably precise experiment has been reported on the reaction

$$\mu^- + {}^3\mathrm{He} \rightarrow \nu_\mu + {}^3\mathrm{H}\,. \tag{1.2}$$

A rate of $1496 \pm 4\,s^{-1}$ was measured and this is in agreement with theoretical estimates for a statistical mixture of the hyperfine states. We shall therefore assume that the particle physics aspects are well understood.

When a muon reaches the $1s$ state of a muonic atom, it can decay or be captured on a bound proton. Except for very light nuclei this capture is far more likely than decay and it is the general features of this capture which will be the focus on this review. We shall show that the many characteristics which are poorly understood are reflections of the complexity of the nuclear environment. This manifests itself in two ways, either the renormalization of the coupling constants, or the complications of nuclear structure. Great strides are being made in understanding both aspects and we shall see that further developments are just around the corner.

When muon capture occurs in any nucleus, the energy release of about 100 MeV is mainly donated to the neutrino, but the nucleus can and does absorb substantial energy, thus many reactions occur. Let us take ^{28}Si as an example because we shall see that many experiments have focussed on this nuclide. First remember that in the $1s$ state of muonic silicon, the muon will decay 34% of the time and capture on the nucleus 66% of the time. Of those captures, about 36% will produce no neutrons, 49% will produce 1 neutron, 14% will produce 2 neutrons and 1% will produce 3 neutrons. Thus, symbolically:

$$\mu^- + {}^{28}\mathrm{Si} \rightarrow {}^{28}\mathrm{Al}^* + \nu_\mu\,. \tag{1.3}$$

Since an excitation of at least 21 MeV is required to produce 2 neutrons, we can see that the nucleus receives more than one might have expected. As a guide one should remember that, for muon capture from a μp atom, the recoiling neutron takes only 5.2 MeV of kinetic energy, whilst the neutrino takes away 99.1 MeV.

Most experiments have concentrated on the small fraction of reactions that leaves the final nucleus in a bound state. In this example ^{28}Al is bound up to 7.7 MeV leaving over a hundred levels able to be excited. Fortunately, there are only a chosen few. It is known that 26% of the captures produce bound states of ^{28}Al. (The difference between this number and the 36% above is that "no neutrons" includes a proton or an alpha being ejected from the nucleus.) The bound state transitions can be observed via their γ-ray emission, but only 16% of muon captures in ^{28}Si have been identified as going to ^{28}Al bound states, i.e., about half of the expected number. This is typical of such comparisons for most nuclei, and we now realize that the other transitions are actually there, but just hidden in the overwhelming background.

These other transitions often produce high energy γ-rays which are Doppler broadened, and the efficiency of the HPGe detector is much lower, so more experimental time is required. Modern experiments with larger, more efficient detectors, could thus study the topic more

comprehensively, and a few examples will be discussed. Such transitions offer the possibility of testing nuclear structure models.

There are several other reactions which excite the nucleus in a similar manner to (μ^-, ν); these are (π^-, γ) at rest and (π^-, π^0), (n, p), $(d, {}^2\mathrm{He})$, $(t, {}^3\mathrm{He})$, $({}^7\mathrm{Li}, {}^7\mathrm{Be})$, and $({}^{13}\mathrm{C}, {}^{13}\mathrm{N})$ in the forward direction. The common signature is a virtual pion and the mode of excitation tends to be a spin (1^+), or spin–dipole $(0^-, 1^-, 2^-)$ transition. Interesting comparisons can also be made to (e, e') at 180° and more data are anticipated from the new DALINAC-S facility. The (p, p') reaction at very forward angles also excites magnetic transitions, but $T = 0$ levels are also excited. Of course in this case one is dealing with excitation of the original nucleus, $^{28}\mathrm{Si}$ in our example above, so the few isoscalar transitions have to be filtered out. Fortunately the (d, d') reaction can be used to confirm $T = 0$ identification. The difficulty is that all the charge exchange reactions have an energy resolution of 0.5–1 MeV whereas γ-rays have a resolution of 2 keV. This factor of a thousand means that comparisons are often difficult. The resolution of (e, e') experiments is excellent (about 50 keV or even better) but the Coulomb difference is often not known well, or there is isospin mixing, so again comparisons can be tricky. Nevertheless a lot has been learnt, and a lot more is within reach.

Reactions where neutrons, protons or alphas are produced can also be studied. If the μ^- absorption on the proton gives a large recoil to the neutron, this is called the pole term. It is effectively a direct reaction where a proton in the target nucleus is suddenly removed, so interesting comparisons can be made with reactions such as (γ, p), $(p, 2p)$, or $(e, e'p)$ where a proton is suddenly ejected from the nucleus. Unfortunately only a few examples exist where there is both (μ^-, ν) and (γ, p) information.

Finally it should be noted that muon capture is often a very useful test for calculations in other weak nuclear reactions. Thus electron capture in stars is critical in the collapse of a supernova [1]. Neutrino nucleus scattering is also important in stars and in the detection of neutrinos [2]. Such reaction calculations are normally tested against muon capture.

1.3. Previous reviews

A few text books have discussed the topic of muon capture and useful introductions have been given by Marshak et al. [3] and Blin-Stoyle [4]; slightly longer discussions have been given by Weissenberg [5] and by Morita [6], but these are only introductions.

There are few in-depth reviews available. At conferences there have been excellent surveys such as those by Cannata et al. [7], an update of two earlier reviews [8,9], but unfortunately these are all difficult to obtain nowadays. There are also the useful reviews by Eramzhyan and his colleagues [10,11], but they are focussed on specific aspects of the problem, and unfortunately also not easy to find. Similarly the review by Singer [330] on nucleon production is an early, but excellent guide to that topic. The only easily accessible review is the thorough survey by Mukhopadhyay [13] which was updated at the Vancouver EICOHEPANS Conference in 1979 [14] and again at WEIN in Montreal in 1989 [15]. Since then there have been isolated talks at various conferences, but none of them claimed to be extensive reviews of the literature. It is thus appropriate to cover some of this earlier work from a modern perspective, and to discuss the significant achievements which have been accomplished in the last twenty years.

2. Fundamental concepts

2.1. Properties of the muon and neutrino

The characteristics of the muon and muon neutrino are very well known, certainly better than we shall need for the study of muon capture. Nevertheless it is worth discussing those properties that we shall use and briefly describing the types of experiments that are the basis for that knowledge.

The mass of the muon is [16]

$$m_\mu = 105.658389\ (34)\,\mathrm{MeV}/c^2\ . \tag{2.1}$$

This 0.3 ppm measurement is derived from experiments on the magnetic moment of the positive muon. A SIN experiment [17] determined the Larmor precession of the μ^+ in bromine, whilst a LAMPF experiment [18] measured the hyperfine Zeeman splitting in muonium, i.e., a μ^+e^- atom. The results are in excellent accord and can also be interpreted in terms of the ratio between the mass of the muon and that of the electron viz:

$$\frac{m_\mu}{m_e} = 206.7683\ (1)\ . \tag{2.2}$$

It is, of course, this large ratio which makes so much difference to the relative properties of these otherwise similar leptons, especially in muon capture.

These measurements were on the μ^+. The most basic of symmetries, CPT, requires that the mass and lifetime (though not partial lifetimes) of particles and antiparticles be identical. However, it is comforting to know that there is a measurement of the μ^- mass using muonic X-rays, which is consistent at the level of 3 ppm [19]. The best experimental check on the CPT theorem is in the $K^o\overline{K^o}$ system. Because these mix, a measurement has to be made on the mass difference of the physically observed K^o_L and K^o_S, and this has been recently remeasured to be [16,20,21]

$$\Delta m = (530.1 \pm 1.4) \times 10^7 \hbar/s \tag{2.3}$$

$$= 3.489\ (9) \times 10^{-6}\,\mathrm{eV}/c^2\ . \tag{2.4}$$

Since the mass of the K^o is $498\,\mathrm{MeV}/c^2$ this represents a difference

$$\Delta m/m \approx 10^{-14}\ . \tag{2.5}$$

This effect for the observed particles can be explained quite accurately as being caused by the weak interactions, so the K^o and $\overline{K^o}$ masses are the same to about 1 part in 10^{16}, a rather impressive precision. As confirmation, the mass of the proton and antiproton are the same to 1 part in 10^{10} [22].

The lifetime of the muon is a key property which is important from many points of view. Because it has a value which is amenable to straightforward electronic techniques, it can be measured quite accurately, since time is the easiest parameter to determine. From the two most precise experiments, one at Saclay [23] and one at TRIUMF [24], the value of the μ^+ lifetime is known to be

$$\tau_\mu = 2197.03\ (4)\,\mathrm{ns}\ . \tag{2.6}$$

This value will be used as a basis for determining muon capture rates in nuclei. It is also the parameter which best determines the leptonic coupling of the weak interactions, since the principal decay

$$\mu^+ \to e^+ + \nu_e + \bar{\nu}_\mu \tag{2.7}$$

does not involve hadrons. Thus taking into account phase space, one can determine that the muon decay rate (λ_μ) is given by

$$\lambda_\mu = \frac{1}{\tau_\mu} = 0.995610 \frac{G_F^2 m_\mu^5 c^4}{192\pi^3 \hbar^7} , \tag{2.8}$$

$$\text{thus } G_F = 1.16639\ (2) \times 10^{-11}\ \text{MeV}^{-2} (\hbar c)^3 \tag{2.9}$$

$$= 8.962 \times 10^{-5}\ \text{MeV fm}^3 \tag{2.10}$$

$$= 1.436 \times 10^{-62}\ \text{J m}^3 . \tag{2.11}$$

The lifetime of the negative muon is more difficult to determine because if the μ^- stops in a material, it will undergo capture when it reaches the 1s muonic state. Even in hydrogen this capture is significant, so one can either assume CPT and obtain the capture rate, or use direct measures of the capture rate and verify CPT, but you cannot have it both ways. Inflight tests would be free of this concern, but at present such experiments cannot attain the required precision. As we have just indicated, the $K^o\ \overline{K^o}$ system offers an impressive test of CPT for masses of particles, so it is reasonable but not logically watertight, to assume that CPT holds for a lifetime to a similar degree of accuracy.

Another property of the muon that we shall focus on is the fact that muons do not transform into electrons, only into muon neutrinos. Similarly for the τ lepton, there is no transformation into muons nor electrons, so in nature there are three families of leptons e, μ, τ which are mutually exclusive. Many attempts have been made to observe the breakdown of this rule but, to date, all have failed (although the solar neutrino problem offers an interesting possible breakdown of this rule). We shall quote two major tests but there are many others [25,26].

The clearest test is to search for

$$\mu^+ \to e^+ + \gamma . \tag{2.12}$$

If the μ^+ were just a heavy electron (like an "excited state") this decay would occur at a branching ratio of about 10^{-5}. In fact the present limit from a recent LAMPF experiment, MEGA [27] is

$$BR < 1.2 \times 10^{-11} \quad \text{at 90\% CL} . \tag{2.13}$$

A similar test is to search for muon conversion into an electron in the 1s state of a muonic atom, for example

$$Ti(\mu^-, e^-)Ti . \tag{2.14}$$

An experiment with SINDRUM II [28,29] improves on the earlier one with the TPC at TRIUMF [30], giving a limit of

$$BR < 6.1 \times 10^{-13} \quad \text{at 90\% CL} . \tag{2.15}$$

Again another factor of a 10 sensitivity is anticipated from further experiments with the SINDRUM II spectrometer. These tests, and related ones, show no evidence for conversion of one lepton into another, although many theories suggest that eventually it might be observed, but often at a level which is beyond the reach of present techniques [31–33].

The final characteristics of the muon that are important to clarify, are its electromagnetic properties. For several decades numerous tests of QED have been made on the muon and the electron. For example Dirac theory predicts that the magnetic moment of a fermion is given by

$$\mu = g\frac{Q}{2m}s = \frac{Q}{2m} \tag{2.16}$$

(where Q is its charge, m its mass, and s its spin $=1/2$) i.e., $g = 2$ apart from radiative connections of order $O(\alpha)$. An experiment on $(g-2)=a$ for the muon continues today at the AGS at Brookhaven, pushing the limits even further [34]. The unanimous conclusion of all existing measurements is that the electron and muon obey the Dirac Equation and so their magnetic moments have $g = 2$, apart from the known corrections, therefore they have no anomalous magnetic moment; however the neutron and proton do because of their compositeness, due to their internal structure of quarks. From high energy scattering experiments, one can express this property of leptons another way by stating that they behave like point particles, and for the muon the compositeness scale $\Lambda > O(1\,\mathrm{TeV})$, i.e., $r_\mu < 10^{-4}$ fm [35]. Such compositeness would change the magnetic moment by $\Delta a_\mu \sim m_\mu^2/\Lambda^2$.

The other important particle in muon capture is the muon neutrino. Every year there are several conferences and dozens of talks and reviews concerning the properties of the neutrinos. In addition, papers on the topic appear in almost every particle physics journal every week. However, for our purposes all of this phrenetic activity can be summarized rather briefly by stating that the neutrino has negligible mass. Nevertheless, it is worth expanding briefly on this topic to give credit to the multitude of experiments on this subject. Although the Standard Model assumes that the mass of the neutrino is zero, there are several indications that this is not true. If the neutrino has mass, it might be a Dirac neutrino or a Majorana neutrino. In either case the helicity of the neutrino is no longer fixed as it is always possible to move faster than the neutrino and see its helicity reverse. A Dirac neutrino can have either left or right handed helicity ν_-^{D}, ν_+^{D} and these states are different from the anti-neutrino which can also have either right or left handed helicity $\bar{\nu}_+^{\mathrm{D}}$, $\bar{\nu}_-^{\mathrm{D}}$. For the Majorana neutrino there is no distinct anti-neutrino, the left-handed helicity is what we normally call a neutrino ν_-^{M} and the right-handed helicity is what we normally call an anti-neutrino ν_+^{M}. Thus the Majorana neutrino is its own antiparticle and therefore it cannot have a magnetic dipole moment nor an electric dipole moment. It can however still interact with a photon as one can have an annular magnetic field. These properties have been thoroughly discussed in two monographs [36,37]. It is interesting that although there is a significant bias towards the Majorana scheme, the Dirac notation is still standard because it has more states and it is easier to transform into Majorana notation than vice versa. One could consider changing the notation to ν_e^{L} and ν_e^{R} instead of ν_e and $\bar{\nu}_e$. However, the phrase "right-handed neutrino" has already been reserved for the massive partner of the neutrino predicted by the See–Saw mechanism. We thus have to continue with the standard convention

of ν and $\bar{\nu}$, though emphasizing that $\bar{\nu}$ is probably NOT an antineutrino in the normal sense of antiparticles, i.e.,

$$\nu_{-}^{\mathrm{M}} \Rightarrow \nu_e \nu_\mu \nu_\tau \,, \tag{2.17}$$

$$\nu_{+}^{\mathrm{M}} \Rightarrow \bar{\nu}_e \bar{\nu}_\mu \bar{\nu}_\tau \,. \tag{2.18}$$

Thus, muon capture is written as

$$\mu^- + p \rightarrow n + \nu_\mu \tag{2.19}$$

and the decay of the muon is written as

$$\mu^+ \rightarrow e^+ + \nu_e + \bar{\nu}_\mu \,. \tag{2.20}$$

It is generally accepted that all direct tests for a massive neutrino have failed to observe an effect. Unfortunately, there have been many false alarms but we restrict ourselves to the recent results [16]

$$m_{\nu_e} < 15\,\mathrm{eV}/c^2 \text{ at } 95\% \text{ CL} \,, \tag{2.21}$$

$$m_{\nu_\mu} < 0.17\,\mathrm{MeV}/c^2 \text{ at } 90\% \text{ CL} \,, \tag{2.22}$$

$$m_{\nu_\tau} < 18\,\mathrm{MeV}/c^2 \text{ at } 95\% \text{ CL} \,. \tag{2.23}$$

The best limit for $\bar{\nu}_e$ is found from a careful analysis of the β^- spectrum from tritium decay. Several experiments are continuing; the Mainz group are now quoting $< 2.8\,\mathrm{eV}/c^2$ [38] and the Troitsk group claim $< 2.5\,\mathrm{eV}/c^2$ [39]. Most experiments used to find that $m_\nu^2 < 0$, and so the Particle Data Group were conservative in their analysis. This problem seems to have been cleared up, so the Particle Data Group will probably lower their limit. For the muon neutrino, the method is to measure the μ^+ recoil momentum in the decay, $\pi^+ \rightarrow \mu^+ + \nu_\mu$, at rest. The most recent analysis indicates that previous pion masses were probably in error [40] and obtains a slightly lower limit on the neutrino mass. Similarly a recent estimate of ν_τ lowers the limit a little [41].

Those limits are model independent. However, if one assumes that neutrinos are Majorana particles, a popular hypothesis, then neutrinoless double β decay becomes possible. There are many experiments continuing to extend the frontiers and 10 nuclides of 9 elements have been studied. Two older but excellent reviews are those of Avignone and Brodzinski [42] and of Moe and Vogel [43]. A more recent experimental review has been given by Morales [44] and recent theoretical studies have been reviewed by Civitarese and Suhonen [45] and by Barbero et al. [46]. At present the most sensitive test is for ^{76}Ge. Some ultrapure germanium detectors have been made from isotopically enriched material. Normally ^{76}Ge is only 7.8% of the natural element, but some material of 86% enrichment has been obtained by the Heidelberg–Moscow group [47]. They have five detectors with a total active mass of 11 kg. Those detectors are placed in the Gran Sasso laboratory to minimize the background from cosmic rays, and they are kept in an air tight enclosure to keep out radon. Taking extreme care to avoid radioactive material in the construction of the detectors, they have been able to lower the background rate

by several orders of magnitude from ordinary detectors at sea-level. A very important fact is that they have been able to detect double β decay with neutrinos, viz:

$$^{76}\mathrm{Ge} \rightarrow ^{76}\mathrm{Se} + \beta^- + \beta^- + \bar{\nu}_e + \bar{\nu}_e \,. \tag{2.24}$$

Their value for the half-life is $\tau_{1/2} = 1.77\ (13) \times 10^{21}$ yr which is critical for verifying the nuclear matrix elements. The double β decay without neutrinos is easier to detect experimentally as it would be observed as a single energy peak at the Q-value of the reaction, viz: 2.046 MeV, which is fortunately quite high in energy and above a lot of the background. The present limit on the decay of

$$^{76}\mathrm{Ge} \rightarrow ^{76}\mathrm{Se} + \beta^- + \beta^- \tag{2.25}$$

is

$$\tau_{1/2} > 5.7 \times 10^{25}\,\mathrm{yr} \text{ at } 90\%\ \mathrm{CL} \,. \tag{2.26}$$

This can then be translated into a limit for the mass of the Majorana neutrino of

$$m_\nu < 0.2\,\mathrm{eV}/c^2 \tag{2.27}$$

Again a negative result, but impressively lower than the tritium decay. Confirming data for ^{76}Ge are coming from the IGEX collaboration, which has 3 detectors, 2 kg each, in the Canfranc Tunnel in Spain, plus some smaller ones in Baksan. Their present limit is [48]

$$\tau_{1/2} > 0.8 \times 10^{25}\,\mathrm{yr} \text{ at } 90\%\ \mathrm{CL} \,. \tag{2.28}$$

There are also important limits set from cosmological constraints on the Big Bang and the Early Universe. The consensus is that

$$m_{\nu_i} \leqslant 30\,\mathrm{eV}/c^2 \,, \tag{2.29}$$

which is a severe constraint on ν_μ and ν_τ [49,50].

All this discussion on neutrino mass would be depressing, were it not for two or three cases in which there is circumstantial evidence for a finite value. One effect is the deficit of solar neutrinos observed at first by Davis in the Homestake mine, and confirmed now by three other experiments. Experiments are continuing and new ones are being prepared. This effect is so important to understand that there are textbooks [51,52] and frequent conferences devoted to this and related subjects. For our limits we refer to some recent discussions and reviews [53–57] and it is certain that this intense interest will continue for many years to come. All four observations agree that there are insufficient solar neutrinos detected at the Earth. The Sun produces a vast number of neutrinos of different energies from a variety of thermonuclear reactions. Each detector is sensitive to different parts of this energy spectrum and thus the ensemble of information is less sensitive to models of the Sun. More and more tests can now be applied to models of the interior of the Sun and especially with recent studies of solar oscillations it is more and more difficult to blame the neutrino deficit on a misunderstanding of the properties of the Sun [58,59].

The most widely held interpretation of the neutrino deficit is the MSW effect (Mikheyev, Smirnov, Wolfenstein). Normal matter on the Sun has electrons but no muons or tau leptons. As the electron neutrinos pass through matter they undergo continuous interactions with the

electrons, a sort of refractive index effect, but muon and τ neutrinos are unaffected. Now if neutrinos have mass, the electron neutrinos have an effective mass which is higher in the centre of the Sun and, as they emerge, this effective mass decreases and may cross that of another neutrino, say the muon neutrino. If there is a mixing between neutrino flavours, the electron neutrinos will transform into muon neutrinos, and thus not be observed on Earth by detectors which can detect only electron neutrinos. Two favoured solutions to the effect are

$$\Delta m^2 = 8 \times 10^{-6}\,\mathrm{eV}^2/c^4 \quad \text{with } \sin^2 2\theta = 7 \times 10^{-3}\,, \tag{2.30}$$

$$\Delta m^2 = 2 \times 10^{-5}\,\mathrm{eV}^2/c^4 \quad \text{with } \sin^2 2\theta = 0.7\,. \tag{2.31}$$

(Δm is the mass difference between the neutrino masses and θ is the mixing angles; all numbers are very approximate). The other major effect is the muon neutrino deficit from the atmosphere interactions of cosmic rays. Now well established from recent data from Superkamiokande [60], the favoured interpretation is $\Delta m^2 \sim 10^{-2}\,\mathrm{eV}^2/c^4$ probably between ν_μ and ν_τ. This may or may not be compatible with evidence from LSND of about 17 oscillation events [61]. The non-observation of $\bar{\nu}_e$ oscillations from the Palo Verde reactor gives a limit of $\Delta m^2 < 10^{-3}\,\mathrm{eV}^2/c^4$ [62]. This confirms that electron neutrinos are probably not involved in the effect observed with atmospheric neutrinos. We shall follow the minimalist framework of supersymmetric unification in *SO* (10), as advocated by Wilczek [63] at the recent conference Neutrino'98. In this approach the neutrino masses are Majorana, and they follow a hierarchical pattern, such as

$$m(\nu_e) \sim \mu\mathrm{eV}/c^2\,, \tag{2.32}$$

$$m(\nu_\mu) \sim \mathrm{meV}/c^2\,, \tag{2.33}$$

$$m(\nu_\tau) \sim 0.1\,\mathrm{eV}/c^2\,. \tag{2.34}$$

This leading scenario is far from the only possibility because there are difficulties fitting the mixing angles in this scheme, especially for the case of the small mixing angle solution for solar neutrinos [64]. Other possibilities are discussed in several detailed reviews [65–71]. Note that if there is strong mixing, it is better to refer to the neutrinos as ν_1, ν_2, and ν_3. However we shall retain the traditional notation.

From now on we shall assume the values of Eqs. (2.32)–(2.34) explicitly or implicitly in our discussions of muon capture. It is important to emphasize however that if the mass of the muon neutrino is not $10^{-3}\,\mathrm{eV}/c^2$ but 1 or even $100,000\,\mathrm{eV}/c^2$, close to the model independent limit, our discussion will not be materially affected. If it were, then such effects would be focussed on for mass searches. One of the best prospects would be the reaction $\mu^-\,{}^6\mathrm{Li} \to tt\nu_\mu$, but the rate is low, and an experiment is impossible at present [72].

2.2. Weak interactions

We shall briefly discuss the aspects of the weak interactions that we need to define the notation. Many reviews and textbooks are available such as Scheck [73,74], Commins and Bucksbaum [75], Greiner and Müller [76], and Holstein [77] as well as those mentioned previously [3–6].

The purely leptonic interaction in a decay such as

$$\mu^+ \to e^+ + \nu_e + \bar{\nu}_\mu \,, \tag{2.35}$$

has been studied in great detail both experimentally and theoretically. Recent confirmation also comes from the related decays of the τ, viz:

$$\tau^+ \to \mu^+ + \nu_\mu + \bar{\nu}_\tau \,, \tag{2.36}$$

$$\tau^+ \to e^+ + \nu_e + \bar{\nu}_\tau \,. \tag{2.37}$$

All three decays are excellent testing grounds for the operators involved in the weak interactions. We shall focus on the muon decay because it has been studied in greatest detail. A full review of this topic has recently been made by Engfer and Walter [78]. The most general amplitude for the muon decay is given by

$$M = \frac{G_F}{\sqrt{2}} \sum_i \overline{u}_e (A_i + A_i' \gamma_5) O_i v_1 u_2 O_i \overline{u}_\mu \,, \tag{2.38}$$

where u_2 and v_1 are ν_μ and $\bar{\nu}_e$ spinors and u_μ and u_e are the muon and electron spinors; the O_i are the usual Dirac matrices and the index i runs through S, V, T, A, and P. An equivalent form is the charge-retention ordering which is normally preferred, viz:

$$M = \frac{G_F}{\sqrt{2}} \sum_i \overline{u}_e O_i u_\mu \overline{u}_2 O_i (C_i + C_i' \gamma_5) v_1 \,. \tag{2.39}$$

Now the decay of the muon can determine which of these couplings is found in nature. The energy spectrum of the muon (neglecting polarization effects) is given by

$$N \,\mathrm{d}x \,\mathrm{d}\Omega \sim \left[6(1-x) + \frac{16}{3}\rho \left(x - \frac{3}{4} \right) + 12\eta \left(\frac{m_e}{m_\mu} \right) \left(\frac{1-x}{x} \right) \right] x^2 \,\mathrm{d}x \,, \tag{2.40}$$

where $x = p_e / p_{\max}$ with $p_{\max} = 52.828\,\mathrm{MeV}/c$ and ρ and η are two of the Michel parameters. Now

$$\rho = (3g_{\mathrm{A}}^2 + 3g_{\mathrm{V}}^2 + 6g_{\mathrm{T}}^2)/D \tag{2.41}$$

and

$$\eta = (g_{\mathrm{S}}^2 - g_{\mathrm{P}}^2 + 2g_{\mathrm{A}}^2 - 2g_{\mathrm{V}}^2)/D \,, \tag{2.42}$$

where

$$D = g_{\mathrm{S}}^2 + g_{\mathrm{P}}^2 + 4g_{\mathrm{V}}^2 + 6g_{\mathrm{T}}^2 + 4g_{\mathrm{A}}^2 \tag{2.43}$$

and

$$g_i^2 = |C_i|^2 + |C_i'|^2 \,. \tag{2.44}$$

Experimentally,

$$\rho = 0.7518\ (26)$$

and

$$\eta = -0.007\ (13) \tag{2.45}$$

Thus, the evidence is that $g_A^2 = g_V^2$ and the other couplings are zero. From the polarization observables we obtain the relative sign

$$g_V = -g_A \tag{2.46}$$

and also that $C_i = -C_i'$. There has even been a measurement of the ν_e energy spectrum [79], which further limits non-standard couplings.

Thus, finally we obtain $C_V = -C_A$ often abbreviated to calling it the V–A interaction. This interaction is universal for the leptons and from the τ decays it is known that [80]

$$\rho_\tau = 0.735\ (13)\ (8) \tag{2.47}$$

and

$$\eta_\tau = -0.015\ (61)\ (62)\ ,$$

where the data are obtained by combining the μ and e decays.

The total rate, including now the radiative corrections and the effects of the finite mass of the electron, is given by

$$\lambda_\mu = \frac{1}{\tau_\mu}\frac{G_F^2 m_\mu^5 c^4}{192\pi^3\hbar^7}\left[1 - \frac{\alpha}{2\pi}\left(\pi^2 - \frac{25}{4}\right)\right] f\left(\frac{m_e^2}{m_\mu^2}\right)\ , \tag{2.48}$$

where

$$f\left(\frac{m_e^2}{m_\mu^2}\right) = f(x) = 1 - 8x - 8x^3 - x^4 + 12x^2\ln\left(\frac{1}{x}\right)\ . \tag{2.49}$$

The radiative correction gives a coefficient of 0.995796 and the finite mass correction is 0.999813 which gives the total correction of 0.995610 as shown in Eq. (2.8). Thus, muon decay defines all the couplings and the total coupling constant for the leptonic weak interactions. The only other useful fact is that the coupling to the muon is the same as the coupling to the electron. This is best illustrated in the decay of the pion

$$\pi^+ \to \mu^+ + \nu_\mu$$

and

$$\pi^+ \to e^+ + \nu_e\ , \tag{2.50}$$

where the branching ratio is given theoretically by

$$\frac{\pi \to e\nu}{\pi \to \mu\nu} = \frac{g_{\pi e\nu}^2}{g_{\pi\mu\nu}^2}\left(\frac{m_e}{m_\mu}\right)^2\left(\frac{m_\pi^2 - m_e^2}{m_\pi^2 - m_\mu^2}\right)^2\left(1 - \frac{16.9\alpha}{\pi}\right) = 1.2345\ (10) \times 10^{-4}\ . \tag{2.51}$$

The suppression of the electron decay is because its helicity is contrary to what the weak interactions prefer. Experimentally there are two values for the $e\nu$ branching ratio [81,82]:

$$\begin{aligned} &\text{TRIUMF [81]}\ 1.2265\ (34)\ (44) \times 10^{-4}\ , \\ &\text{PSI [82]}\qquad 1.2346\ (35)\ (36) \times 10^{-4}\ , \end{aligned} \tag{2.52}$$

which give

$$\frac{g_{\pi\mu\nu}}{g_{\pi e\nu}} = 1.0016\ (16)\ , \tag{2.53}$$

often termed muon electron universality or more recently lepton universality.

Confirming evidence comes from the τ decays which are slightly less precise, but an important verification. There are two useful checks; one is the absolute rate of either $\tau \to e\nu\nu$ or $\tau \to \mu\nu\nu$ compared to $\mu \to e\nu\nu$. The two branching ratios are [83–86]

$$BR(\tau \to e\nu\nu)\ 17.81\ (6)\%\ , \qquad BR(\tau \to \mu\nu\nu)\ 17.36\ (6)\%\ . \tag{2.54}$$

Taking into account the mass of the τ ($1777.05^{+0.29}_{-0.26}\,\mathrm{MeV}/c^2$) from [16] and its overall lifetime ($290.5\,(10)\,\mathrm{fs}$) from [87], the relative rates for e$\nu\nu$ decay give

$$\frac{g_\tau}{g_\mu} = 1.0013\ (25)\ . \tag{2.55}$$

Another technique is a direct comparison of the τ decays of $\mu\nu\nu$ to e$\nu\nu$ which have a relative phase-space factor of 0.9726; this test gives

$$\frac{g_\mu}{g_e} = 1.0014\ (24)\ . \tag{2.56}$$

More detailed tests come from measuring the Michel parameters for the leptonic decays of the τ. Several recent experiments have confirmed the V–A structure of the weak interactions in such decays [80,88–90].

An earlier review by Weinstein and Stroynowski [91] discussed the properties of the τ in general and came to a similar conclusion. A final piece of evidence comes from the decay of Z. The Z and the W are the carriers of the weak interaction and have been studied in great detail at LEP. The lepton–antilepton decays of the Z have the following branching ratios:

$$BR(e^+e^-) = 3.366\ (8)\%, \quad BR(\mu^+\mu^-) = 3.367\ (13\%),$$
$$BR(\tau^+\tau^-) = 3.360\ (15)\%\ . \tag{2.57}$$

Of course this is at a very high energy (M_z=91.186 (2) GeV/c^2), but is an excellent confirmation.

Thus all such evidence strongly establishes

- the V–A character of the weak interaction for leptons,
- the overall coupling constant G_F,
- electron–muon–tau universality.

Now we come to hadrons where several complications enter the picture. For β decay it is known that the coupling to the quarks is slightly reduced because the quarks are mixed, allowing coupling across the generations (otherwise the kaon would not decay). By convention the u, c, and t quarks of charge $2e/3$ are taken to be unmixed. Thus, the mixing is expressed as a 3×3 unitary matrix V which operates on the d, s, and b quarks of charge $-e/3$. This matrix

is called the Cabibbo–Kobayashi–Maskawa matrix and has been the basis for hadronic weak interactions for 25 years. Thus

$$\begin{pmatrix} d' \\ s' \\ b' \end{pmatrix} = \begin{pmatrix} V_{ud} & V_{us} & V_{ub} \\ V_{cd} & V_{cs} & V_{cb} \\ V_{td} & V_{ts} & V_{tb} \end{pmatrix} \begin{pmatrix} d \\ s \\ b \end{pmatrix} . \tag{2.58}$$

The present best values for these are approximately [16]

$$\begin{pmatrix} 0.975 & 0.22 & 0.003 \\ -0.22 & 0.974 & 0.039 \\ 0.01 & -0.04 & 0.9992 \end{pmatrix} . \tag{2.59}$$

The only one that concerns us is the matrix element V_{ud}, but one of the most powerful ways of determining its value is simply by imposing the unitarity of this matrix, so a comprehensive analysis is best. Of course, this assumes that there are only three generations which seems justified at present. At LEP they find from the width of the Z that the number of light neutrinos is 2.992 (11) [16].

This unitarity requirement is that:

$$|V_{ud}|^2 + |V_{us}|^2 + |V_{ub}|^2 = 1 , \tag{2.60}$$

which gives $V_{ud} = 0.9755$ from the above values of V_{us} and V_{ub}.

There is a direct way of determining V_{ud} as well, which is to use the super-allowed β of the light elements, such as ^{10}C, ^{14}O, ^{26}Al^m, ^{34}Cl, ^{42}Sc, ^{50}Mn, and ^{54}Co. Because of the simple matrix element, due to the coupling being vector only, the ft value can be calculated to be

$$(ft)^* = \frac{K}{(2|V_{ud}|^2 G_\mu^{*2}} , \tag{2.61}$$

where K is an accurately known constant and G_μ^* is the Fermi coupling constant which is known from muon decay assuming that g_V is the same for β decay (CVC). Now

$$(ft)^* = ft(1 - \delta_c)(1 + \triangle + \delta_r) , \tag{2.62}$$

where f is the phase-space factor, t the half-life of the transition, and δ_c, $\triangle$, δ_r are small Coulomb and radiative corrections.

There have been many discussions of these correction factors with analyses of all the β-decay data. Two recent assessments, one by Wilkinson [92] ($V_{ud} = 0.9754$ (6)) and one by Towner and Hardy [93] ($V_{ud} = 0.9740$ (5)) come to slightly different conclusions. The latest review by Abele [94] gives the following values from the three methods of determining V_{ud}:

$$\begin{aligned} &\text{Nuclei} : V_{ud} = 0.9740\ (10) , \\ &\text{Neutrons} : V_{ud} = 0.9738\ (23) , \\ &\text{PERKEO II} : V_{ud} = 0.9713\ (14) , \\ &\text{CKM matrix} : V_{ud} = 0.9756\ (4) \end{aligned} \tag{2.63}$$

(PERKEO II is a neutron measurement somewhat different from others.)

This is quite an acceptable agreement for our purposes.

For muon capture on a proton the weak interaction becomes much more complicated than for the purely leptonic case. We shall focus only on muon capture and thus avoid the complications of the strangeness changing interaction. Some of the best constraints on muon capture come from β decay, so we shall discuss that aspect where necessary. In the literature there are many notations, but the most common in the muon capture community is that used by Mukhopadhyay in his reviews [13–15], so we shall follow his definitions.

The muon capture Hamiltonian is thus given by

$$H = \frac{GV_{ud}}{\sqrt{2}}(V_\lambda^\dagger + A_\lambda^\dagger)L_\lambda + h.c.\,, \tag{2.64}$$

where the lepton current is simply

$$L_\lambda = \bar{\psi}_\nu \gamma_\lambda (1+\gamma_5)\psi_\mu\,, \tag{2.65}$$

but the vector and axial vector hadron currents have many extra terms

$$V_\lambda^\dagger = \bar{\psi}_n \left[g_{\rm V}\gamma_\lambda - \left(\frac{g_{\rm M}}{2M}\right)\sigma_{\lambda\rho}q_\rho - {\rm i}\left(\frac{g_{\rm S}}{m_\mu}\right) q_\lambda \right] \psi_p \tag{2.66}$$

and

$$A_\lambda^\dagger = \bar{\psi}_n \left[g_{\rm A}\gamma_\lambda\gamma_5 - \left(\frac{g_{\rm T}}{2M}\right)\sigma_{\lambda\rho}q_\rho\gamma_5 - {\rm i}\left(\frac{g_{\rm P}}{m_\mu}\right) q_\lambda\gamma_5 \right] \psi_p\,. \tag{2.67}$$

Now time reversal invariance requires that the form factors

$$g_{\rm V}\ g_{\rm M}\ g_{\rm S}\ g_{\rm A}\ g_{\rm T} \quad \text{and} \quad g_{\rm P}\,.$$

be real. The subscripts represent their characteristics viz: vector, magnetic, scalar, axial-vector, tensor and pseudoscalar.

The conserved vector current hypothesis gives $g_{\rm S} = 0$. In addition the concept of isospin introduces other constraints. This is introduced as G-parity where the G transformation is defined as

$$G = C\exp({\rm i}\pi T_2) \tag{2.68}$$

where C is the normal charge conjugation operator and the exponential term induces a rotation of 180° about the second isospin axis, i.e., $p \to n$ and $n \to -p$. Thus,

$$G\begin{pmatrix} p \\ n \end{pmatrix} = \begin{pmatrix} \bar{n} \\ -\bar{p} \end{pmatrix} \quad \text{and} \quad G\begin{pmatrix} \bar{n} \\ -\bar{p} \end{pmatrix} = -\begin{pmatrix} p \\ n \end{pmatrix}\,. \tag{2.69}$$

Then G-invariance of the four-fermion Hamiltonian implies that

$$g_{\rm S} = 0 \quad \text{and} \quad g_{\rm T} = 0 \tag{2.70}$$

or in the language of Weinberg [95], the scalar and tensor terms are second class currents. There have been many searches for experimental evidence for non-zero values of these terms, and these have been reviewed by Grenacs [96], and more recently by Govaerts [97,98]. A recent determination by Adelberger et al. [99], from the β^+ decay of ^{32}Ar gave $g_{\rm S} < 0.06$, which is an impressive result, but remember that the theoretical argument for zero is quite strong in itself. There is no convincing evidence for non-zero values but the limits are not very tight. For $g_{\rm T}$

one might expect a small value due to isospin breaking and an estimate is $|g_T/g_M| = 0.0052$ (18) [100]. Such a value is negligible with respect to other uncertainties in muon capture.

For g_V the Conserved Vector Current hypothesis implies that this is the same as for leptons, e.g., $g_V = 1$. Checks on this are the direct measure of V_{ud} from β decay, coupled with the unitarity requirement of the Cabibbo–Kobayashi–Maskawa matrix. There is also the rate for pion β decay $\pi^+ \to \pi^0 + e^+ + \nu_e$ which is an excellent test for CVC but unfortunately it has a very small branching ratio, so it is difficult to measure. The best value comes from the experiment of McFarlane et al., at LAMPF which measured the branching ratio to be $1.026\ (39) \times 10^{-8}$ [101] to be compared with the predicted value of $1.048\ (5) \times 10^{-8}$. An alternative way of expressing this is that for hadrons $V_{ud}^2 = 0.928\ (35)$ to be compared with the value discussed above from β decay of 0.950 (3). This is more than sufficient agreement for our purposes. Note that there is a slight momentum dependence of this form factor [13,102], so that for muon capture $g_V\ (q^2 = -0.88 m_\mu^2) = 0.9755\ (5)$.

The form factor g_M is called the weak interaction magnetism term, and is predicted by CVC. It is called weak magnetism because it is related to the difference between the anomalous magnetic moments of the neutron and proton. The best test comes from comparisons of Gamow–Teller (Axial Vector) transitions in β decay, such as ^{12}B and ^{12}N. In these $1^+T = 0$ to $0^+T = 0$ decays, there is a slight energy-dependent asymmetry which is calculated to be 0.93% MeV, and experimentally is 0.99 (10)% MeV. There is some difficulty with these experiments, but at the 10–20% level this term has been verified. A detailed discussion has been given by Holstein [77]. Theoretically,

$$g_M = \mu_p^a - \mu_n^a = \mu_p - \mu_n - 1 = 3.70589 \tag{2.71}$$

(where μ_p^a is the anomalous magnetic moment of the proton, etc.) The impact of this term is normally small, so the theoretical value is assumed by most authors. Note that there is a slight momentum dependence of this form factor too [13], so for muon capture:

$$g_M(q^2 = -0.88 m_\mu^2) = 0.9666\ (7)(\mu_p - \mu_n - 1) = 3.5821\ (25)\ . \tag{2.72}$$

For the axial coupling, g_A the difference from leptons is quite marked. The best test comes from neutron β decay and there are two critical observations. One is the mean-life which has been very hard to measure dependably because of the difficulty of holding neutrons for the requisite time. The review of particle properties [16] gives

$$\tau = 886.7\ (19)\,\mathrm{s} \tag{2.73}$$

i.e., the half-life is

$$\tau_{1/2} = 614.8\ (14)\,\mathrm{s} = 10.25\ (2)\,\mathrm{min}\ . \tag{2.74}$$

This value has changed somewhat with time, for example, 20 years ago, the recommended value for the mean life was [103]

$$\tau = 918\ (14)\,\mathrm{s}\ , \tag{2.75}$$

so there is a need to remain slightly sceptical about this parameter.

The neutron ft value is given by

$$ft(1+\delta'_{\mathrm{R}}) = \frac{K}{G_{\mathrm{V}}^2|V_{ud}|^2(1+3\lambda^2)}\ , \tag{2.76}$$

where δ'_{R} is an effective, radiative correction and $\lambda = g_{\mathrm{A}}/g_{\mathrm{V}}$.

The other observable is the asymmetry of the neutron β decay for polarized neutrons. This asymmetry is calculated to be

$$A = \frac{-2\lambda(\lambda+1)}{1+3\lambda^2}\ . \tag{2.77}$$

Now λ would be -1 for leptonic interactions, so the asymmetry would be zero. However, experimentally this asymmetry is clearly non-zero and the latest review [16] gives

$$A = -0.1162\ (13)\ . \tag{2.78}$$

Doing a combined analysis of both the total decay rate and the asymmetry parameter one obtains

$$\lambda = \frac{g_{\mathrm{A}}}{g_{\mathrm{V}}} = -1.2670\ (35)\ . \tag{2.79}$$

This is far from the leptonic value of -1 and a major difference for the hadronic sector. These results have been confirmed recently by Liaud et al. [104] but the PERKEO II spectrometer at ILL [105] is obtaining $\mathrm{A} = -0.1189\ (8)$ and $\lambda = -1.2740\ (21)$ so caution should be exercised.

We now appeal to lepton universality and hypothesize that a muon (or tau) interaction with a proton will be dictated by the same couplings as long as the effects of the different masses are taken into account in phase-space and momentum dependence. Direct tests of the coupling for muons have given a result of $g_{\mathrm{A}}^{\mu}/g_{\mathrm{A}}^{e} = 1.00\ (8)$ [96].

The momentum dependence of g_{A} is given by [13]

$$\frac{g_{\mathrm{A}}(q^2)}{g_{\mathrm{A}}(0)} = \left(1 - \frac{q^2}{m_{\mathrm{A}}^2}\right)^{-2} = 0.976\ (5)\ ,$$

since

$$m_{\mathrm{A}} = 0.89^{+0.09}_{-0.08}\,\mathrm{GeV}/c^2 \tag{2.80}$$

thus

$$g_{\mathrm{A}}(-0.88m_{\mu}^2) = -1.237\ (7)\ .$$

A more recent evaluation by Bernard et al. [108], and Fearing et al. [109], gives

$$\frac{g_{\mathrm{A}}(q^2)}{g_{\mathrm{A}}(0)} = \left(1 + \frac{r_{\mathrm{A}}^2}{6}q^2\right) = 0.9823\ (17)$$

using $r_{\mathrm{A}} = 0.65\ (3)\,\mathrm{fm}$ and $q^2 = -0.252\,\mathrm{fm}^{-2}$ thus $g_{\mathrm{A}}(-0.88m_{\mu}^2) = -1.245\ (3)$.

In muon capture on a proton, there is a dramatic consequence of this general value of g_{A}, viz: a very large spin sensitivity. Now the singlet and triplet capture rates are approximately given by [13]

$$\Lambda_{\mathrm{s}} = 30(1-3\lambda)^2 \quad \text{and} \quad \Lambda_{\mathrm{t}} = 30(1+\lambda)^2\ . \tag{2.81}$$

Using $\lambda = -1.26$, we obtain $\Lambda_{\mathrm{s}} \sim 685\,\mathrm{s}^{-1}$ and $\Lambda_{\mathrm{t}} \sim 2\,\mathrm{s}^{-1}$. Corrections to this first order relation change these to $\Lambda_{\mathrm{s}} \sim 660\,\mathrm{s}^{-1}$ and $\Lambda_{\mathrm{t}} \sim 12\,\mathrm{s}^{-1}$. Observation of this spin sensitivity in hydrogen

as well as in the hyperfine effect is an important confirmation of the overall structure of the theory.

Unfortunately there is one coupling which has a very strong dependence on the mass of the lepton, it is the induced pseudoscalar coupling g_P. It is effectively driven by inverse pion decay. Normally a pion decays via

$$\pi \to \mu + \nu_\mu \,, \tag{2.82}$$

so re-arranging there is a virtual effect

$$\mu^- \to \pi^- + \nu_\mu \,, \tag{2.83}$$

which is enhanced for muons because the mass of the muon and pion are so similar. As the pion can interact with hadrons via the strong interaction, this induced coupling must be taken into account on many occasions in muon capture, but cannot be estimated from β decay measurements.

We first need to note that the pion decay rate, Γ_π, to a muon or electron is given by

$$\Gamma_\pi = \frac{F_\pi^2}{4\pi} m_e^2 m_\pi \left(1 - \frac{m_e^2}{m_\pi^2}\right)^2 (1 + O(\alpha)) \,, \tag{2.84}$$

where

$$F_\pi = \frac{G_F V_{ud} f_\pi}{\sqrt{2}}$$

and f_π is the charged pion decay constant and is [16]

$$f_\pi = 130.7\ (0.1)\ (0.36)\,\text{MeV} \,. \tag{2.85}$$

Note. In many papers it is defined without the $\sqrt{2}$, so one frequently sees

$$f_\pi = 92.42\ (0.07)\ (0.25)\,\text{MeV} \,. \tag{2.86}$$

Now this weak decay can be related to nucleon coupling via the Goldberg–Treiman relation

$$f_\pi = \frac{\sqrt{2} M g_A}{g_\pi} \,, \tag{2.87}$$

where M is the mass of the nucleon and g_π is the strong pseudoscalar pion nucleon coupling constant, where

$$\frac{g_\pi^2}{4\pi} = 13.75\ (15) \quad \text{or} \quad g_\pi = 13.14\ (8) \,, \tag{2.88}$$

see Arndt et al. [106], though there is significant debate about this value and sometimes values as high as 14.4 (2) for $g_\pi^2/4\pi$ are still advocated [107].

Some authors prefer to use the effective pseudovector coupling constant where

$$f_\pi^2 = \frac{g_\pi^2}{4\pi} \left(\frac{m_\pi}{2M}\right)^2 = 0.076\ (1) \,. \tag{2.89}$$

(An unfortunate duplication of the notation f_π; furthermore, factors of 4π come and go according to the whims of various authors.)

Now having defined the constants we can return to the weak interaction coupling constant g_P, the induced pseudoscalar one. Partially conserved axial current (PCAC) predicts that

$$g_P = -\frac{2Mg_A m_l}{q^2 - m_\pi^2} \tag{2.90}$$

or using the Goldberger–Treiman relation

$$g_P = +\frac{\sqrt{2} f_\pi g_\pi m_l}{q^2 - m_\pi^2} \ , \tag{2.91}$$

where m_l is the mass of the lepton; if we are discussing β decay $m_l = m_e$ and

$$g_P \simeq g_A/20 \tag{2.92}$$

and this is so small that no experiment has reached sufficient sensitivity to test this value. However for muon capture $m_l = m_\mu$ which makes the effect 200 times larger. It is conventional to calculate the term at the momentum transfer of the free reaction $\mu^- p \to n\nu$ in which the neutrino takes away 99 MeV, so $q^2 = -0.88 m_\mu^2$. Thus, substituting this into the above relation

$$g_P(q^2 = -0.88 m_\mu^2) = 6.77 g_A = -8.53 \ . \tag{2.93}$$

Taking corrections into account, using Chiral Perturbation Theory in the context of QCD there have been two recent evaluations [108,109]:

$$\text{Bernard et al. [108] } g_P(q^2) = -8.44 \pm 0.23 \ ,$$

$$\text{Fearing et al. [109] } g_P(q^2) = -8.21 \pm 0.09 \ , \tag{2.94}$$

where the error comes mainly from the uncertainty in g_π.

We shall see that there is still much experimental uncertainty about the value of g_P, but it should be kept in mind that kinematic factors often suppress its effects, so it is hard to test the relations discussed above.

An important extension of these coupling constants is the Fujii–Primakoff effective Hamiltonian. This is widely used in the literature and is very useful for illustrating a point. In coordinate space it is

$$H_{\text{eff}} = \frac{\tau^+}{\sqrt{2}} \left(\frac{1 - \sigma \cdot v}{\sqrt{2}} \right) \tau_h^{-1} \left[G_V 1 \cdot 1_h + G_A \sigma \cdot \sigma_h - G_P \sigma \cdot v \sigma_h \cdot v + O\left(\frac{p_n}{M} \right) \right] \delta(r - r_h) \ , \tag{2.95}$$

where v is the unit vector along the direction of the neutrino momentum, τ_h^- converts a proton into a neutron, the subscripted operators are 2×2 matrices acting on the non-relativistic nucleon spinors and the unsubscripted operators are 4×4 matrices acting on the relativistic lepton spinors. The Fujii–Primakoff effective form factors are

$$G_V = g_V \left(1 + \frac{q}{2M} \right) \simeq 1.03 \ , \tag{2.96}$$

$$G_A = -\left[g_A + (g_V + g_M) \frac{q}{2M} \right] \simeq -1.47 \ , \tag{2.97}$$

$$G_P = -\left[g_P - g_A + g_V + g_M \right] \frac{q}{2M} \simeq -0.62 \ . \tag{2.98}$$

The terms of order (p_n/M) which are often called the recoil terms are neglected in most demonstrations of typical cases but are included in accurate calculations even though they are generally small and cannot be reliably calculated in nuclei. The point to note about these effective operators is that g_P is multiplied by $q/2M$ or about $1/20$, so that although g_P appears larger than g_A, its effects are normally smaller (slightly).

The discussion so far has been for muon capture on the free proton. Now when the proton is embedded in a nucleus, further complications cloud the picture. It is fairly well accepted that g_A and g_P become modified in the nuclear environment, though there is still some controversy about the extent of this modification, and the best way to describe it. From β decay there is good evidence that the time component (or charge coupling) g_A^C is enhanced by up to 100% in heavy nuclei [110,111]. This is due to two-body exchange current mechanisms, mainly the long-range pion exchange, but there are also short-range exchange currents [112,113]. The space-component (or axial current coupling) g_A^{GT} is however quenched by 30%. This is mainly due to configuration mixing of the nucleon-wave function, which is a failure of the nuclear model and could be improved soon. However, about a third of the effect comes from meson exchange contributions [114]. Again let us emphasize that this information is coming from β-decay and has to be transferred to muon capture.

Now modifications of the pseudoscalar coupling constant are more complex, and also more difficult to substantiate. The effect is too small in β decay as we have already indicated. In muon capture there is considerable uncertainty anyway, so it is difficult to obtain the evidence. Kirchbach and Riska [115] have proposed that the coupling constant be sub-divided into four components, the charge and axial–current coupling, similar to g_A; these they denote as $g_{P,C}$ and g_P respectively, and then they further sub-divide between the parts associated with the $\sigma \cdot q$ operator ($g^{(1)}$) and those associated with the $\sigma \cdot v$ operator ($g^{(2)}$), thus finally giving four distinct components. They show that for ^{40}Ca these all behave differently, viz:

$g_P^{(1)}$ is strongly quenched (0.3),

$g_P^{(2)}$ is weakly quenched (0.73),

$g_{P,C}^{(1)}$ is fairly quenched (0.5),

$g_{P,C}^{(2)}$ is enhanced (1.2).

The only case that they calculate in detail is muon capture in ^{16}O and they find only a 10% effect. This is insufficient as there is already a large discrepancy between theory and experiment. The other general area is radiative muon capture which we shall address later on; the difficulty there is that various calculations differ significantly, so it is not evident which is sufficiently reliable. The overall conclusion is that it is probable that g_A and g_P are modified in nuclei along the lines suggested by Riska and his colleagues. However, we need more reliable evidence than is now available and we shall discuss the possible observations in some detail. It will also be essential to have reliable nuclear wave functions, but that seems quite probable in the near future, at least up to ^{40}Ca, or so.

3. Muonic atom

3.1. Atomic capture

Several reviews have been published on the general properties of muonic atoms, strangely enough most appeared in 1969, viz: Burhop [116]: Devons and Duerdoth [117]: and Wu and Wilets [118]. These are still excellent introductions to the subject. In 1977 another review appeared by Hüfner, Scheck and Wu [119].

Most capture experiments are wisely performed with pure elemental or isotopic targets. However sometimes it is more convenient to use a target which is a material with two or more elements. Studies with fluorine and chlorine are obvious examples. Similarly, there are sometimes impurities in a target and it is useful to be able to estimate the number of muon captures in the other elements. It is critical to realise that it is not easy to estimate the relative number of captures in mixed targets, and the only sure way is to rely on experimental measurements.

When a negative muon stops in a material, it quickly becomes attached to an atom, and the energy released is transferred to Auger electrons, which are simply electrons emitted from the atom. The expression is taken over from radio-active decays in which this effect also occurs. For example in the decay of ^{125}I, on average 21 electrons are emitted with energies up to several kilovolts [120,116]. It is harder to study the process of muon capture, but it must be similar. The details will depend on whether the material is a solid or gas, insulator or metal, but the key feature is the initial choice, because once it is captured, a muon is unlikely to transfer to a neighbouring atom. The first estimate of this effect was by Fermi and Teller [121] who suggested that the probability of being captured was proportional to the total number of electrons in an atom, i.e., to Z. We shall see that this estimate, though giving a rough idea, can be out by a factor of two or more.

Many experiments have been performed to study these capture ratios in various compounds. Oxides have been well studied and fluorides and chlorides to a lesser extent, but few other compounds have been measured. Thus any generalizations must be viewed cautiously because of the very limited data base on which they rest.

There are two principle techniques which have been used to measure the atomic capture ratio. The most common has been to detect the X-rays to identify the element in which the muon is captured, especially the $2p$–$1s$ X-ray. This occurs almost 80% of the time and apart from a few special cases, this is a reliable method, although the energy of the oxygen muonic X-rays is only 134 keV, so care must be taken in estimating self-absorption in the target. The most extensive series of experiments was carried out at SIN (now PSI) by von Egidy et al. [122]. An alternative method was used early on, and taken up again at TRIUMF [123]. It uses the fact that muons when they capture have very different lifetimes and this clearly distinguishes the element on which the muon was captured. The electron from the decay can be used, but then it is necessary to make a large correction for the number of muons which are captured and do not give an electron. Considering the difficulties of both types of measurement, the agreement is quite satisfactory, at the level of 10% or so, in most cases, but some inconsistencies at the level of a factor of 2 still remain.

The results are normally presented as an atomic capture probability in which it is assumed that if there are twice as many atoms of one element, this will double the number of muons

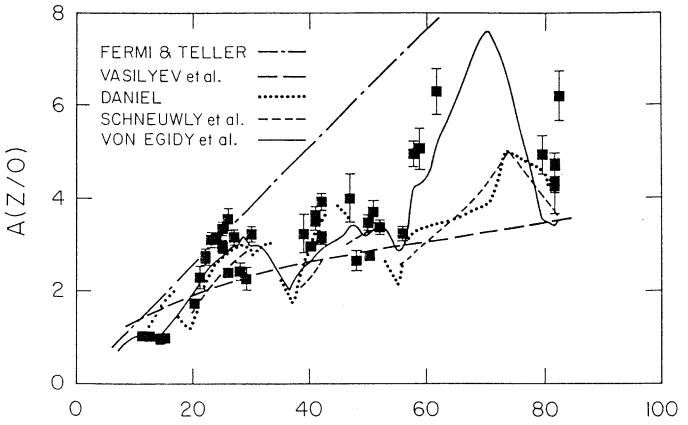

Fig. 3.1. Comparison of experimental and theoretical atomic capture ratios in oxides. The data are those of Stanislaus et al. [123]. The Fermi–Teller Z law is clearly inadequate [121] as is the monotonic form of Vasilyev [124]. Atomic structure is included in the calculations by Schneuwly et al. [125], Daniel [126], and by von Egidy et al. [127], the theory with the best fit.

being captured on that nucleus. Thus, in an oxide Z_mO_n the atomic capture probability A is defined as

$$A\left(\frac{Z}{O}\right) = \frac{nN_\mu(Z)}{mN_\mu(O)}\,, \tag{3.1}$$

where $N_\mu(Z)$ is the proportion of muons being captured on the metal. The results of Stanislaus et al. [123], are compared with various theories in Fig. 3.1. It is immediately clear that there are effects of electronic shells and that a monotonic function of Z as proposed by Fermi and Teller [121] or by Vasilyev et al. [124], is totally unsatisfactory. Effects of the atomic structure were introduced by Schneuwly et al. [125], and Daniel [126], and then refined by von Egidy et al. [127]. In their approach they assume that the probability for the muon to be captured by an atom is proportional to the number of loosely bound electrons. They use a weighting function

$$\sigma = \left(1 - \frac{E_B}{E_O}\right)^{1/2}\,, \tag{3.2}$$

where E_B is the binding energy of the electrons and E_O is a cut off which was fitted and found to be 80 eV. No account was taken of the valence electrons, i.e., the electronic structure of the neutral atom was used. Clearly, their approach greatly improves the fit and give a much better agreement with the fluctuations that are observed experimentally. A related empirical approach was proposed by Stanislaus et al., and it gives a slightly better fit, but it is less satisfying from the point of view of giving an understanding of the physics of the capture process. It was noticed by Stanislaus et al., that the capture ratio was proportional to the density of the material [128]. They then developed a relationship which works quite well for oxides, chlorides

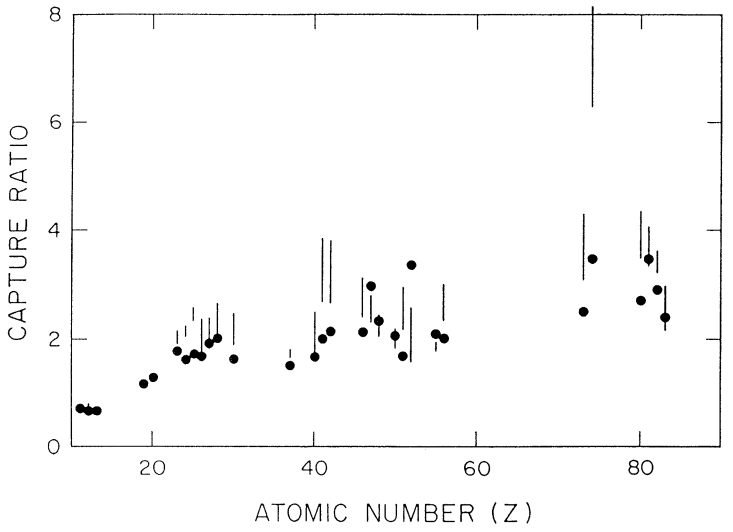

Fig. 3.2. Comparison of experimental (lines) and theoretical (dots) atomic capture ratios in chlorides. The experimental values are a compendium of world data, and the theory is that of Stanislaus et al. [128], see text.

and fluorides. It is

$$A\left(\frac{Z_1}{Z_2}\right) = 0.6\rho(1+\alpha\rho)\left(\frac{Z_2}{Z_1}\right)^{1/8}(1+5.53V^{5.45}10^{-5})\,, \tag{3.3}$$

where ρ is the ordinary density (in g cm^{-3}), V the valency of the metal and α is a parameter which is zero for $Z_1 \geqslant 18$ is -0.164 for oxides with metal $Z_1 < 18$ or -0.222 for chlorides with metal $Z_1 < 18$.

These values of α as well as the coefficients of the valency were all obtained by a minimization of the chi-squared and there is no physics justification. However, the formula can easily be applied to another situation though the reader should be warned again that it was only tested on oxides, fluorides and chlorides and even then the reduced chi-squared was 8.4. Note that even the "perfect" theory would have a poor chi-squared because of the inconsistencies amongst the data. The world data for chlorides is compared to this formula in Fig. 3.2.

Another semi-empirical approach was taken by von Egidy and Hartmann [129]. They simply assessed the capture probability for an element, normalized to 1 for oxygen. In this way they can estimate the capture probability in more complex molecules and they obtain quite good agreement for nitrates and sulphates. This is the easiest approach to apply to unmeasured materials, especially for those with three or more elements.

An interesting test of the initial assumption is now possible. Is the number of muons captured on the metal really just proportional to the number of atoms, and not affected by the valency. In Table 3.1, the experimental data are compared with the empirical formula of Stanislaus et al. [128], and to the theory of Schneuwly et al., who included a small correction for the valency electrons. This table exhibits the poor quality of the data and our uncertain understanding of even this most basic effect. We shall see that for pions, however, there is clear evidence that one should take into account the valency.

Table 3.1
Relative atomic capture ratios of muons for the oxides of the same element, comparing the average of the world data with the theory of Schneuwly et al. [125], and the empirical formula of Stanislaus et al. [128]

Z	Oxides	Experimental	Schneuwly et al.	Stanislaus et al.
11	Na_2O_2/Na_2O	0.79 ± 0.07	1.00	1.06
14	SiO_2/SiO	0.88 ± 0.03	0.95	1.19
22	TiO_2/TiO	0.88 ± 0.05	1.01	0.95
23	V_2O_4/V_2O_3	1.16 ± 0.12	1.00	0.96
	V_2O_5/V_2O_3	1.32 ± 0.11	1.01	0.92
24	CrO_3/Cr_2O_3	1.27 ± 0.05	1.02	1.00
25	MnO_2/MnO	1.04 ± 0.06	1.01	1.02
27	Co_3O_4/CoO	1.08 ± 0.10	1.01	0.96
	Co_2O_3/CoO	1.20 ± 0.14	1.01	0.82
29	CuO/Cu_2O	1.62 ± 0.18	1.01	1.07
41	Nb_2O_5/NbO	0.96 ± 0.07	1.04	0.83
42	MoO_3/MoO_2	1.20 ± 0.07	1.03	1.29
50	SnO_2/SnO	1.19 ± 0.08	1.02	1.19
51	Sb_2O_5/Sb_2O_3	0.55 ± 0.04	1.00	0.67
56	BaO_2/BaO	1.33 ± 0.11	1.00	0.87
82	Pb_3O_4/PbO	0.93 ± 0.14	1.02	1.05
	PbO_2/PbO	1.00 ± 0.06	1.02	1.08

The case of mixtures is interesting because some capture experiments have deliberately mixed another material into the target for calibration purposes [130]. This is definitely a mixed blessing. The added material produces extra γ-rays, and the number captured in the added powder can depend on the grain size [131–133]. For alloys which dissolve in each other uniformly, the capture ratio remains constant after taking into account the relative concentration [134,135], but some concentration dependence is found in gases [136]. We point out these details just as a warning not to use a mixed target unless it is absolutely necessary.

Hydrogen is much less of a problem of course. The presence of hydrogen is a special case, because if the muon is Coulomb captured by a proton, it forms a neutral system μp, which can then easily penetrate nearby atoms, and the muon can quickly be transferred to the higher Z nucleus, because of the stronger binding energy. Thus polyethylene, $(CH_2)_n$, is effectively a carbon target, and water is a convenient oxygen target. If, however, the hydrogen is dominant in a less dense environment, and the heavy element is present at the level of only a per cent or so, then the transfer rate is slower and can be observed. We shall discuss this topic because such gas targets have been used as a technique for transferring the muon to a rare and expensive isotope.

In gases at pressures of a few bars, the transfer of the muon from hydrogen to a heavier element can take hundreds of nanoseconds and the transfer can be monitored by the emission of the $2p$–$1s$ muonic X-ray from the receiving atom. This effect has been studied for many years by Schneuwly's group at PSI, and it was found that some elements, especially oxygen, exhibit complex transfer rates [137,138]. This is now thought to be due to the fact that the μp atoms have a variety of energies, up to several tens of eV, and that the transfer rate depends on this kinetic energy [139]. Thus for oxygen three different transfer rates are required, $8.5 \times 10^{10}\,s^{-1}$

Table 3.2
A comparison of the atomic capture ratios for muons and pions. Also given are the empirical capture probabilities of von Egidy and Hartmann [129], as well as the simple Z law

Z_1Z_2	Muons $A(Z_1Z_2)$	Pions $A(Z_1Z_2)$	vEH	Z Law
B_2O_3	0.22 (5) [A][a]	0.23 (5) [B]	0.25 (7)	0.63
CO_2	0.43 (2) [C]	0.38 (6) [D]		0.75
LiF	0.28 (3) [A][a]	0.10 (1) [E]	0.18 (5)	0.33
	0.10 (8) [F]	0.22 (2) [H]		
NaF	1.56 (12) [A][a]	0.89 (5) [E]	1.01 (5)	1.22
	0.96 (5) [F]	1.02 (15) [D]		
KF	1.89 (18) [G]	2.0 (1) [E]	1.55 (7)	2.11

A[a] [147], B [148], C [149], D [143], E [150], F [151,152], G [154], H [153].

[a]Note that several values by Zinov et al., for other molecules are inconsistent with more recent measurements.

up to 0.12 eV, $36 \times 10^{10}\,s^{-1}$ from 0.12 to 0.22 eV, and zero for higher energies. Thus as the μp atoms thermalize, the capture probability increases, then for about a 100 ns it is quite fast, but falls back again to a lower rate when all the μp atoms have thermalized (0.025 eV) and fall below the 0.12 eV level [140]. Helium is another special case because the transfer rate is very slow, about $10^8\,s^{-1}$, and there is still debate about the mechanism for this transfer [141]. For ^{3}He, the rather unusual $d\mu\,^3$He can be formed, but not for ^{4}He [142].

A final topic is a comparison between the atomic capture probabilities for different negative particles such as muons, pions, kaon and anti-protons. One might anticipate that all captures would have similar characteristics as the strong interaction is not involved, so the only important parameter is the mass of the particle, because heavier particles have a stronger binding energy and so can release more electrons. The only particle apart from the muon for which data exist is the pion. As that has a similar mass to the muon, we can anticipate almost identical characteristics and that is what is observed for the unfortunately few cases in which the same molecule has been studied. In the case of the π^-, one of the interests was the possible use of this particle for cancer therapy, and it was important to know which atom the pion stopped in, and thus which nucleus produced the star of energetic protons and alphas. Measurements were made by Jackson et al. [143], at TRIUMF, on malonic, glutamic, and pimelic acid, and similar C/O ratios were found for pion and muons. Work at KEK has been undertaken with pions on a broader variety of molecules, including comparisons between mixtures and compounds, which were found to be quite different [144,145]. A sample of results is given in Table 3.2 comparing muons and protons for a few compounds. Also given are the predictions from the simple Z law, and for the empirical capture ratios of von Egidy and Hartmann [129], which were obtained for muons. The latter is seen to be a reasonably close estimate. The muon results are taken from various compendia [146,127–129]. It is clear that there is more discrepancy between different results with muons than between muons and pions.

Probably the strongest evidence for the effect of the chemical bond comes from a series of measurements by Imanishi et al., at KEK [144]. They studied a variety of beryllium borides and found a strong dependence on the chemical bonding, even after the atomic ratio is taken

Table 3.3
Measurements of atomic (per-atom) capture ratios for several beryllium borides from Imanishi et al. [144]

Compound	Be_4B	Be_2B	BeB_2	BeB_6	Mixture	vEH	Z law
A(Be/B)	0.40 (2)	0.36 (2)	0.25 (2)	0.10 (3)	0.75 (3)	0.30 (9)	0.8

into account. Their results are given in Table 3.3. They checked the effects of grain size on the mixtures and found no effect, because the energy loss of pions is so similar for neighbours in the Mendeleev chart.

This is one of the strongest effects of valency that has been observed. For example, in chromium, iron and nickel borides the effects is present but less pronounced [145]. We see again that the empirical capture ratios of von Egidy and Hartmann give a better estimate than the Z law for the compounds. Remember the approach of von Egidy et al., ignores such valency effects.

The only major difference between pions and muons is for hydrogenous compounds. The pionic cascade is shortened by strong capture in $n = 3$ or 4. The time it takes is only 10^{-12} s, so typically 1% or 2% of pions will capture on a proton even in water or polyethylene. This is a complex topic and has been thoroughly reviewed by Horvath [155]. Again there is strong evidence for the effects of the chemical binding, but it is not relevant to our main theme here.

3.2. Muonic cascade

Once the muon is securely captured by an atom in the target, it cascades down to the 1s level in a time-scale of the order of 10^{-13} s which is instantaneously as far as typical counters are concerned. The first part of the cascade is by Auger emission, but around $n = 5$ muonic X-rays begin to dominate. The details of the cascade depend upon the chemical and physical environment. For example in a gas the Auger electrons cannot be replaced, whereas in a solid some electrons are replaced as the muon becomes more deeply bound. The X-rays can be a useful calibration standard for an experiment, though sometimes they can be a confusing complication, especially if other elements are in or around the target. It is therefore essential to be aware of their characteristics and especially the energies. The energy levels for a point nucleus are given by

$$E_{n,j} = -\frac{m_\mu c^2}{1 + m_\mu/A}\frac{(Z\alpha)^2}{2n^2}\left[1 + \left(\frac{Z\alpha}{n}\right)^2\left(\frac{n}{j + (1/2)} - \frac{3}{4}\right)\right] . \tag{3.4}$$

When the muon is in the 1s ground-state, it has a radius which is comparable to the nuclear radius, so the binding and thus the energy of the final X-rays are reduced. Equally well for the higher n levels, the nucleus is screened by the inner K electrons so again the binding is reduced, but this is a small effect. The pattern of the levels and the nomenclature is illustrated in Fig. 3.3. The most common transitions are the $E1$ $\Delta n = 1$ transitions such as $4f$–$3d$, $3d$–$2p$, and $2p$–$1s$, but $\Delta n \geqslant 1$ transitions can also occur at a reduced intensity from 20% down to 5% or so. Thus, the transition to the 1s ground-state which are observed are the $2p$–$1s$, $3p$–$1s$, $4p$–$1s$ up to $8p$–$1s$, even $9p$–$1s$. These are often called the Lyman series, K_α, K_β, K_γ, etc., following atomic notation. A typical series is illustrated in Fig. 3.4 for muonic phosphorus. The blur at the

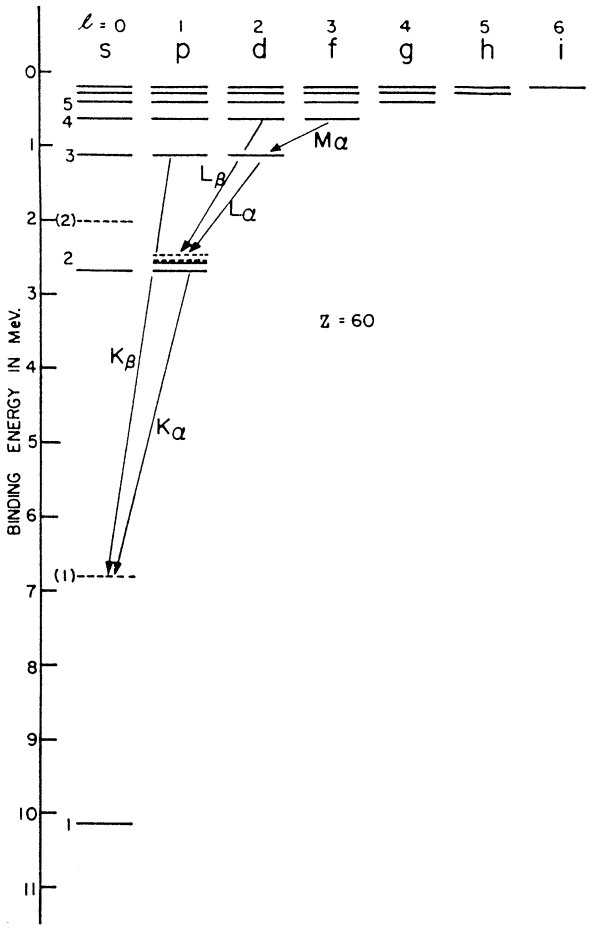

Fig. 3.3. Levels of a muonic atom, showing notation for X-rays. For $Z = 60$ the $1s$ state is raised by 3.3 MeV (dashed level) because of the finite size of the nuclear charge [117].

end is typical and quite characteristic of a series end. Similar transitions end on the $2p$ level, viz., $3d$–$2p$, $4d$–$2p$, $5d$–$2p$, etc., and these are called the L_α, L_β, L_γ lines in the Balmer series.

The situation is unfortunately considerably more complicated than the simple diagram of Fig. 3.3. First there is the fine structure or spin–orbit splitting of the levels. This is caused by the term which includes j, in the square brackets of Eq. (3.4). Thus the p level is split into a $p_{3/2}$ and a $p_{1/2}$ combination, so there are two transitions: $2p_{3/2}$–$1s_{1/2}$ and $2p_{1/2}$–$1s_{1/2}$. The former is more energetic and has twice the intensity. For light elements the transitions cannot be resolved but by silicon or phosphorus the $2p$–$1s$ X-ray is noticeably broadened and by titanium ($Z = 22$) the separation is 2.2 keV; thereafter the lines are clearly distinguished.

In the last 20 years a lot of precise data has been taken on the energies of muonic X-rays. The main goal was to obtain the charge distribution of the nucleus. Major efforts were undertaken at LAMPF and PSI and the results are summarized in the recent compendium of Fricke et al. [157]. There is also an older but still useful compilation by Engfer et al. [78].

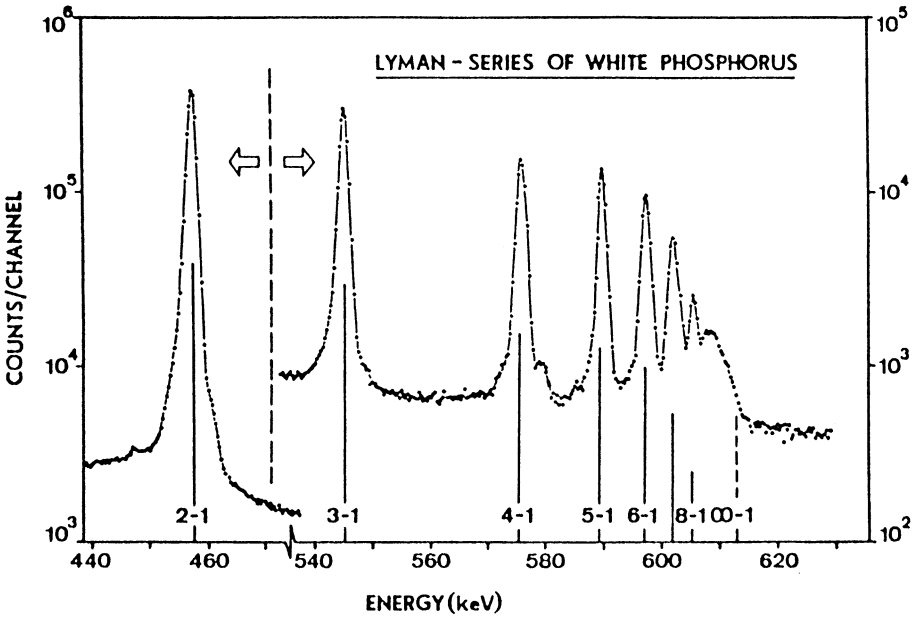

Fig. 3.4. Typical K-series of Lyman series of muonic X-rays [156].

The X-rays energies are illustrated in Fig. 3.5. The curves are the value for a point nucleus and appear to diverge from the data points for $Z = 20$ (Ca) and above for the $2p$–$1s$ transition. In fact the precision is much greater than it appears and even for ^{12}C ($Z = 6$), an excellent value for the charge radius can be obtained. Some typical values for major transitions are given in Table 3.4. These are taken from the review of Fricke et al. [157], but some np–$1s$ transitions are taken from the measurements of Fricke et al. [158], or the older values of Wohlfart et al. [159], Kessler et al. [160], Pratt [161], and Schaller et al. [162]. The latter measurement appears to give values for natural silicon about 70 eV low compared to Fricke et al. ($\sim 3\sigma$). The $4p$–$1s$ has accordingly been corrected and the error raised. (Other elements are within the errors.) For ^{208}Pb the values have been taken from Bergen et al. [163], and Hoehn and Shera [164]. Care must be taken in comparing data sets to check whether natural or isotopic targets were used; also the review by Fricke et al. [157], for light elements gives the centre of gravity of the two fine structure lines (except for ^{28}Si, ^{30}Si, K and Ca), but the measurements [158] list the energy of the $2p_{3/2}$–$1s_{1/2}$ transition. In Table 3.4 we have converted, where necessary, to the centre of gravity of the two lines for the natural combination of stable isotopes (for Ca and heavier the major lines are quoted separately). The accuracy of modern measurements is such that these different definitions are easily distinguishable.

In any experiment studying muon capture these X-ray lines are observed, and cause confusion in the interpretation. Fortunately they are narrow, come in patterns, and are emitted instantaneously with the arrival of the muon. They can thus act as a useful beacon in navigating a spectrum, indicating which elements are present, but they can also be misleading, so care has to be exercised.

The other factor which is useful is the intensity of the muonic X-rays. For most elements the muon must make an np–$1s$ transition, so it has been possible to obtain the yield with

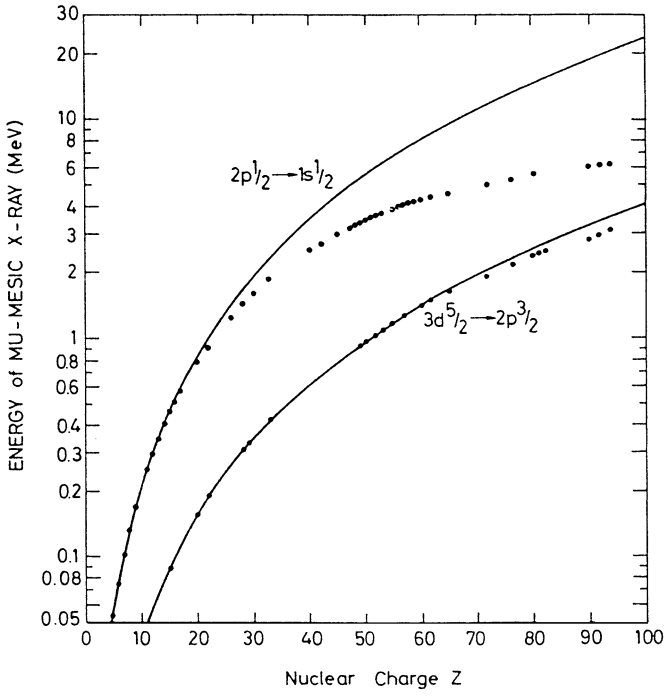

Fig. 3.5. Energies of muonic X-rays. The lines are the predicted values for a point nucleus.

some accuracy. This can then be used in a capture experiment to determine the efficiency of a germanium detector in situ, for energies from very low to very high, with the stop definition included. Even here, however, life is not simple as some X-rays are anomalously low. For deformed nuclei the X-rays spread over complex fine structure. In nuclei such as ^{232}Th or ^{238}U there is a coupling to rotational levels via a dynamic quadrupole interaction, even if the nuclear ground-state spin is zero, as is the case for these two nuclei. Thus for ^{232}Th about 20% of the transitions occur by excitation of the nucleus and are called radiationless. For ^{238}U the proportion is 26% and for both cases the whole of the complex is affected roughly equally [167].

The nuclear excitation during the muonic cascade leads to an interesting effect, because the nuclear de-excitation occurs promptly in the presence of the muon, and so the energy of the transition is modified by a keV or two. This is called the isomer shift and has been studied in great detail, see for example Backe et al. [168], and Walter [169]. This is not relevant to our principal discussion, except that, in heavy elements, the isomer shift can be after an Auger neutron has been emitted, and we shall return to this effect in Section 4.9.

Another type of complexity is that the fine structure intensity may be anomalous. An early discussion of this was given in the review of Wu and Wilets [118]. Now if the levels are populated statistically, the intensity ratios are

$$\begin{aligned}
&(2p_{3/2} - 1s_{1/2}) : (2p_{1/2} - 1s_{1/2}) \text{ is } 2:1\,,\\
&(3d_{5/2} - 2p_{3/2}) : (3d_{3/2} - 2p_{3/2}) : (3d_{3/2} - 2p_{1/2}) \text{ is } 9:1:5\,,\\
&(4f_{7/2} \to 3d_{5/2}) : (4f_{5/2} - 3d_{5/2}) : (4f_{5/2} - 3d_{3/2}) \text{ is } 20:1:14\,. \qquad (3.5)
\end{aligned}$$

Table 3.4
Energies of muonic X-rays in a few elements. For most elements the value given is the centre of gravity of the $2p$–$1s$ lines for all naturally occurring isotopes. Fricke et al. [157], give the values for individual isotopes. For heavier elements the $2p_{3/2}$–$1s_{1/2}$ and $1p_{1/2}$–$1s_{1/2}$ lines are given separately. (The curly brackets denotes values estimated from the systematics.) The parameter c is the nuclear radius at the half-height point of the charge distribution

Element	$2p$–$1s$ (keV)	$3p$–$1s$ (keV)	$4p$–$1s$ (keV)	$3d$–$2p$ (keV)	c (fm)
C	75.2588 (5)	89.212 (15)	94.095 (15)	13.966 (3)	2.001 (2)
N	102.403 (5)	121.437 (15)	128.091 (16)	{19.04 (1)}	2.15 (2)
O	133.535 (2)	158.422 (4)	167.125 (5)	24.915 (6)	2.413 (3)
^{23}Na	250.229 (2)	297.461 (13)	313.961 (18)	{47.26 (2)}	2.9393 (7)
^{27}Al	346.828 (2)	412.877 (10)	435.981 (12)	{66.11 (2)}	3.0554 (4)
Si	400.177 (5)	476.829 (12)	503.59 (4)	76.723 (10)[a]	3.155[b]
Cl	578.6 (3)	{691.4 (3)}	{730.9 (3)}	{113 (1)}	3.50[b,c]
K	712.69 (3)	854.34 (5)	903.84 (5)	143.8 (4)	3.656[b]
Ca	782.7 (2)	941 (1)	997 (1)	156.83 (2)	
	784.15 (3)			158.17 (2)	3.724[b]
Fe	1253.06 (6)	1525 (1)		265.7 (1)	
	1257.19 (5)			269.4 (1)	4.117[b]
^{89}Y	2420.1 (4)	3033.1 (6)		599.4 (4)	[d]
	2439.4 (5)	3038.6 (6)		616.4 (4)	
^{127}I	3667.36 (4)			1101.8 (2)	
	3723.74 (3)			1150.4 (2)	5.5931 (1)
^{197}Au	5591.71 (15)	8091 (1)		2341.2 (5)	
	5760.79 (15)	8135 (1)		2474.2 (5)	
^{208}Pb	5778.1 (1)	8453.95 (10)		2500.59 (3)	
	5962.9 (1)	8501.15 (11)		2642.33 (3)	6.6468 (1)
^{209}Bi	5843.2 (25)			2549.9 (2)	
	6034.0 (22)			2700.5 (2)	6.687 (1)

[a] See Beltrami et al. [165].
[b] Average over natural isotopes.
[c] See Briscoe et al. [166].
[d] See Kessler et al. [160].

In reality the levels are not quite populated statistically, so for example the first ratio is closer to 1.9 than 2. A few well established anomalies occur. In ^{127}I the $p_{3/2}$ level mixes with the 57.6 keV first excited state which has an energy similar to the $p_{3/2}-p_{1/2}$ separation. The ratio of the transition becomes 1.06 (8) instead of 1.9. In ^{209}Bi and ^{141}Pr there is a resonant excitation of nuclear levels and the ratio is 1.39 (10) and 1.69 (10), respectively [170].

Thus one should avoid these complexities when choosing elements for efficiency calibrations. Over 20 years ago this technique was used [171]. Since then there have been extensive studies and also calculations of the cascade. This has turned out to be quite complex as there have to be adjustments to the parameters. Cascade calculations have been made by Vogel [172] and by Hartmann et al. [173], and both achieve good agreement with the intensity of many transitions. They find that muons enter the atom in elemental targets above the principle quantum number $n = 20$. Then the cascade starts, mainly by Auger emission at first. They find that for lighter elements up to iron, the electrons cannot refill fast enough. Thus the M-shell of electrons is depleted when

Table 3.5
Intensity of various muonic X-rays, for solid targets, compared to the cascade calculations of Vogel [172] or Hartmann et al. [173]. For lead the data are from Hoehn et al. [164], Engelhardt et al. [171], and Anderson et al. [174]. For experiments which have used such intensities for normalization, see Giffon et al. [130]

Element	Transition	Energy (keV)	Intensity Exp (%)	Intensity Calc (%)
Na	$2p$–$1s$	250.2	79.2 (1.0)	79.3
	$3d$–$2p$	47.2		60.6
	$4f$–$3d$			33.2
Al	$2p$–$1s$	346.8	79.7 (6)	79.8
	$3d$–$2p$	66.1	62.5 (1.8)	60.2
	$4f$–$3d$		33.5 (5.3)	41.9
Cl	$2p$–$1s$	578.6	85.8 (1.0)	85.2
	$3d$–$2p$		67.6 (1.7)	66.4
	$4f$–$3d$			
Fe	$2p$–$1s$	1255	71.6 (1.7)	74.1
	$3d$–$2p$	267	44.1 (1.2)	44.9
	$4f$–$3d$		33.2 (1.2)	33.2
Au	$2p$–$1s$	5677	89.9 (3.7)	94.7
	$3d$–$2p$	2408	80.4 (2.7)	84.3
	$4f$–$3d$	884	75.6 (1.5)	76.0
Pb	$2p_{3/2}$–$1s_{1/2}$	5974		64
	$3d_{3/2}$–$1s_{1/2}$	2643		30
	$3d_{5/2}$–$2p_{3/2}$	2501		53
	$4f_{5/2}$–$3d_{3/2}$	972		32
	$4f_{7/2}$–$3d_{5/2}$	938		45

L-Auger ejection starts, and similarly the L-shell is heavily depleted when the K-Auger ejection is possible. Thus the K-shell refilling is slower than for an atom with all other electrons present. This affects the details of the cascade and also the electron screening of the nucleus which changes the energy of X-rays slightly. This has been tested by Beltrami et al. [19,165], who found that for the $4f$–$3d$ transition in silicon, the screening is certainly less than for a full K-shell, but probably not as low as the calculated occupancy of 58% from Vogel. Thus the calculations may fit the intensities quite well, but may not predict other properties of the cascade correctly.

Table 3.5 gives some examples of the intensities in some typical atoms. The general trends are obvious; that is that the probability of all the indicated transitions increases, in general, with Z (but chlorine is high). A related effect is that the K_β/K_α intensity ratio decreases steadily from about 10% for $Z = 20$ to 5% for $Z = 70$, see Bergmann et al. [175]. The errors are better than are needed in most muon capture experiments, so these results either calculated or experimental, can be used as an excellent check of the efficiency of a HPGe detector.

However, it must be emphasized that these remarks are true only for solid targets. If a muon is stopped in a gas, the electrons are ejected, and cannot refill before the muon reaches the $1s$ state. Thus, the cascade proceeds more by X-ray emission and the $2p$–$1s$ transition has a higher yield. Table 3.6 compares the yield for solid targets [130] compared to those for a gas obtained by Hauser et al. [176].

Table 3.6
Comparison of the yield of the $2p$–$1s$ muonic X-rays for solid [130] and gaseous [176] targets

Nuclide	Solid (%)	Gas (%)
^{10}B	69.1 (11)	
C	68.4 (7)	
N[a]	57.8 (10)	92.7 (8)
O	57.3 (5)	88.8 (10)
Ne		93.8 (10)
Ti	75.0 (10)	
Fe	71.6 (7)	
Cu	78.0 (10)	
Nb	84.7 (9)	

[a]Solid target was melamine, viz: $C_3H_6N_6$.

It is normal to calibrate the efficiency of a γ-ray detector by using standard sources. The difficulty with that is there are no easily obtainable γ-rays above an energy of 2.6 MeV whereas muonic X- and γ-rays from muon capture can be as high as 8 MeV or even more. Thermal neutron capture in nitrogen has been recommended for efficiency calibrations as there are γ-rays from 1.678 to 10.829 MeV, of known intensities [177]. However, reactors are not common in accelerator facilities. In the range where sources are available, the efficiency typically follows a straight line on a log–log plot, i.e., can be approximated by

$$\ln(\mathrm{Eff}) = a - b \ln E_\gamma \tag{3.6}$$

where Eff is the efficiency and E_γ is the γ-ray energy in MeV. Figs. 3.6 and 3.7 show some typical detector efficiencies and values of the b parameter for different manufacturer's quoted efficiency taken from Helfer and Miller [178]. Other useful data are given by Kamboj et al. [179,180] and also Ludington and Helmer [181]. Note that for typical detectors, the photopeak and efficiency drops by a factor of 10 from 100 keV to 2 MeV and another factor of 4 to 10 MeV. This causes great difficulty in muon capture experiments and is one of the principal reasons that high energy transitions have rarely been identified. The other difficulty is that these transitions are often Doppler broadened, so do not stand out from the background clearly. We shall return to this when discussing the experimental measurements.

3.3. Hyperfine transition

When the muon arrives in the ls level at the end of the atomic cascade, a further complication awaits it. The spin of the muon is 1/2, so if the nucleus has a spin, there are two hyperfine states available. For example in ^{19}F, the nucleus has a spin of 1/2, so there are hyperfine states of spin 0 and 1. The impact of two effects makes this feature very important, especially in fluorine. First the transition rate between these two levels turns out to be comparable to the muon lifetime. Initially it was assumed that this rate would be too small to be noticeable because the radiative rate for an $M1$ photon is small. However, the transition can go by Auger emission of atomic electrons and this speeds it up. Secondly muon capture is highly sensitive to the relative

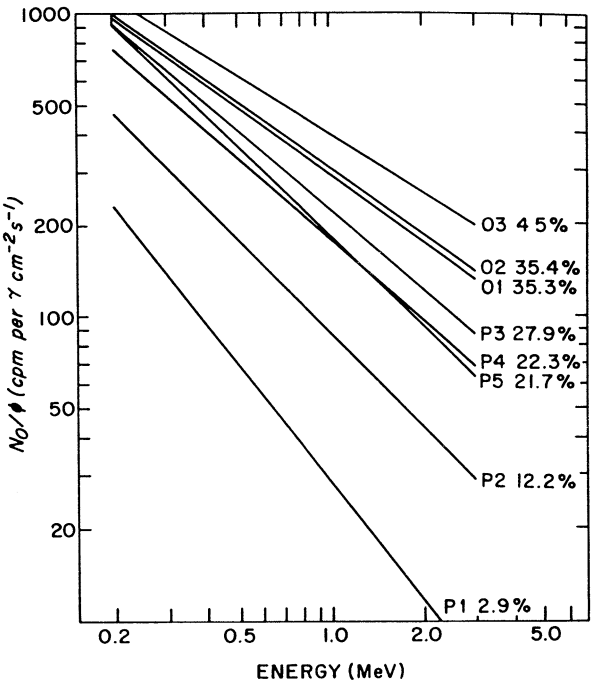

Fig. 3.6. Efficiencies for typical HPGe detectors.

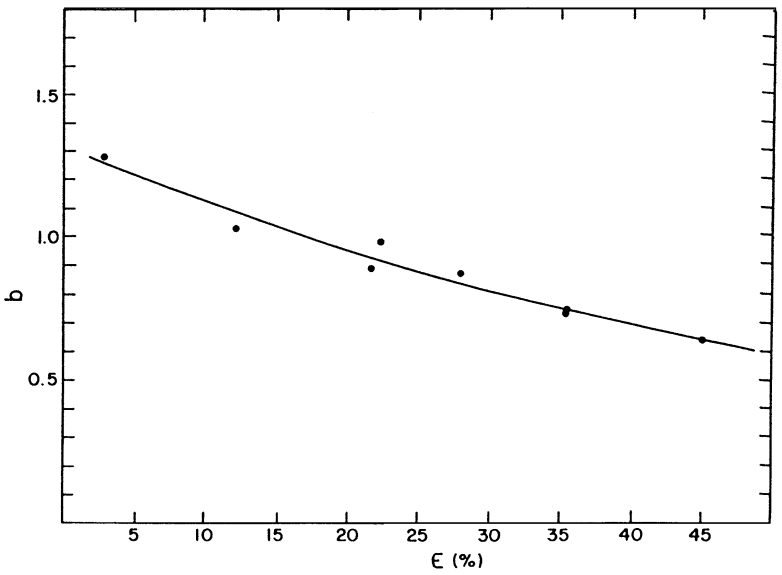

Fig. 3.7. The variation of the b parameter in the efficiency relation Eq. (3.6) for HPGe detectors.

spin alignment of the muon and the proton on which it is captured; remember that for a μp atom, $\Lambda(\text{singlet}) = 660\,\text{s}^{-1}$ but $\Lambda(\text{triplet}) = 12\,\text{s}^{-1}$. Thus for a nucleus with odd Z the relative total capture rate is roughly

$$\frac{\Lambda_{j-1/2}}{\Lambda_{j+1/2}} = \frac{Z/2+1}{Z/2} = \frac{Z+2}{Z},$$

$$\text{i.e.,}\ \Delta\Lambda \sim \frac{2}{Z}\,. \tag{3.7}$$

For nuclei with an odd neutron (viz. ^{3}He, ^{9}Be, ^{13}C, ^{17}O, ^{21}Ne, ^{25}Mg, ^{29}Si, etc.), the capture rates should be the same in the two states, but there would still be a hyperfine transition. Because these nuclei are actually more complex than a neutron outside paired protons, there is a small difference in the capture rates. In addition, for specific transitions, the value of the spin can affect the rates significantly, e.g., ^{13}C.

There are various ways of detecting the hyperfine transition:

(a) Measuring the depolarization of the muon.
(b) Measuring a non-exponential decay for the electron,
(c) Measuring a non-exponential production of γ-rays or neutrons from muon capture.

Each one of these techniques has its weaknesses and its strengths. The test case for any study is fluorine because the effect is large and the time scale for the transition is about 200 ns which makes it particularly convenient. For lighter elements it is slower and for heavy elements faster. Thus for lithium the transition rate is too slow to measure and for elements heavier than titanium it is too fast (< 1 ns). For only a few elements have convincing measurements been made.

3.3.1. Depolarization

Measuring the depolarization of the muon in the 1s state has one great advantage which is that nuclei with even Z can be studied. However, there are two major disadvantages. First the muon loses its polarization during the cascade, so less than 10% of the initial polarization is left for nuclei with spin. Secondly, it is possible for electromagnetic interactions with the crystal to depolarize the muon.

The depolarization of negative muons is a complex topic and has been reviewed by Evseev [182]. During the cascade there are three mechanisms involved. First the radiative transitions depolarize the μ^- to about 20% of its initial polarization for conductors. Carbon is taken to be the standard, and the residual polarization is found to be $20.8 \pm 0.11\%$. The value for other metals, such as Mg, Ca, Zn and Pb, is thought to be similar. Secondly there is a more complex mechanism which can operate in the early part of the cascade if there are interactions with paramagnetic electrons; this can come from radicals caused by the radiation damage or from normal paramagnetic sites. Thus, in liquid oxygen or chromium, no residual polarization is observed. For hydrocarbons the residual polarization can vary from 15% to 80% of that in carbon. Another strange observation is that the oxygen polarization varies from 40% of carbon, for water, to 80% of carbon for hydrogen peroxide. Finally, there is a further depolarization of a factor of 2 or so, if the nucleus has spin.

These are all referring to the polarization when the μ^- first reaches the ls state. Then further mechanisms take over. The hyperfine transition will reduce the asymmetry still further and

other magnetic interactions in the crystal can do so too. Yet with all these complications some important measurements have been made.

3.3.2. Electron detection

Looking for a non-exponential decay of the electrons is the hardest way to detect the hyperfine effect. For light nuclei, where the effect is easiest to observe, the overall capture rate of the muon is much less than its normal decay $\mu^- \to e^- + \bar{\nu}_e + \nu_\mu$ and this is not affected for symmetrical counter arrays. Thus, when detecting electrons, the decay can be approximated by

$$N(t) = A(1 - A_{\mathrm{he}}\mathrm{e}^{-\Lambda_{\mathrm{h}}t})\mathrm{e}^{-\Lambda^- t}\ , \tag{3.8}$$

where Λ_{h} is the hyperfine transition rate, $\Lambda^{\pm}$ is the decay rate for the upper(lower) level, and Λ_{he} is the amplitude of the hyperfine effect for electrons, where

$$A_{\mathrm{he}} = \frac{J+1}{2J+1}\frac{\Delta\Lambda}{\Lambda_{\mathrm{h}}} \quad \text{with } \Delta\Lambda = \Lambda^- - \Lambda^+,\ J = 1/2\ . \tag{3.9}$$

For fluorine $A_{\mathrm{he}} \sim 0.02$, so it is very difficult to observe and only one experiment has done so convincingly [183], and this is the easiest case.

3.3.3. Neutron and γ-ray detection

It is far better to look for the hyperfine effect in the products of the nuclear capture as there is no background from the more prolific muon decay. The effect can be quite large for specific γ-ray transitions, so this method has been used, but the efficiency of γ-ray detectors is poor and so statistics are often limited. In addition the typical timing characteristic of a large HPGe detector is about 7 ns, which makes it impossible to detect fast hyperfine rates. Backgrounds are also problematic and detection should be continued for many lifetimes (but often have not).

The most reliable method is neutron detection, but even here there is a major problem. The neutrons are emitted with energies varying from 0.5 to 20 MeV and have a broad spectrum of velocities. It is normal to cut out the lowest energy neutrons, but taking 2–20 MeV the velocities are 2–6 cm ns^{-1}, thus for a detector 30 cm from the target, all the γ-rays reach the detector after 1 ns, but the neutrons are spread with flight times of 5 to 15 ns. Thus though the intrinsic timing of a neutron detector is excellent, its effective characteristics are not. This makes it very difficult to measure hyperfine transitions with time constants less than 50 ns, i.e., a transition rate $R > 20\,\mu\mathrm{s}^{-1}$.

It might be imagined that the time structure of the neutrons could be calibrated using spin-zero nuclei for which no hyperfine transition occurs. Unfortunately these nuclei have very different nuclear properties and the neutrons produced by the muon capture have a different energy spectrum. For example, capture on ^{16}O, ^{20}Ne or ^{24}Mg cannot be used to calibrate ^{19}F. Thus the spectrum must be obtained for each nucleus which is difficult for all nuclei except ^{19}F.

3.3.4. Results

In spite of all these difficulties, a few measurements have been made and are given in Table 3.7. The reason for the persistence of experimenters is that, using this effect, it is possible to measure the capture rates from the two hyperfine levels, and to test calculations of this asymmetry.

Table 3.7
Experimental results on the muonic hyperfine transition rates in light nuclei. The theoretical calculation is by Winston [184]. He calculated the Auger rate, given the hyperfine energy interval E, as tabulated. For a positive nuclear magnetic moment, the $F^+ = J + 1/2$ lies above the $F^- = J - 1/2$ level. (For ^{3}He and ^{9}Be this is thus reversed)

Nuclide	J^π	Magnetic moment	E(eV)	Method	Λ_H (μs^{-1})	
					Theory	Experiment
^{3}He	$1/2^+$	−2.128	1.5	Ion chamber	0	0.006 ± 0.008 [185]
^{6}Li	1^+	0.822	1.4	μ^-SR	0	< 0.02 [186]
^{7}Li	$3/2^-$	3.256	4.9	μ^-SR	0	< 0.02 [186]
^{9}Be	$3/2^-$	−1.177	4.0	μ^-SR	0	< 0.05 [186]
^{10}B	3^+	1.801	10.1	μ^-SR	0.25	0.21 ± 0.05 [186]
^{11}B	$3/2^-$	2.689	17.3	μ^-SR	0.25	0.33 ± 0.05 [186]
				μ^-SR		0.26 ± 0.06 [187]
				Ge		0.25 ± 0.07 [188]
				Ge		0.181 ± 0.016 [189]
^{13}C	$1/2^-$	0.702	11.2	μ^-SR	0.053	0.020 ± 0.012 [190]
^{14}N	1^+	0.404	7.4	μ^-SR	0	0.076 ± 0.033 [190]
				Ge		NULL [130]
^{19}F	$1/2^+$	2.629	126	Liquid Scint.	5.8	6.1 ± 0.7 [184]
				Ge		4.9 ± 1.2 [191]
				Liquid Scint.		5.6 ± 0.2 [192]
^{23}Na	$3/2^+$	2.218	119	Ge	14	8.4 ± 1.9 [191]
				Ge		15.5 ± 1.1 [193]
^{27}Al	$5/2^+$	3.641	263	μ^-SR	41	41 ± 9 [194]
				Liquid Scint.		36 ± 20 [192]
^{31}P	$1/2^+$	1.132	188	Ge	58	$\geqslant 50$ [191]
				Scintillators		< 1 [195]
				Liquid Scint.		48 ± 10 [192]
^{35}Cl	$3/2^+$	0.822	119	Ge	8	6.5 ± 0.9 [191]
^{37}Cl	$3/2^+$	0.684	99		8	
^{39}K	$3/2^+$	0.391	72	Liquid Scint.	22	25 ± 30 [192]
^{45}Sc	$7/2^-$	4.757	920		460	
^{69}Ga	$3/2^-$	2.016	917		330	
^{71}Ga	$3/2^-$	2.562	1166		650	

The difference in energy of the two hyperfine levels is given by

$$E = 0.0225 \frac{2J+1}{J} \left(\frac{Z_{\text{eff}}^4}{Z} \right) \mu_J \text{ (eV)} , \tag{3.10}$$

where J is the nuclear spin, Z_{eff} is a reduction of the nuclear charge due to the finite size (and will be given later in Table 4.2, and μ_J is the magnetic moment in nuclear magnetons. The calculation of the hyperfine transition rate is from Winston [184]. He assumed that all the electrons were replaced after the atomic cascade and then calculated the Auger rate for those electrons bound less than the energy available. Because the muon is in an orbit very close to the nucleus, the effective nuclear charge for the rest of the atom is $(Z - 1)$, so for a μ^-F

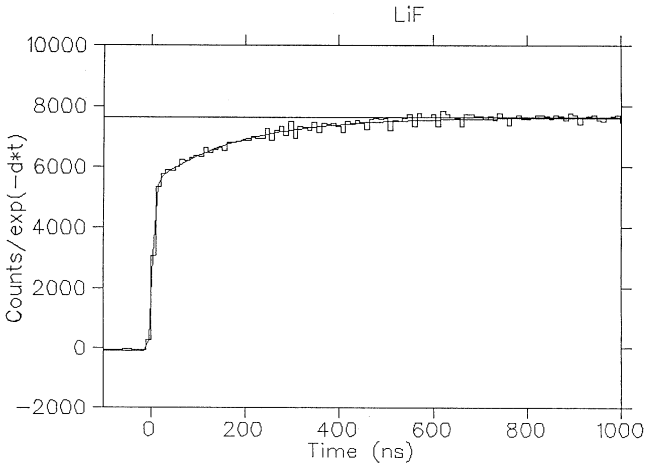

Fig. 3.8. Time distribution for neutrons from muon capture in ^{19}F. The normal decay has been divided out to demonstrate the hyperfine transition clearly which has $\tau \sim 180$ ns.

transition, the electronic structure of oxygen is assumed. For muon capture on He, Li, Be and N, the energy available is less than the binding energy of the least bound electrons in the $Z-1$ atom, so no Auger effect is expected. Of course the radiative transition can still occur, but in fluorine, for example, it is 6000 times slower, so it is totally negligible in such experiments and this has been abbreviated to simply zero in Table 3.7.

Stocki [192] recently completed some measurements of the hyperfine transition rates at TRIUMF using liquid scintillators, for detecting neutrons. For fluorine a full analysis of the neutron time spectrum was accomplished, so we use the errors as quoted. A typical neutron time distribution is presented in Fig. 3.8 where the normal decay has been divided out to emphasize the hyperfine effect. The rise at $t=0$ is well separated and can be fitted independently. It is mainly time of flight effects. For the other elements, the neutron time distribution had to be fixed, so we arbitrarily have doubled the errors as given, to account for systematic uncertainties.

There are several enigmas in Table 3.7. The most serious is that a hyperfine transition has been claimed for nitrogen, but the theory predicts a negligible rate as the energy available is only 7.4 eV but the electrons in a carbon atom are bound by 11.3 eV. Now the calculation is done for free atom, but taking the CN radical makes the situation worse (ionization potential $=14.3$ eV). The result was from a μ^-SR measurement so it could be that an additional depolarizing effect is present.

For phosphorus an initial μ^- polarization measurement by Egorov et al. [195], claimed that an asymmetry had been observed. The measurement was over 0–2.4 μs implying no fast depolarization. Now the upper level has $F=1$ and the lower level $F=0$, so if a fast hyperfine transition occurs, there can be no residual polarization. If an asymmetry is observed then the transition time constant has to be slower than 2 μs. Later asymmetry measurements by Hutchinson et al. [196], and Babaev et al. [197], observed no asymmetry and set limits at 10% of the value observed by Egorov, thus indicating that the hyperfine rate was probably quite fast. This was confirmed by Gorringe et al. [193], though no numerical value could be given. The

Table 3.8
Capture rate asymmetry $\Delta\Lambda/\Lambda$ between the two hyperfine levels for some odd Z nuclei. Note that the calculations are for total capture rates, whereas the neutron experiments detect only neutrons, with a bias towards higher energy products ($E > 2\,\mathrm{MeV}$)

Element	BLYP theory [184]	Primakoff theory [184]	Uberall theory [198]	Neutron experiments
F	0.24	0.36	0.36	0.36 (4) [184] 0.30 (1) [192]
Al	0.09	0.14	0.22	0.14 (8) [192]
P	0.16	0.22	0.25	0.21 (6) [192]
K	−0.05	−0.07		−0.08 (11) [192]

recent experiment of Stocki [192] clearly sees a fast transition rate of $48 \pm 10\,\mu\mathrm{s}^{-1}$, but a more accurate value is difficult to determine because of the neutron time spread in the detector.

For sodium there are two published values $8.4 \pm 1.9\,\mu\mathrm{s}^{-1}$ in NaF and $15.5 \pm 1.1\,\mu\mathrm{s}^{-1}$ in sodium metal. Although there has been discussion that NaF might have a different rate because of its insulating characteristics, that is likely to slow the rate down. The most likely explanation is that the NaF experiment did not estimate the background rates sufficiently well.

What is remarkable about Table 3.7 is that no confirmed experiment contradicts Winston's estimates. This is a resounding confirmation of the assumptions made in the calculations.

In these experiments an important parameter is the difference between the capture rates in the two hyperfine levels. For the γ-ray experiments each transition has to be treated on its own, and this will be discussed later. However, it is worth noting here that sometimes the difference can be quite extraordinary, thus $\lambda^+/\lambda^- = 0.028 \pm 0.021$ for the 320 keV γ-ray in ^{11}Be from muon capture on ^{11}B [189]. This case is particularly clean as this is the only bound excited state in ^{11}B.

For neutron detection it is normally assumed that one is measuring the total capture rates on hyperfine levels. This is not strictly true. Many transitions produce just gamma-rays, and often 2 neutrons are produced so these are double counted. Equally well the detection efficiency for the neutrons is highly energy dependent, so the bias is towards higher energy neutrons. However, it is still worth making a comparison, but you have to assume that the overall capture asymmetry is true for those neutrons which are detected. This assumption seems to be upheld better than might be expected, see Table 3.8. Again we have taken the fluorine results of Stocki as quoted, but have doubled the error on the other elements. The agreement for fluorine is satisfying, though it should be noted that the neutrons detected in different experiments probably do not have the same effective energy spectrum.

4. Muon capture in nuclei

We now come to the meat of the review. We shall first discuss the hydrogen isotopes briefly for completeness, but little substantial progress has occurred for many years. For those interested in these details, we refer them to the excellent reviews by Zavattini [199], Mukhopadhyay [13]

or Blin-Stoyle [4]. We shall next address ^{3}He for which there is a remarkable new result which underpins all theoretical approaches to muon capture. The rest of this section will then be devoted to general features of muon capture to set the scene for the discussion of specific nuclei in Section 5.

4.1. Hydrogen

Muon capture in hydrogen is the most important from the theoretical point of view, but by far the hardest experimentally. First the rate is small ($\sim 460\,\mathrm{s}^{-1}$) in comparison to muon decay ($455\times10^3\,\mathrm{s}^{-1}$) a factor of a thousand which causes great difficulty in an experiment. Secondly the μp atom is neutral and quite reactive as an atom, so it likes to form muonic molecules like $p\mu p$, $p\mu d$ and $p\mu t$. These Coulombic systems and reactions complicate the study of the weak interactions, but are a vast study in their own right, because of the interest in muon catalyzed fusion. Several reviews have surveyed this active area [200–203]. The complication is that most of these molecules ($p\mu d, p\mu t$) and the others ($d\mu d, d\mu t, t\mu t$) then undergo a fast (normally strong) reaction, which fuses the nuclei and produces gammas and neutrons. This can blind any search for muon capture via the weak interactions. Thus such experiments must take stringent precautions to suppress these effects. For hydrogen it is sufficient to reduce the deuterium content, which even for the 150 ppm (parts per million) of natural hydrogen is a problem. Fortunately pure protium (i.e., $^1H_2$) is available with a few ppm of deuterium. Thus, for liquid protium, one is left with only $p\mu p$ molecules, which cannot undergo fusion, so the only competition is muon decay. However, as remarked earlier, this is 1000 times stronger, and the bremsstrahlung from the decay electrons causes significant neutron production in the target container.

It is possible to detect the neutrons directly and two types of experiment have been performed. One is the bubble chamber type which measures all the neutrons produced after a muon stops. The other type measures the neutron production as a function of time. These measure slightly different production sources.

When a μ^- stops in liquid hydrogen it quickly forms a μp atom often in the triplet state. The energy difference between the triplet and singlet states is 0.185 eV, and collisions quickly drive all the atoms into the lower energy singlet state. The formation of a $p\mu p$ molecule occurs more slowly and typically takes about 400 ns. The product is expected to be a $1s\sigma g$ ortho state molecule, that is a singlet state with the proton spins parallel. This is not the lowest molecular state, but the para state is formed less than 1 in 10^4 of ortho molecules and the transition to the para state is expected to be very slow. The ortho to para transition in normal hydrogen liquid can take days.

Capture now occurs from the molecule. If we use values $\Lambda_s = 664 \pm 20$ and $\Lambda_t = 11.9 \pm 0.7$, the molecular capture rates are calculated to be

$$\Lambda_{om} = 2\gamma_o\left(\frac{3}{4}\Lambda_s + \frac{1}{4}\Lambda_t\right) = 506 \pm 20\,\mathrm{s}^{-1}\,, \tag{4.1}$$

$$\Lambda_{pm} = 2\gamma_p\left(\frac{1}{4}\Lambda_s + \frac{3}{4}\Lambda_t\right) = 201 \pm 8\,\mathrm{s}^{-1}\,, \tag{4.2}$$

where $2\gamma_o = 1.01 \pm 0.01$ and $2\gamma_p = 1.147 \pm 0.01$ are factors taking into account the molecular orbital of the muon.

Now if a measurement, such as the bubble chamber type, measures all the neutrons, some are made in the initial singlet state which has a higher capture rate. If a measurement detects the decay curve and extrapolates back, it just measures the molecular rate.

Zavattini [199] discussed two experiments of each type; the decay curve type obtained 515 (85) s^{-1} and 464 (42) s^{-1} to be compared with the Λ_{om} of 506 s^{-1} (Zavattini used 493 s^{-1}) and two bubble chamber experiments which obtained 428 ± 85 and $450 \pm 50\,s^{-1}$ to be compared with the expected 536 s^{-1} (Zavattini used 522 s^{-1}; unfortunately there is a typographical error in his Table 1). The experiments are not very accurate but the agreement is satisfactory, though marginal.

A totally different approach was tried at Saclay 20 years ago [23]. The idea was to measure the μ^- lifetime in liquid hydrogen to high precision. Then the difference between that rate and the equivalent for a μ^+ gives the required capture rate in the ortho molecular state.

This experiment was a major undertaking and is worth describing briefly. As indicated earlier, the liquid hydrogen must be isotopically enriched and they had available gas of 2.7 ± 0.1 ppm of deuterium, sufficient for the 7 litre container. The gas was passed through a palladium filter to reduce contamination below 10^{-9}. The liquid hydrogen was contained in a copper reservoir ($\tau_\mu = 160$ ns) and there was a lead collimator ($\tau_\mu = 75$ ns) in front of a copper degrader.

The great advantage of the Saclay 600 MeV electron linac was the time structure of the beam burst, viz: 3 μs long, at 3000 Hz. Counting was started 1 μs *after* the beam burst to avoid all muons stopped in the copper and lead. Counting was continued for 65 μs, but three 80 μs gates were opened sequentially after the main gate to study backgrounds.

Electrons from the muon decay were detected in plastic scintillator telescopes surrounding the target. The background was 1/1000 of the initial counting rate, so useful data was taken for 20 μs. To test the system the beam could be switched to μ^+, but there is a slight worry about polarization, so two types of run were taken. Sometimes the protium target was surrounded by a magnetic shield, but most of the μ^+ data were taken using sulphur as a target because it depolarizes the μ^+ rapidly.

The result was that

$$\tau_{\mu^-} = 2194.903\ (66)\ \text{ns}, \quad \text{i.e., } \Lambda_{\mu^-} = 455\,601\ (14)\ s^{-1} \tag{4.3}$$

and

$$\tau_{\mu^+} = 2197.182\ (121)\ \text{ns}, \quad \text{i.e., } \Lambda_{\mu^+} = 455\,128\ (25)\ s^{-1}\,, \tag{4.4}$$

but they preferred to use the world average at that time of

$$\tau_{\mu^+} = 2197.148\ (66)\ \text{ns}, \quad \text{i.e., } \Lambda_{\mu^+} = 455\,135\ (14)\ s^{-1}\,. \tag{4.5}$$

Making two minor corrections adding to -6 ± 4, we obtain the final result of

$$\lambda_c = 460 \pm 20\ s^{-1}\,. \tag{4.6}$$

A later measurement of the μ^+ lifetime by the same group [204], led to a recommended value of

$$\tau_{\mu^+} = 2197.093\ (52)\ \text{ns}, \quad \text{i.e., } \Lambda_{\mu^+} = 455\,147\ (11)\ s^{-1} \tag{4.7}$$

or

$$\lambda_c = 448 \pm 18\,s^{-1} . \tag{4.8}$$

It is worth warning the reader that this sort of tinkering with experimental results is highly risky. If the equipment had a problem, it was likely to be the same in the original measurement for the μ^+ and the μ^-. Thus the discussion is whether the dominant errors are statistical or systematic. Anyway, taking either result, they are both somewhat below the prediction of

$$\Lambda_{om} = 506 \pm 20\,s^{-1} . \tag{4.9}$$

The problem thus focuses on whether the $p\mu p$ molecule stays in the ortho state, because the para state has a much lower capture rate of

$$\Lambda_{pm} = 201 \pm 8\,s^{-1} . \tag{4.10}$$

(The worry would be less important for the earlier neutron measurements because data was taken for only 6 μs, but it is interesting that the better measurement is also low at 464 (42) s^{-1}.)

The original assumption had been that the ortho to para conversion rate could be neglected [205], although a later estimate by Ponomarev was $9.6 \times 10^4\,s^{-1}$, quoted in Ref. [206]. The only experimental evidence is from a measurement, again at Saclay, where they detected neutrons in their hydrogen experiment and found a different time constant from the electron detection. Neutrons are problematic as one has a high energy background from cosmic-rays, and lower energy neutrons from photonuclear production. Bremsstrahlung of the muon decay electrons ($E_{max} = 52$ MeV) has a very major part of its spectrum in the giant dipole resonance around 20 MeV. Taking all this into account they obtained $\lambda_{op} = (4.1 \pm 1.4) \times 10^4\,s^{-1}$, i.e., a time constant of 24 μs which is a serious correction for an experiment which takes data over 20 μs. They thus obtain a corrected value $\lambda_{om} = 531$ (33) s^{-1} using $\lambda_c = 460$ (20) or $\lambda_{om} = 517$ (33) if one prefers $\lambda_c = 448$ (18). This is now in agreement with predictions.

This experimental value for the ortho to para transition rate came as a slight surprise, so confirmation is needed and an experiment at TRIUMF has been proposed. However, we shall take the state of affairs to be that there is agreement between theory and experiment at about the 7% level. Although a repeat of the Saclay experiment would also be welcome, the advantages of the Saclay facilities are such that no-one else has attempted the task yet.

We finally mention the two experiments which measured the capture rate in gaseous hydrogen. In this way the capture occurs just from the singlet state and one avoids the problems of capture from the molecular state. Alberigi Quaranta et al. [207], obtained $\Lambda_s = 651 \pm 57\,s^{-1}$ and Bystristky et al. [208], obtained $\Lambda_s = 686 \pm 88\,s^{-1}$, both in excellent agreement with expectations ($664\,s^{-1}$), but again at the 10% level. There is an ongoing experiment at PSI (R-97-05) which hopes to improve significantly on these measurements; it stops a μ^- beam in protium gas, and analyses each stop in the fiducial volume to determine whether an electron is produced or not.

4.2. Deuterium and tritium

The measurement of muon capture in deuterium or tritium is yet more hazardous than that in hydrogen. At first sight the capture in deuterium seems an impossible task because of the molecular reactions alluded to above, but there are two avoidance tactics.

If the experiment is done in a target of mainly hydrogen with some deuterium, the μ^- gets transferred to the deuteron forming μd. Then it may form $p\mu d$ which has a relatively long lifetime as the fusion $p\mu d \rightarrow \mu^- + {}^3\mathrm{He} + \gamma$ is mediated by the electromagnetic interaction; the fusion rate is $(3.0 \pm 0.1) \times 10^5\,\mathrm{s}^{-1}$. (Other fusion rates are of the order of $10^9\,\mathrm{s}^{-1}$.) After the $p\mu d$ fusion the μ^- sticks to the ^{3}He $(84 \pm 4)\%$ of the time and then decays or captures on the ^{3}He at a rate which is about 5 times larger than for deuterium. Thus any experiment must have these effects fully under control. In addition there is the problem of spin dependence of the capture rate. There are two hyperfine states $F = 1 - 1/2$, a doublet and $F = 1 + 1/2$, a quartic. Calculations indicate that the doublet state has a capture rate of $\sim 420\,\mathrm{s}^{-1}$ whereas the capture from the quartic state is only $\sim 10\,\mathrm{s}^{-1}$, so this has to be understood too.

A Columbia group [209] used a target of liquid hydrogen with a deuterium concentration of 0.32%. Neutrons were detected, but because μd molecules are formed, 30% of the neutrons came from the capture on a proton. They observed a rate of $365 \pm 96\,\mathrm{s}^{-1}$.

A second experiment by a Bologna–CERN [210] group used a room temperature target of gaseous hydrogen at 7.6 atm with a deuterium concentration of 5%. Under these conditions the $p\mu d$ molecule is formed slowly so most neutrons come from capture on a deuteron. They observed a rate of $445 \pm 60\,\mathrm{s}^{-1}$.

However, the atomic collision rates are not fully understood for the scattering which takes the higher energy quartet state down to the doublet. Thus, it has been recommended that a conservative analysis gives

$$325 < \lambda_{\mathrm{C}}^{\mathrm{D}} < 557\,\mathrm{s}^{-1}\ . \tag{4.11}$$

The Saclay group [211] has taken a totally different approach, using the same equipment as was used for hydrogen. They use ultra pure deuterium and count the decay electrons. In these conditions the $d\mu d$ system is formed but it immediately fuses via

$$d\mu d \rightarrow n + {}^3\mathrm{He} + \mu^- \tag{4.12}$$

or

$$d\mu d \rightarrow p + t + \mu^-\ , \tag{4.13}$$

which have branching ratios of 60% and 40%, respectively. With a likelihood of $(12.6 \pm 0.4)\%$ the μ^- can stick to the ^{3}He and this has to be taken into account. The main point is however that the fusion is so fast that the μ^- spends most of its time in an atomic state. Thus, overall, 97% of the time a muon is in an atomic doublet state, and 3% in μ^3He (but remember the capture rate is 5 times larger). Also as the μ^- spends most of its time in an atomic state, it is very vulnerable to other impurities. For the hydrogen experiment the μ^- is in a $p\mu p$ state most of the time, so it cannot be transferred. They believed that the nitrogen contamination was smaller than 10^{-10}.

The overall result was that

$$\tau_{\mu^-} = 2194.53\ (11)\,\mathrm{ns}\ , \tag{4.14}$$

Table 4.1
History of the capture rates (in s^{-1} for the μd system in the doublet state. (The first two experiments had an uncertain contamination of the quartic state.)

Year	Exp.	Theory	Ref.
1958		250	[213]
1965	365 (96)		[209]
1965		334	[214]
1972		313	[215]
1973	445 (60)		[210]
1974		377	[216]
1975		387	[217]
1976		405	[218]
1979		413	[219]
1980		450	[220]
1985	470 (29)		[211]
1986	409 (40)		[212]
1990		416 (7)	[221]
1990		402	[222]
1990		399	[223]

which with several corrections then gives

$$\Lambda_{\mathrm{C}}^{\mathrm{D}} = 470 \pm 29\,\mathrm{s}^{-1}\ . \tag{4.15}$$

Another experiment has been performed at SIN [212] by the Austrian groups using a gaseous target and they obtained a rate of $409 \pm 40\,\mathrm{s}^{-1}$.

There has been an equally active theoretical programme summarized in Table 4.1. We shall limit ourselves to a brief discussion of two of the more recent calculations which are the culmination of a decade or two of effort, especially by Truhlik and the Prague group. Adam et al. [221], have completed the most thorough calculation based on the Impulse Approximation. Many apparently minor effects add up as seen by the history of the calculations in Table 4.1. The leading term which produces neutrons in the $1S_o$ state contribute about $260\,\mathrm{s}^{-1}$, but the other final states are major contributors, coming mainly from velocity dependent terms. Meson exchange contributions are about $33\,\mathrm{s}^{-1}$. The final results of Adam et al. [221], were for the doublet state

$$\Lambda_{\mathrm{IA}}^{\mathrm{d}}(^1S_o) = 270 \pm 10\,\mathrm{s}^{-1}\ ,$$

$$\sum_{j=0,1,2} \Lambda_{\mathrm{IA}}^{\mathrm{d}}(^3P_j) = 142 \pm 4\,\mathrm{s}^{-1}\ ,$$

$$\Lambda_{\mathrm{IA}}^{\mathrm{d}}(^1D_2) = 4\,\mathrm{s}^{-1}\ ,$$

giving

$$\Lambda_{\mathrm{IA}}^{\mathrm{d}} = 416 \pm 7\,\mathrm{s}^{-1}\ . \tag{4.16}$$

The uncertainty comes from a sensitivity to the nucleon–nucleon interaction and an imprecise knowledge of the coupling constants.

A different approach was taken by Mintz [220], who worked within the framework of the elementary particle model (EPM). He related the axial form factor F_A to the matrix element for the reaction

$$\gamma + d \rightarrow n + n + \pi^+ \tag{4.17}$$

via the partially conserved axial current hypothesis (PCAC), making use of the Kroll–Ruderman theorem. There might be corrections as large as 10–20% to this estimate. The vector current matrix element was obtained from

$$\gamma + d \rightarrow p + n \tag{4.18}$$

and

$$e^- + d \rightarrow p + n + e^- \,. \tag{4.19}$$

This approach gave

$$\Lambda^{\mathrm{d}}_{\mathrm{EPM}} = 450\,\mathrm{s}^{-1} \tag{4.20}$$

and

$$\Lambda^{\mathrm{q}}_{\mathrm{EPM}} = 7.3\,\mathrm{s}^{-1} \,. \tag{4.21}$$

Unfortunately, the contributions from the various form factors were not given, and so no overall uncertainty can be assessed. However, the EPM result is disturbingly far from that of the Impulse Approximation, but closer to the experimental average of

$$\Lambda^{\mathrm{d}}_{\mathrm{exp}} = 449 \pm 23\,\mathrm{s}^{-1} \,. \tag{4.22}$$

The energy spectrum of the neutrons from

$$\mu^- + d \rightarrow n + n + \nu \,, \tag{4.23}$$

is potentially a perfect way for determining the neutron–neutron scattering length. The final state has no other strongly interacting particles and the energy imparted to the neutrons is quite appropriate. A detailed study has confirmed this assessment [224]. Although attempts have been made to measure this energy spectrum, the experimental difficulties are oppressive. Neutrons are always problematic, especially in the background from a medium-energy accelerator. Furthermore, there is no timing signal at the start of the process, and the detection of the neutrino cannot be included as a confirmation. There has been one attempt to measure the neutron spectrum by Lee et al. [225]. A liquid deuterium target was used, which means that there are lots of fusion neutrons from ($d\mu d \rightarrow n + {}^3\mathrm{He} + \mu$), however the Q-value of this reaction is 3.3 MeV, so the neutron takes only 2.5 MeV. They are also only single neutrons. Thus the experiment focused on higher energy neutrons which requires that the neutron pair go back to back. This means that one of the neutrons can be made to start a timing clock by striking a counter near the target and then the other neutron can be timed over a longer flight path. The estimated energy resolution was 4.4 MeV. The resulting spectrum is shown in Fig. 4.1, compared to the calculation of Doi et al. [222]. The kinematic maximum is marked at about 56 MeV and we can see that the overall shape of the data do not follow the calculation very well. However, this conclusion relies significantly on one datum, so it would be wise to await a second experiment. It is also not clear how the coincidence requirement changes the observed spectrum.

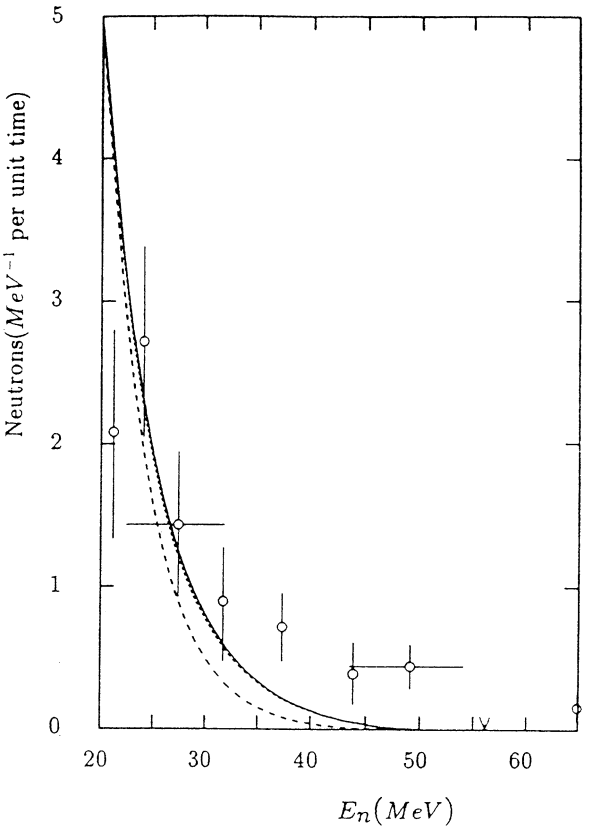

Fig. 4.1. Neutron energy spectrum produced by muon capture from the doublet state of muonic deuterium. The data are those of Lee et al. [225]. The calculations of Doi et al. [222] are with (solid) and without (dashed) meson exchange corrections. The dotted line is when the modification of the electric multipole amplitude is not taken into account.

The focus for studying low energy neutrons has always been the very similar reaction:

$$\pi^- + d \rightarrow n + n + \gamma \, . \tag{4.24}$$

The advantages are quite significant. First, the absorption takes place immediately the pion stops in the target. Secondly, the energy and direction of the photon can be detected as a redundant check on the process. The only disadvantage is that the initial state has two strongly interacting particles, so a small correction is needed. An experimental energy spectrum of the γ-ray is illustrated in Fig. 4.2, taken from Gabioud et al. [226]. Note that the final state interaction peak at 131 MeV is actually a factor of two narrower, but is smoothed out by the spectrometer resolution of 720 keV. The neutrino spectrum for muon capture on the deuteron would be very similar, except that the maximum energy would be at 99.5 MeV instead of 131.5 MeV.

There have been several experiments studying the pion induced reaction. The experiment of Gabioud et al., measured the energy spectrum of the photon only. Most other experiments have detected the neutrons because the effective energy resolution is much better. The results for a_{nn},

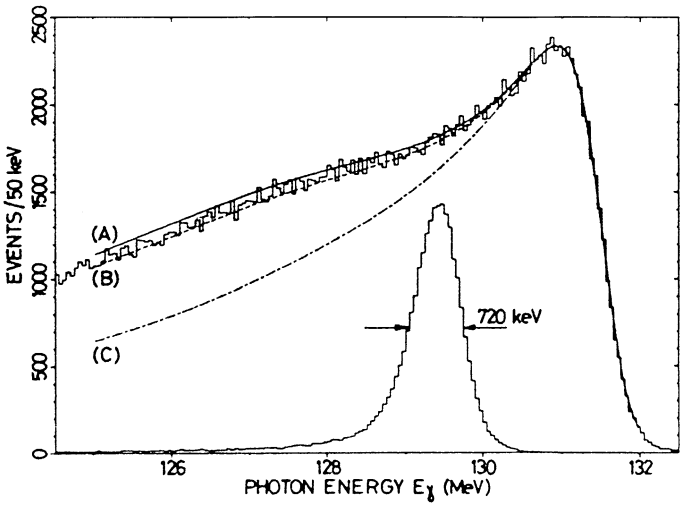

Fig. 4.2. Experimental photon spectrum for the reaction $\pi^- + d \rightarrow \gamma + n + n$ from Gabioud et al. [226]. The resolution of 720 keV is determined with a hydrogen target.

the neutron–neutron scattering length are [226–228]

$$\text{Gabioud et al. [226]:} \quad -18.60 \pm 0.34 \pm 0.26 \pm 0.30\,\text{fm}\,, \tag{4.25}$$

$$\text{Schori et al. [227]:} \quad -18.70 \pm 0.42 \pm 0.39 \pm 0.30\,\text{fm}\,, \tag{4.26}$$

$$\text{Howell et al. [228]:} \quad -18.50 \pm 0.05 \pm 0.44 \pm 0.30\,\text{fm}\,, \tag{4.27}$$

where the errors are statistical, systematic, and theoretical in that order. Summarizing all this one obtains

$$-18.59 \pm 0.27 \pm 0.30\,\text{fm} \tag{4.28}$$

and adding 0.3 for the magnetic moment correction one obtains the final "neutral strong" scattering length of

$$a_{nn}^N = -18.9\ (4)\,\text{fm}\,. \tag{4.29}$$

This is to be compared with -17.3 ± 0.4 fm from proton–proton scattering after a sizable Coulomb correction has been applied [229]. Thus the experimental charge symmetry breaking is 1.6 ± 0.6 fm to be compared with a theoretical estimate of 1.5 ± 0.5 fm. This sort of information is normally inserted into the muon capture problem via the realistic nucleon–nucleon potential that is used in the calculations.

Muon capture on tritium is almost impossible to measure because of the radioactivity of the target and because of the meso-molecular complications. However, pion radiative capture on tritium has been studied [231]. From the theoretical point of view muon capture on tritium is a by-product of calculations for ^{3}He, being the component of the final state with isospin 3/2. Thus, the capture

$$\Lambda(\mu^- + t \rightarrow n + n + n + \nu) \tag{4.30}$$

was first estimated via the Impulse Approximation and a very small value was found, $\sim 9.5\,s^{-1}$. However, Torre and Goulard [230] showed that the rate is quite sensitive to final state interaction and using the Tourreil–Sprung Supersoft Core potential for the neutrons, they obtained

$$\Lambda_s = 137.5\,s^{-1}\,, \tag{4.31}$$

$$\Lambda_t = 3.7\,s^{-1}\,. \tag{4.32}$$

Note that the hyperfine effect is very strong (as for the deuteron), because of the resemblance to the proton case.

4.3. Helium-3

Until recently helium-3 was one of the crowd and the measurements were reasonable, so no particular attention was paid to it. Now there has been a remarkable measurement which has turned the emphasis around.

Capture of helium-3 can occur via:

$$\lambda_t\colon\ \mu^- + {}^3\mathrm{He} \rightarrow {}^3\mathrm{H} + \nu \quad (70\%)\,,$$

$$\lambda_d\colon\ \mu^- + {}^3\mathrm{He} \rightarrow d + n + \nu \quad (20\%)\,,$$

$$\lambda_p\colon\ \mu^- + {}^3\mathrm{He} \rightarrow p + n + n + \nu \quad (10\%)\,. \tag{4.33}$$

We shall focus on the first, and then briefly mention the other reactions. A recent measurement by Ackerbauer et al. [185], at PSI has obtained the partial capture rate as

$$\lambda_t = 1496.0 \pm 4.0\,s^{-1}\,. \tag{4.34}$$

The target was also the detector, a high pressure ionization chamber, filled with ^{3}He at 120 bar at room temperature. The anodes covered an area $2.5 \times 4.0\,cm^2$ and the active volume was $15\,cm^3$. The cathode was held at $-40\,kV$ and a grid at $-3.5\,kV$ which results in a maximum electron drift time of $3.2\,\mu s$. The energy resolution was 30 keV to be compared with the recoil triton energy of 1.9 MeV (and range of 1.52 mm). Most of the time the muon decays, giving off an electron, but this deposits very little energy. The experiment recorded 4×10^8 muon stops and 1.2×10^6 candidate events. The analysis demanded that the triton pulse be clearly distinguished from the incoming muons, so the first $0.5\,\mu s$ is not used directly, but is useful for checking pile-up effects. Events occurring after $6\,\mu s$ were also not analysed. A few small corrections are needed, but on the whole, the experiment is free of systematic trip wires.

Capture is expected to occur from a mixture of the hyperfine states. A hyperfine transition is highly unlikely because the energy difference between the hyperfine states is 1.5 eV whereas the ionization potential for hydrogen (or really pseudotritium) is 13.6 eV. Now in a naive theory you would not expect a difference in the capture rates between the hyperfine states as helium-3 is approximately a neutron with the two protons anti-aligned. However, the magnetic moment of ^{3}He is -2.128 nm, to be compared with that of a free neutron of -1.91 nm, so there are corrections to this simplistic model.

Calculations indicate that for the triton channel [232] $\Delta\lambda_t = 578\,s^{-1}$ and for the total rate $\Delta\Lambda = 450\,s^{-1}$ [233]. Using these estimates, Ackerbauer was able to search for non-exponential

effects in their time spectrum and obtained a hyperfine transition rate of $\Lambda_H = 0.006\ (8)\,\mu s^{-1}$, which is consistent with no transition as expected, and introduces no errors in their measurement. Equally well, they were able to search for possible effects of muons in the $2s$ state, but they showed that there was no effect, consistent with rapid $2s$ quenching (< 50 ns).

Thus the experimental value for muon capture for a statistical population of the hyperfine states has an accuracy of 0.27%. Almost as remarkable is that Congleton and Fearing [232] had studied this problem several years before and had obtained an estimate of

$$\text{Impulse approximation}, \lambda_t = 1304\,s^{-1}\ , \tag{4.35}$$

$$\text{Elementary particle model}, \lambda_t = 1497 \pm 21\,s^{-1}\ . \tag{4.36}$$

The impulse approximation was known to give low estimates; the elementary particle model (EPM) gave perfect agreement. As indicated for deuterium, the EPM is a phenomenological estimate which uses other experimental data to describe the process. Thus muon capture on ^{3}He giving ^{3}H is parameterized with four form factors F_V, F_M, F_A and F_P which have to be obtained at the relevant four momentum transfer of $q_0^2 = -0.954 m_\mu^2$. The vector and magnetic form factors F_V and F_M were estimates from elastic electron scattering off ^{3}He and ^{3}H using the conserved vector current (CVC) theorem. The values were

$$F_V(q_0^2) = 0.834\ (11)\ , \tag{4.37}$$

$$F_M(q_0^2) = -13.97\ (5)\ . \tag{4.38}$$

For the axial form-factor F_A, it is possible to use tritium beta-decay, which gives $F_A(0)$, and then to make a significant extrapolation to give

$$F_A(q_0^2) = 1.052\ (10)\ . \tag{4.39}$$

The final pseudoscalar form-factor can then be estimated from PCAC to be

$$F_P^{PCAC}(q_0^2) = 20.7 \pm 0.2\ . \tag{4.40}$$

An alternative route is to take the experimental result and the previous form-factor values to obtain

$$F_P^{exp}(q_0^2) = 20.8 \pm 2.8\ , \tag{4.41}$$

where the principal contribution to the error is uncertainty on F_A, not the experimental error.

In any case the overall situation is quite clear that the weak interactions of the muon can be obtained from other interactions; something that we addressed earlier, but now the test is valid to 1.5%, which is better than any before, by far.

The impulse approximation calculation has been refined by Congleton and Truhlik [234]. They used techniques developed in the study of muon capture on the deuteron. Many of the parameters which are needed are not known very well, and there are also uncertainties in the nuclear wave functions. They start with the Argonne v_{14} potential (AV14) which is a potential for nuclear calculations which has 14 operators, describing NN channels. Congleton and Truhlik then add the Tucson–Melbourne three-body force (3BF) which improves the three-body results in general. For the meson exchange forces they found that the axial delta-excitation currents

and the vector π-pair (contact) term make the largest contribution. With many tests to check the model dependence they obtain a final result of

$$\lambda_t = 1502 \pm 32 \,, \tag{4.42}$$

which is quite satisfactory.

A rather different approach was taken by Mukhopadhyay and Junker [235]. They take the main weak interaction terms as known, and then solve for the strong pseudoscalar coupling parameter for π–^{3}He–^{3}H. They obtain $G^{\text{eff}}(m_\pi^2) = 45.8 \pm 2.4$ at the pion pole, which is more accurate than (but consistent with) the results of the dispersion relation analysis of $\pi^{\pm}\,^3$He scattering.

One must be careful however; there is only one experimental result, so only one piece of information can be derived. It is still a matter of judgement which logic flow is the most advantageous, but it is clear that the measurement is a very valuable contribution.

The capture rates for the other channels are poorly known. One has to go back to early measurements of Zaimidoroga et al. [236], for a high pressure diffusion chamber and of Auerbach et al. [237], using ^{3}He gas as a scintillator. The results are not of high precision but in agreement. For the total capture rate, they obtained [236,237]:

$$\begin{aligned} \Lambda_{\text{He}} &= 2140 \pm 180\,\text{s}^{-1} \text{ [236]} \\ &= 2170^{+170}_{-430}\,\text{s}^{-1} \text{ [237]} \end{aligned} \tag{4.43}$$

and the sum of the break-up channels as

$$\begin{aligned} \lambda_p + \lambda_d &= 660 \pm 160\,\text{s}^{-1} \text{ [236]} \\ &= 665^{+170}_{430}\,\text{s}^{-1} \text{ [237]} \,. \end{aligned} \tag{4.44}$$

The estimate of Phillips et al. [238],

$$\lambda_p = 209\,\text{s}^{-1} \,, \qquad \lambda_d = 414\,\text{s}^{-1} \,, \tag{4.45}$$

which is in good agreement. (Their estimate for λ_t was $1433 \pm 60\,\text{s}^{-1}$, which is reasonable.)

An interesting comparison can be made with the similar pion induced reactions

$$\begin{aligned} \pi^- + {}^3\text{He} &\to \pi^0 + t \\ &\to \gamma + t \\ &\to \gamma + d + n \\ &\to \gamma + p + n + n \,. \end{aligned} \tag{4.46}$$

These have been studied by several authors. The most recent experiment [239] which detected the photons directly with a high resolution NaI gave

$$\begin{aligned} P_3 = \frac{\omega(\pi^-\,^3\text{He} \to \pi^0 t)}{\omega(\pi^-{}^3\text{He} \to \gamma t)} &= 2.83 \pm 0.07 \text{ (exp)} \\ &= 2.74 \pm 0.23 \text{ (theory)} \end{aligned} \tag{4.47}$$

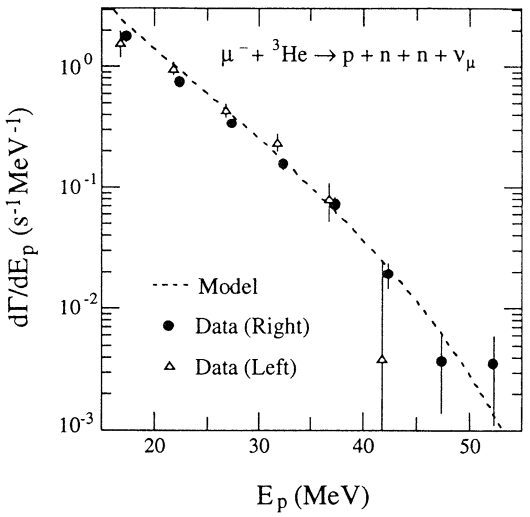

Fig. 4.3. Experimental proton spectrum from muon capture on ^{3}He by Kuhn et al. [242].

and

$$B_3 = \frac{\omega(\pi^- \, ^3\mathrm{He} \to \gamma nd + \gamma nnp)}{\omega(\pi^- \, ^3\mathrm{He} \to \gamma t)} = 1.35 \pm 0.11 \ (\mathrm{exp})$$
$$= 1.05 \pm 0.30 \ (\mathrm{theory}) \, . \tag{4.48}$$

The theoretical results of Phillips and Roig [240] have been added. It is interesting that this second ratio is rather different from the similar ratio in muon capture

$$B_3^{\mu} = \frac{\omega(\mu^- \, ^3\mathrm{He} \to \nu nd + \nu nn p)}{\omega(\mu^- \, ^3\mathrm{He} \to \nu t)} = 0.44 \pm 0.11 \ (\mathrm{exp})$$
$$= 0.43 \ (\mathrm{theory}) \, . \tag{4.49}$$

(We have taken the calculation of Phillips et al. [238], for all three channels as meson exchange effects were neglected in all; an uncertainty is hard to estimate now.)

There have been studies by Kuhn et al. [242] of the energy spectra of the proton and the deuteron channels from muon capture on ^{3}He. The experiment used a cooled gas target at 1 atm pressure giving a density of 11 mg cm^{-3}. A silicon detector was used in the cryostat, followed by a plastic scintillator and wire chambers outside. The set up meant that the proton energy threshold was about 17 MeV and the deuteron threshold about 20 MeV. The background from muon decay electrons is very serious as they are more prolific by a factor of 10^5, so great care had to be taken to identify and reject them. The proton spectrum is given in Fig. 4.3. Remember that most of the protons will have an energy below the experimental threshold. To model the interactions Kuhn et al. took information from the ^{3}He$(e, e' p)$ reaction [243] to estimate the momentum within the ^{3}He, and using the plane-wave impulse approximation (PWIA), they were able to predict the proton energy distribution from muon capture; this is the dashed line, which is in remarkable agreement with the data. More recent data on the ^{3}He$(e, e' p)$ reaction have become available [244], but the agreement is reasonable though some difference is apparent.

For the deuteron channel their estimate was not as satisfactory but a recent calculation of Skibiaski et al. [245], included final state interactions and obtained very good agreement.

There are many other observables in the capture of muons by ^{3}He. One can have polarized muons, polarized ^{3}He, or both polarized [98]. These experiments are very difficult, but capture on a polarized target has been achieved at TRIUMF [241]. The asymmetry of the triton was small, but clearly observed.

4.4. Helium-4

There have been no recent studies of ^{4}He which has a very low capture rate and is thus difficult to study. The possible reactions are

$$\begin{aligned}\mu^- + {}^4\mathrm{He} &\to t + n + \nu \quad (97.75\%)\\ &\to d + n + n + \nu \quad (2\%)\\ &\to p + n + n + n + \nu \quad (0.25\%)\,. \end{aligned} \tag{4.50}$$

The experiments go back to the days of helium bubble chambers and helium gas scintillating targets; the results for the total capture rate are [246,237,247]

$$\begin{aligned}\Lambda &= 336 \pm 75 \text{ [246]}\\ &= 375^{+30}_{-300} \text{ [237]}\\ &= 364 \pm 46 \text{ [247]}\,. \end{aligned} \tag{4.51}$$

The only detailed theoretical study was that of Caine and Jones [248] in 1963. They estimated the branching ratios for the different channels as given in Eq. (4.50), but caution that the numbers are "of qualitative significance only". However, they are in agreement with the intuitive pole-term concept in which most reactions can be described by the muon interacting with a single proton, and the resulting neutron being ejected from the nucleus. (Also there are no bound states in ^{4}H to complicate the issue.) The estimate of Cain and Jones for the total capture rate was $345 \pm 110\,\mathrm{s}^{-1}$. Walecka [249] has also given an estimate of $278\,\mathrm{s}^{-1}$ using the Foldy–Walecka sum rules for the giant dipole excitation. His values for ^{12}C and ^{16}O agree with experiment to better than 10%.

4.5. Total capture rate

The total capture rate for negative muons is simple to define, and relatively easy to measure, but quite perplexing to calculate. Even though apparently straightforward to measure, the experimental measurements are often inconsistent and in some key cases there are few measurements.

For a few low mass cases like helium, the experimental method is to sum the various reaction channels. However, in the vast majority of cases the technique is to measure the apparent lifetime of a negative muon that stops in the element in question, some typical examples are given in Table 4.2. The muon has only two choices, to decay or to capture on the nucleus and the rates simply add. Thus

$$\Lambda_\mathrm{t} = \Lambda_\mathrm{c} + Q\Lambda_\mathrm{d}$$

Table 4.2
Some illustrative total capture rates for μ^- in nuclei. Also given is the mean lifetime. For the hydrogen isotopes, molecular formation complicates the situation. For other light elements (He, Li, Be, ^{10}B) the capture rate is the statistical average of the hyperfine states except for those marked (lhfs), i.e., lower hyperfine state. For $Z > 15$ the rate is always for the lower hyperfine state

Z (Z_{eff})	Element	Mean-life (ns)	Capture rate $\times 10^3$(s^{-1})	Huff factor	Ref.
	μ^+	2197.03 (4)	455.16		[14]
1 (1.00)	^{1}H	2194.90 (7)	0.450 (20)	1.00	[23]
	^{2}H	2194.53 (11)	0.470 (29)		[211]
2 (1.98)	^{3}He	2186.70 (10)	2.15 (2)	1.00	
	^{4}He	2195.31 (5)	0.356 (26)		
3 (2.94)	^{6}Li	2175.3 (4)	4.68 (12)	1.00	[250]
	^{7}Li	2186.8 (4)	2.26 (12)		[250]
4 (3.89)	^{9}Be	2168 (3)	6.1 (6)	1.00	[183]
5 (4.81)	^{10}B	2072 (3)	27.5 (7)	1.00	[183]
	^{11}B (lhfs)	2089 (3)	23.5 (7)	1.00	[183]
6 (5.72)	^{12}C	2028 (2)	37.9 (5)	1.00	[183]
	^{13}C	2037 (8)	35.0 (20)		[183]
7 (6.61)	^{14}N	1919 (15)	66 (4)	1.00	[183]
8 (7.49)	^{16}O	1796 (3)	102.5 (10)	0.998	[183]
	^{18}O	1844 (5)	88.0 (14)		[183]
9 (8.32)	^{19}F (lhfs)	1463 (5)	229 (1)	0.998	[183]
13 (11.48)	^{27}Al (lhfs)	864 (2)	705 (3)	0.993	[183]
14 (12.22)	^{28}Si	758 (2)	868 (3)	0.992	[183]
20 (16.15)	Ca	334 (2)	2546 (20)	0.985	[183]
40 (25.61)	Zr	110.4 (10)	8630 (80)	0.940	[183]
82 (34.18)	Pb	74.8 (4)	12985 (70)	0.844	[183]
83 (34.00)	Bi	73.4 (4)	13240 (70)	0.840	[183]
90 (34.73)	Th	77.3 (3)	12560 (50)	0.824	[251]
92 (34.94)	U	77.0 (4)	12610 (70)	0.820	[252]

where

$$\Lambda_{\text{t}} = (\tau_{\mu^-})^{-1} \quad \text{and} \quad \Lambda_{\text{d}} = (\tau_{\mu^+})^{-1} \,. \tag{4.52}$$

t denotes total, d denotes decay, and Q is the Huff factor [253], which is a small correction which takes into account the fact that the normal muon decay rate is reduced for a bound μ^-, the main effect being that the binding energy reduces the energy available, but there are other smaller effects such as relativistic time dilation. The numerical value of the Huff factor is presented in Table 4.2. There have been attempts to measure the branching ratios and thereby the Huff factor with mixed results [254]. The tendency has been to sweep these problems under the rug, and to assume that the calculation is more dependable than some of the experiments. It should be noted that not only the absolute rate of the muon decay is affected in the atomic state, but also the electron spectrum. For heavier elements the average electron energy is lower,

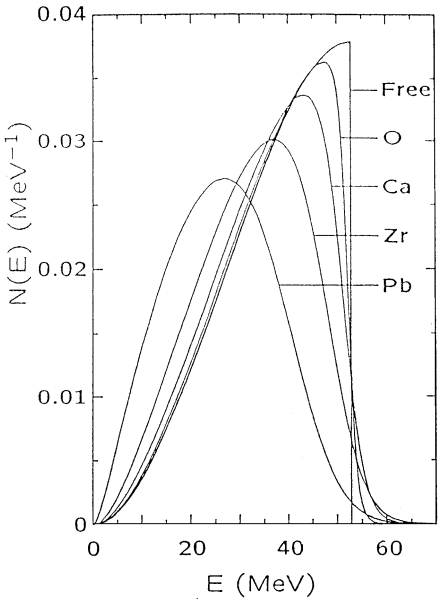

Fig. 4.4. Electron energy spectra for a free muon decay, compared to that for a μ^- bound in O, Ca, Zr and Pb from Watanabe et al. [256].

plus there is a small tail going to energies higher than the 53 MeV allowed in free muon decay. Some selected spectra, calculated by Watanabe et al. [256], are illustrated in Fig. 4.4.

With any measurement that appears simple, the experiments tend to push the limits, often beyond the actual dependability of the equipment. This was often true of some of the early experiments on μ^- lifetimes, which quoted statistical errors without worrying about systematic effects. In particular a lot of the early experiments were on machines with very poor duty cycles and count-rates were contributing to the systematic problems. Most clocks are very dependable, so the problem does not lie there. A typical problem is that there cannot be a second muon in the equipment whilst the first is being studied. These tend to shorten the measured lifetime. If there is a background from the carbon in the counters, or a general background, this tends to lengthen the measured lifetime. Magnetic fields at the experimental target can cause rotation of the muon spin. The actual bias depends on the set up, especially the electronic sorting of events. However, the present agreement for the μ^+ lifetime shows that with care, modern techniques can deliver dependable results. Unfortunately such care has not been lavished on nuclear capture, so serious discrepancies remain.

For light nuclei, the best technique is to detect the electron decay and several experiments have given reasonably consistent results [250,183,189]. For heavier elements neutron detection is quite effective and the extensive measurements of the SREL group are still the best available [255,257]. For elements measured by both the TRIUMF group of Suzuki et al. [183], and the SREL group, the agreement is quite satisfactory. There are however many other experiments and for some elements there is an inconsistency that cannot really be resolved, for example ^{9}Be, ^{13}C, and ^{14}N. In addition it is inadvisable to trust the claimed error of Lathrop et al. [258].

This was an early experiment with a poor duty cycle machine; moreover their lifetime and capture rate for ^{27}Al are inconsistent. However, if we set aside this measurement, there is only the measurement of Suzuki et al. [183], with any precision for the important elements: Mg, Al, Si and P. The reader should use the compendium available in their publication for any study of experimental measurements of the total capture rate.

Since the measurement of Suzuki et al., there have been only three new experiments, all carried out at PSI, that of Wiaux et al. [189], on ^{11}B, that of David et al. [259], on Pu and Np, and that of Hänscheid et al. [252], on uranium isotopes and ^{237}Np. All are very useful additions. Wiaux et al., have clarified the hyperfine rate in ^{11}B and clearly differentiated the capture rate in the two hyperfine levels. The measurements of David et al., and Hänscheid et al., have clarified the results for very heavy elements. In a few elements (Th, U, Np, Pu), the muon's atomic transition can induce fission of the nucleus. Then a few of the muons end up on lighter nuclei, so their lifetime is longer. Thus measurements which detect electrons or neutrons obtain an apparent lifetime a few nanoseconds longer than that for the original nucleus. The best way to measure the capture rate on such nuclei is thus to observe the fission induced by the capture of the muon and this eliminates muons transferred to a lighter element. Of course, sometimes one needs the apparent lifetime observed via neutrons or electrons, and then the other experiments should be used.

To understand the total capture rate for muons, one has to go back first to the phenomenological approach of Primakoff who established the main components for a comprehensive understanding of the major effects. Even though the rates vary from 450 to $12.6\times10^6\,\mathrm{s}^{-1}$, only a few simple concepts are needed for a basic understanding of this phenomenon. First it is assumed that the muon capture on a proton of the nucleus is slow, and therefore additive, depending just on the overlap of the muon with the nucleus. For light nuclei, the point nucleus concept is sufficient, so there are Z protons and since the radius of the muon orbital decreases as Z^{-1}, the probability of finding the muon at the nucleus increases as Z^3, thus the capture rate increases as Z^4. Because the muon radius soon becomes comparable to that of the nucleus, corrections have to be applied and a Z_{eff} is used to take account of this effect; it is listed in Table 4.2, taken from Ford and Wills [260].

Now for heavy nuclei, there are more neutrons than protons, so it becomes more difficult for protons to transform into neutrons because of the Pauli exclusion principle. Thus, Primakoff used closure over the nuclear states to propose the formula

$$\Lambda_{\mathrm{c}}(A,Z)=Z_{\mathrm{eff}}^4 X_1\left[1-X_2\left(\frac{A-Z}{2A}\right)\right] \tag{4.53}$$

where X_1 is the muon capture rate for hydrogen, but reduced because the neutrino has less energy for nuclear capture. The X_2 term in the bracket takes into account the Pauli exclusion principle. This remarkably simple formula provides a reasonable description of the data, see Fig. 4.5. For the Primakoff formula a typical fit gives

$$X_1=170\,\mathrm{s}^{-1}\quad\text{and}\quad X_2=3.125\,. \tag{4.54}$$

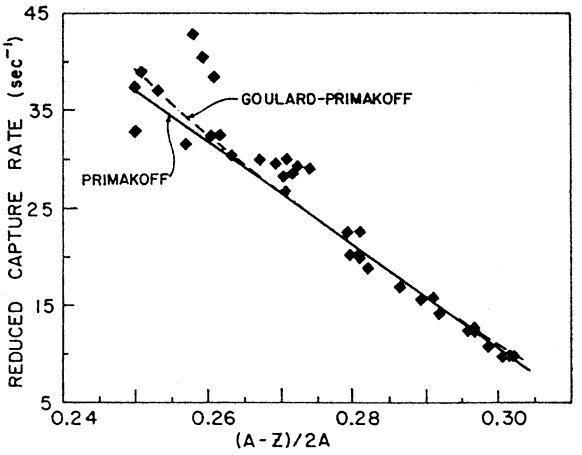

Fig. 4.5. Comparison of the muon total capture rate with the Primakoff formula Eq. (4.53), and the Goulard–Primakoff extension, Eq. (4.55). The data are those of Suzuki et al. [183].

Table 4.3
Fitted parameters for the Goulard–Primakoff formula, Eq. (4.55)

	Number of data	G_1	G_2	G_3	G_4
Pre-TRIUMF data [149]	58	252	−0.038	−0.24	3.23
TRIUMF data [149]	30	261	−0.040	−0.26	3.24
World set 1990 [252]A	91		−0.020	−0.23	3.25
World set 1990 [252]B	91		0.8	−0.02	6.5

Goulard and Primakoff then extended this formula, adding two more terms, viz:

$$\Lambda_c(A,Z) = Z_{\text{eff}}^4 G_1 \left[1 + G_2\frac{A}{2Z} - G_3\frac{A-2Z}{2Z} - G_4\left(\frac{A-Z}{2A} + \frac{A-2Z}{8AZ}\right)\right] . \tag{4.55}$$

This provides a very slight improvement to the description of the data and is given as the dashed line in Fig. 4.5. Two data sets were selected by Suzuki et al., and the fitted parameters are given in Table 4.3. Hänscheid et al., added their new data and obtained similar fits, set A, but then they gave equal weighting to the data points which gives more importance to their new data on the uranium isotopes, and they obtained a totally different parameter set, set B, also given in Table 4.3. This pattern is preferable from the theoretically point of view, but gives a very similar description of the data. Neither set correctly describes the medium mass elements, especially around $Z = 30$ and 55, and so clearly other effects are more important and are distorting this type of fit.

Using the parameters obtained by Hänscheid et al., it is possible to plot the fit in a different manner to bring out other features. In Fig. 4.6 is presented another reduced capture rate, this time defined as

$$\Lambda(\text{reduced}) = \frac{\Lambda_c^{\text{exp}} Z}{Z_{\text{eff}}^4} \tag{4.56}$$

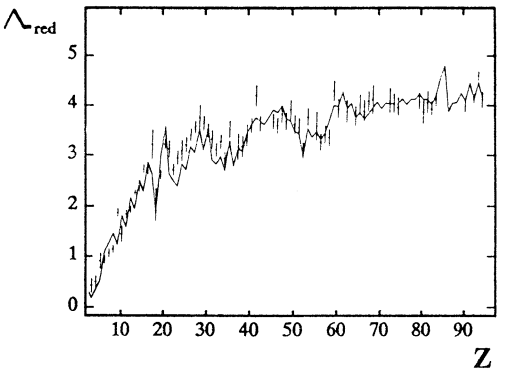

Fig. 4.6. The experimental data for the reduced muon total capture rate (effectively Eq. (4.56)), are compared with the Goulard–Primakoff formula using $G_2 = 0.8$, $G_3 = -0.02$, and $G_4 = 6.5$; taken from Hänscheid et al. [252].

and it is plotted against the atomic number Z. The experimental data are compared with the prediction of the Goulard–Primakoff formula, using the parameter set B of Hänscheid et al. There is a noticeable improvement over the other parameters sets for fitting the region $Z > 82$ (see Fig. 6 of Suzuki et al. [183], for comparison).

Certain aspects such as a clear odd–even Z effect are not described well by the Goulard–Primakoff formula with either parameter set, thus the closure method, inaugurated by Primakoff gives a reasonable, but not perfect, description of the phenomenon.

Many other attempts have been made to calculate the total muon capture rates and we shall focus on more recent publications. The earlier history is more fully described in the reviews by Cannata [8], Mukhopadyay [13] or Walecka [249]. An alternative approach to that of Primakoff was the use of sum rules. This did not work too well until Foldy and Walecka pointed out the importance of the giant resonances on the capture process, and the agreement was much improved, being applied especially to even–even nuclei. Some typical results are given in Table 4.4 and we have taken the revised numbers, published by Walecka [249] to illustrate the effectiveness of this technique. It was pointed out by Cannata et al. [263], that the giant dipole resonance was not the best one to use, but the spin–dipole (1^-) resonance which is a few MeV above the classical electric giant dipole resonance. Their results are also given in Table 4.4 and are a slight improvement over the initial work, especially for ^{4}He and ^{40}Ca.

Early attempts to use the shell-model failed by a factor of two, and it became clear that effective interactions modified the results. Auerbach and his collaborators [264–266] have thus used the random phase approximation with Skyrme-type forces and have obtained excellent agreement with experiment. Their values are given in Table 4.4; using a similar approach, Kolbe et al. [267], have obtained the same type of agreement. Of particular interest is that the most recent publication [266] addresses the problem of neutrino charge exchange cross-sections at the same time, and similar (but not identical) parameters are needed to obtain agreement with experiment. Interest continues with recent studies by Kolbe et al. [268], and by Junker et al. [269]. Most still overestimate the heavy elements.

Another approach is to treat the nucleus as a Fermi sea of nucleons. Initial attempts within this framework also gave values which were a factor of two too large. However, Chiang [262] and collaborators showed that one needs a strong nuclear renormalization of the g_A operator,

Table 4.4
Comparison of some experimental total capture rates with some illustrative calculations by Mukhopadhyay et al. [261], Chiang et al. [262], Cannata et al. [263], Walecka and Foldy [249], and Auerbach et al. [264–266]. All values are given in units of $10^3\,s^{-1}$

Nuclide	Experiment	Eq. (4.53)	[261]	[262]	[263]	[249]	[265,266]
^{4}He	0.356 (26)	0.59			0.300	0.278	
^{6}Li	4.68 (12)	3.01	4.68	4.73			
^{7}Li	2.26 (12)	1.48	3.4	3.4			
^{9}Be	6.1 (6)	5.6	8.84	10.6			
^{12}C	37.9 (5)	40	36	49	34[a]	36	34
^{13}C	35.0 (20)	29	30	38			
^{14}N	66 (4)	71	87	88			
^{16}O	102.5 (10)	117	116	146	98	107	102.5
^{18}O	88.0 (14)	71	90	115			
^{40}Ca	2546 (20)	2530		2771	2520	3180	2480
^{90}Zr	8630 (80)	9644		7194			9290
^{208}Pb	12985 (70)	12399		15338			13930

[a]We have added $6000\,s^{-1}$ to the published calculation to take account of the ground-state transition and to compare more fairly with Walecka's value.

and that this is caused by effective interactions in the nuclear spin–isospin channel. Chiang et al., completed their calculations for the whole of the range of elements and some results are given in Table 4.4. For the heavier elements the agreement is not perfect, but is a significant improvement over earlier attempts with this method. The most recent contribution with this technique has been the work of a similar team [261] who focussed on the lighter nuclei. They improved details of the calculation, in particular accounting for the experimental Q-value, which is important for light nuclei. They also calculate the (ν_e, e^-) and (ν_μ, μ^-) reactions and emphasize the important role of muon capture in providing well established experimental results for comparing with such calculations.

The lesson to learn from these calculations is that we can take the weak interactions for granted, but the presence of the nucleus in muon capture has profound effects, which can change the rate by a factor of two. Different approaches use slightly different language to describe this, but the effect is clear.

4.6. General features in nuclei

4.6.1. The (π^-, γ) reaction as a model

The best way to approach an understanding of the general picture for muon capture is to focus on the neutrino energy spectrum. This has been calculated by several authors, but unfortunately no experimental data are available. Neutrinos are very rarely detectable, and only in the most favourable circumstances. Nevertheless there is a very similar reaction which can serve for a model, viz. radiative pion capture at rest, the (π^-, γ) reaction. It is important to realise that detailed comparisons need sophisticated calculations to guide one's path, but in a general way

the reactions bear a close resemblance. Both start from an exotic atom, thus at rest, with particles of similar mass. The photon and neutrino both leave the nucleus cleanly, with no further interactions, and the interaction with the nucleus tends to be a spin flip transition. The major difference, which is important, is that the muon is always absorbed from the $1s$ atomic state, whereas even for light elements like carbon, the pion is beginning to be absorbed at the $2p$ atomic level and by sodium or magnesium, effectively no pions reach the $1s$ orbit, thus the initial angular momentum configuration is different, opening up more possibilities for the (π^-,γ) reaction. Nevertheless we shall use this reaction as an initial guide.

From the experimental point of view the (π^-,γ) reaction has been studied using pair spectrometers. One group under Crowe started at Berkeley and continued at LAMPF. Another group worked at PSI and obtained a slightly better energy resolution of about 800 keV at the γ-ray energy of 130 MeV or so. This is sufficient to separate transitions to bound levels in light nuclei, but is of limited use for medium or heavy nuclei. To obtain this resolution, however, one has to have a thin converter and thus a low absolute acceptance $\sim 4\times10^{-5}$ of 4π. Added to this is the fact that the reaction under study is typically only 2% of the reactions undergone by a stopped pion [270]. It is thus not surprising that only about 20 nuclides have been studied.

The early work was reviewed by Baer et al. [271], and later by Gmitro et al. [272]. The most recent references are those of Strassner et al. [273], who studied ^{16,18}O and Perroud et al. [274], who studied ^{6,7}Li, ^{9}Be, ^{10,11}B, ^{12}C and ^{14}N with the best energy resolution to date (720 keV for some nuclides). We shall refer to some of these spectra when discussing particular cases. They also had data for some heavier nuclei, in particular ^{28}Si, but these were not published, apart from Conference Proceedings and Annual Reports. For the moment let us use Fig. 4.7 from Baer et al., to point out the general features.

The energy spectrum for the (π^-,γ) reaction shows two distinct characteristics. These are narrow peaks, superimposed on a broad peak extending to high excitation energies. The narrow peaks are subdivided into transitions to bound levels and transitions to broader giant resonances at about 20 MeV. This distinction is not clear in Fig. 4.7 but will become important. The broad peak is due to a quasi-free knock-out of the neutron directly implicated in the capture process and is called the "pole-term". This tends to peak at 20 MeV above the ground-state and is difficult to distinguish from the highly excited giant resonance states. The curves in Fig. 4.7 are estimates of this effect taking into account the Fermi motion of the proton on which the capture occurs, and the binding energy of the resulting neutron. A "phase-space" description gives a poor fit to the observed spectra, see curve P.S. in Fig. 4.7(a) for Li.

The neutrino spectrum for (μ^-,ν) will look fairly similar to these (π^-,γ) spectra, except that it reaches only 95 MeV or so, because the mass of the muon is 34 MeV less than that of a pion. This also implies that the pole-term is less important, because the neutron recoil energy is reduced. Thus, it is not unusual to include this term in the giant resonance excitations and not to distinguish the two mechanisms.

It is worth noting however that, in principle, these are two different mechanisms. This is most easily demonstrated in the case of pion scattering off a nucleus. For pion inelastic scattering off a $T=0$ nucleus, going to pure isospin states, the excitation cross-sections are the same for π^+ and π^-, and in light nuclei, the de-excitation is likely to be n and p emission in equal proportions, (if threshold effects are unimportant). However, if we take quasi-free scattering for

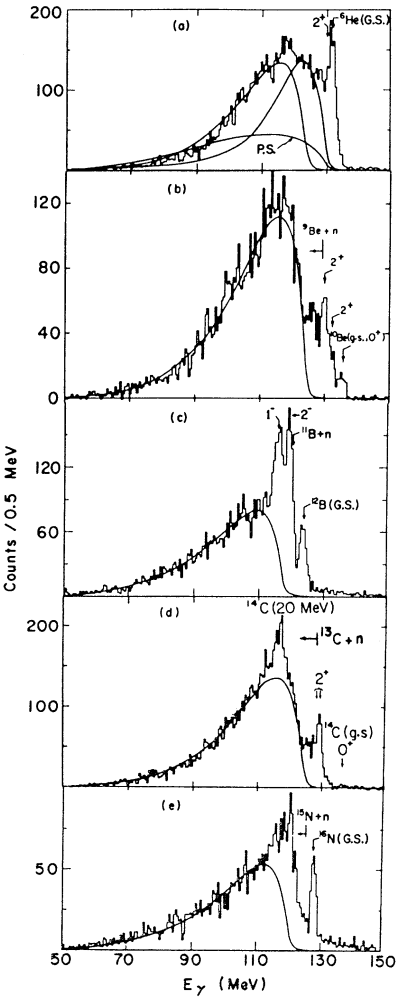

Fig. 4.7. Photon spectra for radiative pion capture (π^-,γ) for ^{6}Li, ^{10}B, ^{12}C, ^{14}N and ^{16}O, taken from Baer et al. [271]. Solid curves are the pole model for neutron knock-out.

about 200 MeV pions, the cross-sections are

$$\frac{\sigma(\pi^+ p)}{\sigma(\pi^- p)} = \frac{\sigma(\pi^-, n)}{\sigma(\pi^+, n)} = \frac{9}{1} \tag{4.57}$$

(or 3 : 1 if the charge exchange channel is included) and the recoil nucleon will be kinematically constrained to go in the direction of the momentum transfer. The reality is that interference occurs and the experimental results are most confusing [275,276]. Thus it would not be surprising if detailed studies of muon capture uncovered complex effects, but no experiment is likely to have the requisite sensitivity.

The only relevant question is what levels are fed in the nucleus that results after the ejection of this nucleon. Giant resonance decay and nucleon knock-out feed similar levels, but resonance decay is the best analogue. Thus the pole term is not necessarily a useful concept for muon capture.

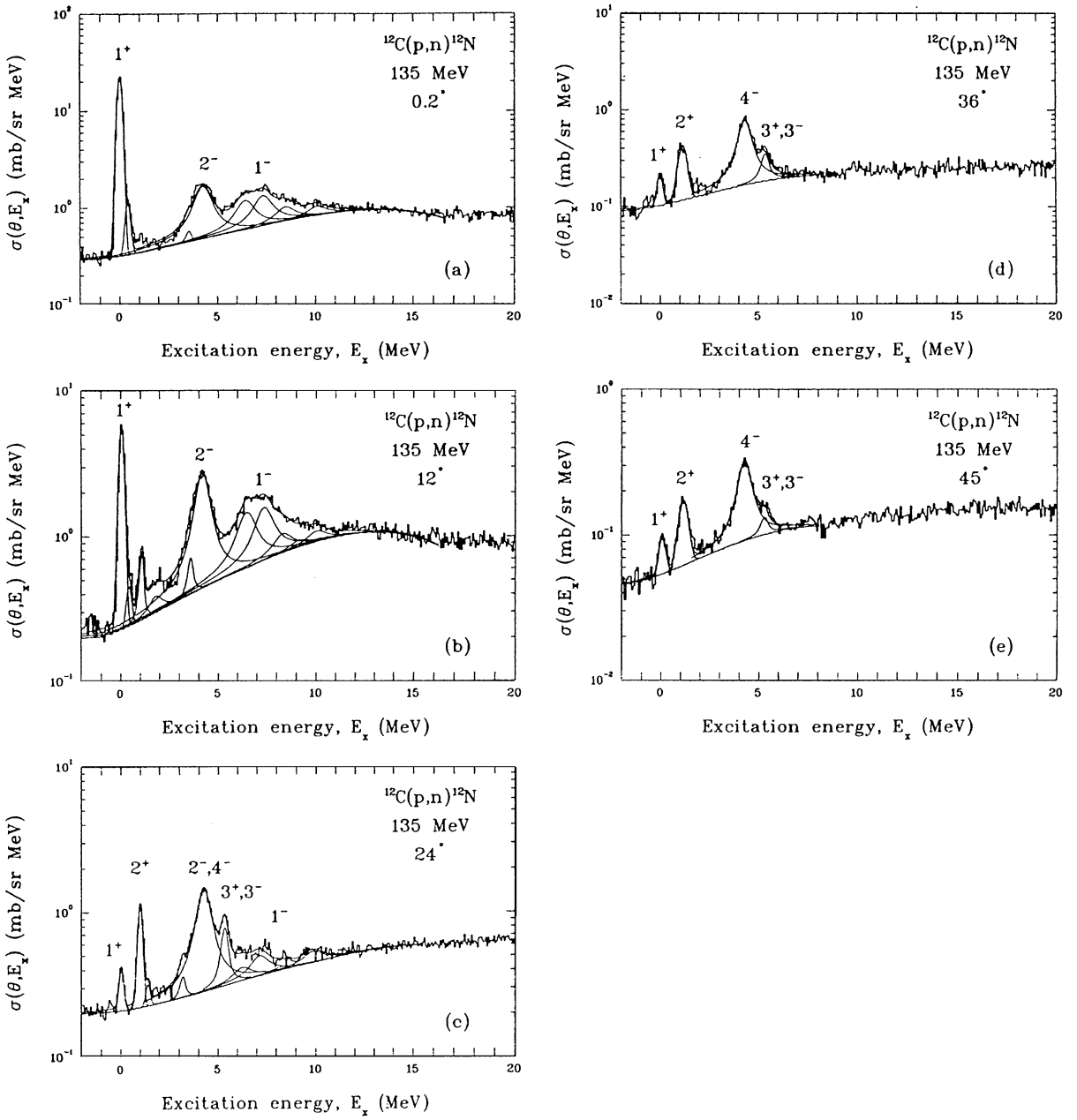

Fig. 4.8. Neutron spectra for the reaction $^{12}C(p,n)^{12}N$ at 135 MeV, with a high resolution of 350 keV out to 36°, and 480 keV at 45°, from Anderson et al. [280]. About 12° is equivalent to muon capture. (The peak at 7.5 MeV is now suspected to be a mixture of 0^-, 1^- and 2^-.)

Table 4.5
The mirror levels in ^{12}N and ^{12}B, with a recommended capture rate for the reaction ^{12}C $(\mu^-, \nu)^{12}$B

J^π	^{12}N energy (MeV)	^{12}N width (keV)	^{12}B energy (MeV)	(μ^-, ν) capture rate (s^{-1})
1^+	0	0	0	6040 (350)
2^+	0.960 (12)	< 20	0.953	210 (100)
2^-	1.191 (8)	118 (14)	1.674	180 (100)
1^-	1.80 (30)	750 (250)	2.621	620 (200)
0^+	2.439 (9)	68 (21)	2.723	(0)
Σ				7050 (270)
Total				37900 (500)

4.6.2. *The* (n, p), (p, n) *and* $(d, ^2\mathrm{He})$ *reactions as models*

The next most useful comparisons are with the (n, p) and $(d, ^2\mathrm{He})$ reactions. If the right kinematic conditions are chosen they feed spin-flip levels in the same manner as muon capture, especially so for the bound levels. This is a very useful comparison, especially for the ground-state transition which cannot be obtained directly in muon capture though it can be inferred in a few cases. There are also many parallels to the opposite charge exchange reaction (p, n), which is equivalent to neutrino induced reactions in nuclei. This topic has recently been reviewed by Ejiri [277].

The (n, p) reaction is simpler, and thus would be preferable in theory, but in practice the $(d, ^2\mathrm{He})$ reaction seems to have more potential. The (n, p) reaction has recently been reviewed by Alford and Spicer [278] in a general discussion of (p, n) and (n, p) reactions at intermediate energies. To compare best with the (μ^-, ν) reaction, one needs an incident nucleon in the range 100–300 MeV, and angles of about 10° which gives a similar momentum transfer of $\sim 100\,\mathrm{MeV}/c$. The (p, n) reaction can be useful for $Z = N$, i.e., $T = 0$ nuclei, but of course the mirror nucleus does not have exactly the same energy levels. The (p, n) reaction is studied using time of flight techniques; excellent data have been produced at IUCF, TRIUMF, to some extent at LAMPF, and more recently at RCNP Osaka. Typically the energy resolution is about 0.5 MeV, although 150 keV has been achieved for ^{16}O for an incident proton energy of 79 MeV [279].

To illustrate the comparison for (p, n) reactions, we give in Fig. 4.8 the spectra obtained by Anderson et al. [280], for ^{12}C$(p, n)^{12}$N at 135 MeV, where the energy resolution is 350 keV up to 36° and 480 keV at 45°. This is a good quality spectrum, yet the energy resolution causes some difficulty when comparing with muon capture. In Table 4.5 we give the mirror energy levels in the mass 12 system [281] for those up to 3.37 MeV for which ^{12}B is bound (all excited states of ^{12}N are unbound). Also given are the capture rates obtained from our re-analysis of the results of Giffon et al. [130], see Table 5.11. The overall comparison is clearly best for 12°; for example the bound levels represent about 1/6 of the spectrum. At 0.2° the 1^+ levels are too dominant and at 24° the higher spin levels are too strong. Detailed comparison however shows that there are differences; for example in the (p, n) reaction, the 2^+ level is thought to dominate over the 2^- at 1 MeV. (Be careful. the apparent peak at 0.5 MeV is an artefact to fit the asymmetric ground-state peak.) The energy resolution of this (p, n) reaction is not sufficient

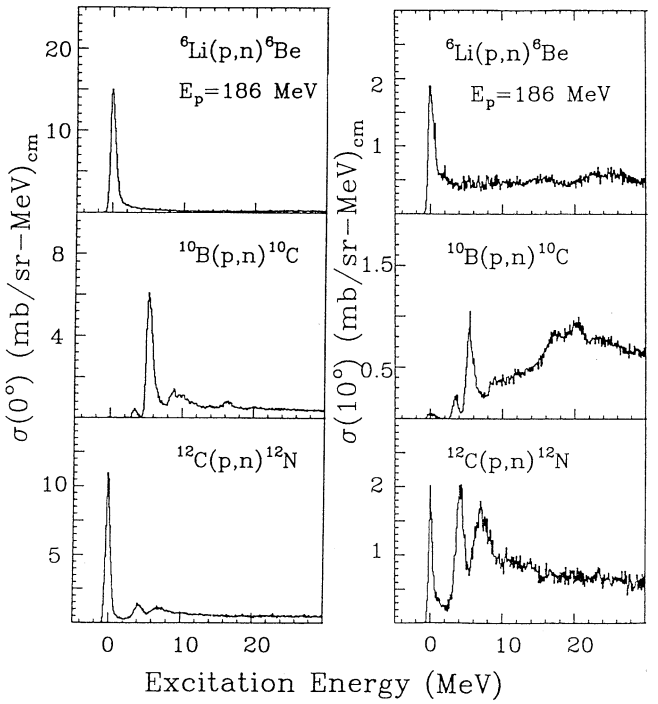

Fig. 4.9. Neutron spectra for several (p,n) reactions on N=Z nuclei. Data are for 186 MeV protons, with a neutron energy resolution of about 1 MeV. The 0° cross-section is mainly 1^+ transitions whereas at 10° spin–dipole resonances $(0^-,1^-,2^-)$ are more noticeable.

to separate the 0.96 and 1.19 MeV levels in ^{12}N, so a comparison is made with the (p,p') reaction in order to make this assertion. Using polarized protons, recent experiments at RCNP have identified the spin-parity of the levels [282].

Other useful (p,n) results are for ^{10}B [283], ^{16}O [279,284], ^{20}Ne, ^{24}Mg and ^{28}Si [285], ^{32}S [286], and ^{40}Ca [287,288]. Unfortunately, it is common practice to present only the 0° spectrum because of the interest in GT strength. For our purposes, this is not the best angle. Most publications do not give the 10° spectra, but the review of Rapaport and Sugarbaker [289] is helpful because they compare the 0° and 10° neutron spectra for ^{6}Li, ^{10}B, and ^{12}C, see Fig. 4.9. The 10° spectra are the closest to muon capture.

For the (n,p) reaction the working energy resolution is at best 1 MeV, often 2 MeV or worse which makes any comparison rather general. The poor energy resolution is caused by fact that the neutron beam is a secondary beam, produced in a primary reaction. The initial experiments at Harvard used the $D(p,n)$ reaction to obtain the neutrons because the cross-section is relatively large, but the intrinsic resolution is then 1.7 MeV at best [290] and 7 MeV in practice [291]. More recent facilities have normally used the ^{7}Li$(p,n)^{7}$Be reaction to produce the neutrons, though the ^{3}H$(p,n)^{3}$He reaction has a larger cross-section and has no excited state transitions. However, the practical disadvantages of a highly radioactive target have outweighed those advantages. The ^{7}Li$(p,n)^{7}$Be reaction at 0° feeds the first excited state of ^{7}Be at 429 keV with a cross-section which is 46% of the ground-state value for 45 MeV [292]. This ratio probably increases with energy, so this would limit the energy resolution achievable with the neutron

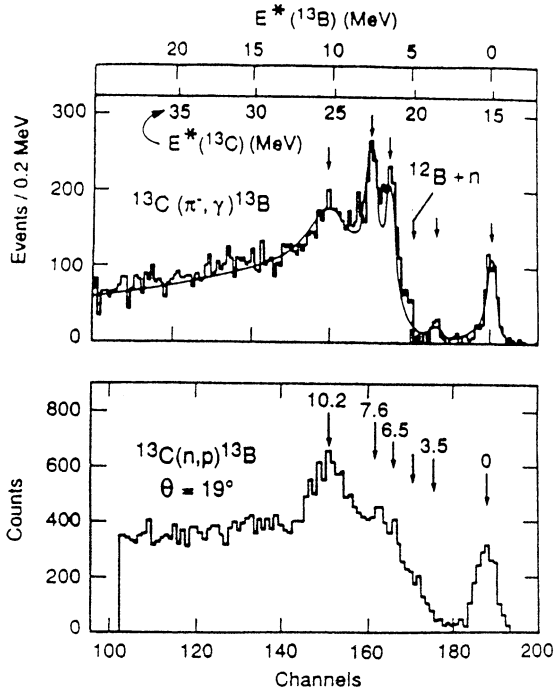

Fig. 4.10. Comparison of the spectra for the reactions $^{13}C(n,p)^{13}B$ and $^{13}C(\pi^-,\gamma)^{13}B$. The (n,p) reaction was at 65 MeV and thus 19° is a reasonable comparison, taken from Wang et al. [298].

beam although present facilities are limited by the target thickness. Such neutron beam facilities have been constructed at Davis, TRIUMF, IUCF and Uppsala, and the working resolution is around 1.5 MeV at Davis, 1 MeV at TRIUMF, and about 2 MeV at IUCF and CELSIUS.

A time of flight type facility was built at the WNR facility at LAMPF with a resolution varying from 1 to 3 MeV [293]; the choice of ^{40}Ca as a target was unfortunate as the experiment by Chittrakarn [288] on the reaction $^{40}Ca(p,n)$ obtained a resolution of about 220 keV and is thus more useful for our purposes. Similarly their ^{32}S measurement [294] is overshadowed by the measurement of $^{32}S(p,n)^{32}Cl$ [286]. Their other choices of ^{6}Li, ^{12}C, ^{13}C [295], and of ^{64}Ni [296] were also sorely handicapped by the energy resolution. The Uppsala data at 100 MeV have been reviewed by Olsson [297]; again the energy resolution is a problem. As an illustration we present a comparison of the $^{13}C(n,p)^{13}B$ and $^{13}C(\pi^-,\gamma)^{13}B$ reactions in Fig. 4.10 taken from the Davis experiment of Wang et al. [298], who studied the $^{13}C(n,p)^{13}B$ reaction at 65 MeV. They chose the 19° spectrum to equalize the momentum transfer for the (π^-,γ) reaction. (Similar results on the $^{13}C(n,p)^{13}B$ reaction were obtained by Martoff et al. [299], at 118 MeV, but with lower statistics.) As indicated on the figure the threshold for $^{13}B \rightarrow {}^{12}B + n$ is at 4.88 MeV, so only 6 excited states can be studied in muon capture. The main structures are above this threshold, as was the case for ^{12}C. Anyway this figure illustrates the strong similarity between these two reactions. The slightly better resolution of the (π^-,γ) reaction is of significant advantage for comparing with muon capture. The resolution achieved at TRIUMF for the (n,p) reaction is about 1 MeV, but they have focussed on heavier elements, where energy resolution is critical, but their results are very useful and we shall return to them.

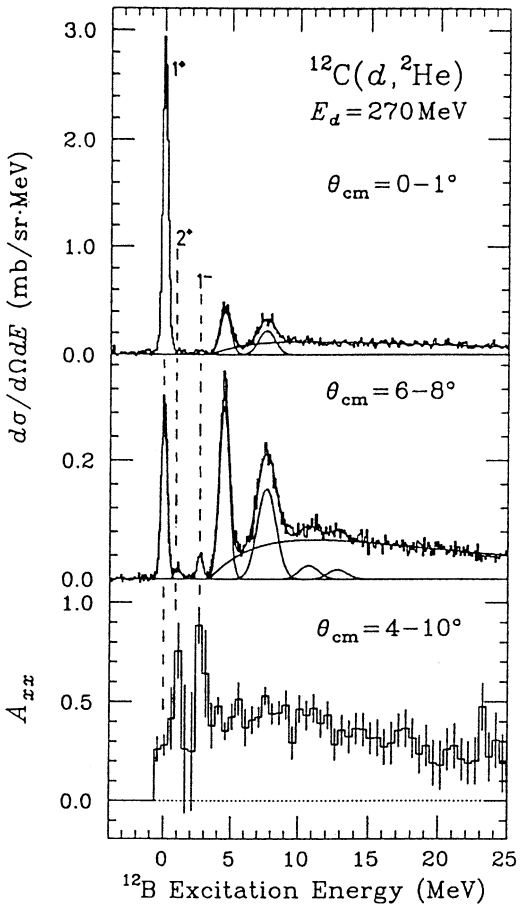

Fig. 4.11. Excitation spectra for the reaction $^{12}C(d,^2He)^{12}B$ with 270 MeV deuterons from Sakai et al. [282,305].

Recently a new tool has entered the arena where an energy resolution of better than 1 MeV has been demonstrated. The $(d,^2\mathrm{He})$ reaction appears strange because the notation ^{2}He is used to designate two protons in a final state interaction. Thus a spectrometer has to detect and measure accurately two co-incident protons which are several degrees apart. At Texas A& M, they use a deuteron beam of 125 MeV and a proton spectrometer which accepts protons for $\Delta\Theta \leqslant 3^\circ$, $\Delta\phi \leqslant 1^\circ$. For an experiment with ^{6}Li, ^{13}C and ^{24}Mg, they obtained an energy resolution of 600–700 keV. The spectra at 0° are almost identical to those for the (n,p) reaction. Unfortunately again they focus on 0°, whereas much higher angles would be preferred for our comparison as the deuteron momentum is only 70 MeV/c. They have also studied ^{26}Mg [300,301] and more recently ^{48}Ti and ^{54}Fe as well [302].

Another facility is in operation at RIKEN, using a 270 MeV deuteron beam. A QQDQD spectrometer, nicknamed SMART, accepts protons a few degrees apart and measures their energy. Initially they had a resolution of about 1 MeV for studying ^{6}Li, ^{12,13}C, and ^{23}Na, [303] but more recently have achieved 460 keV, which is a significant advantage. In Fig. 4.11 we illustrate their results for $^{12}C(d,^2He)$ at 270 MeV, taken from Sakai et al. [282,304]. The similarity to the (p,n)

reaction in Figs. 4.8 and 4.9 is uncanny, so the two nucleon incoming and outgoing channels do not complicate the reaction unduly. The data on the tensor analyzing power A_{xx} are added at the bottom. These confirm the 2^- identification of the peak at 4.5 MeV but indicates 2^- for the strongest component of the peak at 7.5 MeV, as natural parity levels, such as the two small peak of 2^+ and 1^-, have an A_{xx} close to 1. Unfortunately for our purposes, they have concentrated on ^{12}C and taken few spectra on other elements. However, it is clear that this reaction is a very potent tool for studying spin-flip charge exchange reactions. Okamura [305] has been able to reproduce the ^{12}C data very well in his calculations, and also advocates further experiments.

A third facility is in operation at RCNP, Osaka [306]. They use 200 MeV deuterons and detect the two protons in LAS, a Large Angle Spectrometer. They have achieved a very impressive 400 keV for the energy resolution. Again they have concentrated on ^{12}C but also have very useful spectra for ^{10}B and ^{11}B.

4.6.3. *The* $(t,{}^3\mathrm{He})$, $({}^7\mathrm{Li},{}^7\mathrm{Be})$ *and* $({}^{13}\mathrm{C},{}^{13}\mathrm{N})$ *reactions*

Several other charge exchange reactions have been tried. They have been limited by experimental difficulties, but again show remarkable potential. The best data have come from the $(t,{}^3\mathrm{He})$ reaction studied at the NSCL, Michigan, with a 380 MeV beam and a resolution of 160 keV [307,308]. The beam is a secondary beam of $5\times10^6\,\mathrm{p\,s^{-1}}$ and thus experiments are limited by statistics. So far the focus has been on improving the spectrometer and a comparison set using the favourite target, ^{12}C. Spectra with a resolution of 780 keV are also available for ^{9}Be, ^{10,11}B, ^{12}C and ^{13}C [309,310].

The reaction $({}^7\mathrm{Li},{}^7\mathrm{Be})$ seems at first sight to be a strange choice, but several experiments have been performed. At NSCL, Michigan, they have used a 350 MeV beam and obtained a resolution of 1.5 MeV in the S320 spectrometer, studying ^{6}Li, ^{12}C, ^{90}Zr, ^{120}Sn and ^{208}Pb [312,313]. At RCNP, Osaka, they have a 455 MeV beam and have obtained a resolution of about 1 MeV with the Grand RAIDEN spectrometer, for studies of ^{60}Ni [314] and ^{6}Li, ^{12}C, and ^{28}Si [315]. The most powerful part of this reaction is that the ^{7}Be can be excited into its 430 keV state, and if that occurs, the target nucleus must undergo a spin-flip transition. Thus measuring these γ-rays in coincidence distinguishes the $\Delta S=0$ and 1 transitions. Fig. 4.12 shows such a separation for ^{60}Ni. (The shaded area at negative excitation energy is from hydrogen contamination in the target.) The $\Delta S=1$ is close to what would be expected for muon capture. Again the resolution is somewhat of an impediment.

Finally, we mention the reaction $({}^{13}\mathrm{C},{}^{13}\mathrm{N})$ which also favours spin-flip reactions above 1300 MeV. As ^{13}N has no excited state, the reaction is unique. At GANIL they have used a 780 MeV beam which means that some non-spin-flip transitions occur [316]. They have a neutron detector in coincidence with the spectrometer to study the decay of the giant resonances, obtaining an energy resolution of 500 keV and an angular resolution of 0.2°. Only targets of ^{58}Ni and ^{208}Pb were used with limited statistics, so the results are somewhat sketchy. However, there is clearly potential for this reaction.

4.6.4. *Inelastic scattering* (e,e') *and* (p,p')

Another way for exciting magnetic modes is via inelastic scattering. This is most useful for $N=Z$ nuclei and a lot of muon capture data exist for such nuclei, viz, ^{10}B, C, O, Mg, Si, S, and

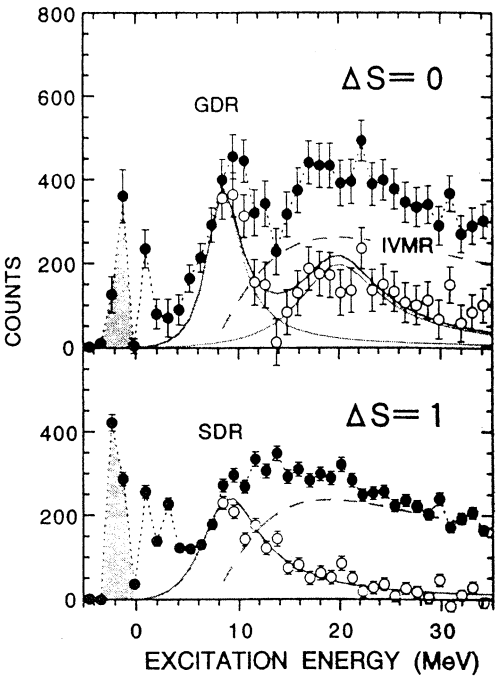

Fig. 4.12. Spin non-flip and spin-flip spectra for the reaction ^{60}Ni(^{7}Li, ^{7}Be)^{60}Co at 65A MeV and at $\sigma < 1.5^{\circ}$. Data are closed circles, and the open circles are the spectra with the background subtracted (the dashed curves). The peak to the left of 0 MeV is due to hydrogen contamination. The data are from Nakayama et al. [314].

Ca. For 180° electron scattering in $N=Z$ nuclei, the $T=1$ operator is about a factor of 100 stronger than the $T=0$ operator. Thus only $T=1$ states are strongly excited, and these are the analogues of those which are important in muon capture. For $T \neq 0$ nuclei this simplicity no longer holds, and levels with the same isospin as the ground-state can be excited, confusing the identifications.

The most extensive set of relevant data is from 180° inelastic electron scattering. Many experiments were performed at the Naval Research Laboratory in Washington, DC, by Fagg and co-workers, and he has reviewed his work and that of many other laboratories (e.g., Stanford, IKO, Orsay, Darmstadt and Saskatoon) [317]. Electron energies in the range 30–100 MeV were found to be useful. Recently constructed facilities at Darmstadt are superb and energy resolutions of 50 keV or better mean that levels can be accurately identified [318].

Similar results can be obtained from proton scattering, but in this case, it is necessary to go to very forward angles to distinguish the spin-flip excitations. The Orsay synchrocyclotron completed several successful experiments for 201 MeV protons at 3–7° in the laboratory [319]. The energy resolution was typically 80–100 keV, and so the data are a useful verification of the electron measurements. More recent results have been reported from RCNP Osaka [320] and LAMPF and IUCF [321] and there is unpublished data from TRIUMF. To clarify the isospin identification it is possible to study deuteron inelastic scattering, (d,d'), for which $\Delta T = 0$.

The difficulty with inelastic scattering is that it is often uncertain which level is the isotopic analogue of the one that is excited in muon capture. Nevertheless these data are important for drawing conclusions about charge exchange reactions or muon capture on $N=Z$ nuclei.

4.6.5. Proton knock-out reactions

We have seen, in the (π^-,γ) reaction, a significant pole term, in which the recoiling neutron is ejected as though it were free. A similar effect is expected in muon capture, although the recoil energy is lower and reduces the quasi-free aspect of this reaction. In any case levels can be excited in the $(A-1)$ nucleus, for example, $^{12}C(\mu^-,\nu n)^{11}B$.

Equivalent reactions are the proton knock-out reactions such as the $(p,2p)$ and $(e,e'p)$ reactions. Both have been studied extensively because of the interest in observing the shell structure of nuclei. For a clean knock-out, the incoming particle should have an energy of several hundred MeV, which then makes it difficult to obtain a good energy resolution in the final state. Early work on the reaction $(p,2p)$ had missing mass resolutions of several MeV, so are not too helpful for muon capture. Recently however significant improvements have been reported. At RCNP in Osaka, they have used 392 MeV protons, and obtained a final state resolution of 350 keV using a two arm spectrometer, Grand Raiden and LAS. A preliminary report by Noro et al. [322], is available for the target nuclei ^{6}Li, ^{12}C, ^{16}O and ^{40}Ca, but no detailed analysis was presented. In an annual report, a resolution of 250 keV was described [323].

More information is available on the reaction $(e,e'p)$, from experiments at NIKHEF and MAMI, for example, see the review by Dieperink and de Witt Huberts [324], or the shorter but more recent ones, by Lapikas [325], Walcher [326] and de Witt Huberts [327]. They typically achieve an energy resolution of 100 keV or so, which can resolve most states in the final nucleus. Many nuclei have been studied, including C, O, P, Ca, V, Zr and ^{208}Pb. From these results, one can obtain the identity of the states most strongly excited, and the spectroscopic factors for them. An alternative reaction, which is also very effective, is the $(d,^3He)$ reaction, which has been extensively studied. The earlier low energy work was difficult to interpret, but the later work for 50 or 70 MeV deuterons has been quite dependable, and gives a comparable pattern of spectroscopic factors to the $(e,e'p)$ reaction, although absolute values can vary somewhat. As energy resolutions of 50 keV or so are possible in the $(d,^3He)$ reaction, it is excellent for our purposes. The (t,α) reaction has sometimes been used, but is not the preferred technique.

When it comes to comparison with muon capture, it is clear that these reactions are useful, but not perfect predictors of the excited state yields. A better comparison is found to hold with the (γ,p) reaction, because the mechanism is more equivalent. In both reactions, levels at 15–20 MeV are excited and decay via proton emission. The slight difference is that γ-rays excite the giant dipole resonance (GDR), whilst the (μ^-,ν) reaction excites the spin dipole resonance (SDR), including some 2^- levels. The experiments on the (γ,p) reaction are not extensive and have their problems. Two techniques are involved. In an early method a bremsstrahlung beam of end point 25 or 30 MeV was used and γ-ray detectors were used to observe the levels excited in the final nucleus. Both (γ,p) and (γ,n) reactions are involved, which causes some confusion, but the (γ,n) yield is often less than the (γ,p) yield for $N=Z$ nuclei. There is also the difficulty that γ-rays can be produced by direct production of a level, or by cascade feeding, but that is a similar problem for muon capture.

A more recent technique has been the direct observation of the ejected protons, using bremsstrahlung difference techniques, or a monochromatic or tagged photon beam. The few experiments which exist are really important for understanding muon capture because the

ground-state transition is observed cleanly, and so are transitions to unbound levels, which give information about the $(\mu^-, \nu 2n)$ reaction.

In general, the situation is that muon capture is the weaker link. Normally, data from one or more of these knock-out reactions is available, and muon capture can be interpreted in the light of this information. However, the energy resolution obtained in muon capture is, of course, more definitive of which is the exact level being excited.

4.7. Neutron production

4.7.1. Neutron multiplicity

We have seen from comparisons with the (π^-, γ) reaction in Fig. 4.7 that muon capture should give nuclear excitations in the range of 10–20 MeV. Now the typical binding energy of a neutron is 8 MeV, so this indicates that many captures will result in the production of one, two, or even more neutrons, as any excitation above the neutron threshold can be assumed to decay via neutron emission. This general picture was confirmed very early on using two different techniques, neutron detection and activation analysis. Both need careful interpretation and comparisons are hazardous, but essential to place these measurements in perspective.

The best experiments are all quite old, but we shall briefly discuss them, as they are an essential basis for understanding more recent results. The neutron detection technique culminated in an experiment by MacDonald et al. [328], at the 184 in Berkeley cyclotron in the early 1960s. A large tank of liquid scintillator was loaded with cadmium and surrounded a target in which the muons were stopped. Pion contamination was $\sim 10^{-4}$ and not important. Neutrons produced in the muon capture process were thermalized and the capture γ-rays recorded in the scintillators. The thermalization time was 7.8 μs, so the process was followed for 35 μs. The efficiency for a single neutron was about 54.5% and was verified using a ^{252}Cf source, although there was some sensitivity to the energy spectrum of the neutrons but it is not of major concern. Multiple neutrons could be detected by this technique, and were the main goal of the experiment. The most accurate measurement is that of the multiplicity and the value is typically 1.5. This is quite well established because, apart from minor corrections

$$\text{observed multiplicity} = \text{efficiency} \times \text{multiplicity} \tag{4.58}$$

and the efficiency is obtained by exactly the same equation for the calibration run with ^{252}Cf, using the known multiplicity of 3.87 (8).

In addition to the overall multiplicity, one also obtains the multiplicity distribution, but this is of lower statistical accuracy and more vulnerable to fluctuations. Even with an efficiency of 54.5% which is excellent from the experimental point of view, it is not really high enough to obtain a reliable multiplicity distribution. Thus the practice arose of comparing calculations to the observed multiplicity and not unfolding the data to obtain the experimental measurement of the actual multiplicity distribution. The difficulty can be illustrated by taking the case of a real 3 neutron event, which will be observed with the distribution of

$$((1-\varepsilon)+\varepsilon)^3 = 0.094N_0 + 0.338N_1 + 0.405N_2 + 0.162N_3\ , \tag{4.59}$$

Table 4.6
Observed neutron multiplicity distributions for a natural Pb target using a counter with an efficiency of 54.5%. Calculated values, corrected for counter efficiency, are from Hadermann and Junker [331], for two choices of effective mass m^*, and from the older calculations of Singer [330] using $m^* = 0.41M$, M being the nucleon mass

	Experiment		Calculated values		
	Kaplan et al. [329]	MacDonald et al. [328]	Hadermann and Junker [331]		Singer model [330]
Multiplicities			$m^* = 0.68M$	$m^* = 0.60M$	
0	0.348 ± 0.100	0.324 ± 0.022	0.362	0.366	0.387
1	0.479 ± 0.057	0.483 ± 0.025	0.470	0.459	0.377
2	0.137 ± 0.027	0.137 ± 0.018	0.154	0.155	0.167
3	0.018 ± 0.012	0.045 ± 0.010	0.014	0.019	0.057
4	0.010 ± 0.005	0.011 ± 0.006	2×10^{-4}	2×10^{-4}	0.011
5	0.005 ± 0.004	—	~ 0	~ 0	0.001

where ε is the efficiency of 0.545 and $N_{0,1,2,3,}$ means that 0, 1, 2, 3 neutrons are detected. Thus, if there are really 3 neutrons, these are all observed only 16% of the time, so the unfolding procedure is very sensitive to errors in the measurements at high multiplicity.

Thus, we shall first take the traditional route and in Table 4.6 present the observed multiplicities for a detector of 54.5% efficiency. Two experiments are given, the most recent by MacDonald et al. [328], and an earlier one by Kaplan et al. [329]. We see that there is excellent agreement, though the older experiment of Kaplan et al., is of lower accuracy. Also included are the older calculation of Singer [330] and the more recent work of Hadermann and Junker [331] for which two values of the effective mass are included. As was indicated earlier, the calculations estimate a distribution of excitation energies, and from the known neutron binding energies obtain the multiplicity. The effective mass is a way of tuning the maximum excitation energy. It was found that evaporation neutrons were not the only mechanism, and thus, Singer introduced the concept of direct neutrons which improved the agreement for the single neutron production.

Now we can take the observed multiplicity and unfold the real multiplicity by using Eq. (4.59) and the equivalent for other multiplicities. However, the observed higher multiplicities are inconsistent and have large fluctuations. Thus to make any sense it is necessary to estimate the highest multiplicity using the models as a guide. We then obtain Table 4.7. Note that the lower multiplicities have large errors, and would be worse if every high multiplicity had been taken from the observations. Also given are the experimental average multiplicities and these do not equate to the multiplicities of the rest of the table because of the necessity of fixing the highest multiplicity.

Now an alternative technique is to measure the activation induced by a stopped muon beam. We consider two experiments, for the moment, though many earlier ones are discussed in these references. Heusser and Kirsten [332] studied muon activation for targets of Mg, Al, Fe, Co and Ni. Natural targets were used, and only for nickel is the result sufficiently comprehensive to be of general use. More recently Wyttenbach et al. [333], studied 18 targets, with a focus on charged particle production. The selection was made, avoiding those targets which had significant activation by neutron production because it is so much stronger. Typical charged

Table 4.7
Actual neutron multiplicity distribution (in %) obtained by unfolding the data of MacDonald et al. [328]. The higher multiplicities have been fixed, using the models as a guide. The average multiplicities are taken directly from the experiment and do not conform to the distribution because it has been adjusted at high multiplicity

	Average multiplicity	0	1	2	3	4
Al	1.262 (59)	9 (6)	75 (10)	5 (10)	9 (6)	0
Si	0.864 (72)	36 (6)	49 (10)	14 (6)	1 (1)	0
Ca	0.746 (32)	37 (3)	54 (5)	8 (3)	1 (1)	0
Fe	1.125 (41)	19 (4)	60 (6)	12 (5)	9 (3)	0
Ag	1.615 (60)	6 (9)	51 (18)	25 (18)	12 (11)	6 (6)
I	1.436 (56)	4 (10)	72 (19)	6 (18)	12 (11)	6 (6)
Au	1.662 (44)	10 (9)	43 (19)	27 (18)	12 (13)	8 (5)
Pb	1.709 (66)	0 (11)	59 (22)	23 (21)	5 (14)	13 (7)

Table 4.8
Activation cross-sections for ^{58}Ni (in %), taken from Heusser and Kirsten [332]. The charged particle probabilities have been estimated from the systematic data of Wyttenbach et al. [333]

No charged particle		Proton production		Alpha production		Neutron distribution	Theory [330]
^{58}Ni$(\mu^-, \nu)^{58}$Co	31.0 (26)	^{58}Ni$(\mu, \nu p)^{57}$Fe	0.2	^{58}Ni$(\mu^-, \nu\alpha)^{54}$Mn	0.2	31.4 (26)	27.3
^{58}Ni$(\mu^-, \nu n)^{57}$Co	58.6 (40)	^{58}Ni$(\mu, \nu pn)^{56}$Fe	1.5[a]	^{58}Ni$(\mu^-, \nu\alpha n)^{53}$Mn	0.1	60.2 (40)	60.1
^{58}Ni$(\mu^-, \nu 2n)^{56}$Co	6.6 (7)	^{58}Ni$(\mu, \nu p2n)^{55}$Fe	1.1[a]	^{58}Ni$(\mu^-, \nu, \alpha 2n)^{52}$Mn	0.1	7.8 (7)	11.9
^{58}Ni$(\mu^-, \nu 3n)^{55}$Co	0.5 (2)	^{58}Ni$(\mu, \nu p3n)^{54}$Fe	0.1[a]			0.6 (2)	0.2

[a] About a fifth of these reactions will have a real deuteron emitted, instead of an independent (pn) pair.

production probabilities are only a few percent of captures, whereas neutron production comprises the rest.

Thus, in Table 4.8 we present the results for ^{58}Ni. The charged particle results have been estimated from the work of Wyttenbach et al., and disagree somewhat with the results of Heusser and Kirsten for the $(\mu^-, \nu\alpha)$ (2.4%) and $(\mu^-, \nu p)$ (2.0%) reactions, but this is a small effect, and not critical for our general discussion. Now in addition Heusser and Kirsten used natural nickel (68.3% of ^{58}Ni) and so corrections have to be applied mainly for activation coming from ^{60}Ni (26.1%). In addition, activation by secondary neutrons has to be subtracted and then the whole set corrected for the isotopic composition, as the original values are given in percentage activation for the natural target.

Now if we wish to compare with the data of MacDonald et al., we must remember that in a neutron detection experiment the reactions (μ^-, ν), $(\mu^-, \nu p)$, $(\mu^-, \nu d)$ and $(\mu^-, \nu\alpha)$ will all be classified as no neutrons. Thus we obtain the activation results for no neutron, 1 neutron, 2 and 3 neutrons as given in the columns marked "neutron distribution", which are compared with the theoretical results of Singer. The experimental multiplicity is 0.78 (4) to be compared with the predicted value of 0.86. Unfortunately, MacDonald et al. [328], did not use nickel as

a target and the closest element was natural iron (91.8% of ^{56}Fe), which was given in Table 4.7. The agreement is marginal and might be affected by the high value for 3 neutron production observed by MacDonald et al. (but removed by us from Table 4.7). Moreover, there is quite a substantial variation in the fraction of transitions going to bound levels of a nucleus.

In Table 4.9 we present some illustrative data for the total (μ^-, ν) reactions, producing bound levels in the final nucleus. In the second column are the MacDonald et al., observations for no neutrons and the third column gives an estimate for the contribution of $(\mu^-, \nu p)$, $(\mu^-, \nu d)$, and $(\mu^-, \nu\alpha)$ reactions, giving the fourth column which is our estimate for the bound level contribution. In the fifth, sixth and seventh columns are activation measurements for the (μ^-, ν) reaction to all bound levels, which will naturally exclude all charged particle reactions. The data have been corrected, if necessary, for the presence of other isotopes. Heavier mass isotopes produce some activation via the $(\mu^-, \nu xn)$ reactions, but then the production probability has to be raised by the isotopic concentration. Such corrections have been applied to the data of Bunatyan et al. [341], and Heusser and Kirsten [332]. However, Miller et al. [340], used isotopically enriched targets to avoid such problems. In the eighth column we present the sum of the transitions observed in γ-ray experiments.

For the lighter elements such as ^{10}B, ^{11}B, ^{12}C, ^{14}N and ^{16}O there are often several experiments and all the transitions have been identified, because there are few bound levels. Details will be given later when we discuss each nucleus. Thus for these nuclei the difference between the activation results and the summation of the γ-ray transitions is just the ground-state transition which is especially strong in ^{12}C and ^{16}O. For most nuclei, however, the ground-state transition for the (μ, ν) reaction is quite weak. Thus for slightly heavier nuclei (^{23}Na, ^{24}Mg, ^{28}Si, ^{31}P and ^{32}S), the γ-ray results of Gorringe et al. [338,339], are less than the total bound state transitions because not all the γ-rays can be identified, even in a modern experiment. This is an old problem which has been of concern for decades, and it used to be even worse. For example Backenstoss et al. [345], studied targets of Sc, Mn, Co, Nb, I and Bi, and observed the (μ^-, ν) reaction to be only 1.9% of captures for ^{59}Co and 1.0% for ^{93}Nb, and nothing for the other elements. It is now clear that in these elements the (μ^-, ν) reaction feeds many levels, and the γ-ray transitions are lost in the general background. Even in the modern experiment of Gorringe et al., they identified only 70% of the (μ^-, ν) transitions in ^{28}Si for example.

The only major disagreement in Table 4.9 is for ^{24}Mg. Heusser and Kirsten observed a production rate of (17.0 ± 2.6)% for ^{24}Na in a natural magnesium target, but the isotopes ^{25}Mg (10%) and ^{26}Mg (11%) must contribute about 7.2% to ^{24}Na production via neutron emission reactions, giving a final estimate of (12.4 ± 3.3)%. This is lower than the yield for just the 472 keV γ-ray transition observed by Gorringe et al. [338], who measured 13.8 (16)%, or by Miller et al. [340], who found 16.7 (12)%. All known transitions cascade through this level, and thus we have to reject the measurement of Heusser and Kirsten.

Now it is clear that the bound state contributions vary significantly from nucleus to nucleus. This could be because fewer levels are bound, so the neutron binding energy in the product nucleus is given in column 10. We see that there is a correlation, but other nuclear structure effects are very important, especially for light elements. Thus, for example, on ^{12}C, 15.3 (9)% of muon capture go to the ground-state of ^{12}B, whereas for ^{14}N (and most nuclei), there is almost no ground-state transition. For the heavier elements nuclear physics effects have their impact as the variation tends to follow the GT strength observed in the (n, p) reaction. The

Table 4.8
Bound state (μ^-, ν) transitions for a variety of nuclei, expressed as a percentage of all captures. Where necessary the experimental measurements have been corrected if a natural target was used. The neutron binding energy for the product nucleus is given in order to indicate the range of bound levels available. Notes: (a) See sections on individual nuclei. (b) Wiaux [189] using activation data of Deutsch et al. [337]. (c) Stocki [192]. (d) Gorringe et al. [338,339]. (e) Miller et al. [340]; isotopic targets. (f) Heusser and Kirsten [332]. (g) Bunatyan et al. [341,342]. (h) Lifshitz and Singer [343]. (i) Winsberg [344]. (j) Wyttenbach et al., quoted in [331]. (k) Budick et al. [335,336]. (l) Hadermann and Junker [331]. (m) Corrected for isotopic composition of the natural target

Target	No neutrons [328]	$(\mu^-, \nu p)(\mu^-, \nu d)$ $(\mu^-, \nu\alpha)$	Bound (μ^-, ν)	Activation			$\Sigma(\gamma)$	Theory	BE (neutron) (MeV)
				[334]	[335]	Others			
^{10}B						19 (4) (a)	19 (4) (a)		6.8
^{11}B (λ^+)						1.5 (10) (b)			0.5
^{11}B (λ^-)						7.6 (12) (b)			0.5
^{12}C						18.6 (7) (a)	3.3 (5) (a)		3.4
^{14}N							9 (2) (c)		8.2
^{16}O						10 (1) (a)	2.9 (2) (a)		2.5
^{23}Na				10.7 (4)			7.2 (9) (d)		5.2
^{24}Mg						22.8 (22) (e)	13.8 (16) (d)	16 (f)	7.0
						12.4 (33) (f)			
^{27}Al	9 (6)	2	7 (6)	11.5 (3)	10 (1)			6 (g) 11 (h)	6.4
^{28}Si	36 (6)	6.5	29 (6)		27 (4) (m)	26 (3) (e)	17.9 (15) (d)	38 (g)	7.7
^{31}P							8.0 (7) (d)		6.6
^{32}S							11.5 (5) (d)		7.9
^{51}V				10.6 (9)	10 (1)			12 (h)	6.4
^{56}Fe	19 (4)	0.5	18.5 (40)	16.5 (19)	17 (3) (m)	20.8 (13) (f, m)		24 (g), 18 (f)	7.3
^{58}Ni						31.0 (26) (f, m)			8.6
^{59}Co				9.6 (2)		15.0 (11) (f)		16 (f)	6.6
^{127}I	4 (10)	0.1	4 (10)			8.2 (16) (i)			9.1
^{208}Pb	8 (11)	0.02	8 (11)	10.5 (12)	9.0 (15)	8.4 (5) (j)	7.9 (14) (k)	8 (l), 14 (h)	~6

1^+ transitions are important (but not the only transitions) for producing the bound states in a nucleus. We shall discuss this in Section 5.9 on γ-ray measurements.

An interesting case is ^{11}B which is rather unusual because there are only two bound levels in ^{11}Be, the ground-state and an excited state at 320 keV; more captures go to this excited state than the ground-state, but the capture is very different for the two hyperfine levels as $\lambda^+/\lambda^- = 0.028\ (21)$. We have thus used the results of Wiaux's experiment to estimate the different contributions to the activation experiment of Deutsch et al. [337], and we estimate that, for the 320 keV level, $\lambda^- = 1700\ (200)\ s^{-1}$, and $\lambda^+ = 48\ (36)\ s^{-1}$. Obtaining estimates for the ground-state transition and total rates from Wiaux, we obtain the results in Table 4.9. The point is not so much the exact numbers, but the high sensitivity to the hyperfine state. Thus data for ^{19}F, ^{23}Na, ^{27}Al and ^{31}P will need refining. Unfortunately, it is hard to go back and correct older experiments. In general, however, the data for these elements would apply more to the lower hyperfine level than to a statistical mixture of the two hyperfine levels.

We shall discuss details of the data in Table 4.9 later when we consider each nucleus separately. The most frustrating aspect however, about the table is how blank it is. People tend to study different nuclei with different techniques, and only for a few famous nuclei such as ^{12}C and ^{16}O is a cross-check available. In the few cases where there is some duplication, there is often confusion as well, so the quoted errors are probably an underestimate in many cases.

4.7.2. High neutron multiplicity

So far we have discussed neutron multiplicities of 3 or 4. This is already surprising as each emitted neutron demands about 8 MeV of binding energy. However, there is now strong evidence that higher multiplicities also occur, even up to 7 or 8. There are a few activation experiments on ^{209}Bi which have observed such multiplicities, and we shall see later that there are confirming γ-ray studies on ^{207}Pb [335]. These observations are difficult to imagine with mechanisms discussed so far, as it is necessary to deposit 50 or 60 MeV in the nucleus. We shall also see that emitted neutrons and charged particles have been observed up to and beyond such energies. Thus although each measurement is difficult and has its own systematic errors, the sum of the evidence clearly indicates that such high energy deposition occurs. The normal impulse approximation can explain depositions of up to 30, maybe even 40 MeV, using high momentum components in the wave-function. However, a single-nucleon absorption cannot explain any of these high energy observations.

Bernabeu et al., related muon capture to pion capture [346,347]. The vector current contributes little, but the axial current contributes in two ways. The time component can be related via PCAC and gives an s-wave absorption of the pion. They note that the effect is stronger than just the $\mu \to \pi\nu$ vertex which is proportional to m_μ, whereas the PCAC term is proportional to m_π^2/m_μ, which gives an enhancement of 3 in the rate. The spatial component of the axial current is also important and gives a p-wave pion absorption. Of course the pion absorption differs from low energy pion absorption in two important ways. First, the pion is below threshold with an energy less than m_μ. Secondly, the absorption follows the muon wave-function and thus is a volume term, whereas for real pions the absorption is so strong that it is restricted to the surface.

The pion is normally absorbed on a nucleon pair with $n-p$ pairs dominating $p-p$ pairs by a factor of 7 or so. Thus high momentum nucleons are created, with neutrons outnumbering

Table 4.10
High multiplicity neutron emission in heavy nuclei given as the probability per thousand muon captures. The calculations of Lifshitz and Singer [348] using meson exchange currents are compared with the impulse approximation. The experiments are the activation experiments on ^{209}Bi by Pruys and Wyttenbach [350] and the γ-ray measurement on ^{207}Pb by Budick et al. [335,336]

Nucleus	$n=6$			$n=7$			$n=8$		
	Calc.	IA	Exp.	Calc.	IA	Exp.	Calc.	IA	Exp.
^{209}Bi	8	0.7	15.0 (15)	3.5	0.01	1.4 (2)	0.7	~ 0	2.8 (2)
^{207}Pb	10		9.2 (23)	3			0.8		
^{165}Ho	5.5			1.5			0.3		
^{107}Ag	3.3			0.52			0.04		

protons by about 20 : 1 (experimentally the ratio is probably somewhat less, but neutrons still dominate).

In a related study Lifshitz and Singer [348], following an earlier phenomenological model by Mukhopadhyay et al. [349], studied high multiplicity neutron emission, induced by meson exchange currents. They argue that such currents contributes 4–10% of the capture rate and the energy deposited in the nucleus peaks at about 60 MeV, and so manifest themselves in high multiplicity events or in the emission of high energy nucleons. We present in Table 4.10 the results of their calculation for neutron multiplicities in several heavy nuclei.

4.7.3. Energy spectrum of neutrons

There have been a few attempts to measure the energy spectrum of the neutrons produced in muon capture because this spectrum gives an indication of the excitation energy of the initial reaction. Unfortunately, the measurement is technically quite hard, and, in addition, it is quite difficult to interpret the results because of the complexity of the reactions.

The best technique for measuring neutron energies is to use the time of flight method. However, one needs a time zero, and in muon capture that is difficult to determine because the muon, after it forms an atom, waits a microsecond or two before being captured. It is very different for pionic atoms or other hadronic atoms as the reaction is instantaneous, and so neutron spectra have been measured quite dependably. For muons one trick is to use de-excitation γ-rays to determine the time zero. This is an excellent idea, but it is important to remember that it is just a measure of those neutrons which feed an excited state, thus direct ground-state transitions are excluded. An alternative method is to use a plastic scintillator as a neutron detector and to unfold the neutron energy spectrum. The difficulty is that single-energy neutrons produce a box-like response, so the unfolding relies on good statistics and an excellent knowledge of the response function. For higher neutron energies (> 20 MeV), inelastic reactions can occur in the carbon of the scintillator, so the box-like response degenerates, adding more low energy events to the response. A final difficulty is that low energy protons from the neutron–proton scattering give a lower pulse in a plastic scintillator than electrons of the same energy. A third technique is a recoil proton spectrometer, in which the neutron scatters off a proton (often in a scintillator) and then the energy of the recoil proton is measured. The efficiency is low $\sim 0.5\%$, but no unfolding is needed. The end result of all this is that measuring the neutron spectrum

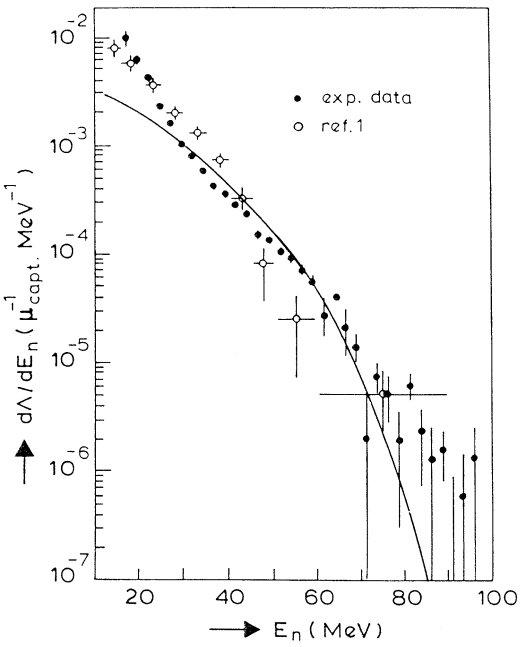

Fig. 4.13. Inclusive spectrum of neutrons emitted after muon capture in ^{40}Ca. The data are those of van der Pluym et al. [351], compared to the earlier data of Kozlowski et al. [352], and a calculation relating muon capture to pion capture.

is a very difficult experiment. In fact it is so difficult that there is no measurement covering the full energy range, and none at all in the region below 1 MeV which is where the peak production lies. Nevertheless some data exist, especially at the higher energies and there seems to be a reasonable experimental consensus in all but one case.

Let us start with the principle that more recent experiments are more likely to be correct than older ones. Although this principle is sometimes violated at the level of 10%, it is a good starting position.

The most recent experiment is by van der Pluym et al. [351], who studied the spectrum from ^{40}Ca at SIN (now PSI). They used a recoil proton spectrometer with an efficiency of 0.5% to 0.8% and an energy resolution of 12% at a neutron energy of 70 MeV. They covered the energy range from 20 to 100 MeV, and their spectrum is illustrated in Fig. 4.13. Of some concern is the fact that there is not good agreement with an earlier experiment by a similar group at PSI, Kozlowski et al. [352]. Factors of 2 discrepancy are worrying, even on a log plot.

The neutron spectrum extends to nearly 100 MeV, the kinematic limit, even though few events are at that high energy. It is difficult to explain how a neutron can acquire 30 or 40 MeV let alone 70 or 80 MeV. It is necessary to invoke a meson exchange mechanism of some sort. The curve is a simple model using the diagrams from the induced pseudoscalar term, which gives an adequate description of this high energy spectrum. A related experiment by McIntyre et al. [353], at TRIUMF used a time of flight technique for ^{165}Ho. Although the lower end of their spectrum is reasonable, data beyond the kinematic limit at 100 MeV indicate that they had

Table 4.11
Neutron yield, per captured muon, for 10 MeV threshold and the exponential constant resulting from a fit of Eq. (4.60) to the neutron spectra in the energy region 10–50 MeV

Nucleus	Yields for 10 MeV threshold			T (MeV)		
	[352]	[354][a]	[355]	[352]	[354]	[355]
O	0.26 (5)			16 (4)		
Si	0.191 (28)	0.156 (25)		10.3 (5)	6.5	
Ca	0.112 (16)	0.114 (8)	0.102 (5)	9.5 (5)	6.6	14 (1)
Pb	0.106 (17)		0.091 (6)	8.6 (5)		12 (2)

[a]Recalculated for 10 MeV thresholds.

a background which they were not controlling correctly. Kozlowski et al. [352], measured the higher energy part of the neutron spectrum for natural O, Si, Ca and Pb, at the $\mu E4$ channel at SIN. They used liquid scintillators, with pulse shape discrimination, and unfolded the neutron energy spectrum using the known response functions of the detectors. A comparison was made with the earlier results of Sundelin and Edelstein [354]. The disaccord is not excessive, but is an indication of the problems in obtaining an experimental consensus. The spectrum clearly falls in an exponential manner, so can be fit to the form

$$N(E_n) = N_o \exp\left(-\frac{E_n}{T}\right) , \tag{4.60}$$

and the values of T are assembled in Table 4.11 with comparisons to earlier work too [355]. McIntyre et al. [353], obtained $T = 10.5 \pm 1.0$ MeV for ^{165}Ho, which seems the consensus for recent experiments. Also given in Table 4.11 are the yields per capture for neutrons above 10 MeV, which are in reasonable agreement. The results show that the majority of neutrons are below 10 MeV especially for the heavier elements since the multiplicity (or total yield) for calcium is 0.746 (32) and for lead is 1.709 (66), see Table 4.7.

A similar group at SIN used the other technique for ^{16}O, see van der Schaaf et al. [356]. They used a NaI crystal to detect the γ-rays of de-excitation in ^{15}N or ^{14}N, and the arrival of that photon can be used as a timing signal for the neutron time of flight. There are two major γ-ray groups from ^{15}N; the most prominent is at $E_\gamma = 6.32$ MeV and another which includes two levels at 5.27 and 5.30 MeV. The neutron energy spectra associated with these two groups is given in Fig. 4.14. Also included are the γ–n correlation coefficients as a function of energy according to the expression

$$N(E_n) = N_o[1 + A_2(E_n)P_2(\cos\theta)] , \tag{4.61}$$

where θ is the angle between the neutron and the γ-ray. Note that the energy spectrum goes down to a much lower energy than the previous experiments, reaching 0.9 MeV, yet the curve still has not turned over. The curve for the 5.3 MeV states falls more rapidly at first, but then changes and parallels the group feeding the 6.32 MeV level. About 30% of the neutrons which excite the 5.3 MeV γ-rays actually excited higher energy levels at about 10 MeV, and the de-excitation of these levels cascaded through the 5.3 MeV pair. Thus the faster fall off could be due to less extra energy being available for the neutron if it excites a 10 MeV state in ^{15}N. Anyway it is significant that a large number of neutrons excite fairly high energy levels in ^{15}N.

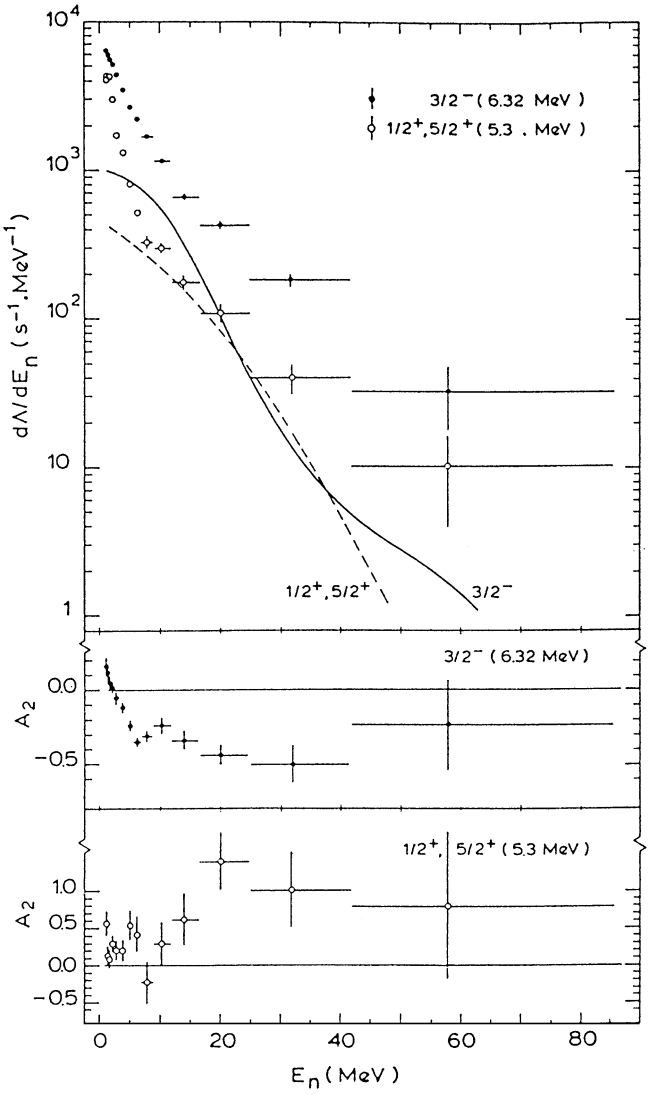

Fig. 4.14. Neutron energy spectra for muon capture in ^{16}O. The experiment by van der Schaaf et al. [356], used a time of flight technique using the 5.3 and 6.32 MeV γ-rays as starting signals. Also shown are the angular correlations. Theory is by Eramzhyan and Salganic [357].

Now for ^{16}O there are also two other experiments which measured the inclusive spectrum, i.e., all neutrons including those which feed the ground-state. These experiments used the unfolding technique. The results of Plett and Sobottka [358] for ^{16}O are illustrated in Fig. 4.15 whereas the results of van der Schaaf [356] show no structure, these results show a strong peak at 5–6 MeV. Now there are also results from Dubna [359,360] which show structures finer than their energy resolution and for ^{16}O show no rise below 3 MeV. As we have seen from the results of van der Schaaf, this rise is to be expected. We therefore reluctantly reject all those Dubna

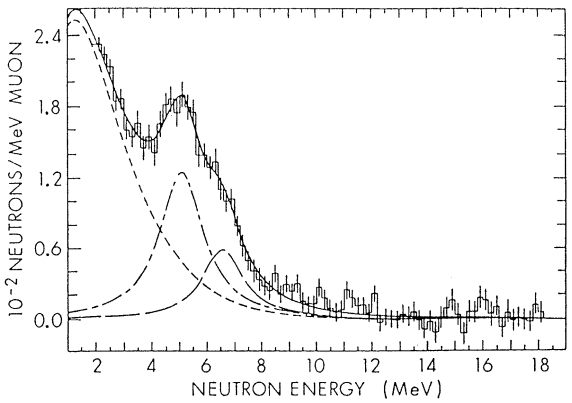

Fig. 4.15. Inclusive neutron energy spectra for muon capture in ^{16}O taken from Plett and Sobottka [358]. The peak at 5 MeV is probably a transition to the ground-state of ^{15}N. The curves are fits to two resonances, and an evaporation spectrum.

results. The results of Plett and Sobottka are compatible with the van der Schaaf measurements if this peak at 5–6 MeV is a ground-state transition. This is in fact what you would expect by referring to analogous results for the (π^-,γ) and (p,n) reactions on ^{16}O. The (p,n) results of Fazely et al. [284], at 135 MeV are illustrated in Fig. 4.16 and show a strong excitation of level at 7.6 (1) MeV (2^-) and weaker excitation of levels at 4.6 MeV (1^+), 6.37 (5) MeV ($1^+,4^-$), 9.4 (1) MeV (1^-) and 11.5 (1) MeV (1^-). These levels are in ^{16}F, of course, and there are likely to be shifts in ^{16}N. Similar results are found for the (π^-,γ) reaction, see Fig. 4.7. Since the neutron separation energy in ^{16}N is 2.5 MeV, the strong excitation at 7.6 (1) MeV would produce a neutron peak at 5.1 (1) MeV and others would be at 2.1, 3.9, 6.9 and 9 MeV, though the last two would have sufficient energy to produce excited levels in ^{15}N. In Fig. 4.15 the curve is a fit to the evaporation spectrum and two peaks, the principal one at 5.07 (7) MeV, with a yield of (15 ± 5)%, and another at 6.55 (13) MeV with a yield of (5 ± 3)%; the lower energy peaks would be in the evaporation spectrum and no obvious peak occurs at 9 MeV which is reasonable. Please note that all these peaks are broader than the experimental resolution. Thus for the (p,n) reaction, the resolution is 0.3 MeV and is illustrated by the 2^- peak in the 9.0° spectrum. (In ^{16}F the 2^- level is not the ground-state, as in ^{16}N, but an excited state at 424 keV with a width of 40 ± 30 keV, since all ^{16}F levels are unbound to (p+^{15}O) decay). For the neutron spectrum work of Plett and Sobottka, the resolution of the detector was 0.33 MeV FWHM at 5.1 MeV and 0.4 MeV at 8 MeV, thus the two peaks are significantly broader than the resolution, and similar to the natural widths observed in the (p,n) reaction. Thus the neutron spectra of Plett and Sobottka, and of van der Schaaf et al., are entirely compatible and logical when the different circumstances are taken into account. There is also a clear warning that γ-coincidence and unfolding techniques give different results in light nuclei because of ground-state transitions, though for heavier nuclei the difference is likely to be less significant.

Another interesting comparison for ^{16}O is to shift the neutron spectra to become the excitation energy in ^{16}N by adding the energy of the γ-ray and the binding energy of the neutron (2.5 MeV). Thus van der Schaaf et al., produced Fig. 4.17. Remember that the neutron

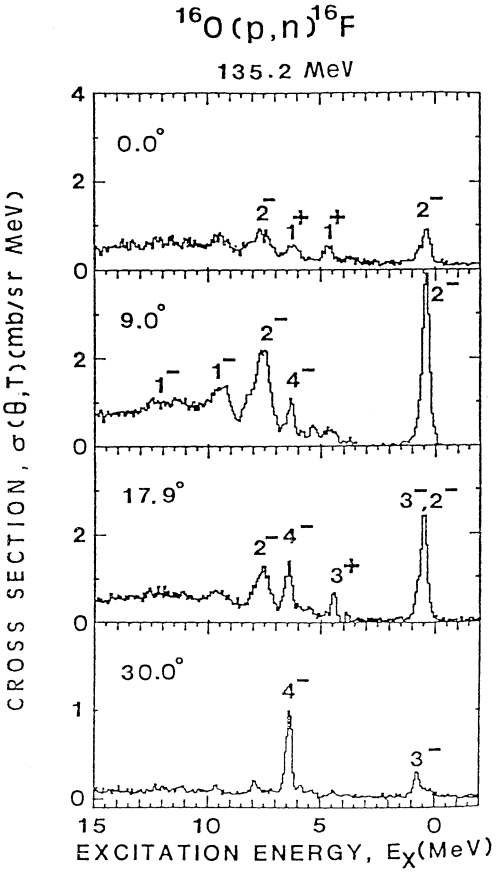

Fig. 4.16. Neutron energy spectra for the reaction $^{16}O(p,n)^{16}F$ at 135 MeV, taken from Fazely et al. [284]. Their spin and parity assignments are indicated. Note that ^{16}F has all levels unbound to neutron emission, whereas ^{16}N is bound up to 2.49 MeV.

minimum energy was 0.9 MeV, so that for both sets of data the actual neutron spectrum continues to lower energy. Below an excitation energy of 8 MeV, ground-state transitions are still allowed, and we have seen in Fig. 4.15 that there is evidence for a neutron peak at 6.55 (13) or 9 MeV excitation, and a stronger neutron peak at 5.1 (1) or 7.5 MeV excitation energy. The curves in Fig. 4.17 are theoretical calculations, A by Ohtsuka [361] and B and B′ by Gmitro et al. [357,362], who also calculated the A_2 coefficient. The obvious discrepancy is that more structure is anticipated in the calculations than is observed, both predicting strong peaks around 9.2 MeV (1^-), 10.6 MeV (2^-), and 12.2 MeV (1^-). They did not have the benefit of the Fazely et al. (p,n) data which indicates somewhat broader, less well defined peaks, at 9.5 and 12 MeV for 1^-, and only one peak at 7.5 MeV of 2^-, which is below threshold for these channels. The 10.6 MeV strength is not visible in the (p,n) spectrum, but is probably submerged in the general broadening. Thus the experimental data are all compatible with an overall larger width for the peaks, and a slight change in the energy of the calculations. We shall discuss more details when we address ^{16}O, but for the moment let us emphasize that it is quite reasonable

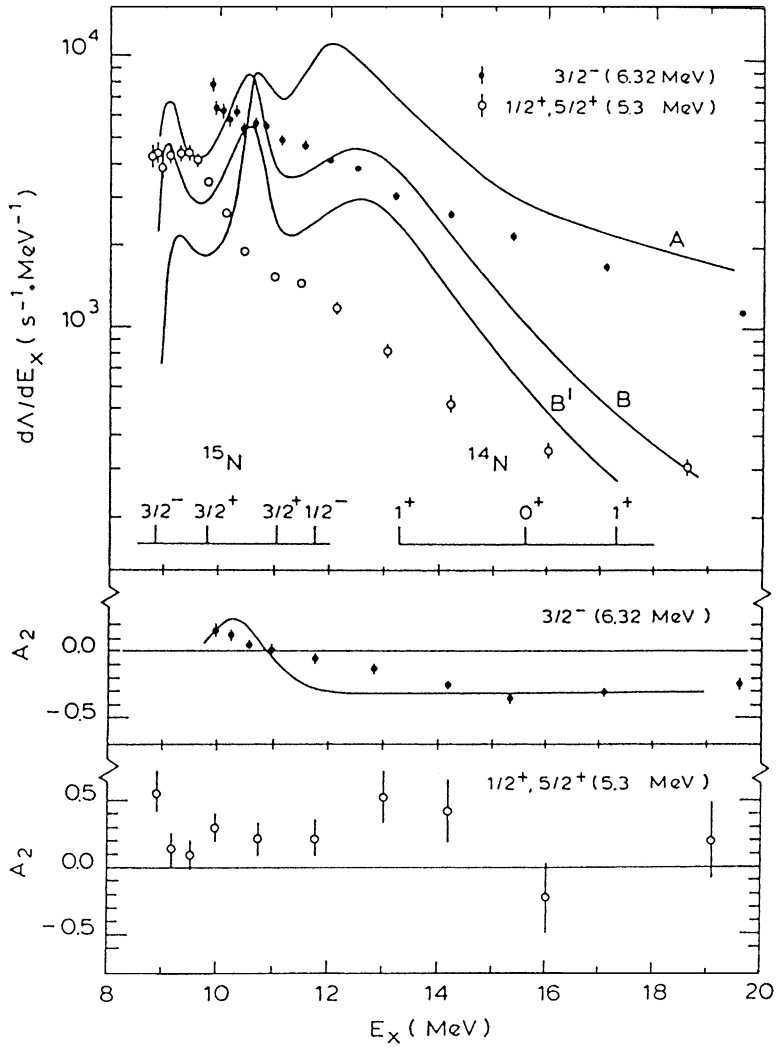

Fig. 4.17. Neutron energy spectra for muon capture in ^{16}O, shifted to present the ^{16}N excitation energy, taken from van der Schaaf et al. [356], including the γ–n correlation coefficients. The theoretical curves A, B and B' are discussed in the text.

that the various neutron energy spectra present only two overlapping broad peaks at 5.1 and 6.5 MeV and no other structure.

In Fig. 4.18 is given the neutron spectrum for ^{12}C as observed by Plett and Sobottka [358] and no obvious structure is visible. The total number of neutrons above 2 MeV is 0.042 (9) per muon stop, or 0.56 (12) neutrons per muon capture. From the ^{12}C$(p,n)^{12}$N reaction, illustrated in Fig. 4.8, we know that there should be excitation of a 2^- level at 4.2 MeV with a width of 0.8 MeV, and levels, maybe 1^-, at about 7 MeV with a total width of about 2.5 MeV. For the ^{12}C$(n,p)^{12}$B reaction, the resolution of Olsson et al. [297], was only 2.3 MeV but the results are similar with peaks at 4.5 and 7.8 MeV. Now in ^{12}B the neutron separation energy is 3.37 MeV, so

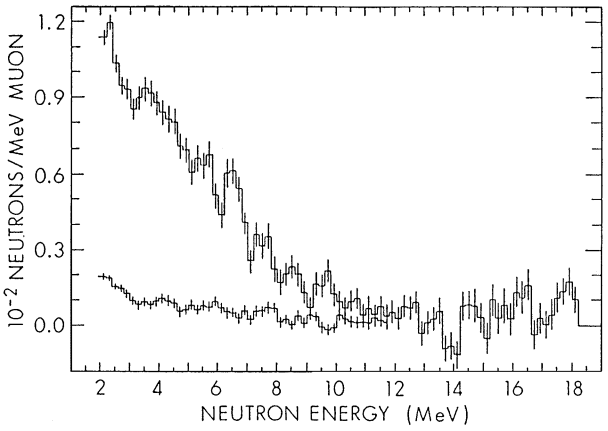

Fig. 4.18. Inclusive neutron energy spectra for muon capture in ^{12}C, taken from Plett and Sobottka [358]. Lower curve is the background. Units are 10^{-2} neutrons/MeV per muon stop (not capture).

one might expect neutron peaks at 1.1 and 4.4 MeV. The first is lost in the evaporation spectrum and the second is very broad and anyway has sufficient energy to excite the first excited state in ^{11}B at 2.12 MeV. This level is observed in γ-ray experiments with a yield of about 0.5% per stopped muon, i.e., 7.5% per capture, which is sufficient to lower the peak, though not to eliminate it entirely. Thus again, the neutron spectrum is compatible with information from the (p,n) and (n,p) reactions.

For heavier nuclei, Schröder et al. [364], used the γ-ray coincidence technique and their results for Tl, Pb and Bi are presented in Fig. 4.19. Note that the neutron spectra go down to 1 MeV, but do not observe the expected turnover. The spectra are very similar and exhibit two clear features, an evaporation spectrum out to about 5 MeV, and then a distinct change to a much harder spectrum. The evaporation spectrum can be fitted to the form

$$\frac{\mathrm{d}N(E)}{\mathrm{d}E} \sim E^{5/11}\mathrm{e}^{-E/\theta}\,, \tag{4.62}$$

and the harder fraction to an exponential falling shape, according to Eq. (4.60). The results are presented in Table 4.12 and can be compared to the high energy results from Table 4.10. The parameter T is very similar, but the yields are difficult to compare because different definitions are used. If we assume that about 4% of the neutrons are between 5 and 10 MeV and about 3% are above 20 MeV, then the results are compatible.

To explain the two components, Schröder et al., developed the model of Singer [330], which had been built on the ideas of Lubkin [365] and Hagge [366]. The direct neutrons are those which are emitted immediately the muon is absorbed on the proton. Thus the target protons are described by a Gaussian momentum distribution, and the recoiling neutron is followed out of the nucleus. The escape probability is calculated using an absorption coefficient and a refractive index to estimate reflection at the nuclear surface. The dot–dash curve in Fig. 4.20 is this component, but it misses the experimental data by a factor of two, and it cannot be improved by changing the model parameters within reasonable limits. Thus, Schröder et al., followed the direct neutrons after the primary scattering until they thermalized or escaped. This escaping

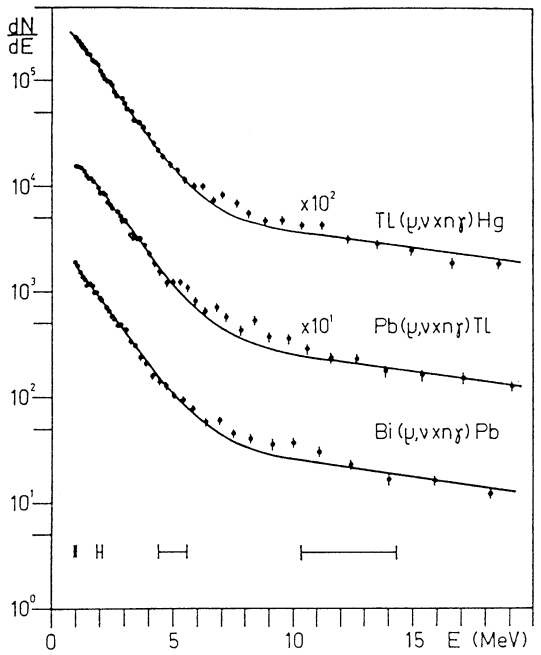

Fig. 4.19. Spectra of neutrons in co-incidence with a gamma, emitted in μ capture on Tl, Pb and Bi, taken from Schröder et al. [364].

Table 4.12
Nuclear temperature parameter θ obtained by Schröder et al. [364]. F is the fraction of high energy neutrons from 4.5 to 20 MeV and T is the exponential parameter in Eq. (4.60)

Target element	θ (MeV)	F	T (MeV)
Tl	1.09 (4)	0.096 (8)	9 (1)
Pb	1.22 (6)	0.102 (10)	9 (1)
Bi	1.06 (5)	0.097 (10)	8 (1)

fraction is called pre-compound and has a surprisingly similar energy spectrum though slightly softer; it is the dashed line in Fig. 4.20, and has a similar intensity to the direct neutrons. The sum of all three components agrees with the experimental spectrum adequately, but clearly not perfectly. The calculation obtains an integral between 5 and 20 MeV of about 7% for each of the direct and pre-compound components, i.e., a sum of 14% per capture. These high energy nucleons are observed in other nuclear reactions, and Singer et al. [367] have shown that there is a strong similarity between muon induced neutrons, and those observed in pion radiative capture, and in nucleon–nucleus interactions.

Before closing this subject it is worth mentioning that some information on the neutron spectrum can be obtained from the Doppler broadening of lines in the γ-ray spectrum. As an example let us use the case of the 6.32 MeV level in ^{15}N which is observed in muon capture

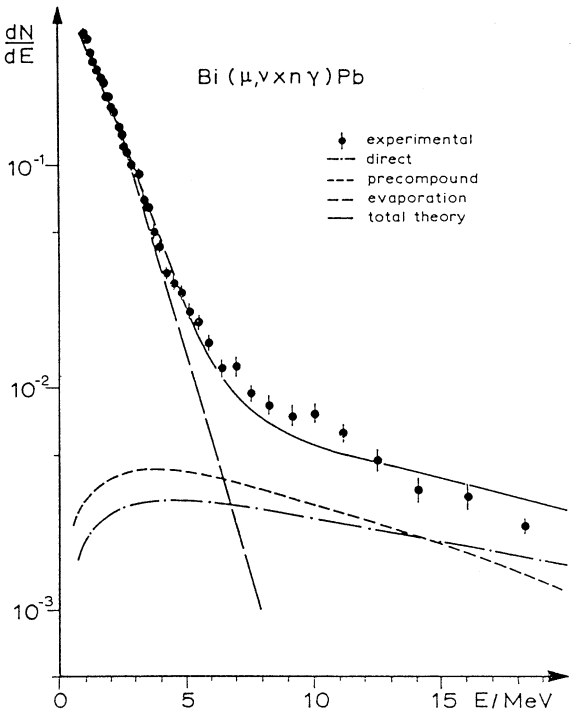

Fig. 4.20. Neutron spectrum for μ capture in Bi from Schröder et al. [364], compared with various descriptions for energies above 5 MeV, see text.

on ^{16}O. First there is the emission of a 90 MeV neutrino which causes the ^{16}N to recoil with a unique momentum of 90 MeV/c. Then a neutron is emitted in any direction, and finally the γ-ray is emitted, again in any direction. If the neutron had no momentum, the 6.32 MeV γ-ray would be Doppler shifted giving a box-like structure with a width of about 76 keV. If the neutron has a low energy, the γ-ray will acquire a trapezoidal like shape. However, a 1 MeV neutron, the most likely energy, has a momentum of 43 MeV/c and a 3 MeV neutron has a moment of 75 MeV/c which are comparable to the momentum of the recoiling ion, and thus the ions' velocity are spread from a very low velocity, to double what it would be without the neutron emission, thus giving a roughly triangular shape to the Doppler-shifted γ-ray, with a total width of over 150 keV.

There are many other complications. First the recoiling ion can slow down, which takes a few hundred femto-seconds to a pico-second or more for light ions. In the case of the 6.32 MeV level, the lifetime is very short, 0.21 fs, so no slowing down occurs, similarly for the 5.299 MeV level in ^{15}N the lifetime is 25 ± 7 fs, so little slowing down occurs, but the 5.27 MeV level has a lifetime of 2.6 ps, so most of the time the ion stops and the Doppler-shift is no longer important.

One also has to worry about n–ν correlations, or n–γ correlations, which though small, are not zero, as the data of van der Schaaf showed (see Fig. 4.14). Also for high energy neutrons which are "direct", the recoil of the ion will be only the Fermi motion of the struck proton in

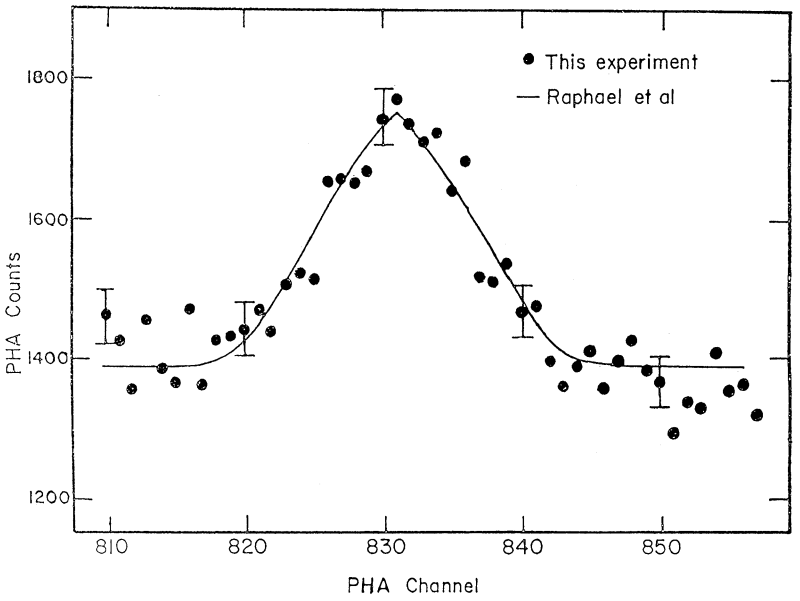

Fig. 4.21. Doppler broadening of the 6.32 MeV γ-ray in ^{15}N from muon capture in ^{16}O, taken from Kaplan et al. [368]. The broadening is more than 150 keV, far greater than the resolution of a germanium detector, which is about 10 keV at this γ-ray energy. The line is a fit for the neutron spectrum of Raphael et al. [369], (which is not a good representation of the experimental spectrum of Fig. 4.14).

the nucleus, not the full momentum of the neutron which escapes. If there is a γ-ray cascade, it is the momentum of the neutrons feeding the upper level which dictates the momentum kick to the ion, as the photon momentum is negligible. Finally this shape has to be folded with the resolution function of the high purity germanium detector, which is typically 2.5 keV FWHM at 1 MeV, 6 keV at 3 MeV and 10 keV at 6 MeV. (These are working resolutions obtained in a meson factory environment, not the best resolutions found in ideal situations.)

Surprisingly there has been only one analysis of the neutron broadening of a γ-ray from muon capture; it was by Kaplan et al. [368], of the 6.32 MeV line from muon capture in ^{16}O. They comment that they could fit the line shape with a neutron group of any energy between 3 and 6 MeV, the fit in Fig. 4.21, which was preferred at the time, because Raphael et al. [369], were predicting a predominant neutron group at about 4 MeV. From the more recent work of van der Schaaf [356], we know that this is not true (Fig. 4.14), and the spectrum is actually very broad and smooth. It would be interesting to reanalyse this, (or other lines), to ascertain the sensitivity to the neutron spectrum. (Unfortunately, Kaplan et al., do not discuss the topic in their only publication [370].) Good statistics would be an essential prerequisite for a useful analysis, but it is an interesting exercise. In practice, one great advantage of this shape is that it helps identify γ-ray lines in a muon capture spectrum.

4.7.4. Neutron–neutron coincidences

From normal muon capture, you would not expect high energy neutrons. Even for the direct process, or quasi-free reaction, it is hard to explain the emission of neutrons above 30 MeV.

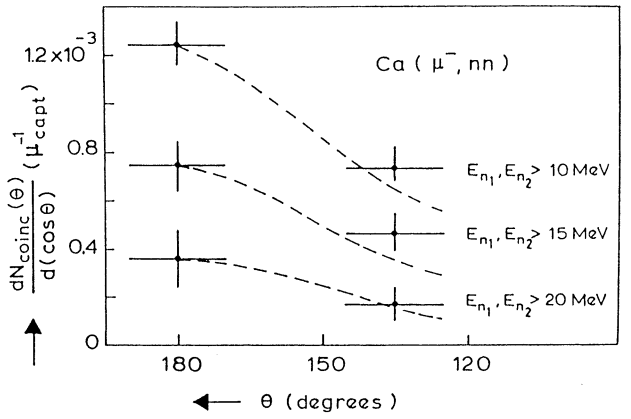

Fig. 4.22. Angular correlation of two neutrons for muon capture in ^{40}Ca. The curves are for similar data for pion capture in ^{59}Co.

A mechanism to do this is to invoke g_P, i.e., to assume that the muon transforms into a pion, which is then absorbed on a correlated nucleon pair. This will give a back to back neutron pair in the final state (the probability for absorption on a p–p pair is much less than on a p–n pair). Thus Kozlowski et al. [352], used their set of multiple neutron detectors to study neutron–neutron pairs.

The n–n angular correlation is given in Fig. 4.22 for ^{40}Ca, and the curves are fits to such a correlation for pion capture in ^{59}Co. (No pion capture had been studied in ^{40}Ca.) We see that n–n coincidences are observed with a similar pattern to that for pion capture. The total probability for the emission of two neutrons given a proton signal above 10 MeV in the counters is about 1×10^{-3} whereas for a single neutron it is 0.11, per captured muon. Thus the yield of coincidences is only 1% of the single neutron yield. For pion capture it is about ten times higher.

There are two plausible reasons why fewer neutron coincidences would be detected for muons. First, the neutrons from muon capture are significantly lower in energy, and thus are more likely to be absorbed in the nucleus, and also less likely to surpass the energy threshold in the detectors. (For pions the neutrons are about 70 MeV each, whereas for muons, the energy available is less because the neutrino takes some, and the muon mass is less anyway.) Secondly for pions the capture takes place mainly at the surface as the atomic pion is absorbed from a p or even a d orbital. However, for muon capture, the interaction site is uniformly distributed throughout the nucleus, so, the neutron has a lower chance of escaping. These mechanisms explain most of this reduction for muons, thus the evidence is clear that a pion-like reaction mechanism makes a significant contribution to the yield of high energy neutrons in muon capture, and to neutron–neutron correlations.

4.7.5. Neutron asymmetry

From the direct reaction yield in muon capture, one would expect some neutron asymmetry with respect to the muon spin. The asymmetry parameter α is normally defined via

$$\frac{\mathrm{d}^2\Lambda}{\mathrm{d}E_n d\omega} = \frac{\Lambda(E_n)}{4\pi}(1 + \alpha(E_n)P_\mu \cos\theta) \,. \tag{4.63}$$

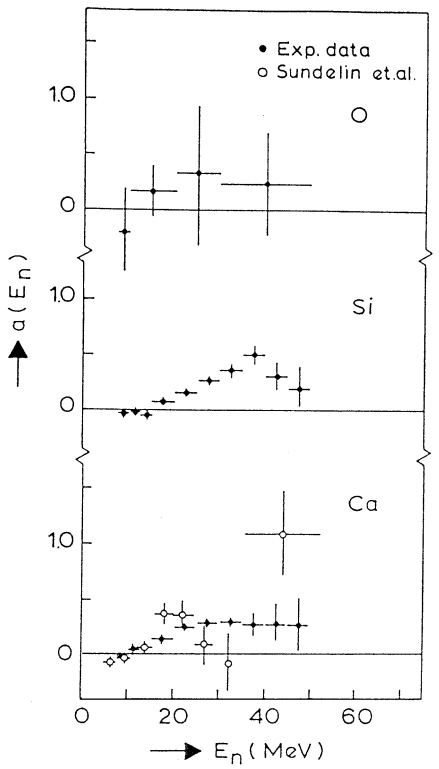

Fig. 4.23. Neutron asymmetry measurements for muon capture in O, Si and Ca, taken from Kozlowski et al. [352].

The residual polarization of the muon in the 1*s* orbit is only 20% for spin zero nuclei (even for a 100% polarized beam), and can be a factor of 2 less for nuclei with spin. Thus, the experiment is searching for a small observable and some early experiments gave incorrect results. Again we refer to the more recent measurements of Kozlowski et al. [352], who obtained the results given in Fig. 4.23, which are in agreement with, but much better than, the earlier results of Sundelin and Edelstein [354]. (Note that the nuclei O, Si, Ca all have a spin zero ground-state.)

At low energies the asymmetry is effectively zero in the evaporation region. As one changes to the direct mechanism, the asymmetry becomes about +0.25. The simplest theoretical estimate using the Primakoff approach predicts $\alpha = -0.4$. It was quickly found that adding momentum dependent terms makes a considerable difference and changes the value to about −0.11 [371–373]. Finally, Boussy and Vinh-Mau [374] studied the impact of final state interactions and found quite a sensitivity to the type of optical potential used to describe the interaction of the outgoing neutron with the nuclei. Unfortunately, they were focussing on trying to describe an asymmetry which had a positive peak of 0.3 at about 20 MeV. This they could do if they exaggerated the surface absorption, but a more conservative volume absorption adequately describes the more recent data. Our knowledge of the nucleon optical potential is now much improved, and so a renewed study would be appropriate. It is thus probable that a reasonable choice of interaction would be satisfactory.

The final conclusion is a familiar refrain. The observed effects are very sensitive to nuclear complications and it is highly unlikely that these can be sufficiently well understood to study the weak interactions via these observables.

4.8. Charged particles

Although the main mechanism of de-excitation after muon capture is neutron emission, it is also possible for charged particles to be emitted. However, this is normally a secondary interaction and thus a minor component of the capture process. However, studying this aspect has clarified other issues too.

Experimentally the study is quite difficult and some very early measurements are still the best that we have. The reason is that the protons, deuterons and alphas which are emitted are typically low energy (2–20 MeV) and thus have a short range. However, even at a meson factory it is necessary to have a relatively thick target in order to get a reasonable muon stop rate. Thus the nuclear emulsion technique is particularly powerful and has been a mainstay of these studies.

As long ago as 1953, Morinaga and Fry [375] studied 24,000 muon tracks stopping in Ilford C2 emulsion, and assumed that 42% stopped in gelatine and 58% stop in Ag or Br. By identifying a capture in a light element by the recoil track of the ion, they were able to study light elements and AgBr separately. They found that for AgBr, 2.2 (2)% of the captures produced protons and 0.5 (1)% produced an alpha particle, whereas for light elements, 9.5 (11)% resulted in proton emission and 3.4 (7)% gave alphas (excluding ^{8}Be production). The errors are statistical only and do not include systematic difficulties. However, the results are very useful, even today.

Kotelchuck and Tyler [376] used Ilford G5 emulsion and obtained 1289 stars from 70,000 stopping tracks, nearly 3 times the sample of Morinaga and Fry. Similar results were obtained by Vaisenberg et al. [377,378], who found that $3.2\ (3) \times 10^{-4}$ of muon captures gave protons above 25 MeV and $4.7\ (11) \times 10^{-5}$ of muon captures gave protons above 40 MeV(13 events).

The higher energy protons can also be measured by scintillator arrays. The most recent experiment by Krane et al. [379], studied proton emission above 40 MeV from Al, Cu and Pb. Earlier references can be found in their publication. They find the energy spectrum to fall with an exponential shape, identical to neutrons, i.e., Eq. (4.60) with $T = 7.5\ (4), 8.3\ (5)$ and 9.9 (11) MeV for Al, Cu and Pb, respectively, see Table 4.10. These high energy protons are a minor contribution to muon capture. The integrated intensity above 40 MeV was found to be $1.38\ (9) \times 10^{-3}$, $1.96\ (12) \times 10^{-3}$ and $0.17\ (3) \times 10^{-3}$ per muon capture, for Al, Cu and Pb, respectively, being a few per cent of the total charge particle emission. Note however that these numbers are an order of magnitude larger than the results of Vaisenberg et al., but comparable to Budyashov et al. [380].

A novel measurement was made by Sobottka and Wills [381] who stopped muons in a Si(Li) detector. The spectrum is given in Fig. 4.24 which has been corrected for electrons from muon decay and for protons which escaped. The lowest part of the spectrum below 1.4 MeV is due to the recoiling heavy ion, mainly ^{27}Al. The higher energy events are protons, deuterons and alphas from muon capture and constitute 15 (2)% of capture events, which is quite consistent with the 12.9 (14)% observed by Morinaga and Fry on gelatine (C, N, O) and 20 (4)% found for neon [384].

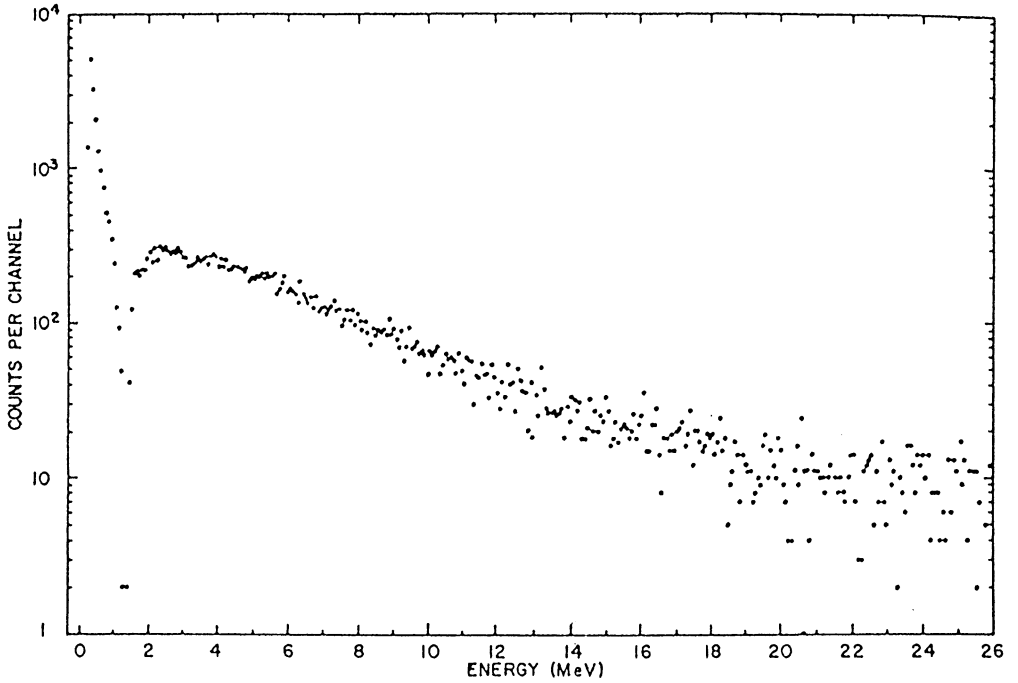

Fig. 4.24. Charged particle spectrum from muons stopping, and capturing in a silicon detector. The peak below 1.4 MeV is from the recoiling heavy ion, mainly ^{27}Al, when no charged particle was emitted. Data are from Sobottka and Wills [381] and are corrected for decay-electron background, and proton escapes.

They also quote that 2% of the events are between 26 and 32 MeV and 1% above 32 MeV. Assuming that they mean the total number of events, this means that 0.3% of captures give protons between 26 and 32 MeV and 0.15% of captures give protons above 32 MeV. (We assume that no α particles reach those energies.) These numbers are consistent with Krane et al. [379], but larger than Vaisenberg et al. Note that although the spectrum in Fig. 4.24 stops at 26 MeV, Sobottka and Wills had events above that but did not present them because of non linearities in the detectors. This should not affect comments about integral numbers.

This technique could be applied to other scintillator materials such as Ge and CsI. Even an organic scintillator could be used, but a major problem of such materials would be that the response to heavy charged particles around 1 MeV is highly non-linear.

It should be noted that deuterons can also be emitted. For particles above about 18 MeV, Budyashov et al. [380], found that they constitute 34 (2)% of the charged particle yield for silicon, falling to 17 (4)% for copper. The spectral shape is similar to that for protons.

In all these experiments neutrons are also emitted in most of the events, thus these numbers are not the probability of only the $(\mu^-, \nu p)$ or $(\mu^-, \nu\alpha)$ reactions, but of $(\mu^-, \nu p(xn))$ and $(\mu^-, \nu\alpha(xn))$. A powerful method to study the likelihood of such reactions is the activation technique which reached its peak in a broad ranging study by Wyttenbach et al. [333]. They studied many nuclei, avoiding those which would have activation from the stronger neutron producing reactions. Their results are given in Figs. 4.25 and 4.26, plotted against the Coulomb

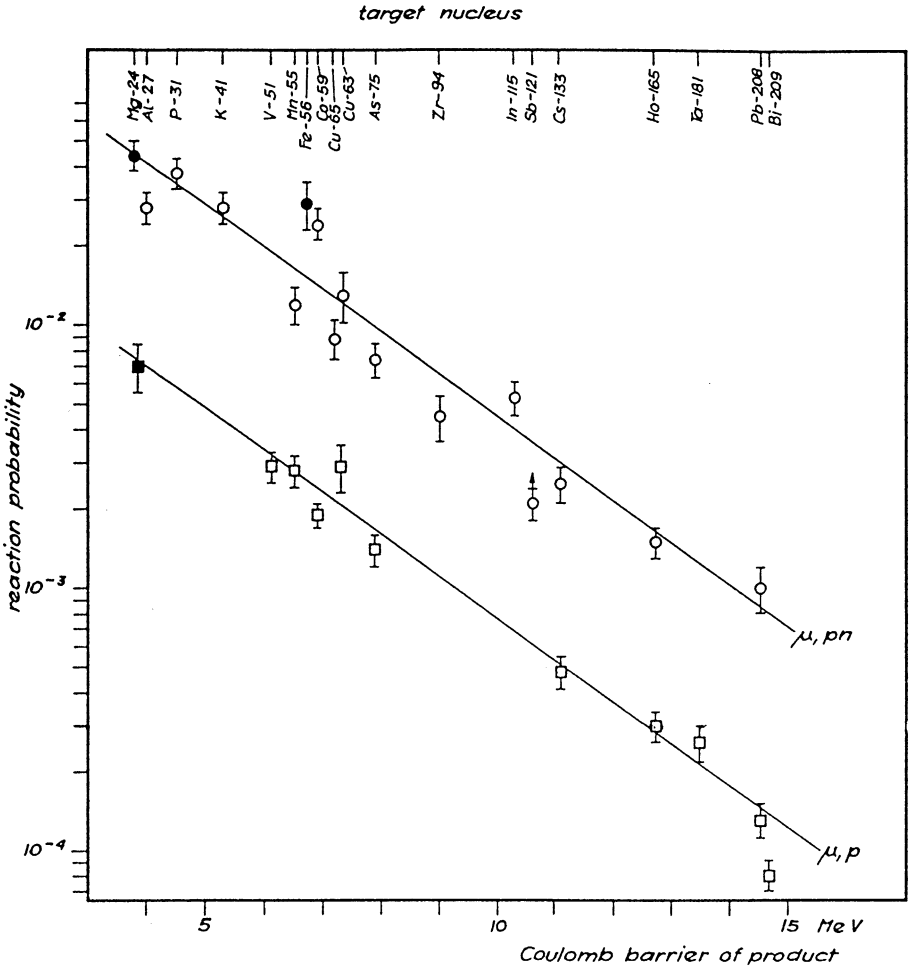

Fig. 4.25. Activation results for the reactions (μ^-, vp) and (μ^-, vnp) taken from Wyttenbach et al. [333]. Filled circles are from γ-ray measurements of Miller et al. [340] and Evans [382]; filled square from Miller et al. [340].

barrier for the outgoing protons. They include some results from γ-ray work, but these are lower limits. They reject the results of Vil'gel'mora et al. [385], as being too high; these are $^{28}\mathrm{Si}(\mu^-, vp) = 5.3\ (10)\%$ and $^{39}\mathrm{K}(\mu^-, vp) = 3.2\ (6)\%$. Although these values seem high, it is not impossible that the (μ^-, vp) reaction becomes more important for light nuclei; there is support for this position from the γ-ray data of Miller et al. [340], and in ^{40}Ca too. Now they comment that the ratio

$$(\mu^-, vp) : (\mu^-, vpn) : (\mu^-, vp2n) : (\mu^-, vp3n) = 1 : 6 : 4 : 4\ , \tag{4.64}$$

roughly holds over a broad mass range, but below $A = 40$ the (μ, vp) reaction could vary significantly from nucleus to nucleus and so caution is advised.

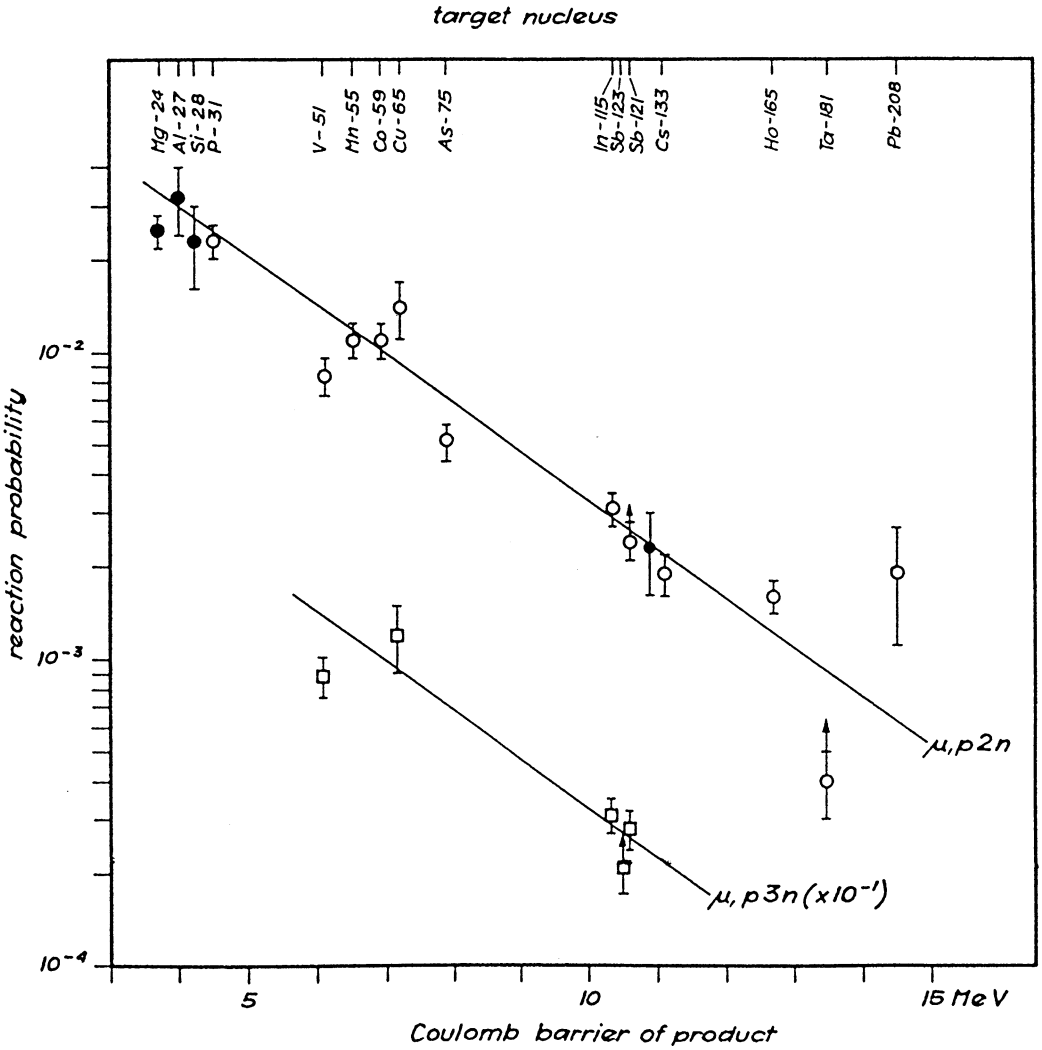

Fig. 4.26. Activation results for the reactions $(\mu^-, vp2n)$ and $(\mu^-, vp3n)$, taken from Wyttenbach et al. [333]. Filled circles are from the γ-ray measurements from Pratt [383], and Miller et al. [340] and the activation measurement of Winsberg [344] for iodine.

The interpretation of the charged particle data was puzzling and many calculations were attempted. The earliest models followed the experience of evaporation from a compound nucleus, excited by a variety of low energy reactions. In Fig. 4.27 we present evaporation spectra for neutrons and protons from ^{68}Ge at an excitation energy of 20 MeV [386]; this was based on the evaporation models of Dostrovsky et al. [387,388]. The parameter a corresponds to the level density. Note that the neutrons peak around 1–2 MeV, but protons need 5 MeV to escape the Coulomb barrier. This threshold energy can be adjusted a little by the choice of the nuclear radius but the overall effect is always present.

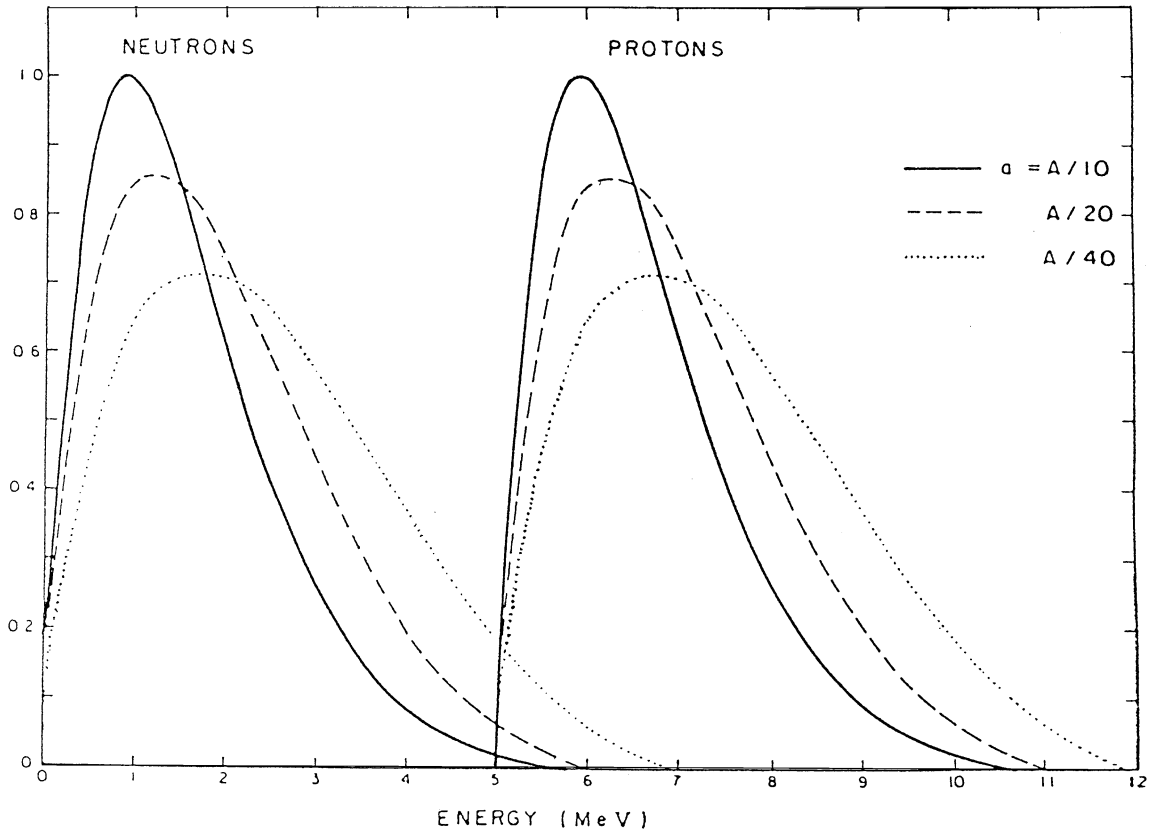

Fig. 4.27. Calculated evaporation spectra for neutrons and protons from ^{68}Ge at 20 MeV excitation energies [386–388]. Note that the Coulomb barrier blocks proton emission below 5 MeV.

Muon capture calculations culminated in the model of Lifshitz and Singer [343,389], which incorporated many of these ideas. For a readable earlier review, see Singer [12]. These references give a short history of the previous theoretical work which is too complex to repeat. Lifshitz and Singer focussed on two major improvements. First a new description of the nucleon momentum in the nucleus, which gave more high momentum components. Fermi gas, shell model, and Gaussian wave functions were all rejected as not adequately describing the high-momentum components which were needed for several measurements [367]. Thus they used a "more realistic" distribution extending up to 400, even 500 MeV/c. The second difficulty was the emission process and they found that both pre-equilibrium and statistical emission was necessary. They used the Griffin model [390] which had been developed to explain other nuclear reactions. The equilibration process is achieved via a series of two-body interactions. Each intermediate stage is characterized by the number of excitons (particles plus holes), and thus a number of unbound particles which have a chance to escape.

The calculation describes a vast amount of data and codified the results in a useful way. Thus Table 4.13 lists the $(\mu^-, \nu\alpha)$ reactions and compares the calculation with the measurements of

Table 4.13
10^3 times the probabilities per muon capture for the $(\mu^-, \nu\alpha)$ reaction, calculated by Lifshitz and Singer [343] compared to 10^3 times the experimental data of Wyttenbach et al. [333]

Capturing nucleus	Lifshitz and Singer	Experiment
^{23}Na	10	11 ± 1.5
^{27}Al	7.3	7.6 ± 1.1
^{28}Si	17	
^{31}P	10	13 ± 2
^{39}K	20	
^{51}V	1.6	1.5 ± 0.2
^{55}Mn	2.3	1.6 ± 0.2
^{56}Fe	3.8	4.6 ± 0.7
^{59}Co	1.4	
^{65}Cu	0.36	0.7 ± 0.2
^{75}As	0.40	$> 0.28 \pm 0.04$
^{79}Br	0.48	

Wyttenbach et al. [333]. In this reaction compound nucleus emission is dominant, as found in other reactions, so pre-equilibrium emission was omitted; the agreement is excellent.

In Table 4.14 we present an abbreviated table from Lifshitz and Singer [343,389] comparing the (μ^-, vp) and $\Sigma(\mu^-, vp(xn))$ reactions. The deuteron reactions are assumed to be incorporated in these channels. The agreement is remarkable and we note in passing that the calculation predicts higher than average (μ^-, vp) reactions for ^{28}Si and ^{39}K, though not as high as Vil'gel'mora et al. [385], obtained.

Finally, we present in Fig. 4.28 the spectrum for protons and alphas from muon capture in AgBr. The calculation of Lifshitz and Singer [389] is compared to the early emulsion work of Morinaga and Fry [375]. The agreement is quite satisfactory over this energy range. At very high energies there is some discrepancy with other experiments, but this part of the spectrum represents a small percentage of events and needs additional complications.

4.9. Fission

When a muon stops in actinide elements, fission products are observed. This is a complex phenomenon, and we can only outline the various effects. Although well established 20 years ago, the measurements were contradictory and at times confusing. Now the topic is much better understood due to a comprehensive program at SIN, led by a group from the University of Bonn, but including many other participants.

There are two types of fission events, prompt and delayed. They are caused by very different mechanisms, but are intimately mingled in the observations, so must be considered together. The prompt events are induced by energy from the atomic cascade of the muon, whereas the delayed events are from muon capture via the weak interactions.

The advantage of a fission event is that it has a much higher energy deposition than other outcomes of a muon stop, so it can be defined without ambiguity, and thus with minimal background. Different detectors have been used such as semi-conductor counters, or a parallel

Table 4.14
Probabilities in units of 10^{-3} per muon capture for the reaction ${}^{A}_{Z}X(\mu, vp)^{A-1}_{Z-2}Y$ and for inclusive proton emission calculated by Lifshitz and Singer [343,348]. The experimental data are from Wyttenbach et al. [333], except when otherwise referenced. For $\Sigma(\mu, vp(xn))$ the experimental figures are lower limits, determined from the actually measured channels. The figures in crescent parentheses are estimates for the total inclusive rate derived from the measured exclusive channels by the use of the approximate regularity noted in Ref. [333], viz: $(\mu, vp) : (\mu, vpn) : (\mu, vp2n) : (\mu, vp3n) = 1 : 6 : 4 : 4$

Capturing nucleus	(μ, vp) calculation	Experiment	$\Sigma(\mu, vp(xn))$ calculation	Experiment	Est.
${}^{27}_{13}$Al	9.7	(4.7)	40	$> 28 \pm 4$	(70)
${}^{28}_{14}$Si	32	53 ± 10[a]	144[b]	150 ± 30[b]	
${}^{31}_{15}$P	6.7	(6.3)	35	$> 61 \pm 6$	(91)
${}^{29}_{19}$K	19	32 ± 6[a]	67		
${}^{41}_{19}$K	5.1	(4.7)	30	$> 28 \pm 4$	(70)
${}^{51}_{23}$V	3.7	2.9 ± 0.4	25	$> 20 \pm 1.8$	(32)
${}^{55}_{25}$Mn	2.4	2.8 ± 0.4	16	$> 26 \pm 2.5$	(35)
${}^{59}_{27}$Co	3.3	1.9 ± 0.2	21	$> 37 \pm 3.4$	(50)
${}^{60}_{28}$Ni	8.9	21.4 ± 2.3[c]	49	40 ± 5[c]	
${}^{63}_{29}$Cu	4.0	2.9 ± 0.6	25	$> 17 \pm 3$	(36)
${}^{65}_{29}$Cu	1.2	(2.3)	11	$> 35 \pm 4.5$	(36)
${}^{75}_{23}$As	1.5	1.4 ± 0.2	14	$> 14 \pm 1.3$	(19)
${}^{79}_{35}$Br	2.7		22	[22][d]	
${}^{107}_{47}$Ag	2.3		18	[11][d]	
${}^{115}_{49}$In	0.63	(0.77)	7.2	$> 11 \pm 1$	(12)
${}^{133}_{55}$Cs	0.75	0.48 ± 0.07	8.7	$> 4.9 \pm 0.5$	(6.7)
${}^{165}_{67}$Ho	0.26	0.30 ± 0.04	4.1	$> 3.4 \pm 0.3$	(4.6)
${}^{181}_{73}$Ta	0.15	0.26 ± 0.04	2.8	$> 0.7 \pm 0.1$	(3.0)
${}^{208}_{82}$Pb	0.14	0.13 ± 0.02	1.1	$> 3.0 \pm 0.8$	(4.1)
${}^{209}_{83}$Bi	0.04	0.08 ± 0.01	1.4	(1.2)	

[a] Ref. [385].
[b] Ref. [381]. The experimental and theoretical figures for $(\Sigma(\mu, vp(xn))$ refer in this case to total charged particle emission, i.e., including α emission.
[c] Ref. [332].
[d] Interpolation values given by Ref. [333].

plate avalanche counter PPAC. For the SIN experiments, the semi-conductor counters had a timing resolution of 1.2 ns, much shorter than the 70 ns time constant for muon capture, so an excellent separation was obtained between prompt and delayed events. The equipment was also augmented with electron counters or germanium detectors, where appropriate. A further advantage at SIN is the superb muon beam, which can stop in a thin target, and of course the 100% duty cycle.

The characteristics of the equipment mean that some observables can be measured very accurately whereas others are subject to systematic difficulties. Thus parameters which are reliably measured are the decay time, and the ratio of prompt to delayed fission events. More difficult is the total fissions per μ stop because the absolute efficiency and μ stop definition are problematic. In fact that has always been the biggest difficulty in this field.

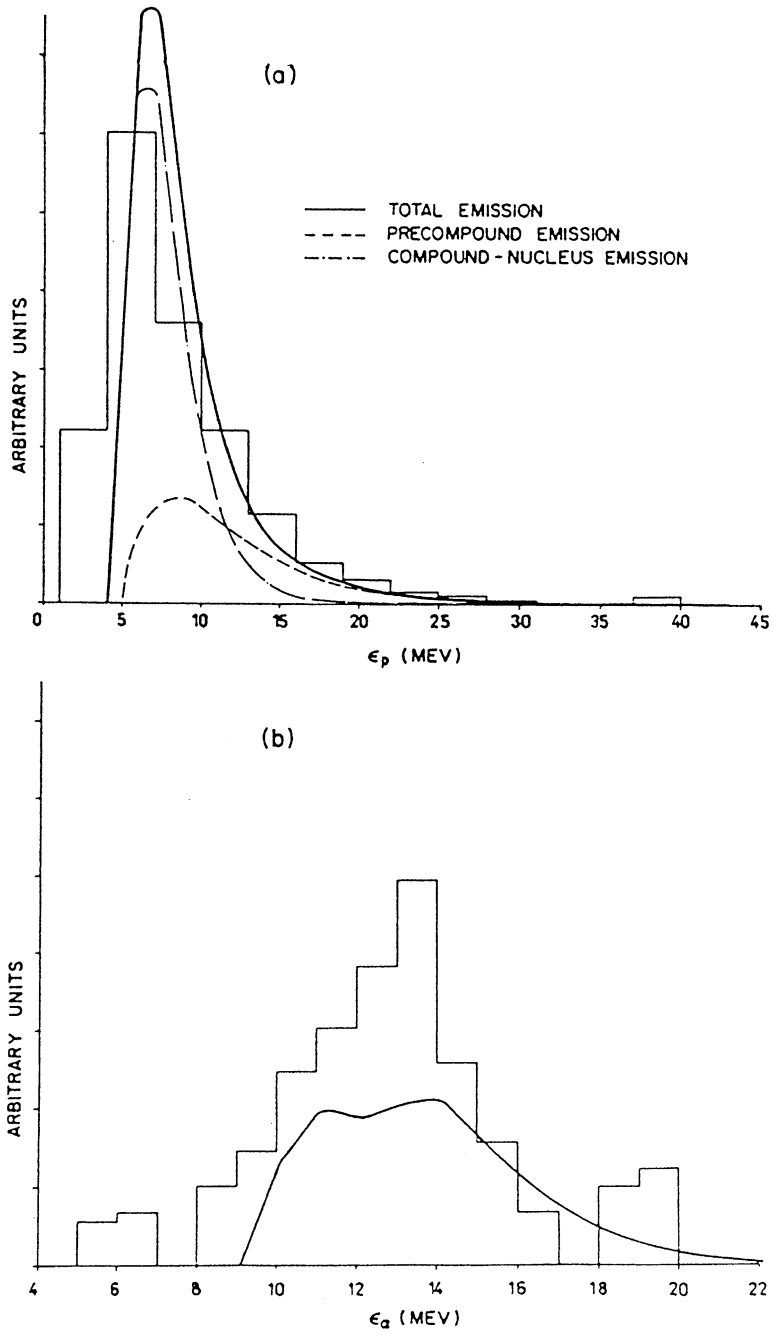

Fig. 4.28. (a) Proton energy spectra from muon capture in AgBr. (b) α particle energy spectra, also from muon capture in AgBr. The data (histograms) are from Morinaga and Fry [375], whilst the calculations are by Lifshitz and Singer [389]. Note the Coulomb barrier effect which blocks the emission of low energy charged particles.

Table 4.15
Basic parameters for fission and Auger events for muon stops in heavy atoms

Nuclide	Lifetime (ns)	Prompt/ delayed fission	Total fissions per μ stop	Prompt/ delayed neutrons	ν_p (prompt fission)	ν_d (delayed fission)	Auger neutrons (%, per stop)
^{207}Pb	75.4 (10)						~ 5[a]
^{209}Bi	73.5 (4)		0.000042 (7)				7 (2)[a]
^{232}Th	77.3 (3)	0.05 (1)	0.02 (1)	0.056 (10)	2.4	3.6	10 (2)[b]
^{233}U	68.9 (3)	0.201 (1)	0.48 (13)		2.4	3.6	
^{234}U	70.6 (2)	0.177 (1)	0.31 (8)		2.5	3.7	
^{235}U	72.2 (2)	0.125 (1)	0.31 (8)	0.11	2.5	3.7	18 (6)[b]
^{236}U	74.3 (3)	0.186 (2)	0.20 (5)		2.6	3.8	
^{237}U			0.17 (5)[c]		2.9	4.1	
^{238}U	77.1 (3)	0.088 (1)	0.14 (4)	0.08	3.1	4.3	15.4 (17)[b]
^{237}Np	69.8 (2)	0.281 (1)	0.54 (17)		2.9	4.1	
^{239}Pu	70.1 (7)	0.20 (5)	0.8 (3)	0.16 (2)	3.2	4.4	~ 5[b]
^{242}Pu	75.4 (9)	0.21 (1)	0.6 (2)	0.17	3.4	4.6	
^{244}Pu	78.2 (4)	0.26 (1)	0.6 (2)		3.4	4.6	

[a]Hargrove et al. [391,392].
[b]Our estimates, see text.
[c]Delayed fission only, see Hänscheid et al. [393].

In Table 4.15 we give some parameters related to muon induced fission for 13 target nuclides. The lifetimes are mainly taken from Hänscheid et al. [252], (but supplemented with [251,149]), and are consistent with many other measurements of a variety of authors. The prompt to delayed ratio for fission events is taken from Rösel et al. [394]. These are in agreement with earlier work, but far more accurate, often an order of magnitude. Next there is the column on the fraction of fissions per muon stop, also taken from Rösel (with bismuth taken from [395]). We have opted to accept their data as presented which were normalized to a recent absolute measurement on ^{237}Np [396]; however the reader is warned that other authors have obtained results which are a half or even smaller [397,13]. Some of these results are relatively recent, and those authors were fully aware of the problems. The difficulty is the absolute efficiency of the detector systems, so often the ratio of the fission probability for different nuclides can be in excellent agreement, thus most authors agree that for ^{235}U/^{238}U the ratio is 2. If it is not, the experiment can be rejected. Confirmation of these higher values for the total fission yield comes from the activation experiment of Baertschi et al. [398], who obtained a total fission yield of $(15 \pm 3)\%$ for ^{238}U. This is a different technique with very different systematic uncertainties.

In column 5 of Table 4.15 we give the ratio for prompt to delayed neutrons. Wilcke et al. [399], gave five values but without errors. Zglinski et al. [400], gave results for ^{232}Th and ^{239}Pu with errors. From the data presented in the paper we estimate that Wilcke et al., would have larger errors, so for ^{232}Th and ^{239}Pu, which both groups studied, we have averaged their results with a weighting of 2 : 1 in favour of Zglinski et al.

Now what is the meaning of this ratio. It is definitely NOT related to the prompt to delayed ratio for fission events, even though Rösel et al. [394], unfortunately mix the two effects in

their tabulation. Thus, for example in ^{232}Th the prompt neutrons are from Auger neutrons, that is neutrons emitted from a nucleus when a non-radiative transition raises the nuclear excitation energy above the binding energy for a neutron. In plutonium isotopes it is related to the fission ratio, but there is evidence that the number of neutrons emitted in a fission event depends on the energy of excitation, so capture fission events give off more neutrons. Thus, in column 6 we given an estimate of the number of neutrons (ν_p) given off in a prompt fission event, where the nucleus is excited to between 6 and 9 MeV. In column 7 is the number of neutrons for capture fission events (ν_d) in which the nucleus is excited to 16–19 MeV. We have used the tables given by Vanderbosch and Huizenga [401], using their estimate that the neutron multiplicity increases by

$$\frac{\mathrm{d}\nu}{\mathrm{d}E} = 0.12\,\mathrm{MeV}^{-1}\,, \tag{4.65}$$

i.e., for 10 MeV higher excitation, we expect 1.2 more neutrons per fission event. Note that Zglinski et al., find that the neutron spectra are different for the same reason. In thorium the prompt neutrons are mainly Auger and cut-off at 4 MeV, whereas delayed neutrons go higher in energy.

Thus for prompt neutrons there are Auger neutrons, and fission neutrons, and for delayed neutrons there are the capture neutrons and more fission neutrons, all with their own multiplicities. However, we have to remember that for all prompt events the muon remains attached to a nucleus for Auger events, it is a nucleus with one less neutron than the target, and muon capture and fission can follow. Equally well after a prompt fission event, the muon normally sticks to the heavy fragment and can capture, giving off more neutrons (though with a slightly lower multiplicity). Thus the ratio for prompt to delayed neutrons includes many contributions:

$$\frac{\text{Prompt}}{\text{Delayed}} = \frac{P_\mathrm{A}M_\mathrm{A} + P_\mathrm{PF}M_\mathrm{PF}}{P_\mathrm{C}M_\mathrm{C} + P_\mathrm{DF}M_\mathrm{DF} + P_\mathrm{PF}M_\mathrm{C}^{Z/2} + P_\mathrm{A}[P_\mathrm{C}^{N-1}M_\mathrm{C}^{N-1} + P_\mathrm{DF}^{N-1}M_\mathrm{DF}^{N-1}][P_\mathrm{C}^{N-1} + P_\mathrm{DF}^{N-1}]^{-1}}\,, \tag{4.66}$$

where P is the probability, per stop, for a type of event, and M is the multiplicity of neutrons given off. The subscript represents the types of events which are A, Auger; PF, prompt fission; C, capture; DF, delayed fission; if the nuclide is not the original nucleus it is the $(N-1)$ isotope because of an Auger event, or $Z/2$ from a fission event.

Obviously with so many terms, most of which are unknown, it is difficult to relate the neutron ratio to the fission event ratio. However, let us use the multiplicities given in Table 4.15, and assume that the $(N-1)$ nucleus has the same properties as the original target nucleus (this is a small correction term anyway). We can assume the capture multiplicity is 1.8 and for a fission fragment is 1.5 (see Table 4.7). Then it is surprising how much sense we can make of the various experiments. For ^{232}Th and ^{235}U we deduce the Auger probabilities given in column 8 of Table 4.15. For ^{238}U we deduce 14 (2)%, which agrees well with Hänscheid et al. [393], who quoted that there were 18.7 (30) prompt neutrons per muon stop, which is excellent agreement. In Table 4.15 we quote a weighted average of these values. For ^{239}Pu the neutron events are mainly fission events, so from a neutron ratio of 0.16 (2) we deduce a fission ratio of 0.25 (4) which is in good agreement with direct measurements which give 0.20 (5). (Unfortunately Rösel et al., did not use ^{239}Pu as a target.) Finally, we tried ^{242}Pu but the highest neutron ratio

we can reasonably reach is 0.16, because the fission event ratio is quite well known, but if we assess an error for the neutron ratio of 0.02, this is all consistent.

Thus, our conclusion is that the measurements for neutron and fission events are quite compatible as long as reasonable estimates are made for the neutron multiplicities. However, apart from the direct measurements for ^{207}Pb and ^{209}Bi [391,392], the probabilities for Auger events, as given in Table 4.15 are subject to the validity of this discussion, and thus liable to systematic uncertainties.

Now we have a general idea of the measurements that can be made, let us delve a little into the complexities of the interpretation. As we have noted in the section on the atomic cascade, there are many complications for heavy nuclei, especially deformed nuclei such as the actinides. First the nuclear deformation couples into the atomic levels of the muon and spreads the energies of the levels, and thus the energies of the muonic X-rays. For example, in ^{238}U the $2p_{3/2}$ level becomes 4 levels between 6.45 and 6.56 MeV. Thus the $2p_{3/2}$–$1s_{1/2}$ X-ray is split into 7 transitions (6.41–6.56 MeV), and the $2p_{1/2}$–$1s_{1/2}$ X-ray becomes 5 transitions (6.10–6.17 MeV). These transitions can all behave differently in fission or Auger events. Equally well, the $3d$ and $4f$ levels are split and the accompanying transitions are complex.

To give a general idea of how a cascade proceeds, we shall describe ^{238}U, taken from Rösel et al. [402], and Hänscheid et al. [393], but in the interests of clarity the numbers will be rounded off and errors omitted, thus small discrepancies may enter in. Those who wish to follow the full complexity should read the original papers.

Down to the $n=3$ level, the ^{238}U cascade proceeds roughly as normal, with Auger transitions, followed by muonic X-rays. About 88% of muons reach the $3d$ level and, 82% of these emit a $3d$–$2p$ X-ray, and 5% emit a $3d$–$1s$ X-ray but 13% excite the nucleus via non-radiative transfer of energy. The nucleus is thus excited to about 9.5 MeV and mostly de-excites via neutron emission, but about 6% of the de-excitations result in fission, which means that 0.7% of all initial stops follow this route, and this is the major contribution to prompt fission.

The next most important contributor is the $2p$ level. About 80% of the muons which stop, reach this level, and 26% undergo a non-radiative transition, exciting the nucleus to over 6 MeV. On average only 1.5% result in fission (though the probability varies significantly with which $2p$ level is populated). Thus in total 0.3% of the initial stops follow this route.

The third most important route is via the $3p$ level but only about 3% reach this level. However, 90% of these undergo a non-radiative transition and 5.3% of these fission, giving finally 0.12% of muons which follow this route. A few higher d-levels give a minor contribution; thus giving the numbers in another form, of the 1.1 (3)% of muons in ^{238}U which induce prompt fission, the following are the contributions (with numbers rounded):

$$3d\text{–}1s, \quad (57 \pm 3)\% , \tag{4.67a}$$

$$2p\text{–}1s, \quad (28 \pm 2)\% , \tag{4.67b}$$

$$np\text{–}1s, \quad (12 \pm 4)\% , \tag{4.67c}$$

$$md\text{–}1s, \quad (4 \pm 2)\% , \tag{4.67d}$$

where $n \geqslant 3$ and $m \geqslant 4$.

There have been several attempts to explain these radiationless transitions. Reasonable agreement with the ^{238}U experiment was obtained by Karpeshin and Nesterenko [403]. They showed that many transitions exhibit this property of exciting the nucleus.

The numbers are different for other nuclides, but this is an excellent illustration of the complexity of the cascade. It is worth noting that when a comparison is made with fission induced by other particles, the presence of the muon is found to raise the outer fission barrier, and thus reduce the probability for fission. We should now divert our attention from fission for a moment and following the other non-radiative transitions. For a while it was wondered whether some nuclei were held in a fission isomer, which then decayed with a short lifetime of a few nano-seconds. Some unusual time structures had been seen in early experiments, but the latest measurements find no evidence for this, so it was probably an artefact of the timing circuits. Thus the nucleus has two main alternative options, neutron emission or γ-ray de-excitation. In ^{238}U the neutron separation energy is 6.15 MeV in the middle of the $2p_{1/2}$ complex, and so most of those transitions have to de-excite by γ-rays. However above this neutron emission is possible and (15.4 ± 1.7)% of muon stops in ^{238}U yield an Auger neutron. This is a feature of many heavy nuclei, including many which do not fission. Such neutron emission means that you are left with a muon in orbit around a nucleus with one neutron less, in this case ^{237}U which cannot be studied directly. Thus, Hänscheid et al. [393], were able to determine that the fission probability per muon capture in ^{237}U is (34 ± 12)%, i.e., higher than in ^{238}U (see Table 4.15).

Note that maybe a half or more of Auger neutron events leave the nucleus in an excited state. These nuclear levels de-excite immediately with the muon still present, and have often been studied because of the energy shift caused by the muon, the so-called isomer effect. However, the intensities of these lines also provide information on the number of Auger events. Thus Budick et al. [404], used a ^{207}Pb target and found that there were 3.5% of prompt γ-rays from ^{206}Pb, to be compared with the total Auger yield of about 5% [391,392].

Returning to prompt fission, we note that the muon can adapt to the fissioning nucleus and stays attached to one of the fragments, even though the pair have a total kinetic energy of about 160 MeV. It was quickly noticed that such events were followed by capture with a muon lifetime of about 130 ns [251,405] this indicates that the muon is attached to the heavy fragment as the light elements would give a muon lifetime of about 200 ns. More recent experiments have confirmed this, showing that the probability for attachment to the light fragment is 5.1 (6)% in ^{237}Np, and estimated to be 5.5 (8)% in ^{238}U, but the probability depends strongly on the mass, going up for heavier light fragments [406–408]. The attachment probability also depends on the kinetic energy of the fragments [409]. Rarely the muon can even be ejected because of the excitation energy available after fission [410]. Some claims have been made that muonic X-rays have been observed from this heavy fragment after the fission process [411], but the evidence is rather slim. Thus at the end of the atomic cascade, in say ^{238}U, the muon is most likely to be in a 1s orbit around a ^{238}U nucleus, (about 84% of the time), about 15% it is bound to a ^{237}U nucleus, and about 1% of the time it is bound to the heavier fragment from a fission event. The nucleus is sometimes in an excited state, but this instantly gives off a γ-ray, so we are quickly left with the ground-state. Now in a time scale of about 70 ns the muon will capture on the heavy nucleus (or 130 ns for the few fragment nuclei). For the heavy nuclei, the weak interactions act as for light nuclei and excite the nucleus to 15 or 20 MeV, but this

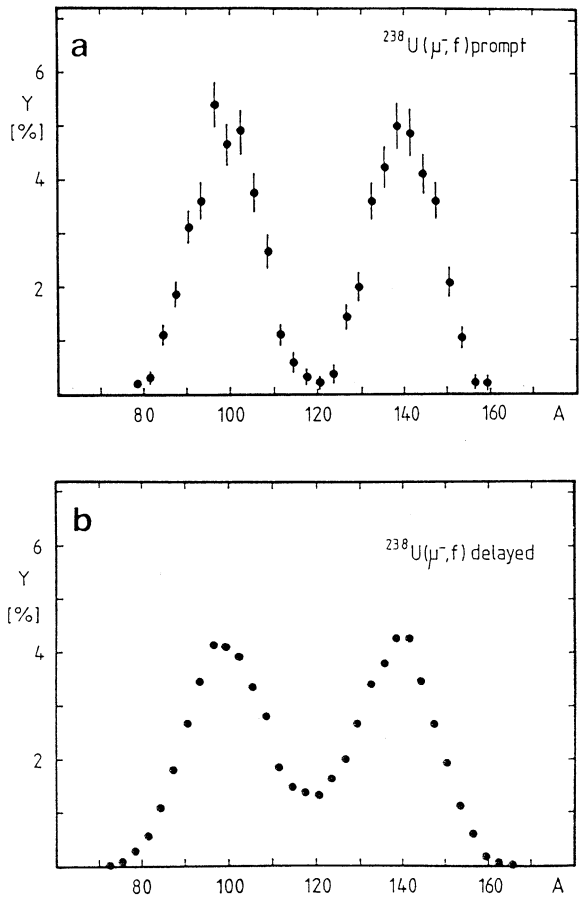

Fig. 4.29. Mass distributions from prompt and delayed fission events from muons stopping in ^{238}U. More energy is available in delayed events from muon capture via the weak interaction.

is more than enough energy to induce fission and this is when most fission events occur. It is known from giant resonance studies with photons that the fission probability is similar to the numbers in Table 4.15, thus above 10 MeV it is 20% for ^{238}U, 40% for ^{235}U or ^{236}U and 10% for ^{232}Th [412]. Remember that the fission threshold is typically 5 or 6 MeV, so some events are not able to fission, thus the pattern of numbers on Table 4.15 is quite reasonable.

The fission event this time occurs after the muon has disappeared and the neutrinos has left the scene. Because the nucleus is quite highly excited, the fission event will not be like a neutron induced fission, or a spontaneous fission, both of which have a mass spectrum for the fragments which has a very deep dip for symmetric fission. This dip gets filled in and David et al. [413,414], have been able to determine this spectrum for muon induced fission in ^{235}U, ^{238}U, ^{237}Np and ^{242}Pu. The results are fairly similar and we give those for ^{238}U in Fig. 4.29. Note that the dip is filled in for delayed fission, but not so much for prompt fission. That is simply because delayed fission occurs after a more energetic excitation. This effect is commonly observed with other excitation mechanisms, and for 190 MeV protons the dip is totally filled

in [415], as it is for pion induced fission. By comparing with other reactions one can estimate that the excitation energy in ^{238}Pa is about 18 MeV, as expected.

Delayed fission has been studied theoretically by several authors. Hadermann and Junker [416] used the impulse approximation to determine the excitation energy of the nucleus with $(Z-1)$ which peaks around 20 MeV. They then used the fission probability, known from other reactions to estimate the overall fission probability. The results depended on which reactions were chosen to obtain the fission probability, but overall the agreement was satisfactory. A similar study of 6 nuclides was made by Zglinski et al. [400], using a collective resonance model and compatible results were obtained.

The probability for muon induced fission in elements other than the actinides is low indeed. However, a probability of $4.2\ (7) \times 10^{-5}$ was found for ^{209}Bi [395] in response to an earlier suggestion by Mukhopadhyay, Haderman and Singer [349] and developed in some calculations by Lifshitz and Singer [417]. They had pursued the ideas of meson-exchange currents exciting the nucleus to high energy. For ^{209}Bi the fission threshold is 22.5 MeV, so fission is rare but not impossible.

In conclusion, we see that the topic of muon-induced fission is now fairly well understood. Because of its complexity there are inevitably many remaining questions and more data would be useful, as always. Thus for example, it is unfortunate that the Bonn group did not include ^{232}Th and ^{239}Pu in their precise measurements of prompt to delayed fission. It would also be interesting to redo some of the neutron experiments, attempting to measure absolute yields, and thus multiplicities (and to give errors, even if we do not believe them).

5. γ-ray studies

5.1. Introduction

5.1.1. Nuclear physics aspects

Significant progress has been made in the last decade by experiments which study the γ-rays emitted after muon capture occurs. Better detectors have helped but longer runs and better statistics make a major difference too.

Many γ-rays are observed in a spectrum, often several hundred, so identification is a critical first step. Modern detectors have a working resolution of about 2.5 keV at 1 MeV and most γ-rays are in the region 500–3000 keV, so there are a few conflicts, and these must be tackled with care. In addition Doppler broadening is severe for lighter elements, ~ 7 keV per MeV in ^{28}Si for example, so overlaps are not uncommon. Many reactions occur and 5–12 nuclides are normally detected in muon capture, and even more are produced, but with transitions too weak to identify.

Comparisons to other reactions help, thus (π,γ), $(d,{}^2\mathrm{He})$, and (n,p) reactions can guide the search, but even the best experiments with these reactions have a resolution of only 200 keV for the final states, so only major transitions can be compared, and often these are obvious anyway. Nevertheless, the comparison gives confidence to the interpretation and is clearly critical for ground-state transitions which produce no γ-rays.

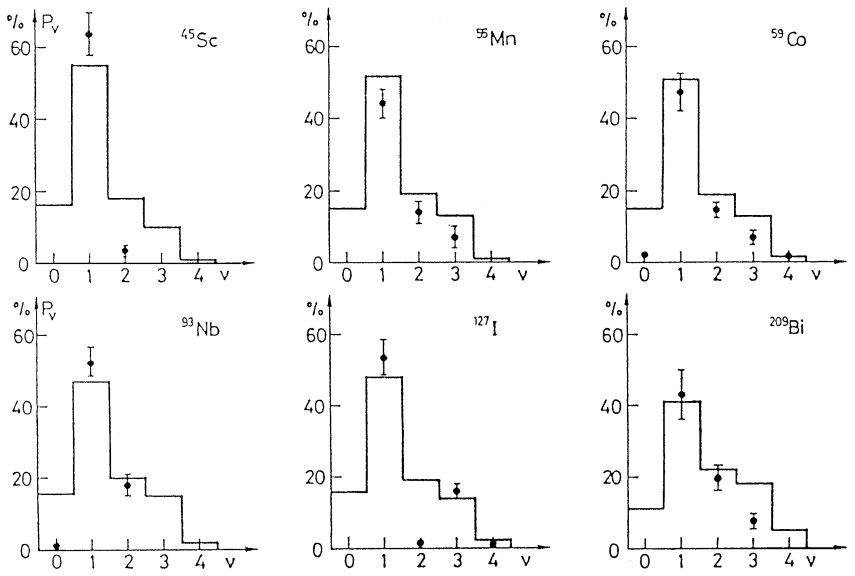

Fig. 5.1. Neutron multiplicities from the γ-ray studies of Backenstoss et al. [345]. (Such measurements give a minimum value.) The calculations are based on Singer's model with a nuclear temperature, $\theta = 0.75$ MeV, and an effective nucleon mass of $m^* = 0.5M$.

Even though many thousands of levels have been tabulated and compiled, it is surprising how many are still not fully described, especially in heavy elements. Even for ^{28}Al, produced via ^{28}Si$(\mu^-, \nu)^{28}$Al, many levels are not known and quite a few parameters in the compilations are clearly inadequate, as excellent as these compendia are. (We shall use the standard references of Endt [418] and the 8th Edition of the Table of Isotopes [419].) Thus, a modern experiment often needs support from classical nuclear structure accelerators.

Even the earliest experiments were remarkably fruitful. Backenstoss et al. [345] stopped muons in ^{45}Sc, ^{55}Mn, ^{59}Co, ^{93}Nb, ^{127}I and ^{209}Bi, elements chosen because the natural target has only one isotope. They were able to identify many transitions and compiled the data given in Fig. 5.1. The dots are their observations for how often the no neutron, $1n$, $2n$, $3n$ and $4n$ reactions were detected. Only γ-ray transitions to the ground-state are included in this plot, to avoid double counting. The comparison is with the Singer model for muon capture. The agreement is remarkable when one considers the limitations of a γ-ray experiment, for example the detector was not sensitive enough to detect γ-rays over 2.6 MeV. Thus the conclusions for these medium to heavy weight nuclei are that:

(a) Most neutrons leave the nucleus in low-lying levels, or levels that cascade through them.
(b) There are few neutron transitions which leave the residual nucleus in the ground-state.
(c) No proton emitting reaction was observed.

The most obvious discrepancy is that very few no neutron transitions were observed. We now realise that they are there, but spread out over many levels, often up to 4 or 6 MeV, and they are very difficult to disentangle, even for a modern experiment. It is important to note that

Table 5.1
Relative strengths (in per cent) of the transitions in muon capture on three nickel isotopes, all having 0^+ ground-states, taken from Eramzhyan et al. [420], using $g_P/g_A = 6.0$

	0^+	0^-	1^+	1^-	2^+	2^-	3^+	3^-	$\Sigma(10^5\,s^{-1})$		B_n (Co)
									Calc.	Exp.	(MeV)
^{58}Ni	2.6	3.2	26.1	35.6	9.6	16.4	5.1	1.3	58	61 (1)	8.6
^{60}Ni	2.8	3.4	25.2	36.5	10.0	15.6	5.2	1.4	53	56 (1)	7.5
^{62}Ni	3.1	3.5	24.9	36.8	10.3	14.7	5.3	1.4	48	47 (1)	10.6

these comments concern nuclei with $A > 40$. For lighter nuclei, the (μ^-, ν) reaction is clearly observed, as are the weaker $(\mu^-, \nu p)$, $(\mu^-, \nu pn)$ and $(\mu^-, \nu p2n)$ reactions, moreover there is indirect evidence that ground-state transitions are important in the $(\mu^-, \nu n)$ reaction.

The simplest transitions to interpret are those from the (μ^-, ν) reaction, unfortunately observed only in the lighter elements. The transition is a matrix element via the weak interactions, and is an excellent test of nuclear structure calculations, as well as being a useful check for astrophysical (e^-, ν) reactions.

To give a general idea of the (μ^-, ν) reaction we shall take a brief glance at muon capture in ^{58,60,62}Ni, studied recently by Eramzhyan et al. [420], using the Random Phase Approximation for the nuclear response. A similar calculation was made 24 years earlier by Nalcioglu et al. [421], with comparable results. This type of calculation is inadequate for a detailed discussion of the excitation spectrum, but it is likely to give a reasonable general impression. All these nuclei have a 0^+ ground-state, so a 1^+ transition goes to a 1^+ final state etc. In Table 5.1, we present the results of Eramzhyan et al., which are given as the relative contributions of the transitions. Also given is the total capture rate, calculated and experimental, and the neutron binding energy in the residual Co nuclide. The main strength is in the 1^+ transitions which tend to go to bound levels, and the spin–dipole 1^- strength which goes to the spin–dipole giant resonance (SDR) at about 15 MeV excitation energy, which is above the neutron binding energy. The spin–dipole 2^- transitions are slightly less important and tend to be a few MeV lower in energy than the 1^- SDR. The 0^- transitions are even less important and tend to be a few MeV above the 1^- SDR. In some reactions the three components of the SDR, i.e., 2^-, 1^-, 0^-, have strengths in the ratio $(2s + 1)$ viz. 5 : 3 : 1, but the (n, p) reaction exhibits a similar pattern to muon capture; Rönnquist [422], using the CELSIUS facility studied the reactions ^{54,56}Fe(n, p) at 97 MeV and also used the RPA to estimate the nuclear responses, so the comparison with Eramzhyan et al., is quite helpful. Rönnquist et al., also point out that the $L = 2$ spin quadrupole resonances have strengths in the proportion $2^+ > 3^+ > 1^+$, which also parallels the muon capture case. Unfortunately, their experimental resolution of ~ 2.8 MeV makes their results of marginal help for guiding analysis of muon capture. Nevertheless a review of their results by Olsson [363] is very useful for helping to compare the (n, p) and (μ^-, ν) reactions in a general way.

Now most of the Gamow–Teller or 1^+ strength goes to low-lying levels; it is also very important for electron capture reactions in the collapse of massive stars. Thus Caurier et al. [423], invested considerable effort in calculating this strength in the pf shell. In Fig. 5.2, we present their calculations for the excitation strength compared to several (n, p) experimental

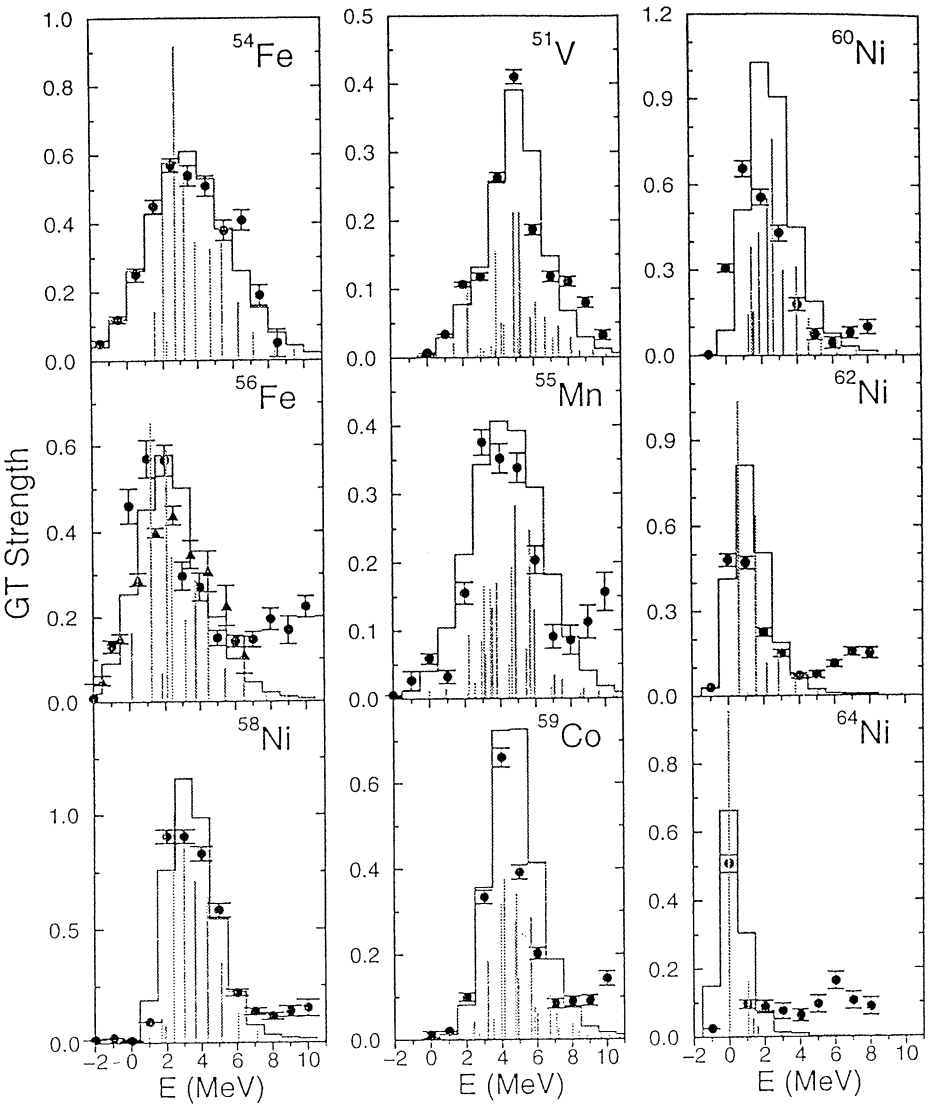

Fig. 5.2. Comparison of GT data from the (n, p) reaction with the calculated strength distributions for even-even nuclei ^{54,56}Fe and ^{58,60,62,64}Ni, and the odd-A nuclei ^{51}V, ^{55}Mn and ^{59}Co taken from Caurier et al. [423]. The shell model results are shown by discrete spikes, and have been folded with the experimental energy resolution to give the histogram. The data are from [424–428].

spectra ^{48}Ti [424] (not illustrated), ^{54}Fe [425], ^{55}Mn, ^{56}Fe and ^{58}Ni [426], ^{51}V and ^{59}Co [427] and ^{60,62,64}Ni [428]. The data are from TRIUMF and use typically 200 MeV neutrons with an energy resolution of 1 MeV or so. We note in passing that the calculations and (n, p) experiment for ^{60}Ni are not really compatible with the experimental results of Nakayama et al. [315], from the reaction ^{60}Ni(^{7}Li, ^{7}Be)^{60}Co in which a double bump structure is observed, peaking at excitation energies of 1.5 and 3.0 MeV for $\Delta S = 1$, see Fig. 4.12.

The calculations and experimental results help us to justify some comments that we have made about muon capture. Firstly, there is every reason to suppose that muon capture will excite the same bound levels as the (n, p) reaction. The reason that Backenstoss et al., did not observe such transitions is that they are splintered, and are often to levels between 4 and 8 MeV, which may have direct transitions to the ground-state. The neutron binding energies for the products of muon capture on ^{58,60,62}Ni were given in Table 5.1; those for the products of the targets ^{54}Fe, ^{56}Fe and ^{64}Ni are 8.9, 7.3 and 6.0 MeV, respectively, whilst the products for the odd nuclei all have neutron binding energies of just over 6 MeV. Thus, a little strength goes to unbound 1^+ levels, but most goes to bound levels. It would be helpful to have a new study of muon capture for such nuclei with a modern large HPGe detector which would have a better efficiency for high energy γ-rays.

Secondly we note that it is worthwhile to make a comparison with the activation results for bound state transitions, given in Table 4.9. The total GT strength for the (n, p) reaction is 1.2 (1) for ^{51}V, 2.8 (3) for ^{56}Fe, 3.8 (4) for ^{58}Ni and 1.9 (1) for ^{59}Co [423]; the inconsistencies for the activation measurements are confusing, but the overall pattern is consistent, giving us some confidence in the activation results, and in the overall pattern of Singer's model though sophistications such as relative GT strength were not included.

We make one final comment on another topic, with respect to the muonic cascade; the muon can have hyperfine levels in the 1s state for nuclei with spin. If it is an odd Z nucleus, the capture rate for a specific transition can vary enormously for these two hyperfine states, and this sensitivity can be used to extract detailed nuclear information. In addition the g_P coupling constant can be studied this way.

5.1.2. Technical aspects

As in all experiments, the quality of the equipment and the beam can make a lot of difference to the outcome of an experiment. Modern large high purity germanium detectors have helped in the study of high energy γ-rays because the efficiency is much better. Detailed efficiency curves have been obtained by Kamboj and collaborators [179,180], and they illustrate the accuracy of such studies, plus the advantages of a 110% detector for high energy γ-rays (a factor of 4 better relative efficiency at 3 MeV over a 20% detector, normalizing at about 150 keV, and a factor of 6 better at 8 MeV. Other useful discussions can be found in texts such as that by Debertin and Helmer [177].

Most muon capture experiments use n-type detectors. Although more expensive they are less vulnerable to degradation by neutron irradiation and they also can detect lower energy γ-rays, though thick targets can nullify this advantage.

Germanium detectors are remarkably stable and permit very accurate energy measurements, even if the resolution is 2 keV for a typical 1 MeV γ-ray. Ideally the centre of gravity of a line can be determined to $N^{-1/2}$ of the resolution, where N is the number of counts, for example, 20 eV for 10,000 counts. In reality it is never that simple because of non-Gaussian responses, and the risks of contaminating lines. Nevertheless accuracies of 0.1 keV are standard, and can be of great help in identifying lines, or in warning of possible weak lines within the resolution function.

Table 5.2
Commonly used calibration γ-rays, showing the changes in the last 20 years. The 1979 data are the compendium of Helmer et al. [431], plus the hydrogen line of Greenwood and Chrien [432]. The latest compendium is that of Helmer and van der Leun [429]. Other data are from [433,434]. We use $E_\lambda = 1239.84244\ (37)$ eV nm

Source	1979 (eV)	1999 (eV)
^{198}Au	411,804.4 (11)	411,802.05 (17)
^{60}Co	1,332,502 (5)	1,332,492 (4)
^{152}Eu	121,782.4 (4)	121,781.7 (3)
	244,698.9 (10)	244,697.4 (8)
	344,281.1 (19)	344,278.5 (12)
^{16}N/^{13}C(α, n)	6,129,270 (50)	6,129,140 (30)[a]
m_e	511,003 (2)	510,998.902 (21)[b]
$np \to \gamma d$	2,223,247 (17)	2,223,258.3 (23)[c]

[a]The site www.nndc.bnl.gov and [435] seem to use an erroneous value of E_x= 6,129,893 (40) eV and E_γ= 6,128,630 (40) eV. We use the average of 3 determinations [436–438], as confirmed by Wapstra [434].
[b]Observed annihilation radiation is slightly less than $m_e c^2$.
[c]Value of [433], as corrected by Wapstra [434].

The calibration lines have gone through a process of re-assessment because of changes in the value of "the gold standard" viz. ^{198}Au [429], due mainly to the conversion between wavelength and eV. New very accurate atomic mass measurements [430] will also change (n, γ) calibrations. These changes will not make a significant difference to γ-ray identification because few lines are measured with precisions better than 1 eV, thus the 20 year old compendium of Helmer et al. [431], is quite adequate for most purposes, but it will be wise to change over to the new standards. In Table 5.2 we compare the 1979 compendium with the best values available today. The biggest difference is the 0.110 keV change in the ^{16}N β decay line, also obtained in ^{13}C(α, n) sources. The use of ^{16}N is convenient in high energy accelerators as the cooling water of magnets or beam stops is quite active [439]. Because the hydrogen (n, γ) line is pervasive in muon capture spectra we have included an old [432] and new [433,434] measurement of this important line. The electron mass is also included as annihilation radiation is so obvious, but one should remember that the observed γ-ray is reduced by a few eV by the binding of the electron in the material.

Identification is critical because in any experiment many background lines and bumps are observed and correct interpretation is essential. Many radioactive materials surround the detector (^{16}N, ^{41}Ar, ^{60}Co) whilst neutron inelastic scattering can excite levels in B, Al, Fe, I, Pb to name the most prominent. Then there is the sea of thermal neutrons around the accelerator and beam lines which creates many (n, γ) lines; H, Cl, Fe are commonly detected. Perhaps the most frustrating background is the neutron interaction in the detector itself. These are often neutrons from muon capture, so the effect can have the same time constant as capture. A neutron collides with a germanium nucleus, exciting it to a nuclear level, and then the nucleus recoils. If the resulting de-excitation γ-ray is absorbed in the detector one measures the γ-ray energy and the recoil energy, creating a triangular shaped structure with a base of about 30 keV. This effect has been studied by Gete et al. [440]; it is also clearly evident in the data of de Laat et al. [441],

Table 5.3
Some typical background lines, observed in muon capture experiments. The yield per muon stop is given as a rough guide; the actual value depends on the target or material around the detector, and on time cuts

Energy (keV)	Approx. yield	Identification
418	0.005	$^{127}\mathrm{I}(n,n')$
476	0.20	$^{10}\mathrm{B}(n,\alpha)^{7}\mathrm{Li}$
511	0.45	$(e^{+}e^{-})$
593	0.10	$^{127}\mathrm{I}(n,n')$
596	0.02	$^{74}\mathrm{Ge}$
693	0.01	$^{72}\mathrm{Ge}$
700	0.07	$^{74}\mathrm{Ge}$
718	0.001	$^{10}\mathrm{B}(n,n')$
803	0.003	$^{206}\mathrm{Pb}(n,n')$
835	0.02	$^{72}\mathrm{Ge}$
844	0.01	$^{27}\mathrm{Al}(n,n')$
847	0.01	$^{56}\mathrm{Fe}(n,n')$
898	0.003	$^{207}\mathrm{Pb}(n,n')$
1014	0.015	$^{27}\mathrm{Al}(n,n')$
1097	0.002	$^{115}\mathrm{In}(n,\gamma)$
1173	0.007	$^{60}\mathrm{Co}(\beta^{-})^{60}\mathrm{Ni}$
1238	0.005	$^{56}\mathrm{Fe}(n,n')$
1294	0.15	$^{41}\mathrm{Ar}(\beta^{-})^{41}\mathrm{K}$
1333	0.007	$^{60}\mathrm{Co}(\beta^{-})^{60}\mathrm{Ni}$
1779	0.01	$^{27}\mathrm{Al}(n,\gamma)$
2223	0.10	$\mathrm{H}(n,\gamma)\mathrm{D}$
2614	0.007	$^{208}\mathrm{Pb}(n,n')$
4438	0.03	$^{12}\mathrm{C}(n,n')$
6129	0.002	$^{16}\mathrm{N}(\beta^{-})^{16}\mathrm{O}$
7631	0.015	$^{56}\mathrm{Fe}(n,\gamma)$
7645	0.01	$^{56}\mathrm{Fe}(n,\gamma)$

who were studying stopped pions and could thus apply time of flight cuts to distinguish neutron effects from γ-ray events. Neutron excitation triangles are seen strongly with the lower edge at 596, 691, 834 and 1041 keV, but de Laat et al., detect many more including 563, 1109, 1204 and 1465 keV which are less clearly detected in muon capture experiments (but are there).

In Table 5.3 we give a few typical background lines to illustrate the variety of causes of such γ-rays. We have used the table given by Miller et al. [340], as a basis, and supplemented it with others from experience at TRIUMF. These are only a sample and two or three times as many have been identified. One might wonder where some come from. Some have obvious sources such as carbon in scintillator detectors, lead from shielding, aluminium and iron from construction materials, and iodine in a NaI suppressor. However, materials in a germanium detector are not so well known, examples are boron nitride insulators and indium contacts, which both unfortunately have very large neutron cross-sections. The ^{41}Ar is from air activation, and ^{60}Co from activated copper in magnets (or a forgotten source). At TRIUMF a persistent

background from ^{152}Eu was traced to activated concrete which had been made from a heavy aggregate from a mine. It is important to realise that the background observed in a specific experiment depends on the material near the detector, and on the target, and most importantly on the timing cuts, so it varies from experiment to experiment quite significantly, but the table illustrates the diverse sources of background.

Most modern experiments have used Compton suppressors around the germanium detector. Normally composed of NaI, but sometimes of BGO, this annulus detects Compton scattered γ-rays from the germanium. Used in anti-coincidence it can reduce the general background by a factor of five, and significantly enhance the signal for weak transitions. Such devices are not without side-effects however. They often add I(n,n') γ-rays to the spectrum for example. One annoying feature is that they can change the efficiency if a cascade is present, as other γ-rays can fire the Compton suppressor. They also create Compton bumps instead of Compton edges as γ-rays which scatter near 180° escape through the hole in the front (which has to be left open to let the γ-rays in).

A final comment should be made about muon stop rate. In meson factories one can often have a muon beam which is more intense than the detectors can handle. It is the old problem of whether you want a little good data or lots of poor data. The faster rates also complicate the timing circuits. Each experiment makes a compromise based on the principal goal, but it is seldom perfect for by-products. Typical rates chosen are 10^4–10^5 μ^- stops s^{-1}, but higher (or lower) may be appropriate in some circumstances. The result however is that weak lines (viz. 10^{-3} per μ capture) are hard to disentangle because of statistical fluctuations in the pulse height spectra.

5.2. Silicon-28

We choose to describe ^{28}Si first, because it is the nucleus for which most information is available. It is a convenient target and many important measurements have focussed on this nuclide.

We commence by presenting in Fig. 5.3 the γ-ray spectrum from the reaction ^{28}Si(π^-,γ) obtained by the SIN group [442]. The analysis of the spectrum is given in Table 5.4. Note that the energy scale in Fig. 5.3 is in error by 0.4 MeV if we assume that all absorption occurs from the $2p$ state, which has a binding energy of about 0.2 MeV. The spectrum can be taken to be roughly the neutrino spectrum from the reaction ^{28}Si(μ^-,ν)(with the energy shifted up by 34 MeV). The continuum has been subtracted off, which means that higher energy excitations will be even more dominant in the total spectrum. Note that although 1^+ levels are dominant around an excitation of 2.2 MeV, as in the (μ^-,ν) reaction, most of the (π^-,γ) reactions will occur from the $2p$ pionic orbit, so 2^+ and 3^+ excitations will be quite prominent and there is no guarantee that the strong excitations at 4.1, 5.2 and 6.1 MeV are 2^- as indicated, and thus there may not be equivalent strong transitions in the (μ^-,ν) reaction. However, even though the details may be inappropriate, the overall impression is an excellent pedagogic illustration.

In Table 5.5 we present a list of the various reactions that can occur in muon capture. Note that for heavier elements the reactions which produce charged particles are lower in probability.

The basic neutron producing reactions are taken from MacDonald et al. [328], which were given in Table 4.7. Activation studies given in Table 4.9 fix the (μ,ν) probability at 26 (3)%.

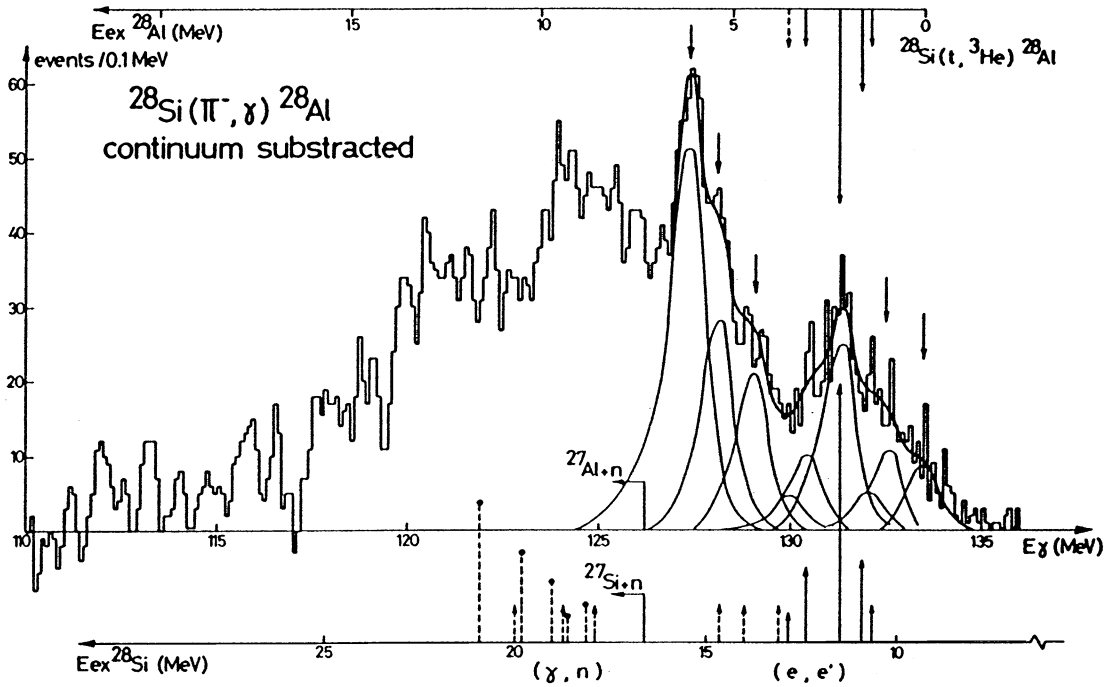

Fig. 5.3. A γ-ray spectrum from the reaction $^{28}\mathrm{Si}(\pi^-,\gamma)$ for pions at rest, mainly in the $2p$ orbit [442]. It is a useful surrogate for the (μ^-,ν) reaction. Note that the γ-ray energy scale is 0.4 MeV too low—see Table 5.4.

Table 5.4
Photon analysis of the reaction $^{28}\mathrm{Si}(\pi^-,\gamma)^{28}\mathrm{Al}$, at rest, from the SIN group; the spectrum is given in Fig. 5.3. The spin and parity assignments are often only suggestions. The B(GT) is normalized to 0.96 for the 2.2 MeV level

Photon energy (MeV)	Excitation in ^{28}Al (MeV)	Spin and parity	Number of events	B(GT)
133.9	G.S.	3^+, 2^+	101	—
132.9	1.0	0^+, 2^+	163	—
132.4	1.4	1^+	75	0.25
131.7	2.2	1^+	288	0.96
130.8	3.1	1^+	82	0.27
130.4	3.5	1^+	21	0.07
129.9	4.1	2^-	179	—
128.7	5.2	2^-	280	—
127.8	6.1	2^-	661	—

For the charged particles Sobottka and Wills [381] found that 15 (2)% of events gave charged particles, and Budyashov et al. [380], found that the yield for deuterons was about half of that for protons. (We make the risky assumption that their measurement for $E > 18$ MeV is true overall.)

Table 5.5
Suggested pattern of muon-capture reactions for ^{28}Si, given as a percentage of all captures. Smaller contributions have an uncertainty of a factor of two, at least

$(\mu^-, \nu)^{28}$Al	26						
$(\mu^-, \nu n)^{27}$Al	45	$(\mu^-, \nu p)^{27}$Mg	2.0				
$(\mu^-, \nu 2n)^{26}$Al	12	$(\mu^-, \nu pn)^{26}$Mg	4.9	$(\mu^-, \nu d)^{26}$Mg	3.1		
$(\mu^-, \nu 3n)^{25}$Al	1	$(\mu^-, \nu p2n)^{25}$Mg	1.4	$(\mu^-, \nu dn)^{25}$Mg	1.0	$(\mu^-, \nu 2pn)^{25}$Na	0.1
		$(\mu^-, \nu p3n)^{24}$Mg	0.6	$(\mu^-, \nu d2n)^{24}$Mg	0.3	$(\mu^-, \nu\alpha)^{24}$Na	1.0
		$(\mu^-, \nu p4n)^{23}$Mg	0.1			$(\mu^-, \nu\alpha n)^{23}$Na	0.8
						$(\mu^-, \nu\alpha 2n)^{22}$Na	0.5
						$(\mu^-, \nu\alpha 3n)^{21}$Na	0.2
$\Sigma(n)$	84	$\Sigma(p)$	9.0	$\Sigma(d)$	4.4	Σ(Na)	2.6

There are problems however. Vil'gel'mora et al. [385], found that the reaction ^{28}Si$(\mu^-, \nu p)$ had a probability of (5.3) (10)% and Wyttenbach et al. [333], found the ratio

$$(\nu p) : (\nu pn) : (\nu p2n) : (\nu p3n) = 1 : 6 : 4 : 4 \, . \tag{5.1}$$

These are clearly incompatible, but Miller et al. [340], found that the yield for the 984 keV γ-ray from $(\mu^-, \nu p)^{27}$Mg was 1.9 (2)%. We thus take this value as a minimum and reject the Wyttenbach ratio for ^{28}Si. (Note that in ^{40}Ca, the $(\mu^-, \nu p)$ and $(\mu^-, \nu$pn) yields are also quite similar, see Section 5.8.) A further complication is that Miller et al., find that the yield for the 1808 keV line from $(\mu^-, \nu$pn$)^{26}$Mg is 10 (1)%, which nearly blows our charged particle budget. We thus push down total the yield of ^{26}Mg to 8% and raise the total charged particle yield to 16%, and the overall result is Table 5.5. We give no errors because of the inconsistencies, but a factor of 2 for smaller yields and $\pm$5% for larger yields is a minimum uncertainty. The point of the table is not the exact numbers, but just the principle of trying to fit all the constraints.

In Table 5.6 we give the yields for γ-rays in ^{28}Al, comparing the recent experiment of Gorringe et al. [338], compared to the older one by Miller et al. [340]. The agreement is satisfactory; the only problem is that Miller et al., probably misidentified the 1620 keV line. The yields for the 2139 keV level are taken from Moftah [443], because there seems to be an error in the yields given by Gorringe et al.

The most obvious feature is that most of the strength is going initially to 1^+ levels, though the 2^-, 2^+ and maybe 0^+ are direct transitions. (Note that the yield of the 972 line is almost all feeding from the 1373 keV and the 2201 keV levels. The 1373–972 keV transition is not listed, as it is the same energy as the $2p$–$1s$ muonic X-ray, see Table 3.4, but it must contribute about 13.4 in these units; thus the results of Miller et al., are internally slightly inconsistent.) Now if one adds all the ground-state transitions, one obtains a yield of about 16 (2)% (averaging the 31 keV yield), but this is far short of the 26 (3)% observed in the activation measurements. Now a line at 4815 keV is observed by Gorringe et al., as well as by Moftah, but is hard to identify, however it is almost certainly from ^{28}Al and would contribute another 1% or so. Yet more lines are needed and there are almost certainly still to be identified transitions between 5 and 7.7 MeV (the neutron binding energy for ^{28}Al).

Table 5.6
Yield of γ-rays from the reaction $^{28}Si(\mu^-, \nu)^{28}Al$, comparing the recent result of Gorringe et al. [338], to the older one of Miller et al. [340]. The yields are given in probability per 1000 captures

		Miller et al. [458]	Gorringe et al. [338]
$31 \rightarrow 0$	$2^+ \rightarrow 3^+$	131 (13)	158 (19)
$972 \rightarrow 31$	$0^+ \rightarrow 2^+$	20 (3)	29.6 (36)
$1373 \rightarrow 31$	$1^+ \rightarrow 2^+$	17 (2)	18.4 (34)
$1620 \rightarrow 31$	$1^+ \rightarrow 2^+$	17 (3)	15.1 (22)
$1620 \rightarrow 0$	$1^+ \rightarrow 3^+$	18 (3)	~ 0
$2139 \rightarrow 31$	$2^+ \rightarrow 2^+$		~ 12
$2139 \rightarrow 0$	$2^+ \rightarrow 3^+$		~ 9
$2201 \rightarrow 972$	$1^+ \rightarrow 0^+$	18 (3)	10.6 (20)
$2201 \rightarrow 31$	$1^+ \rightarrow 2^+$	46 (3)	62.6 (68)
$3105 \rightarrow 31$	$(1,3)^+ \rightarrow 2^+$		12.7 (22)
$3876 \rightarrow 0$	$2^- \rightarrow 3^+$		8.4 (27)

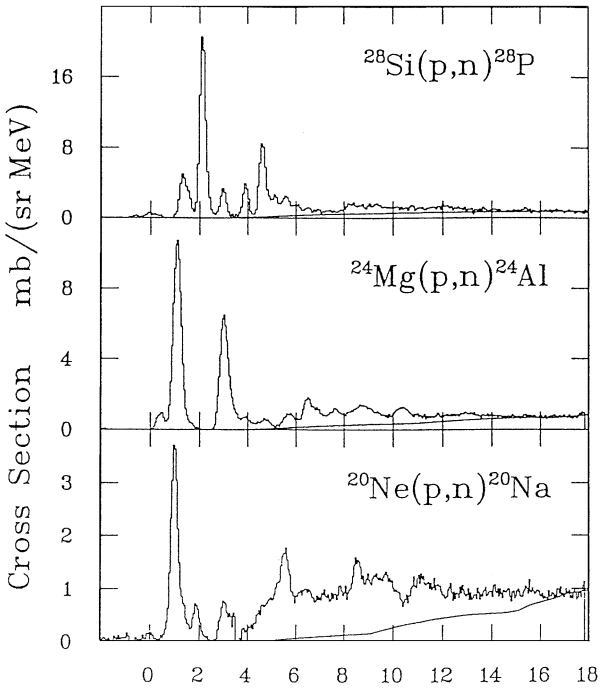

Fig. 5.4. Excitation spectra for the (p,n) reaction at 136 MeV and 0.2° for the $A=Z$ targets of ^{20}Ne, ^{24}Mg, and ^{28}Si. The data are from Anderson et al. [285]. Most of the peaks will be 1^+ transitions and the spin–dipole resonance will be weak at this angle.

In Fig. 5.4 we show the spectra for the (p,n) reaction at 0.2°, $E_p = 136$ MeV, for ^{20}Ne, ^{24}Mg and ^{28}Si, taken from Anderson et al. [285]. Remember that the 0° spectra emphasize the 1^+ transitions and that muon capture has relatively more strength to 2^- and 1^- levels.

Table 5.7
Comparison of 1^+ transitions in ^{28}Si; the data are ^{28}Si(^{3}He, t)^{28}P [446]; ^{28}Si(p,n)^{28}P [285,447]; ^{28}Si(p, p')^{28}Si [448]; ^{28}Si(e,e')^{28}Si [449]; and ^{28}Si(μ^-,ν)^{28}Al [338]. The level identification follows Endt and Booten [450]. To simplify comparisons all data have been normalized to the (p,n) value of B(GT) for the 2.143 MeV level in ^{28}P(2.201 MeV in ^{28}Al)

Excitation energy (MeV)			(^{3}He, t)	(p,n)	(p, p')	(e,e')	(μ^-,ν)
^{28}Si	^{28}P	^{28}Al	B(GT)	B(GT)	σ	σ	capture
10.596	1.313	1.373	0.21	0.20	0.24	0.04	< 0.43[a]
10.725	n.a.	n.a.	—	—	0.09	0.02	—
10.900	1.568	1.620	0.10	0.11	0.10	0.20	0.19
11.446	2.143	2.201	0.96	0.96	0.96	0.96	0.96
12.330	2.973	3.105	0.15	0.15	0.21	0.19	0.17[b]
12.754	3.512	3.542	—	—	—	—	—
13.320	3.90	4.115	0.17	0.16	0.23	—	—
14.095	4.60	4.846	0.35	0.41	0.34	0.08	(~ 0.13?)[c]
14.334	(5.02)	(5.11)	—	0.14	—	—	—
15.147	(5.56)	(5.93)	(0.08)	0.09	0.12	0.05	—
15.500	(5.93)	(6.28)	—	0.09	0.03	0.06	—

[a]May have feeding from higher levels.
[b]We assume no transition to 2201 level.
[c]Possible γ-ray at 4815; branching ratios of level unknown.

Unfortunately the interest of (p,n) experiments is focussed on 1^+ strength, so normally the 0° spectrum is shown, not a 5° or 10° spectrum which might be more relevant for our needs. Thus a comparison with the (π^-,γ) spectrum in Fig. 5.3 shows a much greater strength in the (π^-,γ) reaction feeding levels above 6 MeV extending beyond 20 MeV; this is a better analogy for the (μ^-,ν) reaction. However, the comparison with the (p,n) reaction is very useful, and we can learn a lot from these spectra.

If we consider these 1^+ transitions, it is fortunate that we can compare muon capture with several reactions, viz. the ^{28}Si(p,n)^{28}P and the similar (^{3}He, t) reaction; plus the forward angle ^{28}Si(p, p') and the backward ^{28}Si(e,e') which in these geometries excite 1^+ levels preferentially. There are also results from RIKEN on the reaction ^{28}Si(d, ^{2}He)^{28}Al, but the resolution is only about 1 MeV [444,445]. They also studied the reaction ^{28}Si(^{12}C, ^{12}N)^{28}Al obtaining a slightly better resolution of 700 keV. The results for these reaction are completely consistent with the (p,n) results of Anderson et al., so we do not present those other data in a figure. However, the RIKEN results give data at 0°, 4° and 7° for the (d, ^{2}He) reaction, and the 4° spectrum has greater transition strength at an excitation energy of 5 MeV and above, which is probably more appropriate for muon capture. In Table 5.7 we compare these measurements using, as a basis, the table prepared by Fujita et al. [446], who recently studied the (^{3}He, t) reaction with a 450 MeV ^{3}He beam at RCNP, Osaka. They compared their results with the (p,n) data of Anderson et al. [285,447], which was given in Fig. 5.4, the (p, p') data of Crawley et al. [448], and the (e,e') data of Lüttge et al. [449]. We have adjusted the table to follow the 1^+ identifications of Endt and Booten [450]. We have simplified the table omitting several $T=0$ identifications, and to help in the comparisons, we have normalized the (p, p'),(e,e') and

Table 5.8
Calculations of Kuz'min and Tetereva for $A = 28$ nuclei [451]. They modified the excited state wave functions to fit data for ^{28}Si(e,e') and ^{28}Si$(p,n)^{28}$P. The resulting calculated values for these observables are given, as are the lifetimes and muon capture rates to ^{28}Al

^{28}Al	1^+ Level (keV)	1373	1620	2201	3105	3542	4115	4846	5017	5435	5919
B($M1$)	Calc.(e,e')	0.45	1.04	4.64	0.76		0.26	0.62	0.23	0.29	0.33
B(GT)	Calc.(p,n)	0.30	0.17	1.45	0.22	~ 0	0.25	0.62	0.21	0.14	0.14
τ	Calc.(fs)	152	531	44	12	9.8	7.0	0.88	0.48	0.93	1.8
τ	Exp.(fs)	320 (50)	120 (60)	59 (6)	21 (5)						
(μ,ν)	Calc.(%)	1.48	0.87	7.32	1.29	~ 0	0.97	2.15	0.84	0.76	0.48
(μ,ν)	Exp(%)	3.3 (6)[a]	1.5 (2)	7.3 (9)[b]	1.3 (2)[b]			~ 1			

[a] Probably includes some cascade feeding.
[b] We assume that there is no $3105 \rightarrow 2201$ transition.

(μ^-,ν) data to the strongest level at 11.446 (2.201 in muon capture). The values for the (π^-,γ) reaction were given in Table 5.4, and are also consistent.

The only major complication is that in ^{28}Si the 10.596 and 10.725 MeV levels are of mixed isospin, so the strength is distributed, and is very weak for (e,e') scattering. Otherwise, the comparison is remarkably good, and speaks for itself. Muon capture follows the overall pattern and there is further evidence for missing strength in unidentified transitions, amounting to at least 2% per muon capture for 1^+ transitions alone.

All attempts to calculate muon capture rates in ^{28}Si have failed to obtain agreement with experiment, using standard shell-model methods. A novel approach was tried by Kuz'min and Tetereva who studied the 1^+ transitions. They used experimental observations of the $M1$ strength in ^{28}Si(e,e') and B(GT) from ^{28}Si$(p,n)^{28}$P to modify the wave functions in a phenomenological way to optimize the calculated values of these observables. With the modified wave functions they calculated the muon capture rates. The results are remarkable improvements, and are given in Table 5.8, compared to the direct yields from Gorringe et al. [338]. The experimental B(GT) are given in Table 5.7.

A few important lessons can be learned from this calculation. Firstly, the B($M1$) and B(GT) are normally similar, because the spin operator is usually dominant. However for some cases, the orbital matrix element for B($M1$) can be important and change the similarity (viz. the 1620, 2201 and 3105 levels). Secondly, the calculated values for the lifetimes are quite far off, indicating that there are further modifications still to make. Nevertheless, this calculation is a very useful exercise, as the results indicate that whatever is wrong in the Shell Model codes can eventually be fixed. Note especially that Kuz'min and Tetereva used the canonical values for g_A (-1.263) and for g_p/g_A (7.0).

We now turn our attention to the other types of γ-ray transitions. Although more recent data exist, they have not been fully analyzed, so we revert to the older data of Miller et al. [340], which were in agreement with, but better than the earlier data of Pratt [383]. In Table 5.9 are given their results for the yields of γ-rays for all nuclei apart from ^{28}Al (which were given in Table 5.6). (The most recent level energies are used.) The data have been supplemented with preliminary data of Moftah [443]. After each nucleus is given the total yield, taken from Table 5.4, which includes ground-state transitions. The obvious concerns are ^{27}Al and ^{26}Al

Table 5.9
γ-ray yields from muon capture in ^{28}Si from Miller et al. [340]. Also given are the total yields from Table 5.4, and the threshold for particle emission

Nucleus (total)	Particle threshold (keV)	Transition (keV)	$E\gamma$ (keV)	Yield (%/μ capture)
^{27}Al (45%)	8272	844 → 0	844	11.4 (8)
		1014 → 0	1014	10.3 (8)
		2212 → 0	2212	1.8 (10)
		2735 → 1014	1721	0.8 (7)
		2982 → 0	2982	2.6 (8)
		3004 → 0	3004	~ 0.3[a]
		3680 → 844	2837	0.6 (2)
		3957 → 0	3957	~ 0.9[a]
		4055 → 844	3211	~ 1.9[a]
		4055 → 1014	3040	~ 0.3[a]
		5156 → 0	5156	~ 1.5[a]
		5156 → 1014	4141	~ 0.3[a]
^{27}Mg (2%)	6444	985 → 0	985	1.9 (2)
^{26}Al (12%)	6306	228 → 0	228	0.7 (2)
		417 → 0	417	0.9 (2)
^{26}Mg (8%)	10612	1809 → 0	1809	10 (1)
		2938 → 1809	1130	3.2 (5)
		3941 → 2938	1002	0.9 (6)
^{25}Mg (2.4%)	7331	585 → 0	585	0.6 (3)
		975 → 0	975	0.8 (3)
		1612 → 0	1612	0.9 (6)
^{24}Mg (0.9%)	9312	1369 → 0	1369	0.9 (5)
^{22}Ne (0.5%)	9669	1275 → 0	1275	0.9 (5)

[a]Estimates from Moftah [443] with at least a factor of 2 uncertainty.

which seem under-represented. For ^{27}Al the γ-ray transitions to the ground-state represent about 29% per muon capture. If we estimate another 2% of weak transitions, we then can deduce that 14 (10)% of captures yield neutron emissions to the ground-state directly. For ^{26}Al most of the strength observed by MacDonald et al. (see Table 4.7) is missing. From their results we estimate that the yield of ^{26}Al should be 12 (6)%. There are almost certainly weak transitions which have not been identified, but again, a fair fraction of the time the $(\mu^-, \nu 2n)$ reaction must yield the ground-state directly. Note also that several nuclides were not identified viz.: ^{25}Al, ^{24}Na, ^{23}Na and ^{22}Na to mention those which should be detectable. (Remember that this is one of the best examples that we have.) Similarly, it would be helpful to have the ^{22}Ne identification verified, as this would be a $(\mu^-, \nu\alpha n p)$ reaction.

Table 5.10
Comparison of the reaction ^{28}Si$(\mu, \nu n)^{27}$Al [340] with the related proton knock-out reactions, ^{28}Si$(\gamma, p)^{27}$Al [454,455] and ^{28}Si$(d, ^3\mathrm{He})^{27}$Al [452]. The $(\mu, \nu n)$ results of Miller et al., have been corrected for cascading, and for γ branching ratios to give direct yields. The (γ, p) and $(d, ^3\mathrm{He})$ results have also been normalized to the 844 and 1014 transitions for ease of comparison. The (γ, p) results of Gulbranson et al. [455], are the integral, from 15.6 to 22.5 MeV; those of Thomson and Thompson [454] were from a 28 MeV bremsstrahlung integration

Level (keV)	C^2S (absolute)	$(d, ^3\mathrm{He})$ (renormalized)	$(\mu, \nu n)$ (%)	(γ, p) [454]	(γ, p) [455]
gs	3.39	47	14 (10)	18	27
844	0.79	10.9	8.9 (8)	11.1	12.4
1014	0.48	6.6	8.6 (8)	6.4	5.1
2212	< 0.3	< 4	1.8 (10)	< 0.6	1.0
2735	0.41	5.7	1.1 (7)	4.1	3.1
2982	0.53	7.3	2.6 (8)	3.8	3.2
3004	< 0.06	< 0.08	(~ 0.3)[a]	—	—
3680	0.06	0.8	1.0 (3)	2.5	1.4
3957	—	—	(~ 0.9)[a]	—	3.0
4055	1.3	17.9	(~ 2.2)[a]	2.9	—
4410	0.29	4.0	—	v small	0.7
5156	1.3	17.9	(~ 1.8)[a]		(~ 3)[b]

[a] Estimates from Moftah [443] with at least a factor of 2 uncertainty.
[b] See Fig. 4 of Gulbranson et al. [455].

In Table 5.10 are presented the level yields for the reaction ^{28}Si$(\mu^-, \nu n)^{27}$Al, deduced from the γ-ray yields, with corrections for γ-ray branching ratios and for known cascading. These data are compared to two other knock-out reactions. The reaction ^{28}Si$(d, ^3\mathrm{He})^{27}$Al has been used by many groups to obtain the spectroscopic factors for ^{27}Al levels. We use the data of Mackh et al. [452] for 50 MeV deuterons, but there are several other similar and consistent measurements. In the second column of Table 5.10 is given the absolute spectroscopic factor C^2S, and in the third column it has been renormalized to an average of the $(\mu^-, \nu n)$ yields for the 844 and 1014 keV levels. In addition, results for the (γ, p) reaction are given in columns 5 and 6, similarly renormalized. In column 5 are the results of Thomson and Thompson [454], who used a 28 MeV bremsstrahlung beam and detected γ-rays, just like a muon capture experiment. They corrected the results themselves for branching ratios and cascade feeding. The measurements of Gulbranson et al. [455], column 6, were obtained using the tagged photon facility at Illinois, by detecting the protons directly, which is very dependable for the ground-state transition, but a few levels could not be distinguished because of the energy resolution of about 150 keV. The results used here were an integration from 15.6 to 22.5 MeV. In addition they present a spectrum at $E_\gamma = 21.9$ MeV which shows excitation of the 5156 keV level, comparable to excitation of the 4055 keV level.

The overall comparison shows similarity for all three reactions. However, the pattern for muon capture follows the (γ, p) reaction more closely then it does the spectroscopic factors. The two features which indicate this are the weaker feeding of the ground-state, and the relatively lower feeding of the 4055 and 5156 keV levels. The higher energy levels are probably reduced because of the lower energy available in muon capture and the (γ, p) reaction. The weaker ground-state

transition indicates that muon capture is proceeding more like a de-excitation reaction than a direct knock-out. However, the similarities are also quite noticeable. The only really puzzling discrepancy is the strong feeding of the 1014 keV level in muon capture. This could be partially explained if there is unidentified cascading from higher levels through this level. This might be contributing to the results of Thomson and Thomson too.

Comparisons for the other yields are not worthwhile. As mentioned before ^{26}Al is puzzling because more lines should be observed. In future it would be helpful if limits could be published for obvious candidates which are not definitively observed. Of course, sometimes they are hidden by stronger lines.

We complete our discussion of ^{28}Si by describing two recent experiments, seeking to determine the induced pseudoscalar coupling constant g_P. Many years ago Grenacs et al. [456], pointed out that it was possible to measure the neutrino–gamma correlation by studying the Doppler broadening of a γ-ray from muon capture because the recoil ion was at 180° to the neutrino. It was soon realized that the 2201 keV level in ^{28}Si was a good candidate, because it was a 0^+ to 1^+ transition, followed by a $1^+ \rightarrow 0^+$ decay via a 1228 keV γ-ray.

The correlation between the γ-ray and the neutrino for an initially polarized muon is given by

$$W = 1 + (\alpha + \tfrac{2}{3}c_1)(\mathbf{P}\cdot\mathbf{k})(\mathbf{k}\cdot\mathbf{q}) + (a_2 + b_2(\mathbf{P}\cdot\mathbf{k})(\mathbf{k}\cdot\mathbf{q}))P_2(\mathbf{k}\cdot\mathbf{q})\,, \tag{5.2}$$

where $\mathbf{P}$ is the residual muon polarization, $\mathbf{k}$ is the direction of the γ-ray, $\mathbf{q}$ is the direction of the neutrino, and P_2 is the second order Legendre Polynomial. The coefficients α, a_2, b_2 and c_1 depend on the transition amplitudes. We use the notation of Brudanin et al. [457]; unfortunately there are various usages.

Now if one observes the γ-ray at 90°, $\mathbf{P}\cdot\mathbf{k} = 0$, so only the a_2 term is left, and the correlation does not depend on the value of $\mathbf{P}$. This was the technique used in the initial experiment by Miller et al. [458] working at SREL. Unfortunately, they did not realize that there was a serious background under the line from neutron excitation of levels in the germanium detector. They also omitted to study the slowing down of the ^{28}Al recoil ion, which has a significant impact. Thus their final result is subject to uncertain corrections, and should not be averaged with later experiments.

A recent experiment by Moftah et al. [459] avoided the neutron background by demanding a coincident γ-ray of 941 keV from the succeeding cascade. The slowing down was also determined by studying the 2171 keV γ-ray which originates from the same 2201 keV level. This gave a level lifetime of 61 ± 9 fs, in agreement with recent measurements, but unfortunately long enough to need careful consideration. The analysis of the two γ-rays is given in Fig. 5.5, and gives a correlation coefficient of $a_2 = 0.36$ (6).

A somewhat different approach has been taken at Dubna, as they used polarized muons, and measured the correlation between this spin direction and the γ-ray emission. A recent publication by Briancon et al. [460], presents new results and discusses systematic errors in great detail; it is in excellent agreement with their earlier result [457]. These authors quote their results in terms of the amplitude ratio

$$x = \frac{M(2)}{M(-1)} = 0.239\ (29) \tag{5.3}$$

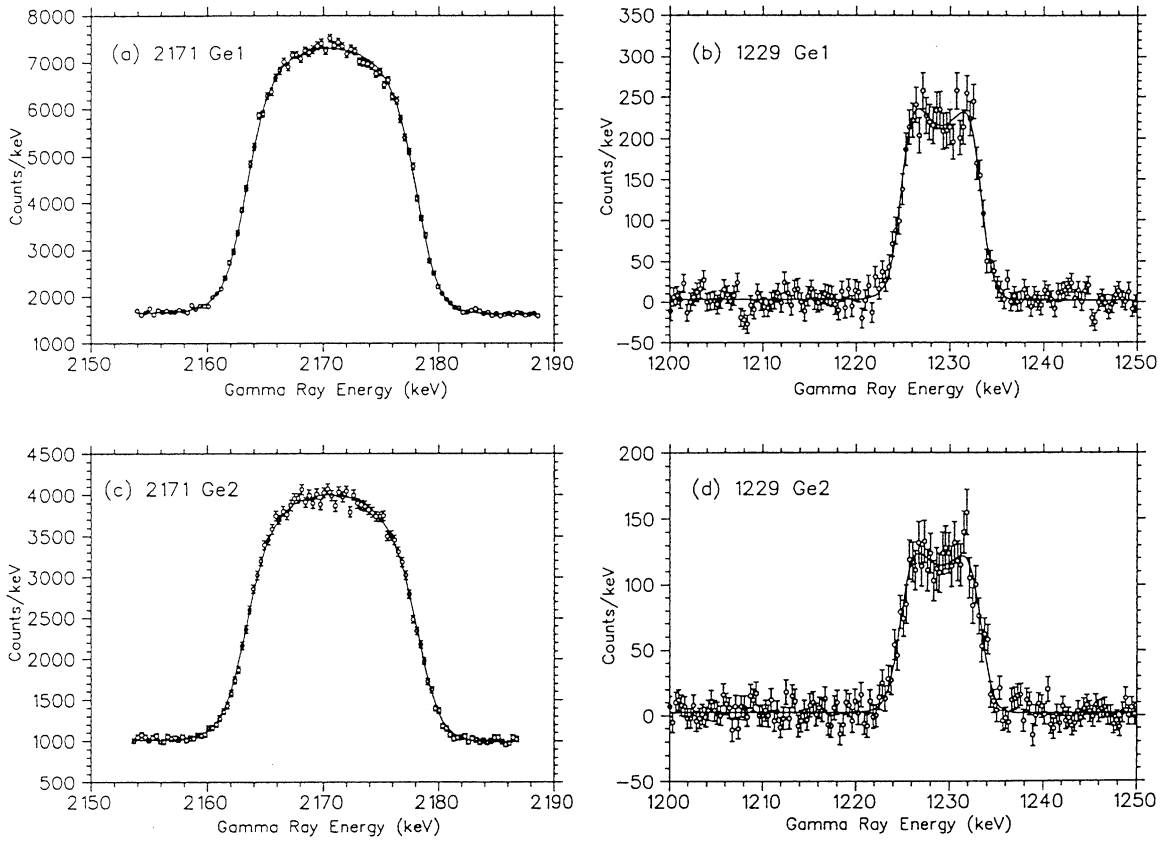

Fig. 5.5. The ν–γ correlation co-efficient is determined from the Doppler broadening of the 1229 and 2171 keV γ-rays in ^{28}Al from muon capture in ^{28}Si. Data are from Moftah et al. [443].

to be compared with their earlier result of 0.254 (34) and the result of Moftah et al., which gives $x = 0.315 \pm 0.080$ where

$$a_2 = \frac{\sqrt{2}x - x^2/2}{1 + x^2} \ . \tag{5.4}$$

Both these experiments are subject to systematic uncertainties, which have to be studied with care. The most obvious is that there might be cascade feeding from higher levels. This was tested by Moftah [443] using co-incidence techniques. The most perplexing possibility is the 3105 keV level which is clearly detected with a yield of the 3074 keV γ-ray of 1.3% per capture [191]. According to Endt's compilation [418,461] the 3105 keV level has a 25% branch to the 2201 keV level [462], but no 903 keV transition is detected in the muon capture spectrum, and a limit of about 5% can be placed on this branch. Similarly the 2201 keV level could be excited from the 4.7% of ^{29}Si present in the natural silicon targets. (The 3.1% of ^{30}Si is less of a problem.) Spectroscopic factors for ^{29}Si [452,453] indicate that only weak feeding would be expected, and experiments with a ^{29}Si target confirm that it is of negligible importance as a contamination for the observed 1229 keV line [458,460]. Both these effects have to be investigated if other nuclei

are proposed for similar studies; for example ^{20}Ne has to be rejected as too vulnerable to these problems.

Although all three experiments are in adequate agreement, the interpretation is puzzling. Junker et al. [463] find that the parameter x is unfortunately quite sensitive to minor parts of the wave function, and even a reasonable value for the calculated branching fraction does not guarantee an adequate description of x by the nuclear model. Similarly Siiskonen et al. [464] confirm that the standard nuclear structure model for ^{28}Si, which uses the OXBASH code and the USD interaction, needs a value of $C_P/C_A = 0 \pm 3$ to fit the experimental value for x. However, in the shell-model calculation, they find that if they use an effective interaction which is similar to the Bonn potential for free nucleon–nucleon scattering, they can describe the experiments with a less worrying $C_P/C_A = 5.1$ (8). It would clearly be more satisfying if a variety of experimental observables demanded the same effective interaction for $A = 28$ nuclei, but this calculation is clearly an important step towards understanding this complex situation. It has been known for a long time that ^{28}Si is not a simple shell-model nucleus, and extensive tests are obviously needed.

5.3. Lithium, beryllium and boron

For the lighter elements, very few bound levels exist, so γ-rays are seldom observed. In addition, most of the time the μ^- decays, and does not undergo capture, thus backgrounds are correspondingly worse.

For muon capture on ^{6}Li and ^{7}Li, no bound excited states are available. For ^{6}Li the capture rate to the ground-state of ^{6}He has been measured to be $1600^{+330}_{-129}\,s^{-1}$ [465], to be compared with the total capture rate of 4680 (120) s^{-1}, see Table 4.2. The $tt\nu_\mu$ final state has been suggested as a means for measuring the ν_μ mass. The rate is small, about 400 s^{-1}, and the interesting kinematic region a minute fraction of this [72]. For ^{9}Be there is only one bound excited state at 2.691 MeV in ^{9}Li, but it has not been observed in muon capture. The only available spectrum is that taken by van der Schaaf [356] as a background check in their ^{16}O experiment. It is a NaI spectrum, and the possible line from muon capture on ^{9}Be is not visible. Radiative pion capture indicates that the strength of feeding to the 2.691 MeV level is about half of that of the ground-state [274]. Similarly, the reaction ^{9}Be$(t,^3$He$)^9$Li shows that the B(GT) is very weak for the ground-state and 2.691 MeV levels in ^{9}Li, though for this reaction the strengths are comparable [309,310]; the results of the (n, p) reaction at 96 MeV are consistent with the other measurements, but are of limited use because of the energy resolution of 2.7 MeV [311].

For boron isotopes there are also few possible γ-rays, but in this case successful experiments have been completed. We show in Fig. 5.6 spectra for the reactions ^{10,11}B$(d,^2$He$)^{10,11}$Be at 0°, taken at Osaka with 200 MeV deuterons by Inomata et al. [306]. As we have emphasized before, the 0° spectrum is not a perfect analogy for the (μ^-, ν) reaction, but it is very close and gives an excellent visual impression of the overall pattern, including the ground-state and excited states which decay via neutron emission. Almost identical excitation spectra are observed in the $(t,^3$He reaction at 380 MeV [309,310]. A similar pattern is observed in the reaction ^{10}B$(p,n)^{10}$C [209]. The (π^-, γ) reactions feeds the ground-state more strongly, but is otherwise similar, see Fig. 4.6, or the better resolution data of Perroud et al. [274].

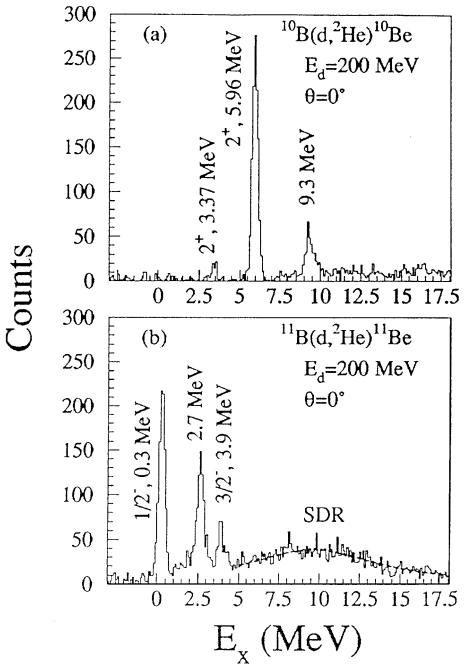

Fig. 5.6. The (d, ^{2}He) reactions on ^{10}B and ^{11}B at a deuteron energy of 200 MeV. The 0° spectrum emphasizes 1^+ transitions. Data are from Inomata et al. [306].

The evidence from muon capture confirms the very weak feeding of the ground-states. For ^{10}B it is found that the 5.96 MeV level is fed about 10 times stronger than the 3.37 MeV, as in Fig. 5.6. These are the only bound levels. For ^{11}B the 320 keV is also detected quite strongly and is the only bound excited state. The main difficulty in the interpretation of the boron experiments is the hyperfine transition rate, which complicates the situation quite significantly. The recent experiment of Wiaux et al. [189] measured many parameters including the hyperfine transition rate for ^{11}B of 0.181 (16) μs^{-1}. This experiment focussed on the time dependence of the 320 keV γ-ray, but also detected the decay electrons as a check. The use of a natural boron target (80% ^{11}B; 20% ^{10}B) means that their results are not useful for the other reactions. There were three previous measurements for the hyperfine rate, given in Table 3.7. Of some concern is the fact that the μSR results are significantly higher, but this could be due to other effects speeding up the muon depolarization. Thus we shall accept the value and error of Wiaux et al., but caution should be exercised. There is no γ-ray measurement for ^{10}B, but the μSR result from Favart et al. [186] of 0.21 (5) is comparable to Wiaux's result, and inconsistent with the same group's value for ^{11}B. The boron isotopes should have comparable hyperfine rates, so we shall accept Favart's result, but again with caution.

The experiment of Wiaux et al., found a very strong difference in the capture rate from the two hyperfine levels to the 320 keV excited state of ^{11}Be, viz. $\lambda^+/\lambda^- = 0.028$ (21). The goal of the experiment was to thereby measure g_P for which they obtain $g_P/g_A = 4.3 + 2.8/-4.3$, using the theory of Suzuki [466]. Junker et al. [463], found a small sensitivity to nuclear structure effects

finding values between 4.3 and 5.1. Thus the present situation is limited by the experimental statistical error, and the measurement is consistent with PCAC.

Now Deutsch et al., measured the total capture rate to bound states of ^{11}Be and found $\bar{\lambda} = 1100\ (80)\,s^{-1}$ [337]. In a later publication [188] they measured the yield of the 320 keV γ-ray line and obtained $\lambda_2 = 1000\ (100)\,s^{-1}$. The techniques were very different, so systematic errors may be uncertain, but let us naively subtract these numbers to determine the ground-state rate of 100 (130) s^{-1}. Now we can estimate the absolute rates for the 320 keV γ-ray line from the two hyperfine levels. The average depends on the hyperfine rate according to

$$\bar{\lambda} = \frac{N_{320}}{N_\mu}(\lambda_o + \lambda_c) = \lambda^+ N_0^+ \left(\frac{\lambda_o + \lambda_c}{\lambda_o + \lambda_c + R}\right) + \lambda^- \left[N_0^- + N_0^+ \left(\frac{R}{\lambda_o + \lambda_c + R}\right)\right] \tag{5.5}$$

using the simplification $\lambda_c = \lambda_c^+ = \lambda_c^-$. Assuming statistical population of the hyperfine levels, $N_0^+ = 5/8$ and $N_0^- = 3/8$, and using $\lambda^+/\lambda^- = 0.028$ (21), then for $R = 0$, $\lambda^- = 2550\ (260)\,s^{-1}$ for $R = 0.25 \times 10^6\,s^{-1}$, $\lambda^- = 1660\ (170)\,s^{-1}$; for $R = 0.18 \times 10^6\,s^{-1}$, $\lambda^- = 1790$ (180). Thus it is certainly necessary to take the hyperfine transition into account, but fortunately the exact value is not too critical with the present errors. Thus we can use $\lambda^- = 1700$ (300) and so $\lambda^+ = 50$ (40). If we assume that the ground-state transition has a rate of 100 (100) in both hyperfine levels (a poor assumption), we then obtain the bound state estimates of 1800 (300) and 150 (100). From the electron time structure Wiaux et al., obtain the total capture rates of $\lambda_c^- = 23.5\ (8) \times 10^3\,s^{-1}$ and $\lambda_c^+ = 10.3\ (20) \times 10^3\,s^{-1}$, thus we can deduce the bound state fractions given in Table 4.9. This difference in the two total rates is expected theoretically; Koshigiri et al. [467], for example predicted $\lambda_c^- = 23\ (3) \times 10^3\,s^{-1}$ and $\lambda_c^- = 12\ (2) \times 10^3\,s^{-1}$.

Theoretical estimates for the ratio λ^+/λ^- for the 320 keV level seem in agreement and are not too sensitive to nuclear structure effects. However, the situation for the absolute rates is totally different and there is a vast difference between various estimates. Let us quote some rates for the lower hyperfine states to the 320 keV level. Kuz'min et al. [468] using standard shell-model approaches obtain 2000–2500 s^{-1} for the older Cohen and Kurath parameters [469], but 2500–3500 s^{-1} for the more recent parameters of Warburton and Brown [470]. However, Suzuki [466] emphasizes the neutron halo effect for ^{11}Be and obtains significant reductions in the transition rate viz 700–1000 s^{-1}. All these are to be compared with our estimate of 1700 (300) s^{-1} for the experimental value. Such variations are confusing and a combined approach might be more appropriate.

For the other γ-rays in ^{11}B we have the experiment of Giffon et al. [130]. They used a natural boron target (20% ^{10}B) and an enriched ^{10}B target (9.1% ^{11}B), so they were able to extract yields for each isotope. Unfortunately they did not have detailed timing information, but they counted for about 4 μs, so the hyperfine transition will have a major impact, and also make it impossible to extract separate hyperfine rates. This thus reduces the usefulness of the data. In ^{10}B there are 5 bound excited states. but only two seem important for our discussion, the 2_1^+ at 3368 keV, and the 2_2^+ at 5958 keV. The other bound levels are at 5960, 6179 and 6263 keV but no direct information is available about possible feeding in muon capture (again limits would be useful).

The 5958 keV level cascades through the 3368 keV level with a 2590 keV γ-ray $> 90\%$ of the time. This complicates the analysis. For ^{11}B, the upper level is not fed strongly, $\lambda = 460$ (460) s^{-1}, i.e., $\sim 2\%$ of captures, and the lower level is seen quite strongly, $\lambda = 7200\ (1080)\,s^{-1}$,

i.e., $\sim 30\%$ of captures. This is consistent with the ^{11}B$(d,^3$He) reaction [471] which find spectroscopic factors of 0.65, 2.03 and 0.13 for the g.s., 3.36 and 5.96 MeV levels respectively. (Note also that the other 3 bound levels are not observed in the $(d,^3$He) reaction.) The data for the $(p,2p)$ reaction are interesting but the energy resolution is several MeV [472,473], so comparisons are frustrating.

For ^{10}B the situation is reversed, as is clear from Fig. 5.6, and the 5.96 MeV level is fed strongly, $\lambda = 4710\ (705)\,\mathrm{s}^{-1}$, i.e., $\sim 19\%$ of captures, and the 3.37 MeV level, hardly at all, $\lambda = 390\ (960)\,\mathrm{s}^{-1}$, i.e., $< 5\%$ of captures, but the exact value is confused by the strong cascade feeding. (Again the other levels are not seen in the $(d,^2$He) reaction, Fig. 5.6: nor the (p,n) reaction, Fig. 4.9: nor (π,γ), Fig. 4.7.) The calculations by Kuz'min et al. [468] confirm that the 5.96 MeV level should be fed more strongly than the 3.37 MeV level. They also find that λ^+/λ^- is small for both transitions, so from the experimental value, assuming the hyperfine transition rate is $210,000\,\mathrm{s}^{-1}$, in Eq. (5.3), we can estimate that for the 5.96 MeV level $\lambda^- \approx 7700\ (1600)$ which is again lower than their calculations, viz. $11,000 < \lambda^- < 14,000\,\mathrm{s}^{-1}$, a puzzling parallel to ^{11}B. If we take the total capture rate in ^{10}B of $27.5\ (7) \times 10^3\,\mathrm{s}^{-1}$ to represent mainly the lower hyperfine level, then the 5.96 MeV level alone accounts for about 28% of the captures for this hyperfine level. (This is a more meaningful estimate than the 19% noted above.)

5.4. Carbon, nitrogen and oxygen

These nuclei have the advantage that hyperfine transitions are probably not important; the only hesitation is that for nitrogen a μSR experiment found depolarization, but we shall assume that this is due to other effects, as there is not enough energy to eject an Auger electron to speed up the hyperfine transition, see Table 3.7. Similarly for ^{13}C there is a weak μSR signal, but the rate is low, so it should not impact muon capture, even if there were data.

For ^{12}C we have inconsistent information which is not surprising considering the difficulty of the capture experiments. We take the total capture rate to be $37.9\ (5) \times 10^3\,\mathrm{s}^{-1}$, which is only 7.7% of muon stops, so the vast majority of muons decay. We take the rate for muon capture to the bound states of ^{12}B to be $7.05\ (27) \times 10^3\,\mathrm{s}^{-1}$ [474] (using modern numbers), i.e., about 18.6 (7)% of muon captures. For the γ-ray experiments the two most recent experiments are inconsistent, and difficult to merge. They both agree however that feeding of the bound excited states is only a small fraction ($\sim 1/6$) of the ground-state transition. That is in agreement with the (p,n) reaction, see Fig. 4.8 as well as the $(d,^2$He) and $(^3$He$,t)$ data of Inomata et al. [306].

For muon capture experiments the first difficulty is that even the strongest excited state is fed only 1.5% of captures, i.e., 0.12% of muon stops, making the spectra vulnerable to background. The other difficulty is that nature has been unbelievably capricious. There are three relevant levels at 2621, 1674 and 953 keV. The 2621 keV is fed most strongly and 80% of the time cascades to the 953 keV level via a 1668 keV γ-ray, and 14% of the time cascades to the 1674 keV level via a 947 keV γ-ray. The 1674 and 953 keV levels then decay to the ground-state directly. Because of the Doppler broadening, the 947 merges with the 953 keV line and the 1668 with the 1674 keV line. Roesch et al. [475], studied the line shapes and concluded that the intensities were

$$\frac{I(1674\,\mathrm{keV})}{I(1668\,\mathrm{keV})} = 0.55\ (15) \tag{5.6}$$

Table 5.11
Feeding of various bound levels in ^{12}B from muon capture in ^{12}C, quoted as rates. We have re-analysed the results of Giffon et al. [130] using information from Roesch et al. [475]. The results of Roesch et al. [475] are also given, and a recommended average. This can then be compared with the calculations of Fukui et al. [476] and Hayes and Towner [477]

^{12}B (keV, J^π)	Giffon et al. [130] ($10^3\,s^{-1}$)	Re-analysis ($10^3\,s^{-1}$)	Roesch et al. [475] ($10^3\,s^{-1}$)	Average ($10^3\,s^{-1}$)	Theory [476] ($10^3\,s^{-1}$)	Theory [477][c] ($10^3\,s^{-1}$)
$2621, 1^-$	1.08 (13)	0.86 (20)	0.38 (10)	0.62 (20)	1.41	0.53 (12)
$1674, 2^-$	0.06 (20)	0.25 (10)	0.12 (8)	0.18 (10)	0.28	0.13 (6)
$953, 2^+$	0	0.14 (10)	0.27 (10)	0.21 (10)	0.30	0.25 (3)
g.s., 1^+	5.91 (35)	5.80 (35)	6.28 (29)	6.04 (35)	6.2[a] 4.5[b]	6.45 (15)
Total bound levels	7.05 (27)	7.05 (27)	7.05 (27)	7.05 (27)		7.36 (15)

[a]Using Hange-Maripuu.
[b]Using Cohen–Kurath.
[c]Unrestricted shell-model partially extrapolated.

whereas if there were no direct feeding of the 953 keV level this ratio would be 0.18 (4). Calculations confirm that some feeding of the 953 keV is expected [476,477]. However, one can deduce that the overall normalization of Roesch et al., is nearly a factor of two lower than the other relevant measurement of Giffon et al. [130], who agree with several earlier measurements.

Giffon et al. [130] however assumed in their analysis that there was no direct feeding of the 953 keV level, a poor assumption. Thus, in Table 5.11 we have re-analysed their results in the light of the experiment of Roesch et al. (and theoretical estimates). The main difference between this re-analysis and the results of Roesch is now a direct consequence of the very different normalizations. We therefore just average to obtain our "recommended experimental" assessment. These capture rates are somewhat lower than the calculations of Fukui et al., but are in good agreement with Hayes and Towner [477]. These recent calculations included 4 $\hbar w$ excitations. Similarly Volpe et al. [478] have some difficulty obtaining perfect agreement with experiment, even though they use a bigger space than Hayes and Towner. These calculations demonstrate vividly how much care is needed to reproduce the rate for the ground-state transition. A similar calculation of ^{12}C properties has been made by Navratil et al. [479].

Why take so much care over a very difficult measurement? Well the reason is that these values are important corrections for recoil–polarization experiments which hope to determine g_P/g_A. It was realized many years ago that for muon capture in ^{12}C, the recoil polarization of the ^{12}B is a parameter which is sensitive to g_P/g_A. Experiments by Possoz et al. [480], and Kuno et al. [481], have measured the ^{12}B recoil polarization by the β-decay asymmetry during the 24 ms half-life. They both measured P_{AV}, that is the polarization of the recoil nucleus along the direction of the initial muon spin. Possoz et al., used a graphite target in a 2 kG magnetic field which retains 75% of the polarization. Kuno et al., used a Grafoil target, which is pyrolitic graphite with a well aligned c-axis. This material does not depolarize the ^{12}B spin. Of course

the μ^- polarization in the initial 1s atomic state was only 16.0 (5)% so all asymmetries are very small. The two measurements are in excellent agreement giving 0.452 (42) [480], and 0.456 (47) [481]. The correction for the excited states is small $\sim$0.006 depending on which γ-ray experiment is assumed to be correct. (We have indicated above that it is inadvisable to use those of Giffon et al., without correction.) However, doing just that Fukui et al. [476], obtained:

either

$$\frac{g_P}{g_A} = 10.6^{+2.3}_{-2.7} \tag{5.7}$$

using Giffon et al., data [130], or

$$\frac{g_P}{g_A} = 9.7^{+2.5}_{-3.0} \tag{5.8}$$

using Roesch et al., data [475]. An alternative parameter to measure is P_L, the longitudinal polarization of the ^{12}B nucleus along its recoil direction. Roesch et al. [482], measured P_L but also measured P_{AV} because the ratio between them does not rely on absolute polarization measurements, yet the result is very sensitive to g_P/g_A. They obtained $R=-0.516$ (41) and also $P_L=-0.96$ (10), deducing that $g_P/g_A = 9.0$ (1.7). In an independent analysis Fukui et al. [476], deduced:

either

$$\frac{g_P}{g_A} = 9.5 \pm 1.7 \tag{5.9}$$

using Giffon et al., data [130], or

$$\frac{g_P}{g_A} = 8.5 \pm 1.9 \tag{5.10}$$

using Roesch et al., data [475]. Finally we note that for ^{12}C, muon capture yields the 2125 keV γ-ray from ^{11}B with a probability of 5.1 (4) $\times 10^{-3}$ per muon stop, taking a weighted average of the data presented by Giffon et al. [130]. This is equivalent to 6.6 (5)% of muon captures. In Section 4.7.3, using Fig. 4.8 from the (p,n) reaction, we expect a significant direct feeding of the ground-state of ^{11}B especially from the peak at 4.2 MeV which may constitute more than 20% of muon captures. Probably other states also give neutron decay to the ^{11}B ground-state as roughly 50% of captures should give a bound ^{11}B nucleus. Other levels in ^{11}B have not been detected. The γ-ray from the 4445 keV is too close to that of the 4439 keV, first excited state of ^{12}C, always profusely excited. However, we can use the superb $(e,e'p)$ data from NIKHEF [483] as a guide. They found that the ground-state has a spectroscopic factor about four times that of the 2125 keV level. They saw no excitation of the 4445 keV level, but the $3/2^-$ level at 5020 keV has a spectroscopic factor only a little less than the 2125 keV level. About a factor of 10 weaker are levels at 6743: 6792: 7286: and 7976 keV. A thorough comparison with spectroscopic factors from other reactions is given in their paper. Thus it appears that the 5020 keV level is the one most likely to be observable in muon capture. The data on the (γ, p) reaction below 30 MeV are somewhat confusing, as clear evidence for excitation of the 4445 keV level was seen in the γ-ray observations by Medicus et al. [484], especially for E_γ of 30–40 MeV. Later direct observations of protons from the (γ, p) reaction by Ferdinande et al. [485], and Ruijter et al. [486], could not resolve the 4445 and 5020 keV levels, but

Ruiter et al., estimate that maybe only 30% of the peak can be ascribed to the 4445 keV level. Of course it is possible that Medicus et al., were observing at least some contamination from neutron inelastic scattering off carbon in and around the target.

For ^{13}C there is still no experimental information on the partial capture rates. Experimentally the total capture rate is 35.0 (1.5) $\times 10^3\,s^{-1}$ and Chiang et al. [270], reproduce this quite well in their calculations, viz. $38.2 \times 10^3\,s^{-1}$. The separate hyperfine capture rates were estimated to be $\lambda(F=1)$, $45 \times 10^3\,s^{-1}$; and $\lambda(F=0)$, 31×10^3. This was estimated by Morita et al., and quoted by Ishida et al. [190]; the statistically weighted average is 41.5×10^3 in reasonable agreement with Chiang et al., Ishida et al., found a very slow hyperfine transition rate of about $0.02\,\mu s^{-1}$, so the hyperfine transition does not affect the average much, but Koshigiri et al. [487], found the $F=0$ rate for the ground-state transition to be much smaller than the $F=1$ rate, a puzzling finding for an even Z nucleus but caused just by the angular momentum of ^{13}B which is 3/2. Their average rate is $\sim 8000\,s^{-1}$. Dogotar et al. [488], and Degroslard and Guichon [489], have also found the average ground-state transition to be about $7000\,s^{-1}$ and the transition to the $1/2^-$ level to be only $133\,s^{-1}$. Experimental confirmation would be really helpful. The (π^-,γ) reaction [299], feeds the ground-state of ^{13}B quite strongly, a state around 3.5 MeV more weakly (there are 4 levels around there), and levels at 6.5 and 7.6 MeV quite strongly, but these are above the neutron separation energy of 4.88 MeV. There are also three recent (n,p) experiments, one at $E_n = 65$ MeV with an energy resolution of about 2 MeV [298], one at $E_n = 118$ MeV with an energy resolution of 2.3 MeV [299], and a LAMPF one over the range 75–210 MeV with a resolution varying between 2 and 3 MeV [295]. The results are all similar to the (π^-,γ) reaction, but hurt by the energy resolution. The comparison was presented in Fig. 4.10. The reaction ^{13}C$(t,^3$He$)^{13}$N has also been studied. The spectrum is similar to the other data, and because the resolution is 780 keV, it can indicate that maybe two states at about 3.9 and 4.7 MeV are excited [309,310].

Until recently there was little information available on ^{14}N. However, the thesis of Stocki [192] provides significant new data. This experiment tried to measure the hyperfine transition, but could not detect any rate. We therefore assume statistical populations of the hyperfine states. Several γ-rays were detected, and limits placed on many others. The results for all the bound states of ^{13}C and ^{14}C are included in Table 5.12. No other γ-rays were positively identified except the ^{12}C 4439 keV γ-ray which is always excited by general neutron background, so no useful statement can be made. Note that the quoted errors in Table 5.12 are for the absolute rate (for which the experiment had some difficulty) and the relative errors are somewhat smaller.

Many of the γ-rays have background lines superimposed on them, so experiments with poor statistics would be vulnerable to having lines included which were not resolved, and thus the older experiments would tend to overestimate yields. Fortunately the major line at 7010 keV (from the 7012 keV level) is particularly clean, at least in Stocki's experiment, so we can compare with earlier experiments with a little more confidence. Giffon et al. [130], obtained a rate for this line of 4640 (700) s^{-1}, i.e., a yield of 6.7 (10)% per capture (using a total capture rate of $69.3 \times 10^3\,s^{-1}$). Note that the yield of Giffon et al., is the lowest of the earlier experiments, the others being of lower accuracy [130]. Mukhopadhyay [496], in notes added in proof on p. 131 of his review, presented a ^{14}N spectrum from Bellotti et al., showing this γ as well as a "6315 keV" line, which was not detected by Stocki, so it was probably background, maybe the 6322 keV line of ^{15}N from muon capture on ^{16}O.

Table 5.12
γ-rays observed in muon capture on ^{14}N, from Stocki [192]. The γ-ray yield is given, as is the direct feeding for each excited state, taking into account the γ-ray branching ratios and cascade feeding. (All bound excited states of ^{13}C and ^{14}C are included.) Also given are the integrated yields in the (γ, p) reaction [491,492], the (π^-, γ) yield of Perroud et al. [274], and the calculations of Kissener et al. [493], plus, in brackets, the calculations of Mukhopadhyay [496] for "allowed muon capture", i.e., 1^+ transitions from the 1^+ ground-state of ^{14}N

Nuclide	Excited state (keV, J^π) (%)		Yield of g.s. transition (%)	Direct feeding of excited state (%)	(γ, p) $\int \sigma \, dE$ (MeV mb)	Theory [493] (%)
^{13}C	g.s.	$1/2^-$	—	—	20	26
	3089	$1/2^+$	1.5 (6)	1.4 (7)	small	—
	3685	$3/2^-$	5.8 (13)	4.7 (13)	7 (2)	16
	3854	$5/2^+$	2.0 (5)	3.1 (8)	1.7 (7)	—
	7550		Unbound	—	17	18
				—	(π^-, γ)	
				—	(%)	
^{14}C	g.s.	0^+	—	—	0.25 (11)	(0.4)
	6094	1^-	1.3 (6)	$1.3^{+0.6}_{-1.0}$		1.1
	6589	0^+	—	0.07 (8)		(0.3)
	6728	3^-	1.3 (5)	1.4 (5)	6.2 (4)	2.7
	6903	0^-	—	< 0.5		—
	7012	2^+	3.4 (14)	3.4 (14)		11
	7341	2^-	< 0.07	< 0.4		
	8318	(2^+)	Unbound		3.4 (3)	11
	11306	(1^+)	Unbound		2.3 (4)	(2)

In Table 5.12 the (π^-, γ) results of Perroud et al. [274], are included. The (n, p) results of Needham et al. [490], are similar with an energy resolution of about 1 MeV. These experiments are then compared with the calculation of Kissener et al. [493] for both ^{13}C and ^{14}C. For ^{14}C they split the strength of the 7012 keV transition equally with the 8318 keV level because of evidence from electron scattering. In the Cohen–Kurath nuclear model that they used, there are no $2p$–$2h$ excitations and these strongly affect these transitions. Note that Kissener et al. [494] also calculated the (π^-, γ) reaction, and obtained reasonable agreement with experiment, especially when they included this empirical splitting of the 7012 keV strength. Also included for ^{14}C, in brackets, are the allowed transitions calculated by Mukhopadhyay [496]. He also found most of the 1^+ strength went just to the 7012 keV level on the Cohen–Kurath model, which gives a 29% yield. He probably would have found a total capture rate higher than experiment which would bring this down to $\sim 22\%$ as found by Kissener et al. [493], who normalized to a total capture rate of $109 \times 10^3 \, s^{-1}$.

For comparison with the ^{13}C lines from muon capture on ^{14}N, there is the experiment of Gellie et al. [491], as well as that by Thompson et al. [492], who, as in their ^{28}Si experiment, measured the γ-rays from a 29 MeV bremsstrahlung beam. The results of Thompson et al., are listed in Table 5.12 and, as in ^{28}Si, show the same pattern as muon capture. Again the $(d, ^3\text{He})$ reaction exhibits a slightly different pattern; the value of C^2S for the ground-state, 3.68 and

7.5 MeV states are 0.8, 0.3 and 1.4, respectively; feeding of the 3089 level is small and of the 3854 level is not even detected [495]. Both Gellie et al., and the $(d,{}^3\mathrm{He})$ reaction observe strong feeding of a state at 7.5 MeV which would decay to the ground-state of ^{12}C; it does not have enough energy to decay to an excited state, as the neutron separation energy in ^{13}C is 4.95 MeV.

The calculation of Kissener et al., for ^{13}C is interesting because they estimate the ground-state transition and find that the only other bound state which is excited is the 3685 keV level. This is because they follow the pattern of the spectroscopic factors. Again the (γ, p) reaction gives a closer pattern to what is observed. (Note that no unknown cascade feeding can affect the muon capture results for ^{13}C γ-rays.) Thus overall the agreement between experiment and theory is adequate, especially if the experimental results are normalized up a little.

Thus, we can now estimate the overall situation for muon capture in ^{14}N. If we average the more recent values for the 7010 keV γ-ray, we obtain a yield of 5.1%; renormalizing the results of Stocki up a little, we suggest about 9 (2)% of muon captures give bound states in ^{14}C and 14 (3)% produce bound excited states in ^{13}C. The (γ, p) reaction then implies about 32 (8)% direct feeding of the ^{13}C ground-state, and 27 (8)% direct feeding of the ^{12}C ground-state via the 7.55 level in ^{13}C. If we add 4% feeding of the first excited state in ^{12}C, and 13% for charged particles, the sum is 99 (10)%, which is reasonable.

The reason for all this detail is that all calculations in ^{14}N find a much higher rate for the transition to the 7012 keV level. Kissener et al., obtained 22%, but empirically divided it up. Mukhopadhyay estimated the rate to be about $20,000\,\mathrm{s}^{-1}$ or about 29% of the total capture rate. This very high value was confirmed by several later calculations by Dogotar et al. [488], and by Desgrolard and Guichon [489]. It is clear that the Cohen–Kurath model does not work well for ^{14}N, and that a more sophisticated model is needed with $2p$–$2h$ excitations built in. For ^{12}C, the Cohen–Kurath model is not too bad, but the modern calculations of Hayes and Towner [2] certainly improve the situation. It would be worthwhile to apply this powerful technique to ^{14}N.

The case of ^{15}N is very difficult experimentally, as this isotope is only 0.37% of natural nitrogen. However, Bely et al. [497], have studied it theoretically. We shall return to their study of ^{32}S later in Section 5.7, but note here that those results are not really consistent with experiments.

The case of ^{16}O was already well investigated in the 1977 review of Mukhopadhyay, and yet still attracts attention today because of its relevance for studying g_{P}. There are only three bound excited states in ^{16}N below the neutron separation energy which is only 2.491 MeV. The main complication is that the first excited state, the important 0^- at 120 keV, has a lifetime of 7.58 (9) μs. Thus, γ-ray experiments must take this into account. An added complication is that the 397 keV level cascades through the 120 keV level 73.4 (16)% of the time, the rest proceeding directly to the ground-state. The interest lies in determining the direct feeding to the 120 keV level, a parameter which is very sensitive to g_{P}. The (π^-,γ) reaction [273] does not have enough resolution to separate the levels nor does the (p,n) reaction normally [284], but an experiment by Madey et al. [279], at 79 MeV, attained an energy resolution of 140 keV, so the spectra resolve the low-lying levels, and confirm the dominance of the 2^- level. The 0^-, 1^- and 3^- levels were all excited less strongly, at about equal amounts, which is different from muon capture. However, the lowish energy of the proton beam may be partially to blame.

Table 5.13
Muon capture rates in ^{16}O to bound states of ^{16}N given in units of $10^3\,s^{-1}$. (The total capture rate is 102.5 (10) × $10^3\,s^{-1}$.)

Level (keV, J^π)		Early exps. (before 1973)	Kane [499]	Guichon [500]	Theory (before 1977)	Theory [501]
g.s.	2^-	7.2 (10)	8.0 (12)		~ 8	7.7
120.4 (1)	0^-	1.2 (4)	1.56 (18)	1.56 (11)	~ 1	1.7
298.2 (1)	3^-	0.13 (8)	< 0.09		~ 0.1	
397.3 (1)	1^-	1.77 (10)	1.31 (11)	1.27 (9)	~ 1.7	1.8

Note that for ^{16}F, the 2^- level is no longer the ground-state but the second excited state. The (n, p) results of Needham et al. [490], have the unusually good energy resolution of 1 MeV but cannot help much for muon capture. The (p, p') reaction has been studied at Orsay at forward angles, and their energy resolution was 100 keV, an excellent achievement [498], but again the results are not too helpful for muon capture.

In Table 5.13 we give the relevant data. The earliest experiments may not have fully taken into account the long-life of the 120 keV level, so we group them together [13]. The two more recent experiments by Kane et al. [499], and Guichon et al. [500], took great care to treat the timing difficulties. The 2^- ground-state is deduced from the total production of ^{16}N which is observed via the 6.13 MeV γ-ray seen in the β-decay. The experimental rates for the 0^- level are in perfect agreement, leading to the experimental value of $\lambda = 1560\ (93)\,s^{-1}$, i.e., a yield of 1.5%.

The early theoretical calculations varied by over a factor of 2.5 for the important 0^- rate. These were discussed in some detail by Mukhopadhyay. We include a later calculation by Eramzhyan et al. [501], who included $2p$–$2h$ effects. We shall focus on the relatively recent calculation by Haxton and Johnson [502], who demonstrated the need for a 4 $\hbar\omega$ shell-model to describe the nuclear structure effects in ^{16}O. They also show that a harmonic oscillator potential gives a poor description of the radial wave functions, and they use a Ginocchio potential, which resembles a Woods–Saxon shape. They still do not quite fit the β-decay rate of 0.489 (20) s^{-1} [503], nor the B(GT) strength below 7 MeV. However, there are adequate reasons for this, so their value of g_P/g_A of 8 (1) is reliable. Warburton et al. [581] in a more recent calculation obtained 7.4 (5). The study of ^{16}O continues and even the most recent calculations cannot totally reproduce properties of this nucleus [504].

We return briefly to the calculations of Eramzhyan et al. [501], because they calculated both the (μ^-, ν) and (π^-, γ) reactions for ^{16}O. We present in Table 5.14 their results for models C and E, those with the inclusion of $2p$–$2h$ wave functions. We see first that even for ^{16}O, more (π^-, γ) reactions proceed from the $1p$ atomic level. Although the (π^-, γ) reaction is similar to muon capture for the $1s$ atomic state, the $2p$ atomic state prefers different levels in ^{16}N, thus the 2^- levels are more strongly fed than the 1^-, and the positive parity are much more important in general.

Thus, although the overall pattern is somewhat similar, some details can be quite different. We thus advise caution in comparing the (π^-, γ) and (μ^-, ν) reactions, especially for elements heavier than ^{16}O for which the $2p$ atomic state dominates more and more. Thus, the (π^-, γ) reaction is a useful guide, but only a guide, no more.

Table 5.14
Comparison of the calculations of Eramzhyan et al. [501] for the (π^-,γ) and (μ^-,ν) reaction in ^{16}O. R_s is the radiative rate from the $1s$ level and R_p from the $2p$ level. For each row it is the sum for all levels of that J^π which is given

Level (J^π)	R_s (π^-,γ) (10^{-4})	R_p (π^-,γ) (10^{-4})	$\sum(\pi^-,\gamma)$ (10^{-4})	(μ^-,ν) rate ($10^3\,s^{-1}$)
0^-	—	1.5	1.5	9
1^-	6.4	20.6	27.0	57
2^-	7.7	73.8	81.5	36
3^-	0.2	8.2	8.4	n.a.
0^+	—	0.3	0.3	0.6
1^+	0.7	15.5	16.2	4.4
2^+	1.2	33.3	34.5	2.3
3^+	1.4	38.2	39.6	1.9

In addition to the weakly excited bound states in ^{16}N, muon capture in ^{16}O produces a significant number of γ-rays in ^{15}N. We have already discussed the experiment of van der Schaaf et al. [356], who focussed on the neutron spectrum from muon capture in ^{16}O. However, they also obtained valuable data on the γ-ray yields, especially the high energy ones. In Table 5.15 we present their results as well as those of Kaplan et al. [370], and compare with the (γ, p) results of Caldwell et al. [505]. Again this is an experiment which detected γ-rays, but in this case they used monochromatic γ-rays up to 28.7 MeV, so the energy dependence of the cross-sections for each excited state is available, and they vary significantly. The integral to 28.7 MeV is used as an average, but a slightly lower band might be more appropriate for comparison with the (μ,ν) reaction. Similar (but not identical) results were obtained by Ullrich and Krauth [506] with 32 MeV bremsstrahlung.

The spectroscopic factors are available from the reaction $(e,e'p)$ studied at NIKHEF by Leuschner et al. [507], and are given in the final column of Table 5.15. Confirmation is available from the MAMI data of Blomqvist et al. [508]. These results confirm the importance of the ground-state. For the other levels a similar pattern is seen, though the 5270 and 5299 keV levels are not as strongly excited as in the (γ, p) or $(\mu, \nu n)$ reactions.

The first surprising thing in Table 5.15 is how strongly the ^{15}N γ-rays are excited, even up to 10 MeV, and yet the (μ^-,ν) and (γ, p) reactions agree on this. Secondly, the sum is a little high. From the (γ, p) data, one can expect the (μ,ν) reaction to produce direct neutron transitions to the ^{15}N ground-state at least 20% of the time (30% or 40% would be more acceptable). Summing the ground-state transitions for the ^{15}N γ-rays and a direct production of 20% we obtain

$$20 + 7.1 + 5.6 + 24.5 + 4.0 + 8.8 = 70\% \,. \tag{5.11}$$

Now we know the ^{16}N bound states contribute 11 (1)%, the $2n$ reaction probably 10% and charged particles 13 (2)% [375], so the ground-state transition for ^{15}N cannot be above 20%. unless there is an overall normalization problem. In any case, the details for ^{16}O are fairly well established and agree with other reactions.

Table 5.15
Yield of γ-rays in ^{15}N and ^{14}N from muon capture in ^{16}O, quoted in % per muon capture. Also given are the (γ, p) data of Caldwell et al. [505], quoted as a % of the integrated cross-section up to 28.7 MeV, which is about 75.4 MeV mb. This measurement also quotes the direct ground-state transition. In the final column are the spectroscopic factors from the $(e, e' p)$ reaction

γ-ray[a] (keV)	Transition (keV)	$(\mu^-, \nu n)$ [370]	$(\mu^-, \nu n)$ [356]	(γ, p) [505]	$(e, e'p)$ [507]
^{15}N					
g.s.			($\leqslant$ 20)	44	1.26 (1)
5269	5270 → g.s.	7.1 (11)			0.114 (3)
5298	5299 → g.s.	5.6 (23)	15 (4)	8.6[b]	0.036 (2)
6323	6324 → g.s.	24.5 (23)	39 (7)	29.4	2.35 (2)
7300	7301 → g.s.		4.0 (10)	7.5	
2297	7567 → 5270				0.023 (25)
3301	8571 → 5270		2.3 (7)		
3923	9222 → 5299		2.4 (7)	2.1	
4558	9829 → 5270		2.4 (7)		
8309	8311 → g.s.				0.041 (3)
8569	8571 → g.s.		(1.2)		0.021 (3)
9220 (9050)	9222 → g.s.		(1.3) 8.8(16)	9.1	0.042 (4)
10067 (9930)	10070 → g.s.				0.133 (2)
10797	10800 → g.s.				0.222 (4)
^{14}N			$(\mu^-, \nu 2n)$		
2313	2313 → g.s.		0.8(4)		
1635	3948 → 2313		0.7(4)		

[a]Note that the γ-ray energy can be 1 or 2 keV less than the transition energy because of the recoil energy.
[b]In Ref. [505], the 5.3 MeV transition was corrected for cascading from the 9.22 MeV level. For fairer comparison van der Schaaf undid this correction, apparently assuming equal branches to the ground-state and the 5299 keV level. Recent branching ratios for the 9222 keV level are more complex.

For the ^{14}N γ-rays from muon capture in ^{16}O, the γ-ray intensities are consistent with strong feeding of the 3948 keV level, with no, or very low, feeding of the first excited state at 2313 keV. (The 3948 keV level has a 96% branching ratio for the cascade via the 2313 keV level.) This low feeding of the 2313 keV level is consistent with the ^{16}O (γ, pn) reaction [509] which feeds roughly equally the g.s., 3948 and 7029 keV levels with $< 7\%$ of these yields to the 2313 keV level. The 7029 keV level has a 99% transition to the ground-state, but would have been lost in the muon capture experiment in the multitude of ^{15}N γ-rays.

For ^{17}O and ^{18}O little is known, except that the total capture rate in ^{18}O is 88.0 $(1.5) \times 10^3\ s^{-1}$, i.e., less than for ^{16}O, and in agreement with the calculations of Mukhopadhyay et al. [261]. The (π^-, γ) reaction feeds the ground-state strongly, levels at 1.3 and 2.9 MeV weakly, and a level at 6.9 MeV quite strongly, but the neutron separation energy for ^{18}N is 2.825 MeV [273].

5.5. Fluorine and neon

Fluorine is a classical case in muon physics because it has such a strong hyperfine transition with a convenient time constant for electronic measurement. The latest value for the rate is 5.6 (2) μs^{-1} [192], but all measurements are in reasonable agreement. Normally a LiF target is used because the muon goes to the fluorine atom 60% of the time and captures for about 33.5% of those events, whereas for lithium, the atom is chosen only 40% of the time and captures for only 0.5% of those events, thus, nuclear capture on the lithium is only 1% of muon captures in LiF. The only γ-ray measurement [178] used NaF and reported just the 1982 keV γ-ray from the decay of the first excited state of ^{18}O. There are 8 bound excited states of ^{19}O, so an experiment is feasible. The (π^-,γ) reaction feeds the g.s, 4.9, 6.3 and 8.0 MeV levels, but ^{19}O is unbound above 3.96 MeV [153], so the major transitions will not be observed via ^{19}O γ-rays; the strongest ^{19}O transitions have been estimated to be about 0.4% of captures to the 97 keV $3/2^+$ level, and about 0.1% each to levels at 1468, 2370 and 3237 keV [272].

Muon capture on ^{20}Ne to three levels in ^{20}F has been reported, viz. the 1^-, at 984 keV, the 1^+, at 1057 keV, and the 2^-, at 1309 keV; the yields of each are similar and are about 3% per muon capture. Calculations by Siiskonen et al. have great difficulty reproducing these values [510,511].

Neon has been discussed many times for a study of the ν–γ correlation coefficient, along the lines of the ^{28}Si experiments. In the ^{20}Ne $(\pi^-,\gamma)^{20}$F reaction [512], the 1^+ level at 1057 keV in ^{20}F is excited clearly (remember that 90% of this reaction proceeds from the $2p$ pionic orbital); this excitation of a 1^+ level is confirmed by the (p,n) reaction [286], see Fig. 5.4, though the strength is less than equivalent transitions in ^{24}Mg or ^{28}Si. Measurements on the (n,p) reaction also exist, but the energy resolution of about 1.1 MeV make comparisons uncertain [513]. Natural neon contains 0.27% ^{21}Ne and 9.22% ^{22}Ne, which is a better situation than silicon because it is the single neutron emission which dominates and might feed this level in ^{20}F. However, cascade feeding is of major concern. The (π^-,γ) and (n,p) reactions feed a complex at about 6.1 MeV with an intensity 10–15 times that of the 1057 keV level. If we assume this complex to be the 2^- levels at 5936 and 6018 keV, then these 2^- excited states cascade down via several other levels with an ultimate sum of 3.5% to the 1057 keV level [514]. Even if the (n,p) reaction exaggerates the feeding that would be observed in the (μ^-,ν) reaction, there is a serious problem. (It could be solved via various co-incidence spectra, but it is a major effort.)

5.6. Sodium, magnesium, aluminium, phosphorus

Johnson et al. [339], have reported all identified γ-rays for muon capture in ^{23}Na. Gorringe et al. [338], recently studied Mg, Si, P and S, but only transitions to the $(A,Z-1)$ nucleus have been reported so far. In Table 5.16 we give the results for Na, Mg, Si and P; citing the direct transitions to specific levels. This requires knowledge of cascade feeding which can sometimes be incomplete, therefore all values might be reduced slightly following the discovery of more transitions. The yields of the ^{28}Al γ-rays were given in Table 5.6 so a comparison illustrates the difficulties involved. For ^{23}Na and ^{31}P there is a hyperfine transition rate which is quite fast so these yields are for the lower state. Information on upper state yields are also available for ^{23}Na, [339], but with larger statistical and systematic errors. The excited states have quite different hyperfine sensitivities.

Table 5.16
Muon capture in ^{23}Na, ^{24}Mg, ^{28}Si and ^{31}P. The results cited are the direct transitions given as a percentage of muon capture, to the bound levels of the $(A, Z-1)$ nucleus, taken from Johnson et al. [339], and Gorringe et al. [338]. γ-ray yields for ^{28}Si were given in Table 5.5. For ^{23}Na and ^{31}P the yields are for the lower hyperfine state

^{23}Na$(\mu^-, \nu)^{23}$Ne			^{28}Si$(\mu^-, \nu)^{28}$Al		
			31	2^+	0.8 (19)
1017	$1/2^+$	1.3 (4)	972	0^+	0.6 (5)
1702	$7/2^+$	0.35 (9)	1372	1^+	3.3 (6)[a]
1823	$3/2^+$	1.08 (24)	1620	1^+	1.5 (2)
2315	$5/2^+$	0.57 (13)	2138	2^+	2.1 (6)
3432	$3/2^+$	1.08 (22)	2201	1^+	7.2 (9)
3458	$1/2^+$	2.8 (6)	3105	1^+	1.3 (3)
			3876		
$\sum$ (^{23}Ne)		7.2 (8)		2^-	1.1 (3)
Activation		10.7 (4)	$\sum$ (^{28}Al)		17.9 (24)
			Activation		26 (3)
^{24}Mg$(\mu^-, \nu)^{24}$Na			^{31}P $(\mu^-, \nu)^{31}$Si		
472	1^+	4.3 (14)[a]	752	$1/2^+$	0.2 (8)
1341	2^+	3.6 (4)	1695	$5/2^+$	1.1 (2)[a]
1347	1^+	3.7 (5)	2317	$3/2^+$	1.0 (1)
1846	2^+	0.7 (1)	3133	$7/2^-$	0.26 (3)
3372	2^-	0.77 (10)	3534	$5/2^-$	2.6 (3)
3413	1^+	0.72 (14)	4383	$3/2^-$	0.35 (4)
			4720	$1/2^+$	2.7 (3)
$\sum$ (^{24}Na)		13.8 (23)	5282	$1/2^+$	1.0 (1)
			$\sum$(^{32}Si)		9.2 (9)

[a]Unidentified cascading to these levels is suspected.

The sum of the γ-ray transitions is given in Table 5.16 and comparison with activation results for ^{23}Na and ^{28}Si indicates that a significant yield of γ-rays is still to be identified. From the identified transitions, it is seen that 1^+ transitions are dominant for bound levels, but 2^- and maybe 2^+ transitions are also identified. Most 2^- transitions and almost all 1^- yield unbound states. This general statement was also true for ^{14}N, see Table 5.12.

A spectrum of the reaction ^{23}Na $(d, ^2\text{He})^{23}$Ne indicates that the ground-state is not strongly fed [303], but it is noted that there is a strong peak at 2 MeV excitation energy, and this is hard to make compatible with Table 5.16. (^{23}Ne is bound up to 5.2 MeV.) The difficulty is the observation of a strong excitation of the 1017 level in the (μ, ν) reaction. The ground-state of ^{23}Na is $3/2^+$, so an $M1$ transition can reach the 1017 keV $1/2^+$ level in ^{23}Ne. Is it maybe cascade feeding in the (μ, ν) reaction?

There are two spectra published, for the reaction ^{24}Mg $(d, ^2\text{He})^{24}$Na; that taken by Xu et al. [300], is for $E_d = 125.2$ MeV, and that by Niizeki et al. [445], at $E_d = 270$ MeV; both achieved an energy resolution of about 650 keV, and the spectra are almost identical. They exhibit weak

feeding of the ground and 472 keV states, but strong excitations at 1.4 MeV and 3.4 MeV, as expected from Table 5.16. There is further weak feeding up to the neutron separation energy of 6.96 MeV. This pattern is confirmed in the (p,n) reaction [285]. The weak excitation of the 472 keV in the $(d,{}^2\mathrm{He})$ reaction further reinforces the suspicion of Gorringe et al., that there is unidentified feeding of that level. The only caveat, an important one however, is that the published $(d,{}^2\mathrm{He})$ and (p,n) spectra are for 0° only, not the preferable 10° or so. Inelastic electron scattering at 165° on ^{24}Mg similarly finds a level at 10.71 MeV (1.35 MeV in ^{24}Na) to take most of the strength and the one at 9.96 MeV (0.47 MeV in ^{24}Na) to have half of that strength, see Richter et al. [515].

For ^{31}P, the GT strength measured in the reaction $^{31}\mathrm{P}(n,p)^{31}\mathrm{Si}$ by Sedlar et al. [516], shows that the direct feeding of the 752 keV level is larger than that to the 2317 keV level, indicating that cascading to the 752 keV level may have been overestimated for muon capture in Table 5.16. Equally well the (n,p) reaction indicates strength at 5600 keV, which has not yet been identified in muon capture; note that ^{31}Si is bound up to 6588 keV. We also remark that there is no peak in the (n,p) reaction at $E_x = 1.7$ MeV, confirming the suspicion of Gorringe et al., that the yield of the level at 1695 keV in muon capture is probably cascade feeding.

Gorringe et al. [338], selected the 1^+ transitions and attempted shell model calculations for these bound levels. Using the OXBASH code, and the universal SD interaction, they calculated a purely theoretical capture rate, Calculation A. Discrepancies can be a factor of two or more, but on average the results are reasonable giving an effective axial coupling $\tilde{g}_\mathrm{A} = -0.91^{+0.15}_{-0.17}$ which is consistent with findings from β-decay, but far from the neutron value of -1.27 (4). They then took the GT matrix element from (n,p) or (p,n) reactions, and used this in place of the shell model value for the $\sigma\tau^+$ matrix elements, also changing $\tilde{g}_\mathrm{A}$ back to -1.26. The other matrix elements were taken from the shell model, resulting in a second version Calculation B. These two methods are compared in Fig. 5.7 and it is clear that Calculation B is certainly better, but not perfect. For the ^{23}Na transitions Johnson et al., found $\tilde{g}_\mathrm{P} = (6.5 \pm 2.4)\tilde{g}_\mathrm{A}$, which illustrates the weak sensitivity to the induced pseudoscalar coupling constant. These findings have been confirmed by Junker et al. [517], who have made calculations for three 1^+ levels in ^{28}Si. They find that for all wave functions the B(GT) from the (p,n) reaction and the capture rates for (μ^-,ν) scale together within 10%. They can also improve the agreement with experiment by transforming the excited state wave functions phenomenologically.

The conclusion to be taken is that the shell-model GT matrix elements do not fit the (n,p), nor the (μ^-,ν) reaction well, but that the experimental values are consistent though with a broad band of uncertainty. From other attempts to study such reactions in the *s–d* shell, it seems that the further theoretical improvement can be anticipated, but with considerable calculational effort.

The γ-rays from the reaction $^{23}\mathrm{Na}(\mu^-,\nu n)^{22}\mathrm{Ne}$ are presented in Table 5.17. Here the transitions are quoted as % per muon capture (Johnson et al., use per muon stop). In this case 52% of captures yield an identified γ-ray in ^{22}Ne, which is close to the 65% or so expected. As ^{22}Ne is bound up to 10.4 MeV many of the transitions have been identified, but not all. We compare the muon capture results with two (γ,p) experiments, one by Gabelko et al. [518], who measured γ-rays, with 32 MeV bremsstrahlung, and the other by Ishkanov et al. [519], who detected protons with a bremsstrahlung difference method up to 30 MeV. This method gives a reliable value for the ground-state transition which is small. For both (γ,p) experiments the

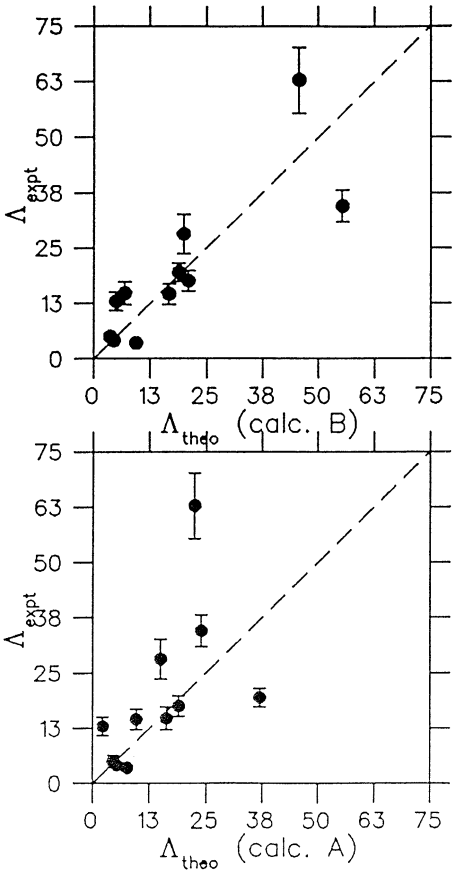

Fig. 5.7. Comparison of 1^+ transitions in muon capture on some *s–d* nuclei. Calculation A used shell-model matrix elements, but Calculation B used $(p,n)/(n,p)$ values for the Gamow–Teller $\sigma\tau^{\pm}$ matrix elements and fits better [338].

results are presented as a % of the total (γ, p) integrated cross-section. Note that the $(\mu, \nu n)$ reaction adds up to only 52% (the true total cannot be much more than 75%).

There are obvious difficulties in Table 5.17. First the (γ, p) results, claiming to measure the same cross-section, are not in agreement. However, remembering that the Ishkanov experiment (last column) had an effective resolution of about 1 MeV helps to explain the differences, though their ^{22}Ne excitation spectrum shows a clear minimum at 5.5 MeV. Their yield curves show that the 8.9 and 11.8 MeV states are predominantly excited for higher γ-ray energies, so one can neglect those levels for comparison with $(\mu^-, \nu n)$, thus the (γ, p) effectively adds to ~70%, comparable to the 52% for $(\mu^-, \nu n)$. The 6.9 MeV level has a strong peak at an excitation energy of 21 MeV, just where the (μ^-, ν) excitation is quite strong. We thus surmise that both the (γ, p) experiment measuring γ-rays and the $(\mu^-, \nu n)$ experiment are missing strength to levels in ^{22}Ne at about 6.9 MeV. Note also that both γ-ray experiments have a higher proportion of excitation of the 1.27 MeV γ-ray. It thus seems reasonable to hypothesize that some of this strength to the 6.9 MeV levels is cascading down via the 1.27 MeV level. (In the $(\mu^-, \nu n)$ experiment the

Table 5.17
Comparison of the reaction ^{23}Na($\mu^-, \nu n$)^{22}Ne [339], with two measurements of the reaction ^{23}Na(γ, p)^{22}Ne, a γ-ray measurement by Gabelko et al. [518], and a proton detection method by Ishkanov et al. [519], both presented as a percentage of the integrated (γ, p) cross-section up to 30 MeV

Level (keV, J^π)	($\mu^-, \nu n$) (% of captures)	(γ, p) [518]	(γ, p) [519]
g.s. 0^+			2
$1275, 2^+$	35 (8)	18.2 (33)	12
$3357, 4^+$	5.6 (11)	8.1 (17)	11
$4457, 2^+$	7.2 (15)	6.2 (17)	16
$5148, 2^-$	2.8 (7)	8.3 (33)	
$5326, 1^+$		0.9 (3)	
$5365, 2^+$		3.1 (11)	
$5523, 2^+$	0.55 (11)		
$5641, 3^+$	1.3 (3)	2.8 (13)	
$6116, 2^+$		2.4 (13)	
6900[a]	unbound	~ 50	27
8900[a]			14
11800[a]			16

[a]Peaks observed in the (γ, p) reaction, using proton detection. Between 5 and 10 levels are candidates for each group.

yield of this γ-ray has already been reduced by a third for known cascading.) Thus with some careful "interpretation", the results can be made compatible, but these suggestions should and can be tested experimentally. The reaction ^{23}Na($d, ^3$He)^{22}Ne was studied a long time ago [520] and few levels were detected, but the results are compatible with the comments above.

For ^{24}Mg($\mu^-, \nu n$)^{23}Na we have only the old data of Miller et al. [458]. This is unfortunate because the data on the (γ, p) reaction are quite extensive [521–523] though with a few inconsistencies, and the reaction ^{24}Mg($d, ^3$He)^{23} is also available and has been summarized by Endt and van der Leun [461]. From the comparison of these results we can conclude that:

(a) The (γ, p) reaction fits the ($\mu^-, \nu n$) data better than the ($d, ^3$He) reaction.
(b) The ground-state of ^{23}Na is fed only weakly.
(c) There is much strength at ^{23}Na excitation energies between 2.8 and 6 MeV which was not identified in the ($\mu^-, \nu n$) reaction.

Of particular value would be a comparison with the (γ, p) results of Bangert et al. [521], who give the γ-ray yields for a variety of bremsstrahlung end points, so the optimum integration could be determined.

For the case of ^{26}Mg there are two experiments on the reaction ^{26}Mg($d, ^2$He)^{26}Na, that of Xu et al. [301], at $E_d = 125.2$ MeV, and the other by Niizeki et al. [445], at $E_d = 270$ MeV. Again the spectra are identical and complex and show excitation of many bound levels (up to 5.62 MeV in ^{26}Na). Both give spectra at various angles so a comparison with (μ^-, ν) would be interesting. An experiment on the (n, p) reaction at 200 MeV exists [524] and gives a similar spectrum.

Table 5.18
Muon capture in the reaction $^{32}S(\mu^-, \nu)^{32}P$, comparing the recent results of Gorringe et al. [338], with the earlier results of Pratt [161]. The results are for the total yields per muon capture, and include cascade feeding. The calculations of Gorringe et al., for the 1^+ levels are for a shell-model calculation, Calculation A, and a phenomenological calculation using information from experimental (p,n) results, Calculation B. Also given are the B(GT) values, obtained by Anderson et al. [286] in the $^{32}S(p,n)^{32}Cl$ reaction

^{32}P level	Pratt exp. [161] (%)	Gorringe exp. [338] (%)	Gorringe Calc. A (%)	Theory Calc. B (%)	B(GT) Anderson et al. [286]
$0, 1^+$					0.01
$1149, 1^+$	1.8 (4)	3.2 (3)[a]	1.10	1.46	0.34
$1323, 2^+$	1.7 (5)	2.0 (2)			
$1755, 3^+$	2.7 (29)	0.66 (7)			
$2658, 2^+$	—	0.73 (8)			
$2740, 1^+$	—	[b]			0.07
$3264, 2^-$	3.5 (15)	2.3 (2)			
$3320, 3^-$	—	0.59 (6)			
$3793, 1^+$	—	[b]			0.03
$4036, 1^-$	1.6 (14)	[c]			
$4205, 1^+$	—	2.6 (3)	1.77	4.09	1.01
$4662, 2^-$	1.6 (6)	[c]			
$4711, 1^+$	—	1.44 (15)	2.73	1.38	0.31
$4877, 1^-$	2.9 (23)	[c]			

[a] At least 1.7% of this is cascade feeding from the 3264 and 4711 keV levels.
[b] Equivalent level observed in (e,e') experiments, at about half the strength of 4711 keV level [527,528].
[c] Not observed by Gorringe et al., in better conditions than for Pratt.

For ^{27}Al and ^{31}P, there are no complete identifications of muon capture γ-rays, although many spectra have been taken [525]. Complete analysis is unfortunately quite time consuming. There are excellent data on the reaction $^{27}Al(\gamma, p)^{26}Mg$ awaiting comparison [526].

5.7. Sulphur, chlorine, and potassium

Sulphur has been studied by Gorringe et al. [338] and there is a much older experiment by Pratt [383]. The complexity of heavier nuclei is beginning to take its toll as many γ-rays have multiple contributions. Thus much hand waving has to take place in the interpretation. The γ-ray yields are given in Table 5.18. Gorringe et al. are able to explain the differences between their results and the older ones of Pratt. The 4036, 4662 and 4879 keV γ-rays were not observed by Gorringe et al. The 1^+ levels at 1149, 4205 and 4710 keV were included in their calculation discussed above, and included in Fig. 5.7, and in Table 5.18. Their phenomenological Calculation B gives a somewhat better matching.

The reaction $^{32}S(p,n)^{32}Cl$ has been studied at 135 MeV by Anderson et al. [286] and is illustrated in Fig. 5.8. The 0° spectrum shows a pattern of 1^+ states very similar to the (μ^-, ν) reaction (as noted in Calculation B of Gorringe et al.). To illustrate this, the B(GT) values of Anderson et al., are included in Table 5.18. The ground-state transition is very weak.

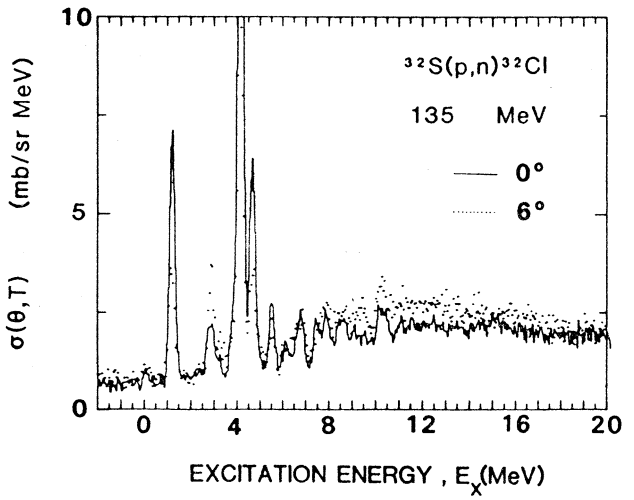

Fig. 5.8. Neutron energy spectrum for the reaction $^{32}S(p,n)^{32}Cl$ at 0° (line) and 6° (dots) for 135 MeV protons, taken from Anderson et al. [286]. For muon capture, viz. $^{32}S(\mu^-,\nu)^{32}P$, the ^{32}P nucleus is bound up to 7.94 MeV.

Fortunately the 6° spectrum is presented as well and shows that a level around 2.8 MeV is excited significantly more than in the 0° spectrum, and other levels at 5.6, 6.2, 6.7, 7.5 and 7.8 are excited and should add another 5% or so of (μ,ν) captures (^{32}P is bound up to 7.94 MeV). Of course the energies may be slightly different in ^{32}P. Note that the sum of the yields for ^{32}P is 11.5% after subtracting known cascade feeding, but using the (p,n) spectrum, we may surmise that there are unidentified transitions, so maybe $\sim$ 16% of muon captures in ^{32}S are to bound states of ^{32}P, a typical number. There is no activation measurement to compare with, because the β-decay of ^{32}P produces no gamma-rays.

Relevant experiments have been reported on 180° inelastic electron scattering on ^{32}S. There is a recent measurement by Petraitis et al. [527], and a similar earlier experiment by Burt et al. [528]. They report strong $M1$ $T=1$ excitations at 8.11 MeV (1149 keV), 11.16 MeV (4205 keV), and 11.65 MeV (4711 keV); the equivalent excitation in ^{32}P is given in brackets and has been observed in muon capture, see Table 5.18. Somewhat weaker excitations are observed at 9.68 MeV (2740 keV), 10.90 MeV (3793 keV), 13.41 MeV ($\sim$ 6410 keV), and 13.78 MeV($\sim$ 6780 keV). These have not been reported yet in muon capture, but should be detectable.

There has been a recent flurry of theoretical activity on shell model calculations for $A=32$; the most recent is by Molique et al. [529], with a previous calculation by Brenneisen et al. [530]. They have made significant progress and have obtained reasonable agreement with γ-ray branching ratios, a sensitive test of the wave functions. Unfortunately, however, they have not addressed the topic of muon capture (nor (p,n) reactions).

For the reaction $^{32}S(\mu^-,\nu n)^{31}P$, there are no results yet available from Gorringe et al. We therefore have to rely on the older experiment of Pratt [161]. In Table 5.19 we compare those results with the (γ,p) results of Varlamov et al. [531] obtained using proton detection and bremsstrahlung differences. A useful feature is that they quote various energy bands and we quote the percentage contributions in the γ-ray ranges 17.4–20.2 MeV and also for 20.2–23.4 MeV. Finally, we present the new analysis by Vernotte et al. [453], of the spectroscopic

Table 5.19
γ-rays observed by Pratt from the reaction $^{32}S(\mu, \nu n)^{31}P$. The yield is given per muon capture; the first three levels, viz. 1266, 2234 and 3134 may be contaminated with other lines. Comparison is made with the (γ, p) reaction studied by Varlamov et al. [531], detecting protons, for two energy ranges. The results of Vernotte et al. [532], are the spectroscopic factors from the $(d, ^3He)$ reaction

Level (keV, J^π)	$(\mu^-, \nu n)$ [161] (%)	(γ, p) [531] 17.4–20.2 MeV (%)	(γ, p) [531] 20.2–23.4 MeV (%)	$(d, ^3He)$ S [532]
0, $1/2^+$		7	2	1.86
1266, $3/2^+$	~ 20	22	11	1.71
2234, $5/2^+$	~ 23	12	8	3.99
3134, $1/2^+$	~ 3			0.22
3295, $5/2^+$	2.9(8)	15	9	1.45
4190, $5/2^+$	1.0(4)			1.41
4260, $3/2^+$	1.6(8)			v. small
4431, $7/2^-$	5.4(13)			visible
4783, $5/2^+$				0.43
5256, $1/2^+$		22	21	0.20
5529, $7/2^+(5/2^+)$	1.9(12)			v. small
5892, $9/2^+$				0.33
5988, $3/2^-$		Small	Small	0.30
6337, $1/2^+$				0.22
7158, $5/2^+$		22	21	1.72
7897, $1/2^-$	Unbound			1.54
9500	Unbound		37	

factors obtained in the $^{32}S(d, ^3He)^{31}P$ reaction by Mackh et al. [452]. Compatible results are found from the $(e, e'p)$ reaction [533]. Comparisons are obviously difficult because of the possible superposition of γ-ray lines in muon capture and the poor energy resolution in the (γ, p) reaction. Clearly lines in muon capture have not yet been identified, but it seems the (γ, p) is a better parallel, in which case the ground-state transition should be about 4% in muon capture, indicating that 63% of muon capture has given identified lines in ^{31}P. This must be most of the yield as we have indicated that 16% give ^{32}P bound states, charged particles about 13%, and the $2n$ reaction about 10% (compare ^{28}Si in Table 5.4). Modern experiments for muon capture and the (γ, p) reaction should settle many of these questions.

Spectra for chlorine and potassium exist, but a detailed analysis is not available. It would be useful to analyse chlorine, as it was an unexpected background in the ^{28}Si of Moftah [443], caused by muons stopping in the black insulating tape used to construct scintillating counters. Other experiments may have the same problem.

5.8. Calcium

For calcium, we have the excellent experiment of Igo-Kemenes et al. [534], who were able to identify over 20 lines. The earlier experiment of Pratt [161] is compatible but observed fewer

Table 5.20
The yield from ^{40}Ca $(\mu^-,\nu)^{40}$K [534], compared to the cross-section for the reaction ^{40}Ca$(p,n)^{40}$Sc at 134 MeV and about 5° [288]. The nucleus ^{40}K is bound up to 6.44 MeV

(p,n) $d\sigma/d\Omega$ (mb/sr)	^{40}Sc (keV)		^{40}K (keV)	(μ^-,ν) (% per capture)
~ 0	0	4^-	0	
~ 0	34	3^-	30	
1.1	772	2^-	800	4.2 (12)
(0.001)	892	5^-	891	
	1667	0^+	1644	
0.25	1799	2^+	1959	0.49(20)
		2^-	2047	0.53(18)
0.01	2300	4^-	2397	
0.09	2300(1^-)	2^-	2419	1.5(2)
0.35	2700	1^+	2730	
0.15	3900	1^-2^-		
0.4	4300	1^+		
(0.2)	5800	(2^-)		
(0.2)	6200	(2^-)		

lines. It is quite clear however that many more are yet to be discovered. The difficulty is that ^{40}K alone has nearly a hundred bound levels, many not well characterized. For ^{39}K there are "only" about 50 bound levels; thus it is no wonder that there is clearly missing yield. The nuclides ^{39}Ar and ^{38}Ar ($\sim 5.9\%$) and ^{38}Ar ($\sim 6.8\%$) were also identified clearly, indicating the importance of proton emission. This could be because of the separation energies in ^{40}K, which require charged particle emission for ^{40}K excitation in the range 6.4 to 7.8 MeV, viz.

$$
\begin{aligned}
^{40}\mathrm{K} \rightarrow\ & ^{36}\mathrm{Cl} + \alpha\text{: } 6.44\,\mathrm{MeV}\ ,\\
& ^{39}\mathrm{Ar} + p\text{: } 7.58\,\mathrm{MeV}\ ,\\
& ^{39}\mathrm{K} + n\text{: } 7.80\,\mathrm{MeV}\ ,\\
& ^{38}\mathrm{Ar} + n + p\text{: } 14.18\,\mathrm{MeV}\ ,\\
& ^{35}\mathrm{Cl} + \alpha + n\text{: } 15.02\,\mathrm{MeV}\ ,\\
& ^{38}\mathrm{K} + n + n\text{: } 20.88\,\mathrm{MeV}\ .
\end{aligned}
\tag{5.12}
$$

Note also that the ratio for $(\mu,\nu p)$:$(\mu,\nu n p)$ is clearly not in the ratio 1 : 6 observed by Wyttenbach et al., see Eq. (4.64).

In Table 5.20 are presented the results of Igo-Kemenes et al. [534], for muon capture quoted as yield per capture. These are compared with the (p,n) results of Chittrakarn et al. [288]. The 4° spectrum is illustrated in Fig. 5.9 and indicates the great advantage of the superb energy resolution of 210 keV. Even with this resolution, comparisons are difficult, but we can conclude that

(a) Muon capture to the ground-state is suppressed.
(b) The unidentified muon capture yield is probably greater than the identified yield.

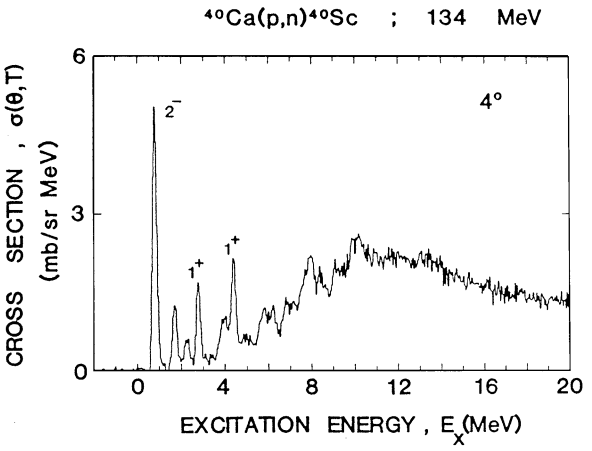

Fig. 5.9. Neutron energy spectrum for the reaction ^{40}Ca$(p,n)^{40}$Si at 134 MeV and 4°; the data are those of Chittrakarn et al. [288]. For muon capture, viz. ^{40}Ca$(\mu^-,\nu)^{40}$K, the nucleus ^{40}K is unbound to ^{36}Cl + α at 6.44 MeV, ^{39}Ar + p at 7.58 MeV and ^{39}K + n at 7.8 MeV; probably enhancing α and p emission in muon capture for this nucleus.

Of course the (p,n) reaction goes to ^{40}Sc and the energy levels are displaced a little, however the results for the reaction ^{40}Ca$(n,p)^{40}$K for $60 < E_n < 260$ MeV have a resolution of only 3 MeV and are not very helpful [294].

Backward electron inelastic scattering off ^{40}Ca adds confusing information. The most recent experiment by Petraitis et al. [535], summarizes the earlier experiments by Burt et al. [536], and by Gross et al. [537], and, most importantly, unpublished Darmstadt theses. Everyone observes a strong M1 transition at 10,319 MeV, the isobaric analogue of the 2730 keV transition in ^{40}K. For a closed shell nucleus one would not expect any coherent 1^+ transition, so this is a surprise anyway. In muon capture the 2730 level was not reported by Igo-Kemenes et al., the level emits a 1086 keV line to the 1643 keV level and a 771 keV line to the 1959 keV level, and only the decay of the 1959 keV level (not the 1643) was observed. Inelastic electron scattering also observes other excitations. That at 8428 keV is the analogue of the 2^- level at 800 keV in ^{40}K. An excitation at 9868 keV in ^{40}Ca is not understood and may be a mixture of a 1^+ transition, with an analogue at 2290 keV, and a 2^+ or 1^- level. An excitation at 10,776 keV in ^{40}Ca is suggested as 1^- and could be the analogue of the 3110, 3128 and/or 3146 keV levels in ^{40}K. Of these three or more transitions, only the 800 keV level is reported and it could be the result of cascade feeding. Another puzzle is the 1^+ level at 4.3 MeV which is strongly excited by the (p,n) reaction; this is equivalent to about 11.96 MeV in ^{40}Ca. Now a line at 12.03 MeV is observed in small angle proton scattering [319], so it seems that a 1^+ assignment is acceptable. However, it was not observed in the earlier electron scattering experiments, but Petraitis et al., report a 1^+ excitation at 11.76 MeV and a weak one at 12.04 MeV, so the different excitation mechanisms observe different proportions, and muon capture would be a useful adjunct. Small angle scattering for 319 MeV protons also exist from LAMPF [539], but the energy resolution is not sufficient for our present discussion.

Table 5.21
The yield of the reaction $^{40}Ca(\mu^-, \nu n)^{39}K$ [534] compared to the reaction $^{40}Ca(\gamma, p)^{39}K$ for 24.6 MeV bremsstrahlung from Brajnik et al. [538]. The $(d, ^3He)$ spectroscopic factors are from the compilation by Endt [418]

Level (keV, J^π)	$^{40}Ca(\mu^-, \nu n)^{39}K$ yield/capture (%)	$^{40}Ca(\gamma, p)^{39}K$ (MeV mb)	Spectroscopic factor $S_{\vec{p}}$
g.s., $3/2^+$	—	100 (7)	6.0
2523, $1/2^+$	8.8 (5)	49 (5)	3.3
2814, $7/2^-$	4.4 (4)	11 (3)	1.0
3019, $3/2^-$	2.1 (4)	14 (3)	0.1
3598, $9/2^-$	—	2 (1)	
3883, $5/2^-$	1.0 (2)	2.8 (8)	0.04
3939, $3/2^+$	< 12	11 (4)	
4082, $3/2^-$		3.6 (10)	
4930, $3/2^+$	< 2.7	5 (1)	
5262, $5/2^+$	0.50 (27)	8 (1)	2.3
5318, $3/2^+$		3.5 (15)	
5598, $5/2^+$	0.50 (27)[a]	9 (3)	1.6
5826, $1/2^-, 3/2^-$		< 1	0.1
5940, $5/2^+$		< 1	0.6
6350, $5/2^+$		6 (1)	2.8
Unbound (> 6380)		97 (15)	

[a]Given as excitation of a 5.62 MeV γ-ray, therefore identification uncertain.

Petraitis et al., also report 1^+ excitations in ^{40}Ca at 12.49, 12.83, 13.05 and 13.48 MeV, equivalent to 4.88, 5.22, 5.44 and 5.87 MeV in ^{40}K. All these would be bound levels, but are hard to identify. Even though ^{40}K is relatively well established, the reaction $^{39}K(n, \gamma)^{40}K$ probably does not excite these levels strongly; that was the case with ^{28}Al anyway.

The muon induced reaction $^{40}Ca(\mu^-, \nu n)^{39}K$ was clearly observed by Igo-Kemenes et al. [534], and their results are presented in Table 5.21 as the γ-ray yield per capture. (All levels observed have a 100%, or close to 100%, branching ratio for γ-ray decay to the ground-state, an unprecedented simplification.) The yields are compared with the (γ, p) results of Brajnik et al. [538]. This experiment detected both γ-rays and protons for a variety of bremsstrahlung energies; we compare with their data for an end-point energy of 24.6 MeV. The (γ, p) cross-section peak around 18–20 MeV which is an excellent match for the excitation energy in muon capture. Their results are compatible with, but not identical to those of Ullrich and Trauth [506] who studied γ-rays excited by a bremsstrahlung beam with an end-point energy of 32 MeV. Finally in the last column is given the spectroscopic factor for the $(d, ^3He)$ reaction, averaged over three experiments [418]. There are also results for the first four levels from the (e, e') reaction [582]. The $(p, 2p)$ reaction gives consistent, but not such detailed information [540,541]. Once again all five reactions are similar, but the closest match is between muon capture and the (γ, p) reaction; compare for example the yield for the 2814 keV level with those for the 3019 and 5262 keV levels.

As we would anticipate a single neutron yield of 50–60% in muon capture (see Table 4.7), it is clear that many ^{39}K gamma-rays have yet to be identified, even when taking into account

Table 5.22
Experiments on muon capture in heavy elements, in historical order

Anderson et al., 1969 [174]	^{206}Pb
Povel et al., 1970 [542]	^{nat}Br[^{79}Br(51%); ^{81}Br(49%)]
Kessler et al., 1970 [160]	^{89}Y
Backenstoss et al., 1971 [345]	^{45}Sc, ^{55}Mn, ^{59}Co, ^{93}Nb, ^{127}I, ^{209}Bi
Petitjean et al., 1971 [543]	^{nat}Eu[^{151}Eu(48%); ^{153}Eu(52%)]
Backe et al., 1972 [544]	^{nat}Tl[^{203}Tl(30%); ^{205}Tl(70%)]
Evans, 1973 [382]	Si, Ti, ^{55}Mn, Fe, ^{59}Co, Ni, ^{89}Y, Ag, ^{197}Au
Dubler et al., 1978 [545]	^{138}Ba, ^{203}Tl, ^{205}Tl
Budick et al., 1983 [335,336,404,546]	^{207}Pb

a ground-state transition of about 17%. Equally well there are probably more gammas to be found in ^{38}K for which only two were identified with a summed yield of 1.4%.

In conclusion ^{40}Ca has been a valuable element because many auxiliary data are available. It is clearly time to have a modern experiment on muon capture which should search for the many suggested γ-rays.

5.9. Heavy elements

Even for sulfur and calcium it is beginning to get difficult to identify γ-rays. For heavier elements the problems multiply. Most nuclides are poorly characterized, and the γ-ray energies overlap. The good news is that the ion recoil is reduced, so Doppler broadening is less of a problem, and the spectrum is less vulnerable to room background because the timing gate is only ~ 100 ns long, instead of the 5 μs used for the lightest elements.

The measurements on heavy elements are listed in Table 5.22. In an early attempt on the separated isotope ^{206}Pb, Anderson et al., reported 15 capture γ-rays, most of which they could not identify. It is now possible to identify most of them, see Table 5.23. However, identification from such a list is quite risky as secondary clues cannot be used, as when the original spectrum is available. Thus the shape of the line, and reliability of the energy assessment are important, as is the search for other known branches of a level. Note that the expected lines in ^{204}Tl were not reported.

We have already discussed the excellent survey by Backenstoss et al. [345], (see Fig. 5.1). They used mono-isotopic elements and established the main patterns of muon capture in heavy elements; viz. the ln emission is dominant, with $2n$ and often $3n$ emission detectable. Also the transitions to the $(A, Z-1)$ nucleus were hard to detect and only in ^{59}Co and ^{93}Nb were tentative assignments made.

The experiment of Petitjean et al., on natural Eu confirmed this pattern. Although there are two naturally occurring isotopes, ^{151}Eu and ^{153}Eu, this did not significantly impede the experiment. They identified 17 γ-rays with excellent evidence for 3 and even 4 neutron emission. Again the transitions to ^{153}Sm were not observed. The nuclide ^{151}Sm was observed, but most likely from the reaction ^{153}Eu $(\mu^-, \nu 2n)$.

Table 5.23
Observed γ-rays from muon capture in ^{206}Pb; in the original experiment by Anderson et al. [174], few of the lines could be identified

E_γ (keV)	Intensity per μ capture (%)	Identification
203.9 (8)	18	^{205}Tl (203.7)
266.4 (5)	3	^{206}Tl (265.8)?
279.3 (6)	4	^{203}Tl (279.2)
416.1 (6)	6	^{205}Tl (415.7)
439.2 (6)	3	
536.5 (11)	1	^{203}Tl (536.9), ^{206}Tl (535.5)
599.0 (7)	2	
719.9 (5)	7	^{205}Tl (720.1)
764.3 (5)	1	^{203}Tl (764.9), ^{204}Tl (764.3)
794.3 (4)	2	^{203}Tl (793.2, 794.8)
1014.1 (4)	1	^{27}Al(n,n')(1014.45), ^{205}Tl (1015.5)
1136.7 (6)	1	^{205}Tl (1136.6)
1218.0 (5)	1	^{205}Tl (1219.0)?
1233.6 (7)	1	^{205}Tl (1230.1, 1234.8)
1434.2 (16)	1	^{205}Tl (1433.4)

The same group studied natural thallium, see Backe et al. [544]. Again there are two naturally occurring isotopes, ^{203}Tl and ^{205}Tl, but the experiment is still very useful. Hardly any identifications were made at the time (and about half of those are probably wrong). Their results are listed in Table 5.24 to illustrate how much has changed in our knowledge of the mercury isotopes. We should note again that these new identifications were made just from this list, without the help of secondary clues. However, the energy is an excellent criterion, and strong lines are right on the modern value (and often off the value of the time). Clearly great care was taken with the energy calibration. Dubler et al. [545] also studied muon capture in natural thallium (as well as barium), but focussed on energy determinations of one major line per isotope.

Note that of the 52 lines in Table 5.24, 14 are still unidentified (and several of the identifications are debatable). In contrast to the original identification, the present ones follow the established patterns, viz. the ln emission is very strongly represented with $2n$ emission clearly established. ^{205}Hg has two weak, but probably correct, identifications: there is no convincing identification of ^{204}Au or ^{203}Au, which would represent proton emission.

Evans [382] also made a survey of various heavy elements, but only half were mono-isotopic. The others, though important, are more difficult to interpret. There is reasonable agreement with earlier experiments which gives us overall confidence in the database.

Finally, we come to the most recent of this set of experiments, that by Budick et al. [335,336,404], on muon capture on a separated ^{207}Pb target. They observed 57 lines, and identified 47 of them. Their identifications are also useful for understanding the earlier results of Anderson et al. on ^{206}Pb.

Their analysis is complete and presents an excellent view of the overall picture. In Table 5.25 we present their summary situation, compared to the results of Backenstoss et al., for the neighbouring element of ^{209}Bi, and the theory of Lifshitz and Singer for ^{207}Pb [343,389]. The overall agreement is excellent and essentially defines our knowledge of muon capture in heavy elements. Remember that γ-ray experiments cannot detect direct neutron emissions to a ground-state. Equally well the efficiency of the germanium detector is uncertain at the 10–20% level. It tends to affect all major lines in the same sense, so the accuracy on the summation is probably optimistic. The final column is the re-analysis of the thallium data of Backe et al., derived from Table 5.24. (No corrections for internal conversion have been made.) It is reasonable but indicates that many more ground-state transitions are yet to be identified (^{203}Hg and ^{201}Hg have many very low energy lines which will be missed because of internal conversion, and absorption in the target material.)

Comparison with spectroscopic factors or with the (γ, p) reaction is not worthwhile unless several levels are identified. Wene [547] studied the (γ, p) reaction in ^{45}Si, ^{51}V, ^{59}Co, ^{58}Ni and ^{63}Cu (the latter two were separated isotopes). There is also the $(p, 2p)$ survey of Ruhla et al. [540], with an energy resolution of about 2 MeV. Best are the spectroscopic studies via the $(d, ^3\mathrm{He})$ reaction, for example the study by Reiner et al. [548], on ^{58}Ni. High resolution results from the $(e, e'p)$ reaction are available for ^{51}V and ^{90}Zr [324], but no muon capture data. All these experiments indicate that proton knock-out reactions feed many levels, often between 2 and 6 MeV excitation energy, and such transitions are not reported in the muon capture results of Evans and Backenstoss et al. It is quite clear that the muon capture experiments should have identified more lines; in addition the ground-state transition is often quite strong in the other knock-out reactions.

For gold there is an excellent experiment on the reaction $^{197}\mathrm{Au}(d, ^3\mathrm{He})^{196}\mathrm{Pt}$ for 50 and 108 MeV deuteron energy. This reaction feeds the three lowest levels about equally, viz: ground-state, 356 keV and 689 keV. A dozen other levels between 1 and 2 MeV are also fed strongly. The muon capture data of Evans [382] includes lines not strongly fed by the $(d, ^3\mathrm{He})$ reaction, but cascade feeding is clearly present. The situation is such that comparisons are futile.

The situation for ^{207}Pb is hopeful because of the detailed information available. In addition there are results from Barnes et al. [551], of a study of the reaction $^{207}\mathrm{Pb}(t, \alpha)^{206}\mathrm{Tl}$ at 20 MeV. Comparison with the muon capture results of Budick turns out however to be difficult, especially as the 266 keV level is strongly fed by cascade feeding. The general effect noted before is present here, viz that the higher energy levels are not so strongly fed in muon capture as in the (t, α) reaction. In addition details disagree, for example the 801 keV level appears to be fed fairly well in muon capture but no via the (t, α) reaction. Clearly we need more information about muon capture, in particular limits on transitions observed via (t, α). One particularly frustrating conflict is that the 1711 keV level, strongly fed via (t, α), decays with a 304.9 keV γ-ray which is exactly the same energy as the second excited state. Note also that one would expect some direct feeding of the ground-state in ^{206}Tl. For ^{208}Pb we have beautiful data from the $(e, e'p)$ reaction from NIKHEF [549], but no muon capture data.

Bismuth is interesting because we have three experiments on other reactions. Uegaki et al. [550], studied the reaction $^{209}\mathrm{Bi}(\gamma, p)^{208}\mathrm{Pb}$ from $E_\gamma = 17$–23 MeV; McClatchie et al. [552], studied the reaction $^{209}\mathrm{Bi}(d, ^3\mathrm{He})^{208}\mathrm{Pb}$ at 50 MeV, and higher energy states were investigated later with better energy resolution by Mairle et al. [553]. These experiments indicate that several levels

Table 5.24
Capture γ-ray transitions in muonic thallium with original and modern identifications

E (keV)	I per μ-stop(%)	Original identification	Modern identification
109.68 ± 0.12	0.98 ± 0.18	—	—
125.49 ± 0.30	0.29 ± 0.08	—	—
158.37 ± 0.22	0.38 ± 0.11	^{199}Hg (158.37)	^{199}Hg (158.38)
197.05 ± 0.18	0.63 ± 0.15	—	—
203.67 ± 0.18	0.92 ± 0.18	^{205}Tl (n,n') (203.75)	^{205}Tl(n,n')(203.75)
222.37 ± 0.15	1.65 ± 0.83	—	^{202}Hg (222.3)
318.55 ± 0.21	1.64 ± 0.37	—	^{203}Hg (318.4)
351.86 ± 0.19	1.70 ± 0.38	—	^{202}Hg (351.7), ^{201}Hg (352.4)?
368.07 ± 0.19	4.34 ± 0.84	^{200}Hg (367.97)	^{200}Hg (367.94), ^{203}Hg (369.0)
370.35 ± 0.21	1.72 ± 0.48	—	^{203}Hg (370.4)
379.64 ± 0.22	1.00 ± 0.23	—	^{205}Hg (379.5)
388.17 ± 0.23	0.76 ± 0.19	—	^{202}Hg (388.1), ^{201}Hg (388.3)
412.21 ± 0.30	0.95 ± 0.31	^{198}Hg (411.8)	^{198}Hg (411.8)
414.86 ± 0.36	0.68 ± 0.22	—	^{201}Hg (414.5)
436.70 ± 0.19	25.41 ± 4.12	^{204}Hg (430)	^{204}Hg (436.55)
439.68 ± 0.19	17.01 ± 2.78	^{202}Hg (439.1)	^{202}Hg (439.51)
467.13 ± 0.30	0.73 ± 0.22	—	^{205}Hg (467.5)
497.80 ± 0.33	0.77 ± 0.22	—	^{204}Hg (497.6), ^{203}Hg (498.3)
520.36 ± 0.22	7.22 ± 1.35	^{202}Hg (523)	^{202}Hg (520.1), ^{201}Hg (521.1)
542.76 ± 0.31	0.78 ± 0.22	—	^{203}Hg (541.2), ^{201}Hg (542.6)
548.96 ± 0.28	1.09 ± 0.29	—	^{203}Hg (548.8)
579.25 ± 0.26	1.76 ± 0.43	^{200}Hg (579.4)	^{200}Hg (579.3)
654.57 ± 0.36	1.16 ± 0.31	—	^{204}Au(654.9)?
680.09 ± 0.29	2.37 ± 0.56	—	^{202}Hg (680.1)
691.71 ± 0.17	7.60 ± 0.93	^{200}Hg (691.3)	^{204}Hg (691.8)
706.48 ± 0.27	1.30 ± 0.27	—	—
720.58 ± 0.29	0.95 ± 0.22	—	^{202}Hg (718.3)??
735.61 ± 0.32	0.87 ± 0.23	—	—
742.37 ± 0.33	0.80 ± 0.23	—	^{202}Hg (742.6)
758.61 ± 0.42	0.52 ± 0.14	^{200}Hg (759.6)	—
801.33 ± 0.41	0.56 ± 0.15	—	—
904.26 ± 0.50	0.66 ± 0.18	—	—
908.41 ± 0.51	0.67 ± 0.18	—	^{202}Hg (908.4)
960.18 ± 0.43	0.55 ± 0.14	^{200}Hg (959.9)	^{202}Hg (959.7)
968.94 ± 0.37	0.75 ± 0.17	—	—
1014.53 ± 0.39	0.59 ± 0.15	—	^{27}Al(n,n')(1014.45), ^{205}Hg (1015.4)
1134.67 ± 0.20	3.00 ± 0.56	—	^{204}Hg (1134.65), ^{205}Tl(n,n')(1136.56)
1199.36 ± 0.27	1.20 ± 0.25	—	^{204}Hg (1199.2)
1204.56 ± 0.41	0.52 ± 0.14	^{200}Hg (1207)	^{200}Hg (1205.7), ^{202}Hg (1203.7)
1279.91 ± 0.40	0.93 ± 0.18	—	^{204}Hg (1280.2)
1391.29 ± 0.35	0.68 ± 0.17	^{200}Hg (1389)	^{204}Hg (1392.2)
1511.59 ± 0.28	1.50 ± 0.34	—	^{204}Hg (1511.1)
1553.86 ± 0.35	0.96 ± 0.24	—	^{204}Hg (1552.8)
1597.91 ± 0.45	0.62 ± 0.17	^{200}Hg (1593)	^{204}Hg (1598.3)
1606.33 ± 0.75	0.54 ± 0.20	^{200}Hg (1604)	—
1660.03 ± 0.47	0.58 ± 0.17	—	—
1681.49 ± 0.49	0.51 ± 0.16	—	^{204}Hg (1680.8)
1703.85 ± 0.40	0.70 ± 0.20	—	^{204}Hg (1704.3)
1722.84 ± 0.66	0.34 ± 0.12	^{200}Hg (1718)	—
1744.06 ± 0.72	0.30 ± 0.12	^{200}Hg (1745)	—
1827.98 ± 0.51	0.50 ± 0.16	—	^{204}Hg (1827.5)
1975.90 ± 0.85	0.21 ± 0.09	^{200}Hg (1973)	—

Table 5.25
Experimental neutron multiplicities are compared with the calculations of Lifshitz and Singer for lead [343,389] and in brackets, a supplemental calculation [348]. Experiments which detected γ-rays are by Budick et al. [335,336,404] on separated ^{207}Pb, by Backenstoss et al. [345] on ^{209}Bi, and by Backe et al. [544], on ^{nat}Tl. The high multiplicity experiment by Pruys and Wyttenbach on ^{209}Bi used the activation technique [350]

Mode	^{207}Pb(exp) [336] (%)	Pb(calc) [343] (%)	^{209}Bi(exp) [345] (%)	^{209}Bi(exp) [350] (%)	^{nat}Tl [544] (%)
$0n$	7.9 (14)	22	—	—	2.4 (3)
$1n$	42.9 (57)	31	43.0 (70)	—	36.3 (50)
$2n$	24.5 (52)	26	19.3 (36)	—	5.7 (7)
$3n$	10.4 (39)	14	7.7 (13)	—	9.6 (34)
$4n$	5.4 (8)	5.9	—	—	0.0 (4)
$5n$	1.3 (3)	1.1	—	—	1.4 (9)
$6n$	0.9 (2)	0.07 (1.0)	—	1.50 (15)	0.4 (1)
$7n$	—	(0.3)	—	0.14 (2)	—
$8n$	—	(0.08)	—	0.28 (2)	—
$\sum$	93.3 (88)	100(+)	70.0 (80)	1.92 (15)	55.8 (51)

between 3 and 5 MeV should be excited. In both reactions the three lowest levels are excited about equally viz the ground-state, 2615 and 3198 keV. Comparison with the muon capture results of Backenstoss et al., implies that there is cascade feeding, so it is difficult to estimate the direct feeding of the 2615 and 3198 keV levels in muon capture, and thereby suggest a value for the direct feeding of the ground-state.

In general then, the comparison of muon capture in heavy elements with the (γ, p), $(d, {}^3\mathrm{He})$ and $(e, e'p)$ reactions is confusing, and it seems that muon capture, though similar to these other knock-out reactions, has its own idiosyncrasies.

6. Other topics

6.1. Radiative muon capture

Although relatively rare, radiative muon capture has been studied because of its potential for measuring g_P. The reality is, however, that confusion reigns.

We shall first discuss radiative muon capture in hydrogen, viz:

$$\mu^- + p \rightarrow n + \nu + \gamma \,. \tag{6.1}$$

This is a doubly rare reaction; first ordinary muon capture is already $\sim 10^{-3}$ of muon decay in muonic hydrogen. Then, one loses another factor of 10^{-4}. However, in a real experiment, the bremsstrahlung from normal μ^- decay drowns the observable effect below about 60 MeV. Thus the observable γ-rays for reaction (6.1) have a branching ratio of $\sim 10^{-8}$.

It is not surprising therefore that only one experiment has attempted the monumental task of studying this reaction. A letter was published by Jonkmans et al. [554], and a full report has

recently been published by Wright et al. [555]. Because of the low branching ratio it is clear that an intense muon bean is required ($\sim 6 \times 10^5\,s^{-1}$) and a high efficiency detector, with a reasonable energy resolution. The choice fell on a pair spectrometer in the form of a cylindrical drift chamber with lead converters, so a detection efficiency of a few per cent was achieved.

The potential backgrounds are often quite subtle and great care has to be taken to control any contribution; for example

- *pion contamination in the beam*—since a pion stopping in hydrogen undergoes pion radiative capture and π^0 production giving two gammas, an rf mass separator reduced pions to 2×10^{-4} of the muon beam. Since the pion capture is prompt, a time cut eliminates the few pions that get through. Fortunately the energy spectrum is quite unique, so it is straightforward to confirm the effectiveness of these avoidance tactics.
- *heavy gas contamination in the target*—if there is any gas present in the target with a higher Z (viz N_2, O_2, Ar), the muon is transferred from the hydrogen to that atom, so the contamination must be kept $< 10^{-9}$, using bake out techniques, and a palladium filter.
- *deuterium contamination in the target*—normal hydrogen has about 120 ppm of deuterium. This causes difficulty because of muon induced fusion from the $p\mu d$ molecule, which produces μ^3He atoms. Radiative capture in ^{3}He is 20 times that in H_2. Normal hydrogen thus creates a background three times the expected signal. Therefore protium gas is used; one sample had 1.4 (2) ppm of deuterium, the other < 0.1 ppm.
- *cosmic ray and machine background*—high energy neutrons can produce a π^0 background. These can be tested with the machine off, or the beam off. The contribution is about 10%, but can be monitored as the energy of many events is between 100 and 200 MeV, where no muon radiative capture is expected.

This gives a flavour of the technical complications for this experiment. The final result was the accumulation of 279 (26) events of radiative muon capture above 60 MeV, i.e., a branching ratio of $2.10\ (21) \times 10^{-8}$. It is the branching ratio which is most sensitive to g_P as the spectral shape does not change much. Using the theoretical calculation of Beder and Fearing [556], the experimental result gives

$$\frac{g_P(q^2)}{g_A(0)} = 9.8\ (7)(3) \tag{6.2}$$

for a $q^2 = -0.88 m_\mu^2$. i.e.,

$$g_P(q^2) = -12.5\ (10)\,, \tag{6.3}$$

including a liberal uncertainty for the various values of $g_A(0)$. This is over 4σ above the theoretical estimates for g_P (-8.21 (9)), see Eq. (2.94). Many suggestions have been made to explain this difference, including a recent one that the answer may lie in which levels of the $p\mu p$ molecule are formed [557]; however, no consensus has yet been reached on this discrepancy. We shall come back to the topic when we assemble all the evidence for g_P.

Radiative muon capture on several nuclei has been studied over many years by a variety of techniques and a consensus has now been reached. There were a few experiments before the meson factory era, for example Hart et al. [558], who studied ^{40}Ca with a NaI crystal and an external converter. As discussed above for hydrogen, it is difficult to measure low energy

gammas, because of the bremsstrahlung from ordinary muon decay. This is less of a problem for heavy elements, so most of the discrepancies are for light nuclei. The early experiments started the convention of quoting the results for γ-ray energies above 57 MeV, and for a branching ratio with respect to ordinary muon capture. This has become standard, which makes comparisons easier.

In Table 6.1 are given the results of the modern experiments. The earlier experiments had used NaI spectrometers, but had difficulty distinguishing γ from neutron induced events. We omit all these earlier measurements. More modern experiments have avoided that difficulty by using an external converter, or by using the totally different technique of a pair spectrometer. At SIN the experiments started off using their pair spectrometer [559,560] and their results, together with Hart et al., are given in column 3. Later the SIN experiments used a NaI array, and surveyed 7 elements [561], see column 4. TRIUMF started off using a NaI [562] but then used the time projection chamber (TPC) which was designed for their (μ^-, e^-) experiment [563]. When this facility was redesigned to study radiative capture on hydrogen, it became an excellent tool for studying nuclei too, so the most recent results have been taken with that cylindrical pair spectrometer [564–566]. It should be noted that sometimes a theoretical curve is used to fix the shape of the γ-ray spectrum and then slightly different values of the branching ratio are obtained, so results from one experiment can be quoted differently. The values in Table 6.1 are an attempt at "model independent" determinations.

The most important thing to note about Table 6.1 is that there is remarkable experimental agreement. For all experiments after Hart et al., in 1977, the measurements are within or very close to within the error bars. The only exception is the ^{16}O measurement of Frischknecht et al. [560], which is about a factor of 2 too high. This problem is understandable as in ^{16}O the muon is decaying most of the time, and the electrons produce a serious bremsstrahlung background.

The general feature of the data is that there is a slow decrease of the branching ratio with Z. The only exception is the ^{27}Al–^{28}Si comparison, which has been confirmed in the most recent experiment. This leads to the idea of plotting the branching ratio against neutron excess, not Z.

The theoretical interpretation of radiative muon capture goes back to the pioneering work of Rood and Tolhoek in 1965 [567]. This was later developed by many authors and there is a thorough survey of this work (and the SIN and earlier experiments) by Gmitro and Truöl in 1987 [568]. It is unnecessary to duplicate this review, and so we just note the conclusions.

First it is clear that radiative muon capture is very sensitive to g_P, the induced pseudo scalar coupling constant. Fig. 6.1 is taken from Rood and Tolhoek [567] and illustrates this effect for ^{40}Ca. The γ-ray energy is normalized to the maximum available energy (~ 90 MeV), thus experiments start at $x = 0.63$ ($E_\gamma = 57$ MeV). The main effect is that a higher value of g_P means a higher cross-section. There is also a very slight change in shape, but that is hard to determine experimentally.

However, as discussed by Gmitro and Truöl, not only is radiative muon capture sensitive to g_P, but it is also sensitive to the nuclear model. It is necessary to include all excitations of the final nucleus; these are similar to ordinary muon capture and have been discussed in some detail, see for example the recent calculations by Eramzhyan et al. [420], for the nickel isotopes. The main effect is that higher energy excitations are reduced in radiative capture because of the lower energy available. Thus, many of the original uses of closure are questionable. Remember also that many calculations of ordinary muon capture were a factor of 2 too high. This same

Table 6.1
Muon radiative capture on nuclei for $E_\gamma > 57$ MeV in units of 10^{-5} per ordinary muon capture

Element	Z	Early exp.	Döbeli [561]	TRIUMF	Armstrong [564]	Bergbusch [566]
^{12}C	6		2.7 (18)	2.3 (2)[d]		
^{16}O	8	3.8 (4)[a]	2.44 (47)	2.2 (2)[d]		1.67 (18)
^{27}Al	13		$1.83^{+0.55}_{-0.25}$		1.43 (13)	1.40 (11)
^{28}Si	14				1.93 (18)	2.09 (20)
^{40}Ca	20	2.07 (20)[b] 2.11 (14)[c]	2.30 (21)	2.11 (15)[d]	2.09 (19)	
Ti	22					1.30 (12)
Fe	26		1.71(17)			
^{58}Ni	28			1.48 (8)[e]		
^{60}Ni	28			1.39 (9)[e]		
^{62}Ni	28			1.05 (6)[e]		
Zr	40					1.31 (15)
Mo	42				1.11 (11)	
Ag	47					1.12 (13)
Sn	50				0.98 (9)	
^{165}Ho	67		0.75 (13)			
Pb	82				0.60 (7)	
^{209}Bi	83		0.62 (8)			

[a]Ref. [560].
[b]Ref. [559].
[c]Ref. [558].
[d]Ref. [563].
[e]Ref. [565].

factor of 2 is present in various approximations made by Eramzhyan et al., though amongst the various models, there is agreement that radiative muon capture is smaller for the heavier isotopes of nickel.

Another recent calculation is that of Fearing and Welsh [569] who used a relativistic mean field theory approach. For the nucleus they took a relativistic Fermi-gas model and the local density approximation. Their results showed a fairly simple sensitivity to the neutron excess, viz:

$$\alpha = \frac{N - Z}{A} \tag{6.4}$$

and thus Bergbusch et al., found this was a useful way of illustrating the branching ratio.

The calculation of Fearing and Welsh [569] is shown in Fig. 6.2, taken from the recent publication of Bergbusch et al. [566]. The difficulty is that their values have to be renormalized by a factor of 0.4. Note also that Fearing and Welsh believe that their approximations are not valid for lighter nuclei ($A < 40$).

From these recent calculations, and their criticism of earlier work, there is only one conclusion that can be drawn, viz. that the nuclear effects are still not sufficiently understood that

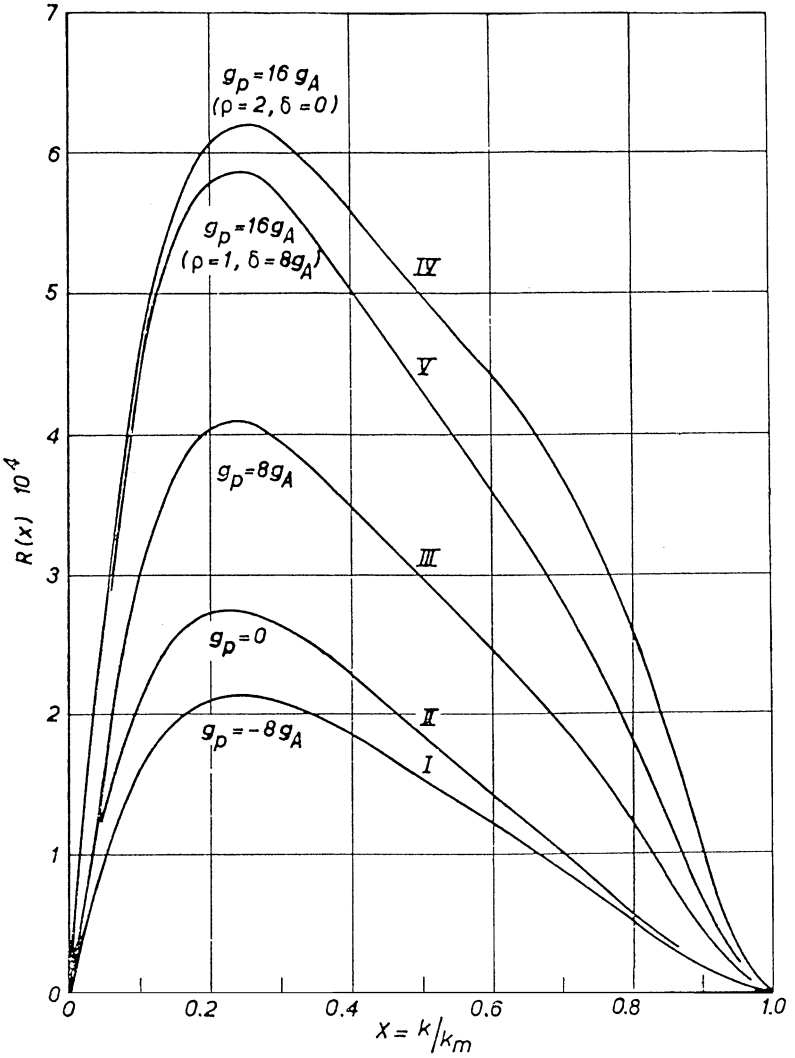

Fig. 6.1. Energy spectrum for the photon in radiative muon capture on ^{40}Ca, taken from Rood and Tolhoek [567]. The sensitivity to g_P is large, but mainly affects the absolute rate. Typically $k_m \approx 90$ MeV, and experiments can study only $E_\gamma \geqslant 57$ MeV (i.e., $x \geqslant 0.63$).

one can reliably derive a value of g_P from the experimental measurements. This is somewhat disappointing after so much effort by all parties, but nature does not always reward perspiration as much as inspiration.

6.2. Summary of g_p determinations

It is now worthwhile to bring together all the attempts to measure g_P in muon capture. The discussion in Section 6.1 implies that we must reluctantly set aside any claims to determine g_P from radiative muon capture in nuclei.

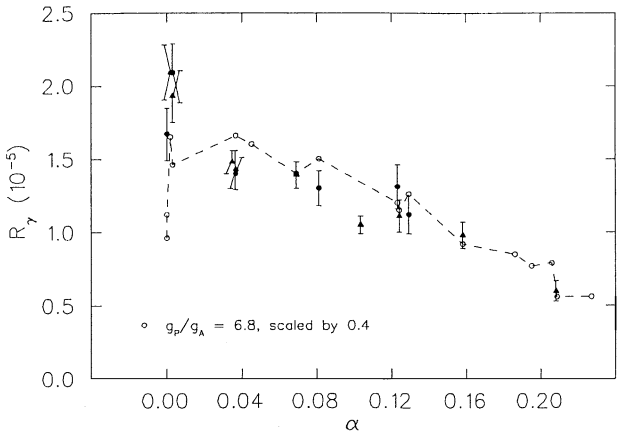

Fig. 6.2. Absolute rate for radiative muon capture on various nuclei, plotted against the neutron excess, Eq. (6.4). Data and calculation are for $E_\gamma \geqslant 57$ MeV, taken from Bergbusch et al. [566]. The calculation of Fearing and Welsh [569] had to be renormalized by a factor of 0.4 (open circles, connected by a dashed line).

Table 6.2
Experimental determinations of $g_P(q^2)/g_A(q^2)$ from muon capture experiments. We use $g_A(q^2) = -1.245(3)$. This is an abbreviated listing and only the most recent discussion of a measurement is given

Nucleus	Observable	Experimental reference	Theoretical reference	$g_P(q^2)/g_A(q^2)$
	PCAC		[109]	6.59 ± 0.07
^{1}H	Ordinary capture	[23]		6.9 ± 1.5
^{1}H	Radiative capture	[555]	[556]	10.0 ± 0.8
^{3}He	Capture to triton	[185]	[234]	6.9 ± 1.2
^{11}B	Hyperfine λ^+/λ^-	[189]	[463]	$4.7^{+2.8}_{-4.3}$
^{12}C	Capture to g.s.	[570]	[571]	6.7 ± 2.0
^{12}C	P_{AV}	[480,481]	[130,476]	$10.6^{+2.3}_{-2.7}$
			[475,476]	$9.7^{+2.5}_{-3.0}$
	P_{AV}/P_L	[482]	[130,476]	9.5 ± 1.7
			[475,476]	8.5 ± 1.9
^{16}O	Capture to ^{16}N(0^-)	[499,500]	[502,581]	7.5 ± 0.5
^{23}Na	Hyperfine rates	[339]	[573]	6.5 ± 2.4
			[574]	7.9 ± 2.2
^{28}Si	ν–γ correlation	[459]	[464]	5.1 ± 0.8
		[460]	[464]	4.4 ± 0.3

We list the various measurements of g_P/g_A in Table 6.2 and will discuss them briefly one by one. Ordinary muon capture in hydrogen was discussed in Section 2.2. The most recent assessment is given by Bardin et al. [23]. They average the results in gas and in liquid to get $g_P = -8.7 \pm 1.9$, i.e., $g_P/g_A = 6.9 \pm 1.5$. This value is still debated because of the uncertainty covering the ortho to para conversion in liquid hydrogen.

The measurement of muon capture in ^{3}He has been analysed in a variety of ways. For the present purposes we follow Ackerbauer et al. [185], who give $g_P = -8.53 \pm 1.54$ or $g_P/g_A = 6.9 \pm 1.2$. Again it is important to emphasize that the error is dominated by uncertainties in the other factors going into the calculation. The experiment itself has a precision of 0.27%.

The experiment of Wiaux [189] measured the ratio of the hyperfine capture rates in ^{11}B to give the 320 keV state in ^{11}Be. This was discussed in detail in Section 5.3. Junker et al. [463] estimate the uncertainty in g_P/g_A due to nuclear structure to be only ± 0.4, indicating that this value of g_P/g_A is limited by the experimental uncertainty.

For ^{12}C there are a variety of measurements. The ground-state transition rate can be used to estimate g_P/g_A as shown by Holstein [571]. The more recent calculation of Hayes and Towner [477] must have a similar estimate, but do not present their results in that manner.

The polarization recoil of the ^{12}B ion was discussed in detail in Section 5.4. Although Fukui et al. [476], did not make the corrections for excited states in an optimal manner, this correction is small and does not affect the results dramatically. Again it would be useful to use the nuclear structure results of Hayes and Towner as these polarization observables seem to be fairly robust.

For muon capture in ^{16}O, the transition to the 120 keV level in ^{16}N has been the centre of much attention. We quote the latest assessment by Warburton et al. [581], but note that Towner and Khanna [572] made an extensive review of this transition. Again this transition is sensitive to nuclear effects, but it seems that modern codes are reaching the requisite accuracy.

Johnson et al. [339] analysed six capture transitions in ^{23}Na. Using the OXBASH code they obtained $\tilde{g}_P/\tilde{g}_A = 6.5 \pm 2.4$ for the USD interaction [573] and 7.9 ± 2.2 for the Brown and Kuo interaction [574]. The tilde represents the fact that it is an effective coupling constant as they found $\tilde{g}_A = -1.01 \pm 0.07$ for the USD interaction and -1.34 ± 0.08 for the KUO interaction. These values are found in β-decay calculations too. However, it is difficult to assess what $\tilde{g}_P/\tilde{g}_A$ represents.

Finally, we come to ^{28}Si which was discussed in detail in Section 5.2. The γ–ν correlation has been measured for the muon capture transition to the 2201 keV level. Moftah et al. [459] measured the unpolarized correlation and obtained an amplitude ratio $x = 0.315$ (80); Briancon et al. measured the polarization effect and obtained an amplitude ratio of $x = 0.239$ (29). The normal OXBASH interpretation of this is that $g_P \sim 0 \pm 1$, but Siiskonen et al. [464], have suggested modified shell model interactions and obtained the values of g_P in Table 6.2. Clearly, their motivation was to "explain" the discrepancy in g_P, so it is not an unbiassed calculation. A similar "explanation" has been made by Junker et al. [517].

The overall conclusion from Table 6.2 is that experiments confirm the approximate value of g_P, but every measurement has its problems. There has been extensive discussion that g_P is quenched for heavier nuclei. The evidence one way or the other is very weak, so that remains an open problem. The main difficulty being that, for heavier nuclei, viz ^{23}Na and ^{28}Si in Table 6.2, the uncertainties in the calculations are manifest.

6.3. The $(\mu^-, e^\pm)$ reaction

We conclude with a brief discussion of the search for lepton number non-conservation in the reactions (μ^-, e^-) and (μ^-, e^+). These attempts are related to searches for muon decays

such as:

$$\mu^+ \to e^+ + \gamma\,, \tag{6.5a}$$

$$\mu^+ \to e^+ + \gamma + \gamma\,, \tag{6.5b}$$

$$\mu^+ \to e^+ + e^+ + e^+\,. \tag{6.5c}$$

The decay (6.5a) has been estimated to have a branching ratio of $\sim 10^{-5}$ if the muon was an excited state of the electron. In fact the latest LAMPF measurement from MEGA [26] has given the limit

$$BR(\mu \to e\gamma) < 1.2 \times 10^{-11} \quad \text{at 90\% CL} \tag{6.6}$$

and thus leptons do not transform into one another to high accuracy. This topic of lepton flavour conservation has recently been reviewed by Depommier and Leroy [25] who discuss evidence from many decays and reactions. (See also the slightly earlier reviews by van der Schaaf [575] and Kosmos et al. [576].) Apart from neutrino oscillations, which is a special case, no lepton flavour violation has been observed, and some limits (such as Eq. 6.6) are quite impressive. More recent discussions of (μ^-, e^-) conversion have been given by Raidel and Santamaria [33] and by Schwieger [32].

If there was some coupling between muons and electrons, the (μ^-, e^-) reaction would be a sensitive test as the nucleons act coherently and would enhance the rate. A related aspect is that the ground-state to ground-state transition would dominate ($\sim 80\%$ of the strength).

The signature for the (μ^-, e^-) reaction is particularly simple and unique as the e^- will be mono-energetic with an energy of 106 MeV. For free muon decay the electron reaches only 53 MeV, but in an atomic orbit, because of the momentum uncertainty, the μ^- produces electrons to a higher energy. Heavier nuclei with a tighter binding energy have a broader spread, see Fig. 4.4. However, the (μ^-, e^-) conversion is enhanced at high Z, so conflicting requirements mean that titanium has been a popular compromise as a target.

Because of the sensitivity which is reached, other backgrounds have to be considered; one is radiative muon capture followed by photon conversion. As we have seen, this occurs at a very low level, but is of concern. Bergbusch et al. had this in mind as one of the motivations for their experiment on radiative capture. Other backgrounds on the (μ^-, e^-) experiment are cosmic rays, and pion radiative capture, followed by photon conversion.

At TRIUMF the Time Projection Chamber was designed expressly for this search. Muons were stopped in various targets and high energy electrons were tracked in a magnetic field. Low energy electrons from muon decay circled at lower radius and did not trigger the data acquisition system.

For titanium the limit set by Ahmad et al. [577,30] is

$$BR(\mathrm{Ti}(\mu^-, e^-)) < 4.6 \times 10^{-12} \quad \text{at 90\% CL} \tag{6.7}$$

and for lead

$$BR(\mathrm{Pb}(\mu^-, e^-)) < 4.9 \times 10^{-10} \quad \text{at 90\% CL}\,. \tag{6.8}$$

Equally well one can search for the (μ^-, e^+) reaction which is permitted within certain theories. The ground-state transition has a low limit

$$BR(\mathrm{Ti}(\mu^-, e^+)\mathrm{Ca}(g.s.)) < 9 \times 10^{-12} \quad \text{at 90\% CL} \tag{6.9}$$

but a more likely transition would be to the giant resonance region. Thus an analysis was made with that hypothesis, but is limited by the tail from radiative muon capture, followed by photon conversion, thus:

$$BR(\mathrm{Ti}(\mu^-, e^+)\mathrm{Ca}^*(GDR)) < 1.7 \times 10^{-10} \quad \text{at 90\% CL .}$$

The SINDRUM II facility at PSI has been used for several searches for lepton flavour violation. It is a set of concentric cylindrical chambers with a superconducting solenoid. Their present limits are for titanium [28,29]

$$BR(\mathrm{Ti}(\mu^-, e^-)) < 6.1 \times 10^{-13} \quad \text{at 90\% CL} \tag{6.10}$$

and for lead [578]

$$BR(\mathrm{Pb}(\mu^-, e^-)) < 4.6 \times 10^{-11} \quad \text{at 90\% CL} \tag{6.11}$$

and again for the (μ^-, e^+) reaction [579]

$$BR(\mathrm{Ti}(\mu^-, e^+)\mathrm{Ca}(g.s.)) < 1.7 \times 10^{-12} \quad \text{at 90\% CL} \tag{6.12}$$

$$BR(\mathrm{Ti}(\mu^-, e^+)\mathrm{Ca}^*(GDR)) < 3.6 \times 10^{-11} \quad \text{at 90\% CL .} \tag{6.13}$$

These are all impressive limits and are often quoted in discussions of the basic structure of the leptonic sector of particle physics [580]. This structure has been assumed in our discussion of ordinary muon capture, but it is useful to take a brief glance at these difficult experiments on which our understanding is firmly founded. Because of the key nature of such tests, experiments are ongoing and further improvements are anticipated (and maybe even the detection of these "forbidden" reactions). SINDRUM II continues at PSI and MECO has been proposed at Brookhaven to study $^{27}\mathrm{Al}(\mu^-, e^-)$ [580].

7. Summary

We are at the close of our tour of the secluded garden of muon capture. We have learnt a lot in the last 25 years since Nimai Mukhopadhyay wrote his monumental review, yet there is clearly much more to understand.

Perhaps the most important contribution to our understanding of muon capture has come from other reactions such as (p, n) and $(d, {}^2\mathrm{He})$. These excite the same magnetic transitions and give an excellent general picture of the overall strength. However, transferring that knowledge to the muon capture reaction requires better identification of the final states, and thus even better energy resolution in these experiments. Hopefully work will continue at RCNP Osaka, and RIKEN. We shall also need continuing efforts to identify these excited states from traditional nuclear physics facilities. Not only is there intrinsic interest in this field, but there are also important applications to astrophysics.

In all of these direct transition reactions it has become clear that our understanding of nuclear structure is still sorely limited. Gorringe et al. made a major step experimentally for ^{23}Na, ^{24}Mg, ^{28}Si and ^{31}P, but showed that standard shell model codes calculate transition rates which can be as much as a factor 2 out. However, recent developments from Strasbourg and other centres are leading the way in massive shell model calculations. As complex as this work is, it is unfortunately very necessary and we can now begin to understand the failings of earlier calculations on muon capture. In the few cases where modern computational technology has been applied, such as ^{12}C and ^{16}O, it is clear that a much better description of experimental results is now possible.

For the proton knock-out aspects of muon capture, many more identifications have now been made for the $(\mu^-, \nu n)$ reaction, and, again, a lot has been learnt from comparison with other reactions such as $(e, e'p)$ and $(d, ^3\mathrm{He})$. High energy resolution is required and is now achieved, though the demise of NIKHEF will not help. We still need more results on that difficult reaction (γ, p) which bears a close similarity to the $(\mu^-, \nu n)$ reaction. Again energy resolution is a problem, but a deeper understanding is reached when several reactions are compared. It will be interesting to see whether one can excite 1^- and 2^- spin–dipole resonances, and study their nucleon decay. That would be an even closer match to what is happening in muon capture. Equally well, muon capture results should help in the identification of the levels detected in the (γ, p) reaction.

One of the biggest developments in the last decade has been our understanding of muon induced fission. This has come about because of the coherent effort of the Bonn group at PSI. This topic is such a fascinating blend of atomic physics, nuclear excitation and fission physics. A few lacunae remain, but the overall picture is now firmly established. It is certainly far more complex than was thought when the initial experiments were attempted.

What about our understanding of particle physics, and the fundamental properties of matter; have we made an impact there? It is tempting to shrug off this aspect and assert that not much has been achieved, but is this negative attitude truly fair. The impact has been subtle and in specific areas, but nonetheless there has been an impact. The very precise measurement of muon capture on ^{3}He has confirmed the overall structure of the weak interactions in the non-leptonic sector and important comparisons have been made with β-decay. Searches for the (μ^-, e^-) reaction have set impressive limits on lepton number conservation; limits which are at least as good as any other limits in particle physics experiments. Overall many measurements on muon capture have confirmed our basic understanding and often pushed forward the limits of our knowledge, especially about the weak interactions, which historically have been one of the most straightforward ways of learning profound ideas about our universe. Yes, a secluded garden, but beautiful, and with rare and unique species.

Acknowledgements

Many people have contributed to this review, sometimes unknowingly. It was mainly written while I was on administrative leave from the University of British Columbia. Therefore I would like to thank those colleagues who helped make this year so successful: at Louvain-la-Neuve,

J. Deutsch and R. Prieels; at Jerusalem, A. Gal and E. Friedman; and at PSI, C. Petitjean and K. Gabathuler.

At TRIUMF over the last few years, we have tried to contribute to this field, and my colleagues have helped greatly to further my understanding of this complex topic; many thanks to D.S. Armstrong, J. Brewer, T.P. Gorringe, M.D. Hasinoff, and most importantly to the students who have spent many hours of frustrating labour on the essential toil of experimental physics, E. Gete, B.A. Moftah, and T.J. Stocki.

My debt to Nimai Mukhopadhyay is clear for all to see. His masterful review is still worthwhile reading after nearly a quarter century. He continued to have a strong interest in this field, even during his final illness; in the spring of 2000 he died before this present review was completed, and we are all the poorer because of his passing.

Such a review is not possible without the dedication of someone to type from scrawled handwriting, sent from half-way around the globe. Raso Samarasekera of TRIUMF has handled almost all this aspect and has devoted great care to such a complex task; many thanks for such a superb product.

References

[1] M. Hirsch et al., Atom. Data Nucl. Data Tables 53 (1993) 165.
[2] A.C. Hayes, Phys. Rep. 315 (1999) 257.
[3] R.E. Marshak, Riazuddin, C.P. Ryan, Theory of Weak Interactions in Particle Physics, Wiley-Interscience, New York, 1969.
[4] R.J. Blin-Stoyle, Fundamental Interactions and the Nucleus, North-Holland/American Elsevier, Amsterdam, 1973.
[5] A.O. Weissenberg, Muons, North-Holland, Amsterdam, 1967.
[6] M. Morita, Beta Decay and Muon Capture, Benjamin, New York, 1973.
[7] F. Cannata, R. Graves, H. Uberall, The capture of muons by complex nuclei, Riv. Nuovo Cim. 7 (1977) 133.
[8] F. Cannata, R. Graves, H. Uberall, The capture of muons by complex nuclei, in: A.O. Barut (Ed.), Muon Physics, Reidel, Dordrecht, 1975.
[9] H. Uberall, Springer Tracts in Modern Physics, Vol. 71, Springer, Berlin, 1974, p. 1.
[10] V.V. Balashov, G.Ya. Korenman, R.A. Eramzhyan, Sov. J. Particles Nucl. 4 (1973) 247.
[11] R.A. Eramzhyan, Muon capture, present status and perspectives, Proceedings of WEIN, 1992.
[12] P. Singer, Springer Tracts in Modern Physics, Vol. 71, Springer, Berlin, 1974, p. 39.
[13] N. Mukhopadhyay, Phys. Rep. 30C (1977) 1.
[14] N. Mukhopadhyay, Nucl. Phys. A 335 (1980) 111.
[15] N. Mukhopadhyay, in: P. Depommier (Ed.), Proceedings of WEIN Conference, Editions Frontieres, Dreux, 1989, p. 51.
[16] C. Caso et al., Review of particle properties, Eur. Phys. J. C 3 (1998) 1.
[17] E. Klempt et al., Phys. Rev. D 25 (1982) 652.
[18] F.G. Marian et al., Phys. Rev. Lett. 49 (1982) 993.
[19] I. Beltrami et al., Nucl. Phys. A 451 (1986) 679.
[20] R. Adler et al., Phys. Lett. B 369 (1996) 367; and CERN Courier 37 (January/February 1997) 22.
[21] A. Angelopoulos et al., Phys. Lett. B 444 (1998) 38.
[22] G. Gabrielse et al., Phys. Rev. Lett. 82 (1999) 3198.
[23] G. Bardin et al., Phys. Lett. B 137 (1984) 135.
[24] K.L. Giovanetti et al., Phys. Rev. D 29 (1984) 343.
[25] P. Depommier, C. Leroy, Rep. Prog. Phys. 58 (1995) 61.

[26] A. van der Schaaf, Prog. Part. Nucl. Phys. 31 (1988) 1.
[27] M.L. Brooks et al., Phys. Rev. Lett. 83 (1999) 1521.
[28] C. Dohmen, Phys. Lett. B 317 (1993) 631.
[29] P. Wintz, in: A. Astbury et al. (Eds.), High Energy Physics, ICHEP'98, World Scientific, Singapore, 1999, p. 967.
[30] S. Ahmad, Phys. Rev. D 38 (1988) 2102.
[31] R.N. Mohapatra, Prog. Part. Nucl. Phys. 31 (1993) 39.
[32] J. Schwieger et al., Phys. Lett. B 443 (1998) 7.
[33] M. Raidal, A. Santamaria, Phys. Lett. B 421 (1998) 250.
[34] R.M. Carey et al., Phys. Rev. Lett. 82 (1999) 1632; see also H.N. Brown et al., Phys. Rev. Lett. 86 (2001) 2227.
[35] P. Langacker, M. Luo, A.K. Mann, Rev. Mod. Phys. 64 (1992) 87.
[36] B. Kayser, F. Gibrat-Debu, F. Perrier, The Physics of Massive Neutrinos, World Scientific, Singapore, 1989.
[37] F. Boehm, P. Vogel, Physics of Massive Neutrinos, Cambridge University Press, Cambridge, 1987.
[38] C.H. Weinheimer et al., Phys. Lett. B 460 (1990) 219.
[39] V.M. Lobashev et al., Phys. Lett. B 460 (1999) 227.
[40] K. Assamagan et al., Phys. Rev. D 53 (1996) 6005.
[41] D. Buskulic et al., Phys. Lett. B 349 (1995) 585.
[42] F.T. Avignone III, R.L. Brodzinski, Prog. Part. Nucl. Phys. 21 (1998) 99.
[43] M. Moe, P. Vogel, Annu. Rev. Nucl. Part. Sci. 44 (1994) 247.
[44] A. Morales, Nucl. Phys. B Proc. Suppl. 77 (1999) 335.
[45] O. Civitarese, J. Suhonen, Nucl. Phys. A 653 (1999) 321.
[46] C. Barbero et al., Nucl. Phys. A 650 (1999) 485.
[47] L. Baudis et al., Phys. Rev. Lett. 83 (1999) 41.
[48] C.E. Aalseth et al., Phys. Rev. C 59 (1999) 2108.
[49] E.W. Kolb, M.S. Turner, The Early Universe, Addison-Wesley, Reading, MA, 1990.
[50] G.G. Raffelt, Stars as Laboratories for Fundamental Physics, University of Chicago Press, Chicago, 1996.
[51] J.N. Bahcall, Neutrino Astrophysics, Cambridge University Press, Cambridge, 1989.
[52] R.N. Mohapatra, P.B. Pal, Massive Neutrinos in Physics and Astrophysics, World Scientific, Singapore, 1991; 2nd Edition, 1998.
[53] W. Haxton, Annu. Rev. Astr. Astrophysics 33 (1995) 459.
[54] G. Gelmini, E. Roulet, Neutrino Masses, Rep. Prog. Phys. 58 (1995) 1207.
[55] M. Spiro, D. Vignaud, Nucl. Phys. A 654 (1999) 350c.
[56] K. Zuber, Phys. Rep. 305 (1998) 295.
[57] P. Fisher, B. Kayser, K.S. McFarland, Annu. Rev. Nucl. Part. Phys. 49 (1999) 481.
[58] J.N. Bahcall et al., Phys. Rev. Lett. 78 (1997) 171.
[59] S. Parke, Phys. Rev. Lett. 74 (1995) 839.
[60] Y. Fukuda et al., Phys. Rev. Lett. 82 (1999) 2644.
[61] C. Atharassopoulus et al., Phys. Rev. C 54 (1996) 2685.
[62] F. Boehm et al., Phys. Rev. Lett. 84 (2000) 3764.
[63] F. Wilczek, Nucl. Phys. B Proc. Suppl. 77 (1999) 511.
[64] E. Ma et al., Phys. Lett. B 444 (1998) 391.
[65] N. Hata, W. Haxton, Phys. Lett. B 353 (1995) 422.
[66] J.N. Bahcall, M.H. Pinsonneault, Rev. Mod. Phys. 64 (1992) 885; J.N. Bahcall, M.H. Pinsonneault, Rev. Mod. Phys. 67 (1995) 781.
[67] P.I. Krastev et al., Phys. Rev. D 54 (1996) 7057.
[68] L. Oberauer, F. von Feilitzsch, Rep. Prog. Phys. 55 (1992) 1093.
[69] O. Cremonesi, Solar neutrinos, Riv. Nuovo Cimento 16 (1993) 1.
[70] P. Langacker, Nucl. Phys. B Proc. Suppl. 77 (1999) 241.
[71] J. Ellis, Nucl. Phys. A 663/664 (2000) 231c.
[72] K. Junker, Nucl. Phys. A 407 (1983) 460.
[73] F. Scheck, Leptons, Hadrons and Nuclei, North-Holland, Amsterdam, 1983.

[74] F. Scheck, Electroweak and Strong Interactions, Springer, Berlin, 1996.
[75] E.D. Commins, P.H. Bucksbaum, Weak Interactions of Leptons and Quarks, Cambridge University Press, Cambridge, 1983.
[76] W. Greiner, B. Müller, Gauge Theory of Weak Interactions, 2nd Edition, Springer, Berlin, 1996.
[77] B.R. Holstein, Weak Interactions in Nuclei, Princeton University Press, Princeton, NJ, 1989.
[78] R. Engfer, H.K. Walter, Annu. Rev. Nucl. Part. Sci. 36 (1986) 327.
[79] K. Armbruster et al., Phys. Rev. Lett. 81 (1998) 520.
[80] R. Ammar et al., Phys. Rev. Lett. 78 (1997) 4686.
[81] D.I. Britton et al., Phys. Rev. Lett. 68 (1992) 3000; Phys. Rev. D 49 (1994) 28.
[82] G. Czapek et al., Phys. Rev. Lett. 70 (1993) 17.
[83] A. Anastassov et al., Phys. Rev. D 55 (1997) 2559.
[84] B. Stugu, Nucl. Phys. B Proc. Suppl. 76 (1999) 123.
[85] OPAL, Phys. Lett. B 447 (1999) 134.
[86] P. Abreu et al., Eur. Phys. J. C 10 (1999) 201.
[87] S.R. Wasserbaech, Nucl. Phys. B Proc. Suppl. 76 (1999) 107.
[88] K. Abe et al., Phys. Rev. Lett. 78 (1997) 4691.
[89] M. Acciarri et al., Phys. Lett. B 438 (1999) 405.
[90] K. Ackerstaff et al., Eur. Phys. J. C 8 (1999) 3.
[91] A.J. Weinstein, R. Stroynowski, Annu. Rev. Nucl. Part. Sci. 43 (1993) 457.
[92] D.H. Wilkinson, in: H. Ejiri et al. (Eds.), Proceedings of WEIN Conference, World Scientific, Singapore, 1995, p. 307; and TRIUMF 97-74, in preparation.
[93] I.S. Towner, J.C. Hardy, in: W.C. Haxton, E.M. Henley (Eds.), Symmetries and Fundamental Interactions in Nuclei, World Scientific, Singapore, 1995, pp. 183–249; and Phys. Canada 55 (1999) 91.
[94] H. Abele, Nucl. Instr. and Meth. A 440 (2000) 499; also Nucl. Phys. A 663/664 (2000) 947c.
[95] S. Weinberg, Phys. Rev. 112 (1958) 1375.
[96] L. Grenacs, Annu. Rev. Nucl. Part. Sci. 35 (1985) 455.
[97] J. Govaerts, Hyperfine Interactions 118 (1999) 25.
[98] J. Govaerts, Nucl. Instr. and Meth. A 402 (1998) 303.
[99] E. Adelberger et al., Phys. Rev. Lett. 83 (1999) 1299.
[100] D.H. Wilkinson, Eur. Phys. J. A 7 (2000) 307.
[101] W.K. McFarlane et al., Phys. Rev. D 32 (1985) 547.
[102] P. Mergell, U.-G. Meissner, D. Drechsel, Nucl. Phys. A 596 (1996) 367.
[103] Particle Data Group, Rev. Mod. Phys. 48 (1976) S1.
[104] P. Liaud et al., Nucl. Phys. A 612 (1997) 53.
[105] J. Reich et al., Nucl. Instr. and Meth. A 440 (2000) 535.
[106] R.A. Arndt et al., Phys. Rev. C 49 (1994) 2729.
[107] T.E.O. Ericson et al., Phys. Rev. Lett. 75 (1995) 1046. This latest value is in T.E.O. Ericson et al., πN Newsletter 12 (1997) 16.
[108] V. Bernard, N. Kaiser, U.-G. Meissner, Phys. Rev. D 50 (1994) 6899; Int. J. Mod. Phys. E 4 (1995) 193.
[109] H.W. Fearing, R. Lewis, N. Mobed, S. Scherer, Phys. Rev. D 56 (1997) 1783.
[110] K. Kubodera, J. Delorme, M. Rho, Phys. Rev. Lett. 40 (1978) 755.
[111] E.K. Warburton, Phys. Rev. Lett. 66 (1991) 1823; E.K. Warburton, Phys. Rev. C 44 (1991) 233.
[112] M. Kirchbach, D.O. Riska, K. Tsushima, Nucl. Phys. A 542 (1992) 616.
[113] I.S. Towner, Nucl. Phys. A 542 (1992) 631.
[114] K. Tsushima, D.O. Riska, Nucl. Phys. A 549 (1992) 313.
[115] M. Kirchbach, D.O. Riska, Nucl. Phys. A 578 (1994) 511.
[116] E.H.S. Burhop, High Energy Physics, Vol. III, Academic Press, New York, 1969, p. 109.
[117] S. Devons, L. Duerdoth, Adv. Nucl. Phys. 2 (1969) 295.
[118] C.S. Wu, L. Wilets, Annu. Rev. Nucl. Sci. 19 (1969) 527.
[119] J. Hüfner, F. Scheck, C.S. Wu, Muon Physics, Vol. I, Academic Press, New York, 1977.
[120] D.E. Charlton, J. Booz, Radiat. Res. 87 (1981) 10.
[121] E. Fermi, E. Teller, Phys. Rev. 72 (1947) 399.

[122] T. von Egidy et al., Phys. Rev. A 23 (1981) 427.
[123] S. Stanislaus et al., Nucl. Phys. A 475 (1987) 630.
[124] V.A. Vasilyev et al., Dubna Report, JINR, R1, 10222, 1976.
[125] H. Schneuwly et al., Nucl. Phys. A 312 (1978) 419.
[126] H. Daniel, Z. Phys. A 291 (1979) 29.
[127] T. von Egidy et al., Phys. Rev. A 29 (1984) 455.
[128] S. Stanislaus et al., Nucl. Phys. A 475 (1987) 642.
[129] T. von Egidy, F.J. Hartmann, Phys. Rev. A 26 (1982) 2355.
[130] M. Giffon et al., Phys. Rev. C 24 (1981) 241.
[131] H. Daniel, Nucl. Instr. and Meth. 150 (1978) 609.
[132] G.A. Grin, R. Kunselman, Phys. Lett. B 31 (1970) 116.
[133] V.M. Abazov et al., Nucl. Instr. and Meth. 169 (1980) 423.
[134] R. Bergmann et al., Phys. Rev. A 20 (1979) 633.
[135] R.A. Naumann et al., Phys. Rev. A 21 (1980) 639.
[136] P. Ehrhart et al., Phys. Rev. A 27 (1983) 575.
[137] F. Mulhausser, H. Schneuwly, J. Phys. B 26 (1993) 4307.
[138] H. Schneuwly, Phys. Lett. A 191 (1994) 416.
[139] L. Schellenberg et al., Hyperfine Interactions 101/102 (1996) 215.
[140] A. Werthmüller et al., Hyperfine Interactions 101/102 (1996) 271.
[141] S. Tresch et al., Hyperfine Interactions 101/102 (1996) 221.
[142] M. Augsburger et al., PSI Scientific Report, Vol. 1, 1999, p. 16.
[143] D.F. Jackson, C.A. Lewis, K. O'Leary, Phys. Rev. A 25 (1982) 3262.
[144] N. Imanishi et al., Phys. Rev. A 32 (1985) 2584.
[145] N. Imanishi et al., Phys. Rev. A 35 (1987) 2044.
[146] D. Horvath, F. Entezami, TRIUMF Report TRI-83-1, 1983.
[147] V.G. Zinov et al., Sov. J. Nucl. Phys. 2 (1966) 613.
[148] N. Imanishi et al., Phys. Rev. A 35 (1987) 5244.
[149] T. Suzuki et al., Phys. Lett. B 95 (1980) 202.
[150] N. Imanishi et al., Phys. Rev. A 37 (1988) 43.
[151] W. Wilhelm et al., Chem. Phys. Lett. 55 (1978) 478.
[152] F.J. Hartmann et al., Z. Phys. A 308 (1982) 103.
[153] C.J. Martoff et al., Phys. Rev. C 27 (1983) 1621.
[154] R.A. Naumann et al., in: V.N. Prokrovsky (Ed.), Proceedings of the International Symposium, Dubna, 1977, p. 110.
[155] D. Horvath, Radiochim. Acta 28 (1981) 241.
[156] E.B. Shera, Nucl. Phys. A 335 (1980) 75.
[157] G. Fricke et al., Atom. Data Nucl. Data Tables 60 (1995) 177.
[158] G. Fricke et al., Phys. Rev. C 45 (1992) 80.
[159] H.D. Wohlfahrt et al., Phys. Rev. C 23 (1981) 533.
[160] D. Kessler et al., Can. J. Phys. 48 (1970) 3029.
[161] T.A.E.C. Pratt, Nucl. Instr. and Meth. 66 (1968) 348.
[162] L.A. Schaller et al., Nucl. Phys. A 300 (1978) 225.
[163] P. Bergen et al., Phys. Rev. C 37 (1988) 2821.
[164] M.V. Hoehn, E.B. Shera, Phys. Rev. C 30 (1984) 704.
[165] I. Beltrami et al., Nucl. Phys. A 429 (1984) 381.
[166] W.J. Briscoe et al., Nucl. Phys. 344 (1980) 475.
[167] Ch. Rösel et al., Z. Phys. A 340 (1991) 199.
[168] H. Backe et al., Nucl. Phys. A 234 (1974) 469.
[169] H.K. Walter, Nucl. Phys. A 234 (1974) 504.
[170] W.Y. Lee et al., Phys. Rev. Lett. 23 (1969) 648.
[171] H.D. Engelhardt et al., Nucl. Phys. A 258 (1976) 480.
[172] P. Vogel, Phys. Rev. A 22 (1980) 1600.

[173] F.J. Hartmann et al., Z. Phys. A 305 (1982) 189.
[174] H.L. Anderson et al., Phys. Rev. 187 (1969) 1565.
[175] R. Bergmann et al., Z. Phys. 291 (1979) 129.
[176] P. Hauser et al., Nucl. Instr. and Meth. A 411 (1998) 389.
[177] K. Debertin, R.G. Helmer, Gamma-ray and X-ray Spectrometry with Semiconductor Detectors, Elsevier, Amsterdam, 1988, p. 240.
[178] I.K. Helfer, K.M. Miller, Health Phys. 55 (1988) 15.
[179] S. Kamboj et al., Health Phys. 64 (1993) 300.
[180] S. Kamboj, B. Kahn, Health Phys. 70 (1996) 512.
[181] M.A. Ludington, R.G. Helmer, Nucl. Instr. and Meth. A 446 (2000) 506.
[182] V.S. Evseev, in: V.W. Hughes, C.S. Wu (Eds.), Muon Physics III, Academic Press, New York, 1975, p. 235.
[183] T. Suzuki et al., Phys. Rev. C 35 (1987) 2212.
[184] R. Winston, Phys. Rev. 129 (1963) 2766.
[185] P. Ackerbauer et al., Phys. Lett. B 417 (1998) 224.
[186] D. Favart et al., Phys. Rev. Lett. 25 (1970) 1348.
[187] K. Koshigiri et al., Prog. Theor. Phys. 68 (1982) 687; and University of Tokyo, Meson Science Newsletter, May 1982, p. 46.
[188] J.P. Deutsch et al., Phys. Lett. B 28 (1968) 178.
[189] V. Wiaux, Ph.D. Thesis, Université de Louvain, 1999.
[190] K. Ishida et al., Phys. Lett. B 167 (1986) 31.
[191] T.P. Gorringe et al., Phys. Lett. B 309 (1993) 241.
[192] T.J. Stocki, Ph.D. Thesis, University of British Columbia, 1998.
[193] T.P. Gorringe et al., Phys. Rev. Lett. 72 (1994) 3472.
[194] J.H. Brewer, Hyperfine Interactions 17–19 (1984) 879.
[195] L.B. Egorov et al., Sov. Phys. JETP 14 (1962) 494; I.E. Ignatenko et al., Nucl. Phys. 32 (1962) 563.
[196] D.P. Hutchinson et al., Phys. Rev. Lett. 9 (1962) 516.
[197] A.I. Babaev et al., Sov. J. Nucl. Phys. 10 (1970) 554.
[198] H. Überall, Phys. Rev. 121 (1961) 1219.
[199] E. Zavattini, in: V.W. Hughes, C.S. Wu (Eds.), Muon Physics II, Academic Press, New York, 1975, p. 219.
[200] L. Bracci, G. Fiorentini, Phys. Rep. 86 (1982) 169.
[201] W.H. Breunlich et al., Annu. Rev. Nucl. Part. Sci. 39 (1989) 311.
[202] P. Froelich, Adv. Phys. 41 (1992) 405.
[203] L. Ponomarev, Annu. Rev. Nucl. Sci. 23 (1973) 395; L. Ponomarev, Contemp. Phys. 31 (1991) 219.
[204] G. Bardin et al., Nucl. Phys. A 352 (1981) 365.
[205] S. Weinberg, Phys. Rev. Lett. 4 (1960) 575.
[206] G. Bardin et al., Phys. Lett. B 104 (1981) 320.
[207] A. Alberigi Quaranta et al., Phys. Rev. 177 (1969) 2118.
[208] V.M. Bystritskii et al., Sov. Phys. JETP 39 (1974) 19.
[209] I.T. Wang et al., Phys. Rev. B 139 (1965) 1528.
[210] A. Bertini et al., Phys. Rev. D 8 (1973) 3774.
[211] G. Bardin et al., Nucl. Phys. A 453 (1986) 591.
[212] M. Cargnelli et al., Workshop on fundamental μ physics, Los Alamos, 1986, LA 10714C; also Yamada Conference XXIII, Osaka, 1989.
[213] H. Uberall, L. Wolfenstein, Nuovo Cimento 10 (1958) 136.
[214] I.T. Wang, Phys. Rev. B 139 (1965) 1539.
[215] P. Pascual et al., Nuovo Cimento A 12 (1972) 241.
[216] M. Sotona, E. Truhlik, Nucl. Phys. A 229 (1974) 471.
[217] Nguyen Tien Nguyen, Nucl. Phys. A 254 (1975) 485.
[218] F. Dautry et al., Nucl. Phys. A 264 (1976) 507.
[219] E. Ivanov, E. Truhlik, Nucl. Phys. A 316 (1979) 451.
[220] S.L. Mintz, Phys. Rev. C 22 (1980) 2507.

[221] J. Adam, E. Truhlik, Nucl. Phys. A 507 (1990) 675.
[222] M. Doi et al., Nucl. Phys. A 511 (1990) 507.
[223] N. Tatara et al., Phys. Rev. C 42 (1990) 1694.
[224] G.E. Dogatar et al., Nucl. Phys. A 326 (1979) 225.
[225] Y.K. Lee et al., Phys. Lett. B 188 (1987) 33.
[226] B. Gabioud et al., Nucl. Phys. A 420 (1984) 496.
[227] O. Schori et al., Phys. Rev. C 35 (1987) 2252.
[228] C.R. Howell et al., Phys. Lett. B 444 (1998) 252.
[229] G.A. Miller et al., Phys. Rep. 194 (1990) 1.
[230] J. Torre, B. Goulard, Phys. Rev. Lett. 43 (1979) 1222.
[231] J.A. Bistirlich et al., Phys. Rev. Lett. 36 (1976) 942.
[232] J.G. Congleton, H.W. Fearing, Nucl. Phys. A 552 (1993) 534. See also J. Govaerts, J.-L. Lucio-Martinez, Nucl. Phys. A 678 (2000) 110.
[233] J.G. Congleton, Nucl. Phys. A 570 (1994) 511.
[234] J.G. Congleton, E. Truhlik, Phys. Rev. C 53 (1996) 956.
[235] N.C. Mukhopadhyay, K. Junker, Phys. Rev. Lett. 77 (1996) 5342.
[236] O.A. Zaimidoroga et al., Phys. Lett. 6 (1963) 100.
[237] L.B. Auerbach et al., Phys. Rev. B 138 (1967) 127.
[238] A.C. Phillips et al., Nucl. Phys. A 237 (1975) 493.
[239] F. Corriveau et al., Nucl. Phys. A 473 (1987) 747.
[240] A.C. Phillips, F. Roig, Nucl. Phys. A 234 (1974) 378.
[241] P.A. Souder et al., Nucl. Instr. and Meth. A 402 (1998) 311.
[242] S.E. Kuhn et al., Phys. Rev. C 50 (1994) 1771.
[243] E. Jans et al., Nucl. Phys. A 475 (1987) 687.
[244] R.E.J. Florizone et al., Phys. Rev. Lett. 83 (1999) 2308.
[245] R. Skibinski et al., Phys. Rev. C 59 (1999) 2384.
[246] R. Bizzari et al., Nuovo Cimento 33 (1964) 1497.
[247] M.M. Block et al., Nuovo Cimento 55 (1968) 501.
[248] C.A. Caine, P.S.H. Jones, Nucl. Phys. 44 (1963) 177.
[249] J.D. Walecka, in: V.W. Hughes, C.S. Wu (Eds.), Muon Physics III, Academic Press, New York, 1975.
[250] G. Bardin et al., Phys. Lett. B 79 (1978) 52.
[251] Dz. Ganzorig et al., Nucl. Phys. A 350 (1980) 278; earlier report, Phys. Lett. B 78 (1978) 41.
[252] H. Hänscheid et al., Z. Phys. A 335 (1990) 1.
[253] L.W. Huff, Ann. Phys. (N.Y.) 16 (1961) 288.
[254] I.M. Blair et al., Proc. Phys. Soc. London 80 (1962) 938.
[255] T.A. Filippas et al., Phys. Lett. 6 (1963) 118.
[256] R. Watanabe et al., Atom. Data Nucl. Data Tables 54 (1993) 165.
[257] M. Eckhause et al., Nucl. Phys. 81 (1966) 575.
[258] J.L. Lathrop et al., Phys. Rev. Lett. 7 (1961) 107.
[259] P. David et al., Z. Phys. A 330 (1988) 397.
[260] K.W. Ford, J.G. Wills, Nucl. Phys. 35 (1968) 295.
[261] N.C. Mukhopadhyay et al., Phys. Lett. B 434 (1998) 7.
[262] H.C. Chiang et al., Nucl. Phys. A 510 (1990) 591.
[263] F. Cannata, R. Leonardi, M. Rosa Clot, Phys. Lett. B 32 (1970) 6.
[264] Nguyen Van Giai, N. Auerbach, A.Z. Mekjian, Phys. Rev. Lett. 46 (1981) 1444.
[265] N. Auerbach, A. Klein, Nucl. Phys. A 422 (1984) 480.
[266] N. Auerbach, Nguyen Van Giai, O.K. Vorov, Phys. Rev. C 56 (1997) R2368.
[267] E. Kolbe et al., Phys. Rev. C 50 (1994) 2576.
[268] E. Kolbe et al., Phys. Rev. C 62 (2000) 055502.
[269] K. Junker et al., Conference on Nuclear Physics, St. Petersburg, June, 2000.
[270] H.C. Chiang et al., Nucl. Phys. A 510 (1990) 573.
[271] H.W. Baer, K.M. Crowe, P. Truöl, Adv. Nucl. Phys. 9 (1977) 177.

[272] M. Gmitro, R.A. Eramzhian, H. Kissener, P. Truöl, Sov. J. Part. Nucl. 13 (1982) 513; M. Gmitro, R.A. Eramzhian, H. Kissener, P. Truöl, Sov. J. Part. Nucl. 14 (1983) 323.
[273] G. Strassner et al., Phys. Rev. C 20 (1979) 248.
[274] J.P. Perroud et al., Nucl. Phys. A 453 (1986) 542.
[275] Q. Ingram, AIP Conference #54, 1979, p. 455.
[276] R.J. Ellis, AIP Conference #54, 1979, p. 274.
[277] H. Ejiri, Phys. Rep. 338 (2000) 265.
[278] W.P. Alford, B.M. Spicer, Adv. Nucl. Phys. 24 (1998) 1.
[279] R. Madey et al., Phys. Rev. C 56 (1997) 3210.
[280] B.D. Anderson et al., Phys. Rev. C 54 (1996) 237.
[281] F. Ajzenberg-Selove, Nucl. Phys. A 506 (1990) 1.
[282] H. Sakai et al., Nucl. Phys. A 599 (1996) 197c.
[283] L. Wang et al., Phys. Rev. C 47 (1993) 2123.
[284] A. Fazely et al., Phys. Rev. C 25 (1982) 1760.
[285] B.D. Anderson et al., Phys. Rev. C 43 (1991) 50.
[286] B.D. Anderson et al., Phys. Rev. C 36 (1987) 2195.
[287] J.M. Watson et al., Nucl. Phys. A 599 (1996) 211c.
[288] T. Chittrakarn et al., Phys. Rev. C 34 (1986) 80.
[289] J. Rapaport, E. Sugerbaker, Annu. Rev. Nucl. Part. Sci. 44 (1994) 109.
[290] B.D. Anderson et al., Phys. Rev. C 54 (1996) 1531.
[291] D.F. Measday, J.N. Palmieri, Phys. Rev. 161 (1967) 1071.
[292] S.M. Austin et al., Phys. Rev. Lett. 44 (1980) 972.
[293] B.K. Park et al., Phys. Rev. C 45 (1992) 1791.
[294] B.K. Park et al., Phys. Rev. C 48 (1993) 711.
[295] D.S. Sorenson et al., Phys. Rev. C 45 (1992) R500.
[296] A. Ling et al., Phys. Rev. C 44 (1991) 2794.
[297] N. Olsson et al., Nucl. Phys. A 599 (1996) 185c.
[298] K. Wang et al., Phys. Rev. C 53 (1996) 1718.
[299] C.J. Martoff et al., Phys. Rev. C 54 (1996) 2767.
[300] H.M. Xu et al., Phys. Rev. C 52 (1995) R1161.
[301] H.M. Xu et al., Phys. Rev. C 54 (1996) 3266.
[302] C.A. Gagliardi et al., in: H. Sakai et al. (Eds.), New Facets of Spin Giant Resonances in Nuclei, World Scientific, Singapore, 1998, p. 50.
[303] H. Ohnuma et al., Phys. Rev. C 47 (1993) 648.
[304] H. Okamura et al., Phys. Rev. B 345 (1995) 1.
[305] H. Okamura et al., Phys. Rev. C 60 (1999) 064602.
[306] T. Inomata et al., Phys. Rev. C 57 (1998) 3153.
[307] S.M. Austin, Nucl. Phys. A 649 (1999) 279c.
[308] B.M. Sherrill et al., Nucl. Instr. and Meth. A 432 (1999) 299.
[309] I. Daito et al., Phys. Lett. B 418 (1998) 27.
[310] M. Fujiwara, I. Daito, in: H. Sakai et al. (Eds.), New Facets of Spin Giant Resonances in Nuclei, World Scientific, Singapore, 1980, p. 80.
[311] S. Dangtip et al., Nucl. Phys. A 677 (2000) 3.
[312] J. Jänecke et al., Nucl. Phys. A 599 (1996) 191c.
[313] T. Annakkage et al., Nucl. Phys. A 648 (1999) 3.
[314] S. Nakayama et al., Phys. Rev. Lett. 83 (1999) 690.
[315] S. Nakayama et al., Phys. Rev. C 60 (1999) 047303.
[316] I. Lhenry, Nucl. Phys. A 599 (1996) 245c.
[317] L.W. Fagg, Rev. Mod. Phys. 47 (1975) 683.
[318] P. von Neumann-Cosel et al., Phys. Rev. Lett. 82 (1999) 105.
[319] N. Anantaraman et al., Phys. Rev. Lett. 46 (1981) 1318.
[320] A. Tamii et al., Phys. Lett. B 459 (1999) 61.

[321] F.T. Baker et al., Phys. Rep. 289 (1997) 235.
[322] T. Noro et al., Nucl. Phys. A 629 (1998) 324c.
[323] T. Ishikawa et al., Annual Report, RCNP, Osaka, 1998.
[324] A.E.L. Dieperink, P.K.A. de Witt-Huberts, Annu. Rev. Nucl. Sci. 40 (1990) 239.
[325] L. Lapikas, Nucl. Phys. A 553 (1993) 297c.
[326] T. Walcher, Prog. Part. Nucl. Phys. 34 (1995) 1.
[327] P.K.A. de Witt-Huberts, Prog. Part. Nucl. Phys. 34 (1995) 17.
[328] B. MacDonald, J.A. Diaz, S.N. Kaplan, R.V. Pyle, Phys. Rev. B 139 (1965) 1253.
[329] S.N. Kaplan, B.J. Moyer, R.V. Pyle, Phys. Rev. 112 (1958) 968.
[330] P. Singer, Phys. Rev. 124 (1961) 1602; Nuovo Cimento 23 (1962) 669.
[331] J. Hadermann, K. Junker, Phys. Lett. B 55 (1975) 141; J. Hadermann, K. Junker, Nucl. Phys. A 271 (1976) 401.
[332] G. Heusser, T. Kirsten, Nucl. Phys. A 195 (1972) 369.
[333] A. Wyttenbach et al., Nucl. Phys. A 294 (1978) 278.
[334] A. Wyttenbach et al., quoted in note 9 added in proof, Mukhopadhyay, Ref. [13].
[335] B. Budick et al., Phys. Lett. B 110 (1982) 375.
[336] B. Budick et al., Nucl. Phys. A 393 (1983) 469.
[337] J.P. Deutsch et al., Nuovo Cimento B 52 (1967) 557.
[338] T.P. Gorringe et al., Phys. Rev. C 60 (1999) 055501.
[339] B. Johnson et al., Phys. Rev. C 54 (1996) 2714.
[340] G.H. Miller et al., Phys. Rev. C 6 (1972) 487.
[341] G.G. Bunatyan et al., Sov. J. Nucl. Phys. 9 (1969) 457; G.G. Bunatyan et al., Sov. J. Nucl. Phys. 11 (1970) 444; G.G. Bunatyan et al., Sov. J. Nucl. Phys. 15 (1972) 526.
[342] G.G. Bunatyan et al., Sov. J. Nucl. Phys. 2 (1966) 619; G.G. Bunatyan et al., Sov. J. Nucl. Phys. 3 (1966) 613.
[343] M. Lifshitz, P. Singer, Phys. Rev. C 22 (1980) 2135.
[344] L. Winsberg, Phys. Rev. 95 (1954) 205.
[345] G. Backenstoss et al., Nucl. Phys. A 162 (1971) 541.
[346] J. Bernabeu, T.E.O. Ericson, C. Jarlskog, Phys. Lett. B 69 (1977) 161.
[347] T.E.O. Ericson, J. Bernabeu, Phys. Lett. B 70 (1977) 170.
[348] M. Lifshitz, P. Singer, Phys. Lett. B 215 (1988) 607.
[349] N.C. Mukhopadhyay, J. Haderman, P. Singer, Phys. Rev. Lett. 44 (1980) 1653.
[350] H.S. Pruys, A. Wyttenbach; quoted in [348].
[351] J. van der Pluym et al., Phys. Lett. B 177 (1986) 21.
[352] T. Kozlowski et al., Nucl. Phys. A 436 (1985) 717.
[353] E.K. McIntyre et al., Phys. Lett. B 137 (1984) 339.
[354] R.M. Sundelin, R.M. Edelstein, Phys. Rev. C 7 (1973) 1037.
[355] M.H. Krieger, Ph.D. Thesis, Columbia University, 1969.
[356] A. van der Schaaf et al., Nucl. Phys. A 408 (1983) 573.
[357] R.A. Eramzhyan, Yu.A. Salganic, Nucl. Phys. A 207 (1973) 609.
[358] M.E. Plett, S.E. Sobottka, Phys. Rev. C 3 (1971) 1003.
[359] V. Evseyev et al., Phys. Lett. B 28 (1969) 553.
[360] I. Wojtkowska et al., Sov. J. Nucl. Phys. 15 (1972) 639.
[361] N. Ohtsuka, Nucl. Phys. A 370 (1981) 431.
[362] M. Gmitro et al., Czech. J. Phys. B 31 (1981) 499.
[363] N. Olsson et al., Nucl. Phys. A 559 (1993) 368.
[364] W.U. Schröder et al., Z. Phys. 268 (1974) 57.
[365] E. Lubkin, Ann. Phys. (N.Y.) 11 (1960) 414.
[366] D.E. Hagge, thesis, UCRO-10516, University of California, 1963.
[367] P. Singer, N.C. Mukhopadhyay, R.D. Amado, Phys. Rev. Lett. 42 (1979) 162.
[368] S.N. Kaplan et al., in: S. Devons (Ed.), High Energy Physics and Nuclear Structure, Plenum, New York, 1970, p. 163.

[369] R. Raphael, H. Überall, C. Werntz, Phys. Lett. B 24 (1967) 15.
[370] S.N. Kaplan et al., Phys. Rev. Lett. 22 (1969) 795.
[371] R. Klein, T. Neal, L. Wolfenstein, Phys. Rev. B 138 (1965) 86.
[372] A. Bogan, Nucl. Phys. B 12 (1969) 89.
[373] C.A. Piketty, J. Procureur, Nucl. Phys. B 26 (1971) 390.
[374] A. Bouyssy, N. Vinh-Mau, Nucl. Phys. A 185 (1972) 32; A. Bouyssy, H. Ngo, N. Vinh-Mau, Phys. Lett. B 44 (1973) 139.
[375] H. Morinaga, W.F. Fry, Nuovo Cimento Ser. 9 (10) (1953) 308.
[376] D. Kotelchuk, J.V. Tyler, Phys. Rev. 165 (1968) 1190.
[377] A.O. Vaisenberg et al., Sov. J. Nucl. Phys. 1 (1965) 467.
[378] A.O. Vaisenberg et al., Sov. J. Nucl. Phys. 11 (1970) 464.
[379] K.S. Krane et al., Phys. Rev. C 20 (1979) 1873.
[380] Yu.G. Budyashov et al., Sov. Phys. JETP 33 (1971) 11.
[381] S.E. Sobottka, E.L. Wills, Phys. Rev. Lett. 20 (1968) 596.
[382] H.J. Evans, Nucl. Phys. A 207 (1973) 379.
[383] T.A.E.C. Pratt, Nuovo Cimento B 61 (1969) 119.
[384] V.I. Komarov, O.V. Savchenko, Sov. J. Nucl. Phys. 8 (1969) 239.
[385] L. Vil'gel'mora et al., Sov. J. Nucl. Phys. 13 (1971) 310.
[386] M. Kawai, K. Kikuchi, Nuclear Matter and Nuclear Reactions, North-Holland, Amsterdam, 1968.
[387] I. Dostrovsky, P. Rabinowitz, P. Bivins, Phys. Rev. 111 (1958) 1659.
[388] I. Dostrovsky, Z. Fraenkel, L. Winsberg, Phys. Rev. 118 (1960) 781.
[389] M. Lifshitz, P. Singer, Phys. Rev. Lett. 41 (1978) 18.
[390] J.J. Griffin, Phys. Rev. Lett. 19 (1966) 57.
[391] C.K. Hargrove et al., Phys. Rev. Lett. 23 (1969) 215.
[392] K.P. Lohs et al., Nucl. Phys. A 236 (1974) 457.
[393] H. Hänscheid et al., Z. Phys. A 342 (1992) 111.
[394] Ch. Rösel et al., Z. Phys. A 345 (1993) 89.
[395] H. Paganetti et al., Z. Phys. A 343 (1992) 113.
[396] W. Schrieder et al., Z. Phys. A 339 (1991) 445.
[397] S. Ahmad et al., Phys. Lett. B 92 (1980) 83.
[398] P. Baertschi et al., Nucl. Phys. A 294 (1978) 369.
[399] W.W. Wilcke et al., Phys. Rev. C 18 (1978) 1452.
[400] A. Zglinski et al., Nucl. Phys. A 305 (1978) 381.
[401] R. Vandenbosch, J.R. Huizenga, Nuclear Fission, Academic Press, New York, 1973.
[402] Ch. Rösel et al., Z. Phys. A 340 (1991) 199.
[403] F.F. Karpeshin, V.O. Nesterenko, J. Phys. G 17 (1991) 705.
[404] B. Budick et al., Nucl. Phys. A 350 (1980) 265.
[405] W.U. Schröder et al., Phys. Rev. Lett. 43 (1979) 672.
[406] F. Risse et al., Z. Phys. A 339 (1991) 427.
[407] J.A. Maruhn et al., Phys. Rev. Lett. 44 (1980) 1576.
[408] L. Bracci, G. Fiorentini, Nucl. Phys. A 423 (1984) 429.
[409] F.F. Karpeshin, Nucl. Phys. 2000, in preparation.
[410] F.F. Karpeshin, J. Phys. G 16 (1990) 1195.
[411] Ch. Rösel et al., Z. Phys. A 345 (1993) 425.
[412] J.T. Caldwell et al., Phys. Rev. C 21 (1980) 1215.
[413] P. David et al., Z. Phys. A 328 (1988) 37.
[414] P. David et al., Phys. Lett. B 124 (1983) 161.
[415] M.C. Duijvestijn et al., Phys. Rev. C 59 (1999) 776.
[416] J. Hadermann, K. Junker, Nucl. Phys. A 256 (1976) 521.
[417] M. Lifshitz, P. Singer, Z. Phys. A 332 (1989) 311.
[418] P.M. Endt, Nucl. Phys. A 521 (1990) 1.
[419] R.B. Firestone et al., Table of Isotopes, 8th Edition, Wiley, New York, 1996.

[420] R.A. Eramzhyan et al., Nucl. Phys. A 642 (1998) 428.
[421] O. Nalcioglu, D.J. Rowe, C. Ngo-Trong, Nucl. Phys. A 218 (1974) 495.
[422] T. Rönnquist et al., Nucl. Phys. A 563 (1993) 225.
[423] E. Caurier et al., Nucl. Phys. A 653 (1999) 439.
[424] W.P. Alford et al., Nucl. Phys. A 514 (1990) 49.
[425] M.C. Vetterli et al., Phys. Rev. C 40 (1989) 559.
[426] S. El-Kateb et al., Phys. Rev. C 49 (1994) 3128.
[427] W.P. Alford et al., Phys. Rev. C 48 (1993) 2818.
[428] A.L. Williams et al., Phys. Rev. C 51 (1995) 1144.
[429] R.G. Helmer, C. van der Leun, Nucl. Instr. and Meth. A 450 (2000) 35.
[430] F. Di Filippo et al., Phys. Rev. Lett. 73 (1994) 1481.
[431] R.G. Helmer et al., Atom. Data Nucl. Data Tables 24 (1979) 39.
[432] R.C. Greenwood, R.E. Chrien, Phys. Rev. C 21 (1980) 498.
[433] G.L. Greene et al., Phys. Rev. Lett. 56 (1986) 819.
[434] A.H. Wapstra, Nucl. Instr. and Meth. A 292 (1990) 671.
[435] D.R. Tilley et al., Nucl. Phys. A 564 (1993) 1.
[436] T.J. Kennett et al., Nucl. Instr. and Meth. A 247 (1986) 420.
[437] P.F.A. Alkemade et al., Nucl. Instr. and Meth. 197 (1982) 383.
[438] E.B. Shera, Phys. Rev. C 26 (1982) 2321.
[439] E.L. Hull et al., Nucl. Instr. and Meth. A 385 (1997) 489.
[440] E. Gete et al., Nucl. Instr. and Meth. A 388 (1997) 212.
[441] C.T.A.M. de Laat et al., Nucl. Phys. A 523 (1991) 453.
[442] J.P. Perroud, Seminar on Electromagnetic Interactions of Nuclei at Low and Medium Energies, Moscow, June 1981. See also the SIN Annual Report, 1976, E45.
[443] B.A. Moftah, Ph.D. Thesis, University of British Columbia.
[444] T. Ichihara et al., Nucl. Phys. A 569 (1994) 287c.
[445] T. Niizeki et al., Nucl. Phys. A 577 (1994) 37c.
[446] Y. Fujita et al., Phys. Rev. C 55 (1997) 1137.
[447] P. von Neumann-Cosel et al., Phys. Rev. C 55 (1997) 532.
[448] G.M. Crawley et al., Phys. Rev. C 39 (1989) 311.
[449] C. Lüttge et al., Phys. Rev. C 53 (1996) 127.
[450] P.M. Endt, J.G.L. Booten, Nucl. Phys. A 555 (1993) 499.
[451] V.A. Kuz'min, T.V. Tetereva, Dubna preprint E4-99-210, 1999.
[452] H. Mackh et al., Z. Phys. 269 (1974) 353.
[453] J. Vernotte et al., Phys. Rev. C 49 (1994) 1559.
[454] J.E.M. Thomson, M.N. Thompson, Nucl. Phys. A 285 (1977) 84.
[455] R.L. Gulbranson et al., Phys. Rev. C 27 (1983) 470.
[456] L. Grenacs et al., Nucl. Instr. and Meth. 58 (1968) 164.
[457] V. Brudanin et al., Nucl. Phys. A 587 (1995) 577.
[458] G.H. Miller et al., Phys. Rev. Lett. 29 (1972) 1194.
[459] B.A. Moftah et al., Phys. Lett. B 395 (1997) 157.
[460] Ch. Briancon et al., Nucl. Phys. A 671 (2000) 647.
[461] P.M. Endt, C. van der Leun, Nucl. Phys. A 310 (1978) 1.
[462] B. Lawergren, J. Beyea, Phys. Rev. C 6 (1972) 2082.
[463] K. Junker et al., Phys. Rev. C 61 (2000) 044602.
[464] T. Siiskonen et al., Phys. Rev. C 59 (1999) R1839.
[465] J.P. Deutsch et al., Phys. Lett. B 26 (1968) 315.
[466] T. Suzuki, Proceedings of the International Symposium on Non-nucleonic Degrees of Freedom, Detected in the Nucleus, September 2–5, 1996, Osaka, Japan.
[467] K. Koshigiri et al., Prog. Theor. Phys. 71 (1984) 1293.
[468] V.A. Kuz'min et al., Phys. Atom. Nuclei 57 (1994) 1954.
[469] S. Cohen, D. Kurath, Nucl. Phys. 73 (1965) 1.

[470] E.K. Warburton, B.A. Brown, Phys. Rev. C 46 (1992) 923.
[471] U. Schwinn et al., Z. Phys. A 275 (1975) 241.
[472] J.P. Garron et al., Nucl. Phys. 37 (1962) 126.
[473] H. Tyren et al., Nucl. Phys. 79 (1966) 321.
[474] E.J. Maier et al., Phys. Rev. 133 (1964) 663.
[475] L.Ph. Roesch et al., Phys. Lett. B 107 (1981) 31.
[476] M. Fukui et al., Prog. Theor. Phys. 70 (1983) 827; M. Fukui et al., Prog. Theor. Phys. 78 (1987) 343.
[477] A.C. Hayes, I.S. Towner, Phys. Rev. C 61 (2000) 044603 and private communication.
[478] C. Volpe et al., Phys. Rev. C 62 (2000) 015501.
[479] P. Navratil et al., Phys. Rev. Lett. 84 (2000) 5728.
[480] A. Possoz et al., Phys. Lett. B 70 (1977) 265.
[481] Y. Kuno et al., Phys. Lett. B 148 (1984) 270.
[482] L.Ph. Roesch et al., Phys. Rev. Lett. 46 (1981) 1507; L.Ph. Roesch et al., Helv. Phys. Acta 55 (1982) 74.
[483] G. van der Steenhoven et al., Nucl. Phys. A 480 (1988) 547; G. van der Steenhoven et al., Nucl. Phys. A 484 (1988) 445.
[484] H.A. Medicus et al., Nucl. Phys. A 156 (1970) 257.
[485] H. Ferdinande et al., Phys. Rev. C 39 (1989) 253.
[486] H. Ruijter et al., Phys. Rev. C 54 (1996) 3076.
[487] K. Koshigiri et al., Prog. Theor. Phys. 74 (1985) 736.
[488] G.E. Dogotar et al., Nucl. Phys. 282 (1977) 474.
[489] P. Desgrolard, P.A.M. Guichon, Phys. Rev. C 19 (1979) 120; see also P. Desgrolard, P.A.M. Guichon, Nuovo Cimento A 43 (1978) 475.
[490] G.A. Needham et al., Nucl. Phys. A 385 (1982) 349.
[491] R.W. Gellie et al., Can. Journ. Phys. 50 (1972) 1689.
[492] M.N. Thompson et al., Phys. Lett. B 31 (1970) 211.
[493] H.R. Kissener et al., Nucl. Phys. A 215 (1973) 424.
[494] H.R. Kissener et al., Nucl. Phys. A 312 (1978) 394.
[495] F. Hinterberger et al., Nucl. Phys. A 106 (1968) 161.
[496] N. Mukhopadhyay, Phys. Lett. B 44 (1973) 33.
[497] Yu. Bely et al., Nucl. Phys. A 204 (1973) 357.
[498] C. Djalali et al., Phys. Rev. C 35 (1987) 1201.
[499] F.R. Kane et al., Phys. Lett. B 45 (1973) 292.
[500] P. Guichon et al., Phys. Rev. C 19 (1979) 987.
[501] R.A. Eramzhyan et al., Nucl. Phys. A 290 (1977) 294.
[502] W.C. Haxton, C. Johnson, Phys. Rev. Lett. 65 (1990) 1325.
[503] A.R. Heath, G.T. Garvey, Phys. Rev. C 31 (1985) 2190.
[504] A. Fabrocini et al., Phys. Rev. C 61 (2000) 044302.
[505] J.T. Caldwell et al., Phys. Rev. Lett. 19 (1967) 447.
[506] H. Ullrich, H. Krauth, Nucl. Phys. A 123 (1969) 641.
[507] M. Leuschner et al., Phys. Rev. C 49 (1994) 955.
[508] K.I. Blomqvist et al., Phys. Lett. B 344 (1995) 85.
[509] L. Isaksson et al., Phys. Rev. Lett. 83 (1999) 3146.
[510] T. Siiskonen et al., Nucl. Phys. A 635 (1998) 446.
[511] T. Siiskonen et al., J. Phys. G 25 (1999) L55.
[512] C.J. Martoff et al., Phys. Rev. Lett. 46 (1981) 891.
[513] B.W. Pointon et al., Phys. Rev. C 44 (1991) 2430.
[514] D.R. Tilley et al., Nucl. Phys. A 636 (1998) 249.
[515] A. Richter et al., Phys. Rev. Lett. 20 (1990) 2819.
[516] R.M. Sedlar et al., Phys. Rev. C 59 (1999) 789.
[517] K. Junker et al., International Conference on Nuclear Structure and Related Topics, Dubna, June, 2000.
[518] A.S. Gabelko et al., Sov. J. Nucl. Phys. 44 (1986) 741.
[519] B.S. Ishkanov et al., Sov. J. Nucl. Phys. 33 (1981) 303.

[520] B.H. Wildenthal, E. Newman, Phys. Rev. 175 (1968) 1431.
[521] K. Bangert et al., Nucl. Phys. A 261 (1976) 149.
[522] P.J. Ryan et al., Nucl. Phys. A 411 (1983) 105.
[523] V.V. Varlamov et al., Sov. J. Nucl. Phys. 30 (1979) 617.
[524] S. Yen, Can. Journ. Phys. 65 (1987) 595.
[525] N. Saurel, Thesis, University of Clermond-Ferrand, 1998.
[526] P.J.P. Ryan et al., Nucl. Phys. A 371 (1981) 318.
[527] M. Petraitis et al., Phys. Rev. C 49 (1994) 3000.
[528] P.E. Burt et al., Phys. Rev. C 29 (1984) 713.
[529] H. Molique et al., Phys. Rev. C 61 (2000) 044304.
[530] J. Brenneisen et al., Z. Phys. A 357 (1997) 377.
[531] V.V. Varlamov et al., Sov. J. Nucl. Phys. 28 (1978) 302.
[532] J. Vernotte et al., Nucl. Phys. A 655 (1999) 415.
[533] J. Wesseling et al., Nucl. Phys. A 547 (1992) 519.
[534] P. Igo-Kemenes et al., Phys. Lett. B 34 (1971) 286.
[535] M. Petraitis et al., Phys. Rev. C 51 (1995) 1014.
[536] P.E. Burt et al., Phys. Rev. C 25 (1982) 2805.
[537] W. Gross et al., Phys. Lett. B 84 (1979) 296.
[538] D. Brajnik et al., Phys. Rev. C 9 (1974) 1901.
[539] F.T. Baker et al., Phys. Rev. C 61 (2000) 037302.
[540] C. Ruhla et al., Nucl. Phys. A 95 (1967) 526.
[541] P.G. Roos et al., Phys. Rev. Lett. 40 (1978) 1439.
[542] H.P. Povel et al., Phys. Lett. B 33 (1970) 620.
[543] C. Petitjean et al., Nucl. Phys. A 178 (1971) 193.
[544] H. Backe et al., Nucl. Phys. A 189 (1972) 472.
[545] T. Dubler et al., Nucl. Phys. A 294 (1978) 397.
[546] B. Budick et al., Phys. Lett. B 106 (1981) 51.
[547] C.-O. Wene, Z. Phys. A 272 (1975) 77.
[548] K. Reiner et al., Nucl. Phys. A 472 (1987) 1.
[549] I. Bobeldijk et al., Phys. Rev. Lett. 73 (1994) 2684.
[550] J. Uegaki et al., Nucl. Phys. A 371 (1981) 93.
[551] P.D. Barnes et al., Phys. Rev. C 1 (1970) 228.
[552] E.A. McClatchie et al., Phys. Rev. C 1 (1970) 1828.
[553] G. Mairle et al., Phys. Lett. B 121 (1983) 307.
[554] G. Jonkmans et al., Phys. Rev. Lett. 77 (1996) 4512.
[555] D.H. Wright et al., Phys. Rev. C 57 (1998) 373.
[556] D.S. Beder et al., Phys. Rev. D 35 (1987) 2130; D.S. Beder et al., Phys. Rev. C 39 (1989) 3493.
[557] S.-C. Ando, F. Myhrer, K. Kubodera, arXiv:nucl-th 0008003.
[558] R.D. Hart et al., Phys. Rev. Lett. 39 (1977) 399.
[559] A. Frischknecht et al., Phys. Rev. C 32 (1985) 1506.
[560] A. Frischknecht et al., Phys. Rev. C 38 (1988) 1996.
[561] M. Döbeli et al., Phys. Rev. C 37 (1988) 1633.
[562] C. Virtue, Ph.D. Thesis, University of British Columbia, 1987.
[563] D.S. Armstrong et al., Phys. Rev. C 43 (1991) 1425; see also D.S. Armstrong et al., Phys. Rev. C 40 (1989) R1100.
[564] D.S. Armstrong et al., Phys. Rev. C 46 (1992) 1094.
[565] T.P. Gorringe et al., Phys. Rev. C 58 (1998) 1767.
[566] P.C. Bergbusch et al., Phys. Rev. C 59 (1999) 2853.
[567] H.P.C. Rood, H.A. Tolhoek, Nucl. Phys. 70 (1965) 658.
[568] M. Gmitro, P. Truöl, Adv. Nucl. Phys. 18 (1987) 241.
[569] H.W. Fearing, M.S. Welsh, Phys. Rev. C 46 (1992) 2077.
[570] G.H. Miller et al., Phys. Lett. B 41 (1972) 50.

[571] B.R. Holstein, Phys. Rev. D 13 (1976) 2499.
[572] I.S. Towner, F.C. Khanna, Nucl. Phys. A 372 (1981) 331.
[573] B.A. Brown, B.H. Wildenthal, Atom. Data Nucl. Data Tables 33 (1985) 347.
[574] G.E. Brown, T.T.S. Kuo, Nucl. Phys. 85 (1966) 40; G.E. Brown, T.T.S. Kuo, Nucl. Phys. A 103 (1967) 71.
[575] A. van der Schaaf, Prog. Part. Nucl. Phys. 31 (1993) 1.
[576] T.S. Kosmas et al., Prog. Part. Nucl. Phys. 33 (1994) 397.
[577] S. Ahmad et al., Phys. Rev. Lett. 59 (1987) 970.
[578] W. Honecker et al., Phys. Rev. Lett. 76 (1996) 200.
[579] J. Kaulart et al., Phys. Lett. B 422 (1998) 334.
[580] T. Siiskonen et al., Phys. Rev. C 60 (1999) 062501; T. Siiskonen et al., Phys. Rev. C 62 (2000) 035502.
[581] E.K. Warburton, I.S. Towner, B.A. Brown, Phys. Rev. C 49 (1994) 824.
[582] G.J. Kramer et al., Phys. Lett. B 227 (1989) 199.